

AN ABSTRACT OF THE THESIS OF

Abbas Dadkhah-Nikoo for the degree of Doctor of Philosophy  
in Mechanical Engineering presented on May 2, 1991.

Title: Experimental Investigation of Wood Combustion and  
Combustion Profiles in a Cylindrical Combustion Chamber

Abstract approved: \_\_\_\_\_

*Redacted for Privacy*

Dwight J. Busnell

This study presents the results of an experimental investigation of wood combustion. Variables chosen for investigation were fuel feed rate, fuel moisture content, fuel particle size, excess air, fraction and temperature of under-fire air. Data recorded during the experiments included the composition and temperature of the combustion products in the combustion chamber, particulate emissions and combustible fraction of the particulate.

Most mathematical models describing the combustion of wood particles require numerical solutions. For this investigation, an alternative model was used to generate closed form solutions for the determination of the burning times for wood particles in the combustion chamber. The model results were in good agreement with the experimental findings.

The temperature profiles of combustion products within the combustion chamber were closely estimated, using an analytical model developed for this investigation. The com-

position profiles within the combustion chamber were estimated with the use of a chemical equilibrium model. These models were in good agreement with the experimental results for the estimation of the oxygen and carbon dioxide contents of the combustion products. The chemical equilibrium model proved to be inadequate for the determination of the  $\text{NO}_x$  and CO contents of the combustion products.

Based upon the experimental data, a linear regression model was developed to investigate the variables affecting the combustion process. A computer model was used to calculate the temperature and composition of the combustion products under adiabatic conditions. Over the range of the variables considered, it was concluded that combustion efficiency and particulate emissions were most influenced by the factors that increased the volume and velocity of combustion products in the chamber. Moreover, it was also concluded that the part-load operation of the combustion unit resulted in higher particulate emissions and lower combustion efficiency.

Experimental Investigation of Wood Combustion and  
Combustion Profiles in a Cylindrical Combustion Chamber

by

Abbas Dadkhah-Nikoo

A THESIS

submitted to

Oregon State University

in partial fulfillment of  
the requirement for the  
degree of

Doctor of Philosophy

Completed May 2, 1991

Commencement June 1991

APPROVED:

*Redacted for Privacy*

Associate Professor of Mechanical Engineering in charge of  
major

*Redacted for Privacy*

Head of the Department of Mechanical Engineering

*Redacted for Privacy*

Dean of Graduate School

Date thesis presented May 2, 1991

Typed by B. McMechan for Abbas Dadkhah-Nikoo

© Copyright by Abbas Dadkhah-Nikoo  
May 2, 1991

All Rights Reserved

Dedicated To:

My first and best teachers,  
who sacrificed their dreams  
so that I could achieve mine;

My parents.

## ACKNOWLEDGEMENTS

A special thanks to my major advisor, Dr. Dwight J. Bushnell, for his help, encouragement and guidance. Throughout my graduate studies at Oregon State University, Dr. Bushnell has been a great teacher, a generous supporter and a wonderful friend to me. Without his help, my graduate program would have been impossible to complete.

I would also like to thank Dr. Gordon M. Reistad for his support and help over the past eleven years. Special gratitude is also extended to Dr. Richard Peterson for providing valuable advice on the design and improvement of the experimental facilities. I would like to express my appreciation to Dr. Charles K. Sollitt for his time and assistance.

I wish to thank my fellow graduate students, Charles Haluzack and Kerry Harmon, who provided indispensable assistance for this project.

Finally, to my wife Zahra Khaze and our sons, Neama and Navid: You have been extremely patient, understanding and supportive. Your love and support has given me strength when I needed it the most. I will be eternally grateful to you and hope to make up for the lost time.

## Table of Contents

<u>Chapter</u>		<u>Page</u>
1	INTRODUCTION.....	1
	1.1 Composition of Wood.....	3
	1.2 Combustion of Wood.....	4
	1.3 Combustion of Single Wood Particles.....	6
	1.4 Factors Affecting the Combustion of Wood.....	9
	1.4.1 Moisture Content .....	9
	1.4.2 Size of the Wood Particles .....	11
	1.4.3 Combustion Air Temperature .....	11
	1.4.4 Excess Air .....	12
	1.5 Combustion Profile.....	13
	1.6 Experimental Facilities.....	16
	1.7 Experiments.....	21
2	BURNING TIME OF WOOD PARTICLES IN A COMBUSTION CHAMBER.....	25
	2.1 Mathematical Modeling of Wood Combustion....	25
	2.1.1 Pyrolysis Time .....	27
	2.1.2 Char Combustion .....	34
	2.2 Experiments.....	41
	2.2.1 Radiation Heat Transfer from the Refractory Wall.....	42
	2.2.2 Radiation Heat Transfer from Adjacent Particles.....	44
	2.2.3 Radiation from Flame .....	45
	2.2.4 Heat Conduction to the Grate .....	46
	2.2.5 Additional Experiments .....	47
	2.2.5 Properties .....	48
	2.3 Results.....	49
	2.3.1 Effect of Moisture Content on Particle Burning Times.....	55
	2.3.2 Effect of Reynolds Numbers on Particle Burning Times.....	60
	2.3.3 Effect of Heat Flux on Particle Burning Times.....	62
	2.3.4 Effect of Size on Particle Burning Times.....	62
	2.3.5 Effect of Combustion Air Temperature on Particle Burning Times.....	65
	2.4. Conclusion.....	66



## Table of Contents (continued)

<u>Chapter</u>		<u>Page</u>
3	TEMPERATURE AND COMPOSITION PROFILES IN THE COMBUSTION CHAMBER.....	68
3.1	Combustion Profile.....	68
3.1.1	Temperature Profile .....	68
3.1.2	Composition Profile .....	72
3.2	Experiments.....	73
3.3	Experimental Results.....	74
3.3.1	Temperature Profile .....	74
3.3.2	Composition .....	83
3.3.2.1	NO <sub>x</sub> and CO Content.....	83
3.3.2.2	O <sub>2</sub> and CO <sub>2</sub> Profiles.....	91
3.4	Conclusion.....	91
4	PERFORMANCE OF THE COMBUSTION SYSTEM.....	95
4.1	Adiabatic Combustion Model, Experiments and Regression Analysis .....	96
4.1.1	Adiabatic Combustion Model .....	96
4.1.2	Experiments .....	98
4.1.3	Regression Model .....	100
4.2	Experimental Results.....	107
4.2.1	Part-Load Operation (Off-Design) ....	108
4.2.2	Moisture Content .....	114
4.2.3	Excess Air .....	119
4.2.4	Under-Fire Air .....	122
4.2.5	Fuel Particle Size .....	124
4.2.6	Under-Fire Air Temperature .....	127
4.3	Conclusions.....	131
5	CONCLUSION AND RECOMMENDATIONS.....	134
5.1	Conclusion.....	134
5.2	Recommendations.....	136
	REFERENCES.....	137
	Appendices.....	143
	A: COMPUTER PROGRAMS.....	143
	B: COMBUSTION PROFILES FOR EXPERIMENTS, CHAPTER 2.....	181
	C: EXPERIMENTAL CODE AND DATA.....	187

## List of Figures

<u>Figure</u>	<u>Page</u>
1.1 Stages of wood combustion .....	6
1.2 Schematic of the experimental facilities .....	17
1.3 Cutaway view of the combustion chamber .....	18
1.4 Components of the combustion chamber .....	19
2.1 Effect of moisture content on endothermicity and time of pyrolysis .....	33
2.2 Effect of particle size and ratio of $a/bR$ on pyrolysis time .....	34
2.3 Variation of $\tau$ as a function of $\delta$ for different Reynolds number values .....	39
2.4 Variation of $\tau$ as a function of $\delta$ for different Reynolds number values .....	39
2.5 Comparison of the results obtained from equations (2.37) and (2.39), calculating $\tau$ as a function of $\delta$ for different Reynolds numbers .....	40
2.6 Comparisons of model predictions for pyrolysis times of red oak and sugar pine to experimental data .....	53
2.7 Comparison of model predictions of char combustion times for red oak and sugar pine and experimental data .....	54
2.8 Comparison of model predictions of total combustion times for Douglas-Fir, red oak and sugar pine and experimental data for red oak and sugar pine .....	56
2.9 Comparison of model predictions and experimental data for pyrolysis and total combustion times of red oak cubes as a function of moisture content .....	57

## List of Figures (continued)

<u>Figure</u>		<u>Page</u>
2.10	Comparison of model predictions and experimental data for total combustion times as a function of moisture content, Douglas-fir .....	58
2.11	Comparison of model predictions of pyrolysis and total combustion times as a function of moisture content, sugar pine, and experimental data .....	59
2.12	Comparison of model predictions of pyrolysis and total combustion times for red oak as a function of Reynolds numbers and experimental data .....	61
2.13	Comparison of model predictions of pyrolysis and total combustion times as a function of Reynolds numbers for 1 cm sugar pine and experimental data .....	62
2.14	Comparison of model predictions of pyrolysis and total combustion times for red oak as a function of heat flux and experimental data .....	63
2.15	Comparison of model predictions of pyrolysis and total combustion times for sugar pine as a function of heat flux and experimental data .....	63
2.16	Comparison of model predictions of total combustion times for Douglas-fir as a function of heat flux and experimental data .....	64
2.17	Comparison of model predictions for pyrolysis and total combustion times as function of particle size for sugar pine and experimental data .....	65
3.1	Temperature profile for experiment A .....	76
3.2	Temperature profile for experiment B .....	77
3.3	Temperature profile for experiment C .....	78
3.4	Temperature profile for experiment F .....	79

## List of Figures (continued)

<u>Figure</u>	<u>Page</u>
3.5 Temperature profile for experiment D .....	80
3.6 Temperature profile for experiment L .....	80
3.7 Temperature profile for experiment O .....	81
3.8 Temperature profile for experiment P .....	82
3.9 Temperature profile for experiment Q .....	82
3.10 NO <sub>x</sub> profile for experiment A .....	85
3.11 NO <sub>x</sub> profile for experiment C .....	85
3.12 NO <sub>x</sub> profile for experiment H .....	86
3.13 NO <sub>x</sub> profile for experiment K .....	86
3.14 NO <sub>x</sub> profile for experiment O .....	88
3.15 NO <sub>x</sub> profile for experiment P .....	88
3.16 NO <sub>x</sub> profile for experiment Q .....	89
3.17 CO profile for experiment A .....	89
3.18 CO profile for experiment H .....	90
3.19 CO profile for experiment Q .....	90
3.20 O <sub>2</sub> and CO <sub>2</sub> profiles for experiment A .....	92
3.21 O <sub>2</sub> and CO <sub>2</sub> profiles for experiment B .....	92
3.22 O <sub>2</sub> and CO <sub>2</sub> profiles for experiment K .....	93
4.1 Comparison of the results for the adiabatic model, the experiments, and regression models for combustion temperatures .....	106

## List of Figures (continued)

<u>Figure</u>	<u>Page</u>
4.2 Comparison of the results for the adiabatic model, the experiments, and regression models oxygen content of combustion products .....	107
4.3 Combustion temperature vs. fuel feed rate .....	109
4.4 Oxygen and carbon dioxide content of combustion products vs. fuel feed rate .....	110
4.5 CO and NO <sub>x</sub> content of the combustion products as a function of fuel feed rate .....	110
4.6 Particulate emissions and combustibles in the particulate as a function of fuel feed rate ....	112
4.7 Efficiencies vs. fuel feed rate .....	113
4.8 Combustion temperature as a function of fuel moisture content .....	115
4.9 Combustion products oxygen and carbon dioxide content as a function of fuel moisture content .....	115
4.10 Combustion products CO and NO <sub>x</sub> content as a function of fuel moisture content .....	116
4.11 Particulate and combustibles in particulate as a function of fuel moisture content .....	117
4.12 Efficiencies as a function of fuel moisture content .....	118
4.13 Combustion temperature and heat loss as a function of fuel moisture content .....	118
4.14 Combustion temperature as a function of excess air .....	120
4.15 Temperature, CO, and NO <sub>x</sub> content of combustion products as a function of excess air .....	120
4.16 Particulate emissions and combustibles in particulate as a function of excess air .....	121

## List of Figures (continued)

<u>Figure</u>	<u>Page</u>
4.17 Efficiencies as a function of excess air .....	122
4.18 Combustion temperature and heat loss as a function of under-fire air .....	123
4.19 Efficiency as a function of under-fire air .....	124
4.20 Temperature, CO and NO <sub>x</sub> content of combustion products as a function of particle size .....	125
4.21 Particulate emissions and combustibles in particulate as a function of particle size .....	126
4.22 Efficiency and heat loss as a function of particle size .....	127
4.23 Heat loss and combustion temperature as functions of under-fire temperature .....	128
4.24 Particulate emissions and combustibles in particulate as functions of under-fire air temperature .....	129
4.25 Efficiencies as functions of under-fire air temperature .....	130

## List of Tables

<u>Table</u>	<u>Page</u>
1.1 Analysis of the experimental fuels .....	22
2.1 Experimental conditions, results and model predictions for Douglas-Fir and wood pellets ..	50
2.2A Experimental conditions and calculated heat transfers for red oak and sugar pine .....	51
2.2B Experimental and calculated results for red oak and sugar pine .....	52
3.1 Experimental test conditions .....	74
4.1 Experimental settings for the experiments and independent variables for regression analysis .....	99
4.2A Experimental results .....	101
4.2B Experimental results (continued) .....	102
4.3 Adiabatic model results for the experimental settings .....	103
4.4 Table of regression coefficients .....	104

# Experimental Investigation of Wood Combustion and Combustion Profiles in a Cylindrical Combustion Chamber

## CHAPTER 1

### INTRODUCTION

During the past two decades fossil fuel availability and cost as well as concerns for protection of the environment have motivated new efforts in the search for renewable, clean, affordable, and reliable sources of energy. Biomass fuels, particularly wood and wood waste fuels, present an attractive choice for energy production. In 1983, biomass resources supplied 2.8 quads ( $2.8 \times 10^{15}$  btu) of energy per year, representing 3.7 percent of annual energy consumption in the United States. By the year 2000, biomass resources can provide from 6 to 16.6 quads (i.e., 5 to 15 percent) of the annual energy consumption in the United States [SERI 1983].

Today, concern for the safety and protection of the environment is a decisive factor in the selection, design, and operation of the energy conversion systems. Primary pollutants generated during the combustion process include nitrogen oxides, carbon monoxide, carbon dioxide, sulfur compounds, and particulate emissions.



Fossil fuel combustion and harvesting of the forests are principal contributors to the green house effect (caused by an increase in carbon dioxide in the earth's atmosphere). Biomass fuel combustion seems to play only a minor role in increasing the levels of carbon dioxide in the earth's atmosphere. In fact, a balance between harvesting, combustion, and the recultivation of biomass would not contribute significantly to the increase of carbon dioxide on a global basis [Klass 1980]. Nitrogen oxides and sulfur compounds are other forms of pollutants resulting from the combustion of fossil fuels. In comparison to fossil fuels, biomass fuels contain considerably lower amounts of nitrogen or sulfur. Therefore, combustion of the biomass fuels does not generate high levels of nitrogen oxides or sulfur compounds.

In comparison to fossil fuels, biomass fuels pose several limitations. Biomass fuels have lower energy content per unit volume and can absorb higher levels of moisture. Wide variations in composition and lack of standards are other disadvantages of biomass fuels. Compared to natural gas and oil, biomass fuels have higher levels of ash. However, compared to coal the ash content of biomass fuels is considerably lower.

Despite the length of time that wood has been used as a source of fuel, our knowledge is far from complete in understanding the process of wood combustion. The current study presents an experimental investigation of the influ-

ence of some of the variables involved in the combustion of wood.

This investigation is presented in four chapters. In addition to this brief introduction, a review of the literature related to the combustion of wood is presented in Chapter 1. Descriptions of the experimental facilities and the experiments performed for the current study are also given in this chapter. Chapter 2 is concerned with the burning time of wood particles in a combustion chamber. Chapter 3 describes the temperature and composition profiles of the gaseous combustion products in the chamber. Finally, in Chapter 4 the overall performance of the combustion process and the combustion unit is examined.

### 1.1 Composition of Wood

The major components of dry wood are cellulose, hemicellulose and lignin. The minor (extraneous) components of wood are resins, mineral matters, and nitrogenous organic compounds with traces of organic acids [Benson 1932]. On a dry basis, wood contains about 7 percent extractives and mineral compound or ash. Extracted hardwoods contain about 43 percent cellulose, 35 percent hemicellulose, and 22 percent lignin. Softwoods contain approximately 43 percent cellulose, 28 percent hemicellulose and 29 percent lignin [Shafizadeh 1977]. According to Siau [1971], the woody cell wall contains approximately 50 percent cellulose, 20

to 35 percent hemicellulose, 15 to 25 percent lignin, and extractives and mineral compounds in a range from 0 to 25 percent.

Cellulose is the principal constituent of the cell wall. It is the main source of the mechanical and hydroscopic properties of wood [Siau 1971]. The cellulose component, which is macro-molecular, is the same in all types of wood, with the exception of the degree of polymerization. Cellulose has been shown to have an empirical formula, which is somewhat akin to  $(C_6H_{10}O_5)_n$ , with a molecular weight of about  $10^6$  [Kanury et al. 1970b].

Hemicelluloses in the cell wall have a similar composition to cellulose, but have different molecular configurations. They are low molecular weight polysaccharides. The hemicelluloses are amorphous and have a lower degree of polymerization [Siau 1971].

Lignin is a randomly linked amorphous polymer, consisting of Phenyl-propane units. Lignin has a lower molecular weight than cellulose (i.e., about 1000). The elementary composition of lignin is  $C_{47}H_{52}O_{16}$  [Kanury et al. 1970b].

## 1.2 Combustion of Wood

Upon exposure to heat flux, wood particles do not burn directly [Browne 1958]. Combustion of wood takes place in three stages. The first stage involves the drying or evap-

oration of moisture in the wood. This is an endothermic process which requires the supply of heat to the particles. The energy required in this process has been discussed in detail by Dadkhah-Nikoo [1987; 1985].

Since the ignition temperature of dry wood is higher than its charring temperature [Wise et al. 1952], wood undergoes thermal degradation or pyrolysis under the influence of a sufficiently strong source of energy. Pyrolysis is "an endothermic irreversible chemical degradation of wood in which virgin wood is transformed into char and combustible vapors" [Kanury 1972]. The amount, rate and composition of pyrolysis products depends upon the imposed temperature and pressure, exposure time, the geometry of the particle and the environment under which pyrolysis takes place as well as the chemical and physical properties of the wood [Browne 1958; Kanury 1974]. When Combustible pyrolysis products are driven off they can react with oxygen and burn in the gas phase with flaming combustion. This reaction generates heat for further drying and pyrolysis of the fuel.

The residue remaining after pyrolysis is a highly reactive carbonaceous char. Oxidation of char in the solid phase results in glowing combustion that has a slower rate of burning than flaming combustion. If the intensity of the heat flux or the oxygen supply fall below a minimum level, smoldering combustion takes place. In smoldering combustion unoxidized volatile products and aerosol parti-

cles are emitted as smoke. During the combustion process the cellulosic component is mainly converted to volatile products, while lignin is mainly converted to char [Shafizadeh 1977].

The three successive or overlapping processes of wood combustion are controlled partly by the chemical and physical properties of the wood and partly by the prevailing conditions of heat and mass transfer imposed on the wood particles. A simplified version of wood combustion process is shown in Figure 1.1.

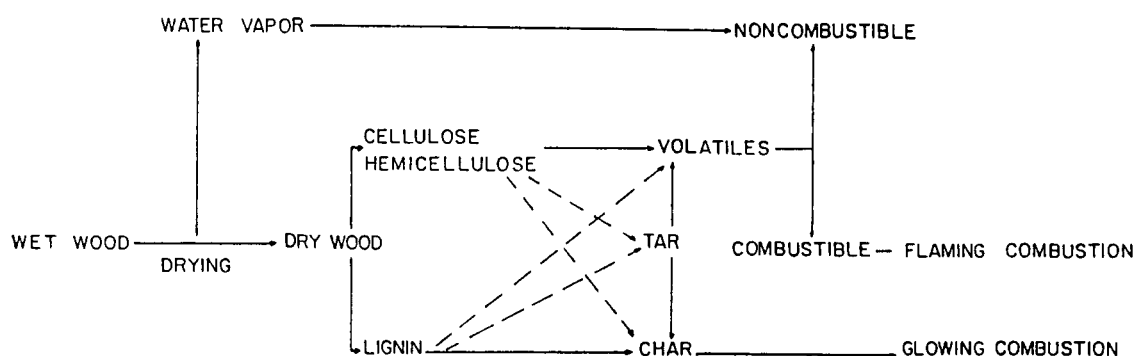


Figure 1.1 Stages of wood combustion.

### 1.3 Combustion of Single Wood Particles

When a wood particle is exposed to intense heat flux, a temperature gradient develops between the surface of the particle and its interior. Noting that the thermal conductivity of the wood is anisotropic [Siau 1971], the rate of heat transfer is therefore not isotropic in the particle. In an inert environment, the increase in the temperature of

the wood particle up to 400°F results in vaporization of free and bond water with traces of carbon dioxide, formic acid and acetic acid and glyoxal [Browne 1985]. Part of the vapors formed during this phase reaches the surface of the particle through the pores. The other portion of the vapors is convected back into the particle and condenses upon reaching the cooler interior [Kanury et al. 1970a]. This endothermic process continues until this zone is dehydrated. As the zone moves farther into the particle, the temperature in the zone it approaches continues to rise. Drying of the wood is a separate category of research in itself and is not considered in detail in the current study [Malte et al. 1983-84; Kamke 1984; Mujumdar et al. 1980; 1983; 1984; 1987; 1990; Simpson 1983-84].

Between 400 and 540°F additional vapors form, largely including noncombustible gases, but also some amount of carbon monoxide. This is also an endothermic process. Between 540 and 930°F active pyrolysis begins. At this stage combustible gases, including carbon monoxide, methane, formaldehyde, formic and acetic acids, methanol and hydrogen as well as some noncombustible gases, such as carbon dioxide and water vapor, are released. The gases escaping the particle at this stage also carry droplets of tars that appear as smoke. The products of pyrolysis also undergo secondary reactions with one another before reaching the surface of the particle. This stage of pyrolysis is an exothermic process [Martin et al. 1980]. At tempera-

tures above 930°F, carbonization of char becomes more complete. When the particle temperature reaches 1830°F and beyond, carbon is consumed at the surface with a yellowish-red glowing combustion [Browne 1985].

According to Browne [1958], hemicellulose is pyrolyzed first at temperatures between 390 and 500°F. Cellulose is then pyrolyzed at 460 to 660°F, followed by lignin at 530 to 930°F. Depending on the conditions of heat and mass transfer imposed on the particle as well as the size and properties of the particle, the processes described above could take place simultaneously or consecutively.

The pyrolysis rate of wood in general may be described as an Arrhenius type of decomposition reaction [Kung 1972; Wichman et al. 1987; Gullett et al. 1987; Kailasanath et al. 1981]. A review of kinetic data for pyrolysis of wood is given by Roberts [1970].

The energy equation describing the pyrolysis of wood is usually described by an unsteady state equation provided by an Arrhenius source term. However, it has been shown that though this is valid in certain zones of space and time, there exist other zones in which the secondary physicochemical effects of energy and mass transfer become dominant in the determination of pyrolysis rate [Kanury 1970a]. The influence of internal convection on the pyrolysis rate has been examined by several researchers, including Kanury [1970b], Kansa et al. [1977] and Dosanjh et al. [1987].

A similar approach is applicable to the case of char combustion [Daw et al. 1988; Walker 1982; Satyendra 1982].

#### 1.4 Factors Affecting the Combustion of Wood

Performance of the wood-fired combustion units and boilers depends upon the design and operating conditions of the combustion system as well as fuel preparation and properties. Some of these factors include fuel moisture content, fuel particle size, excess air used for combustion, temperature of the combustion air, and fraction of the under-fire air. This section provides a qualitative discussion of the impact of some of these factors on performance of wood combustion.

##### 1.4.1 Moisture Content

Moisture content of the biomass fuels may vary from 2 to 75 percent (wet basis) [Junge et al. 1980; Howlett et al. 1977]. This variation depends on wood species, storage, handling, site, and the season of the year. Moisture content of the fuel affects the combustion process in a variety of ways. Variation in fuel moisture content alters the net heating value of the fuel, rate of combustion of the fuel, flame temperature, volume and velocity of the combustion products in the combustion chamber.

Evaporation of moisture in wet wood is an endothermic process that requires approximately 1000 btus of energy per pound of water. This energy requirement reduces the net



heating value of the fuel [Dadkhah-Nikoo 1985]. It has been shown that for fuels with moisture contents higher than 68 percent (wet basis), furnace blackout occurs [Drucker 1984]. Therefore, for wood-fired boilers it is necessary to use supplementary fuels to sustain the combustion.

Since the net heating value of the wood fuel decreases in proportion to increased moisture content, the flame temperature reduces accordingly. Reduction of the adiabatic flame temperature due to increased wood moisture content has been studied by Tillman and Anderson [1983] for some wood species. The effect of moisture content on the combustion temperature of Douglas-fir is discussed by Dadkhah-Nikoo [1985]. The burning rate of wood particles decreases as the moisture content of the fuel increases [Simmons 1983; Junge 1975]. Therefore, the burning time of the wood fuel increases accordingly.

As a result of vaporization, the volume of the moisture content of the fuel increases by a factor of 5700. This increase in volume and a consequent increase in the velocity of the combustion gases, with the slower rate of burning and lower flame temperature, increases the emissions of unburned particulate and reduces the efficiency of wood-fired boilers [Johnson 1975].

#### 1.4.2 Size of the Wood Particles

Similar to moisture content, the size of wood fuel particles offers a wide range of variation [Junge 1980]. Wood fuel particles used in typical wood-fired boilers vary from  $8 \times 10^{-5}$  to 4 inches; this is a ratio of  $5 \times 10^4$ .

Smaller particles have a larger surface to mass ratio than larger particles. This results in a higher rate of heat transfer to the smaller particles and therefore a faster rate of combustion than for the larger particles. Experiments conducted by Simmons [1983] illustrate the influence of particle size on the reactivity and combustion time of sugar pine and red oak samples. For example, these experiments showed that increasing the size of a pine cube from 0.2 inches to 1 inch increases the burning time of the particle from 30 seconds to 400 seconds.

Wood combustion systems are designed for a limited range of fuel particle sizes [Dadkhah-Nikoo 1985]. The use of fuels containing particles with sizes outside the specified range of a particular system reduces system efficiency. The decrease in efficiency is due to an increase in emissions of the amount of unburned fuel. The combined effects of moisture content and particle size on wood-fired boilers are discussed by Junge [1975].

#### 1.4.3 Combustion Air Temperature

Increasing the combustion air temperature has been shown to improve the performance of a combustion system. Junge [1975], recommended that the highest possible temper-

ature be used in hogged-fuel boilers. For oil- and gas-fired boilers, increasing the combustion air temperature increases the boiler efficiency [KBV, Inc. 1980]. The experiments of Simmons [1983], showed that increasing the combustion air temperature reduces the combustion time of single wood particles. The combustion of wood char at high temperatures is a diffusionally controlled process [Browne 1958]. For diffusionally controlled regimes, the combustion rate of carbon particles is inversely proportional to the combustion air temperature [Kanury 1977]. Simmons' [1983] experiments seem to demonstrate this point for wood combustion as well.

#### 1.4.4 Excess Air

To promote the complete combustion of the fuel, air in excess of the stoichiometric requirement is supplied to combustion systems. For wood-fired boilers, the amount of excess air is dependent upon the design of the particular system and the conditions of the fuel. Use of excess air above the optimum amount required for combustion increases particulate emissions and reduces boiler efficiency, flame temperature, and combustion rate.

Besides the amount of excess air, the ratio of under-fire air and the location of over-fire air are also important factors in combustion processes. Junge [1979] examined the optimum amount of excess air and fractions of under-fire air for hogged-fuel boilers. Similar studies by

Haluzak [1989] have identified the optimum operating conditions for the combustion of wood-pellets.

Other factors affecting the wood combustion process include the fuel bed thickness for systems using grates [Tuttle 1977] and the physical and chemical properties of wood.

### 1.5 Combustion Profile

To improve the combustion or gasification process of wood and coal, knowledge of fuel bed composition and temperature profiles is essential. For combustion systems using a grate, this profile can be divided into two parts: first, the combustion profile on the grate or in the fuel bed, and second, the combustion profile in the space above the fuel bed.

The combustion of coal [Britten 1986] or wood [Tuttle 1977] on the grate is dependent upon the amount of under-fire air supplied through the grate. A qualitative description of the combustion profile on the grate, based on the assumption that the fuel is fed from the top and that the under-fire air is less than the stoichiometric requirement for complete combustion of the fuel, is given here.

When the wet fuel particles are delivered to the combustion chamber they form a layer on top of the fuel bed. As high temperature combustion gases pass through this layer the moisture is removed while dry fuel travels down

toward the grate. This is also the preheating zone in which the fuel temperature is raised as the fuel moves down. In the next layer, dry fuel, upon exposure to high temperature combustion gases, undergoes volatilization. In this zone most of the fuel volatile matters are released. The upward movement of the gases through the bed continues until the free surface of the bed is reached. Above the fuel bed, over-fire air is supplied to complete the combustion of the gases that is released in the fuel bed. The low volatile content fuel travels down until it reaches the reduction zone. In this zone, due to lack of oxygen, the primary product of combustion is CO. The next stage is the oxidation zone, in which the char reacts with the oxygen that is supplied for this stage. The main product of char combustion in this zone is carbon dioxide. Finally, when the char is completely consumed, it forms the ash layer that rests on the grate.

The composition of the gas in the layers noted above can be described as follows. In the ash layer, the gas composition is the same as under-fire air. In the oxidation zone, oxygen is rapidly consumed while the carbon dioxide concentration increases until the reduction zone is reached. At this point the oxygen concentration is at its minimum and carbon dioxide is at its maximum concentration. Through the reduction zone, the carbon dioxide concentration decreases while the carbon monoxide concentration increases. This trend continues until the gases reach the

volatilization zone, in which the products of pyrolysis are added to the gases flowing through the bed. In the drying zone, water vapor is added to the gas stream. The gases finally escape the bed when they reach the over-fire air and flaming combustion in the gas phase begins.

The temperature in the fuel bed starts from a low temperature on the grate that is very close to that of under-fire air. The air temperature increases slightly as it passes through the ash layer, which is in the process of being cooled. The bed temperature increases rapidly in the char combustion zone (oxidation zone) and reaches its maximum. The maximum temperature and the  $\text{CO}_2$  concentration are reached at the same location [Barriga et al. 1980]. The temperature of the bed decreases continuously from the start of the reduction zone up to the top of the bed.

The profile described above for the fuel bed is similar to the profile found in a coal gasification process [Barriga et al. 1980; Eapen et al. 1976; Winslow 1976]. In actual fuel beds found in most wood-fired boilers, the zones and profiles are not so well-defined.

In the gas phase above the grate, the composition and temperature profiles are dependent upon the amount and location of the over-fire air. The method of introducing the over-fire air, which affects the flow and mixing of the gases, also influences the profile. The temperature profile is also affected by heat loss through the combustion chamber wall. The temperature and composition profile of

the combustion products in the gas phase is discussed in detail in Chapter 3.

## 1.6 Experimental Facilities

The experimental facility used for the current study consists of a combustion chamber, an air delivery and pre-heat system, a fuel delivery system, an exhaust system, and a data acquisition and control system. Figure 1.2 is a schematic illustration of the overall experimental facility.

Figure 1.3 shows a cutaway view of the combustion chamber. The combustion chamber has an ash pit, an under-fire air port, a grate, a ceramic refractory, an over-fire tube, a stainless steel casing, a fuel feed tube, an auger, an exhaust port, and a cooling water tube. The components of the combustion chamber are illustrated in Figure 1.4.

The outer shell of the combustion chamber is made of schedule 20, 304 stainless steel tube with a nominal diameter of 12 inches. A high temperature ceramic refractory is used to protect the outer shell and promote thermal stability in the chamber. The combustion chamber inside diameter is 6.5 inches. The height of the combustion chamber is 36 inches.

Fuel is delivered from the hopper through a metering drum and the auger to the combustion chamber. A compressor

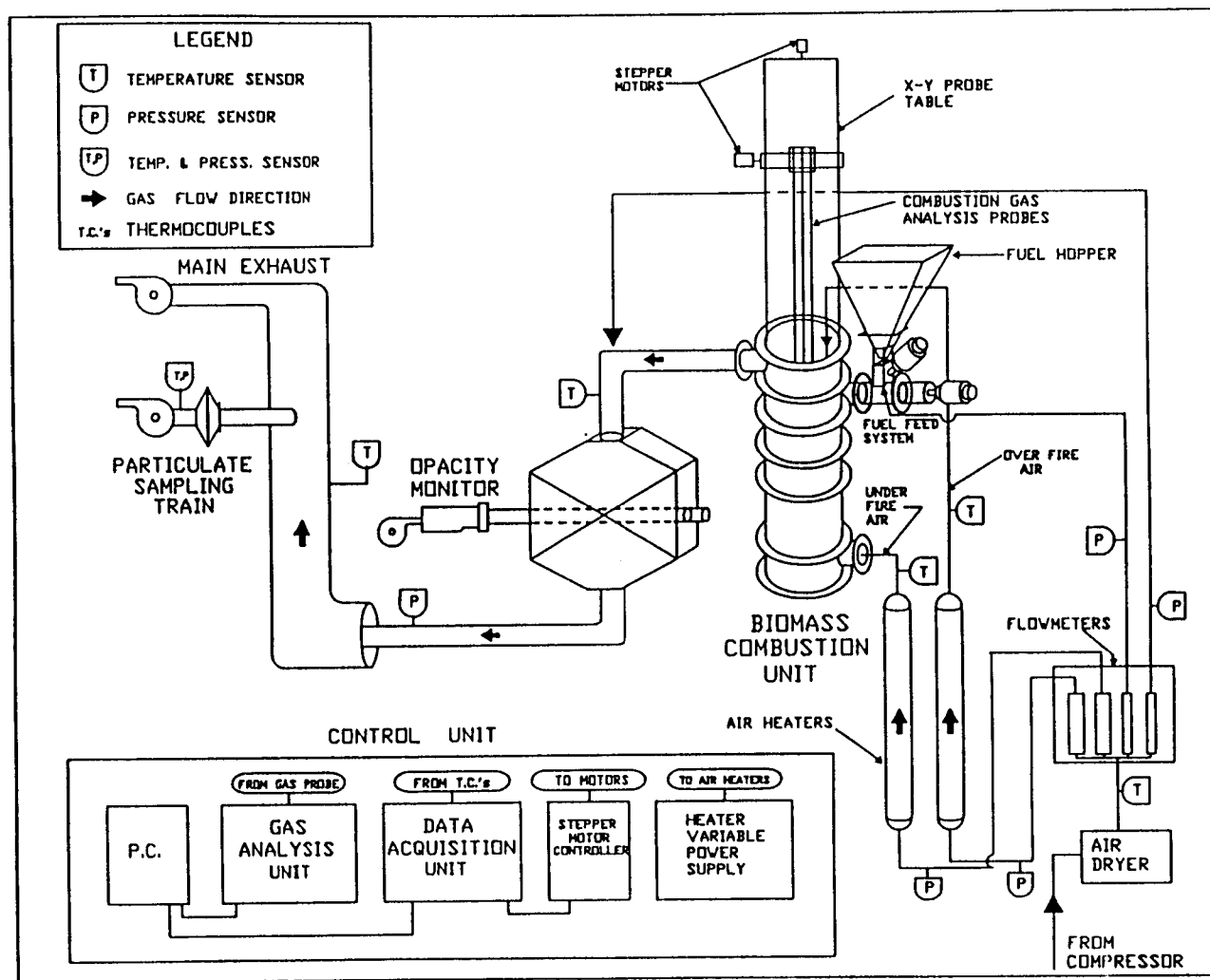


Figure 1.2 Schematic of the experimental facilities.



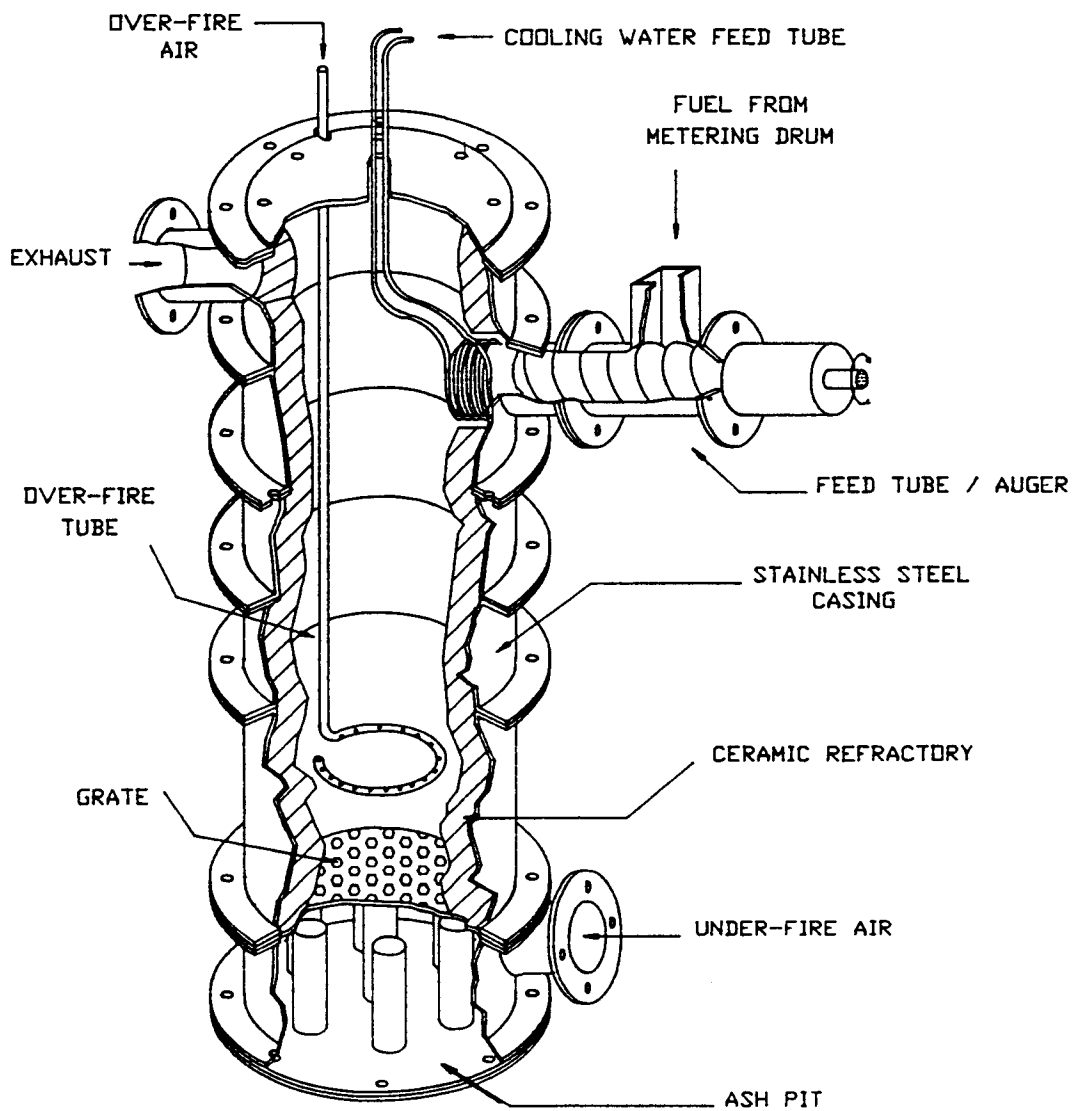


Figure 1.3 Cutaway view of the combustion chamber.

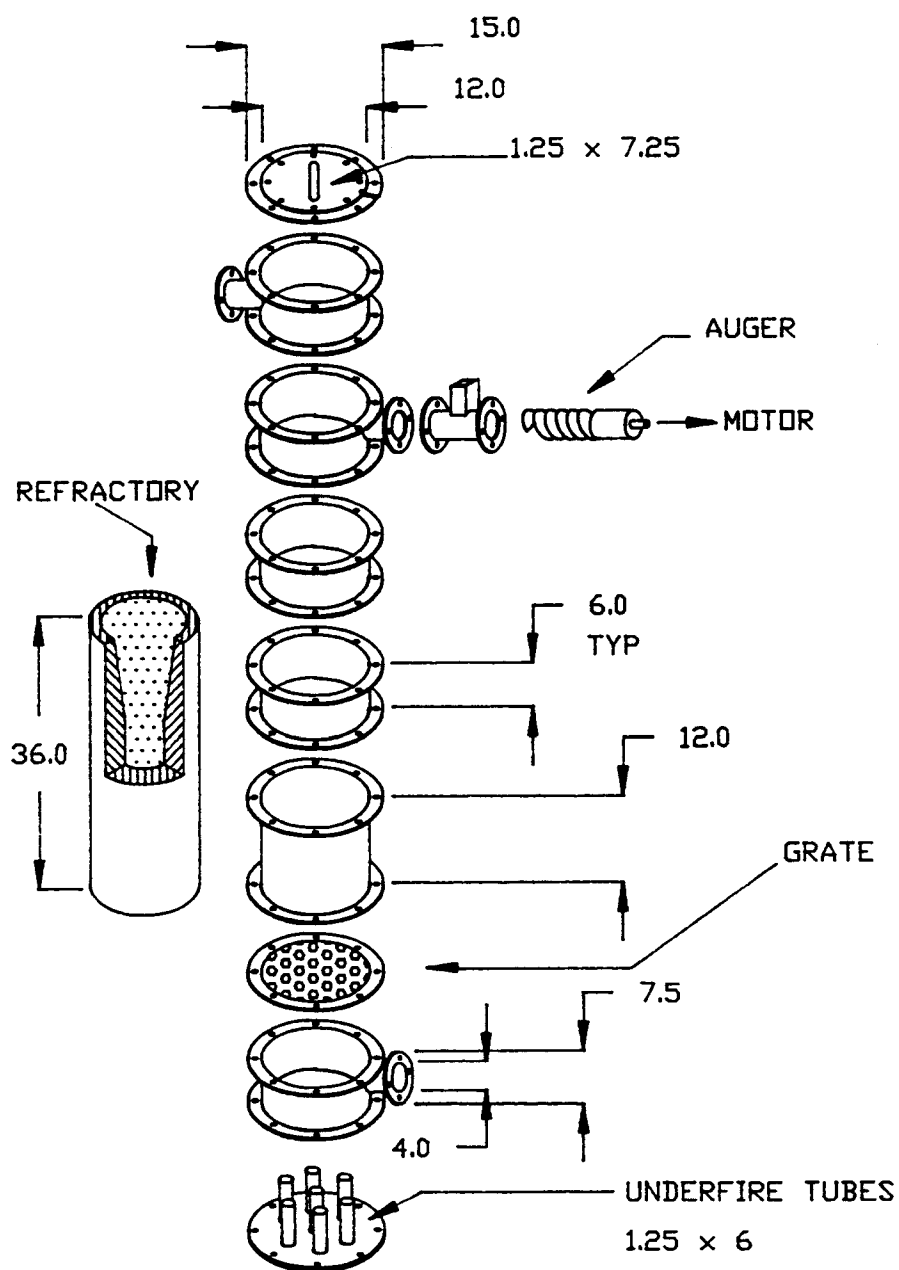


Figure 1.4 Components of the combustion chamber.

supplies the combustion air that passes through an air-drier to remove moisture. Four flow meters divide and measure the supplied air into under-fire, over-fire, dilution, and cooling air streams. To gain higher temperatures (when desired), under-fire and over-fire air pass through separate air heaters. The products of combustion exit the combustion chamber through the exhaust port. Dilution air is added to the exhaust stream to protect the visible emission monitoring system (opacity meter). Cooling water is provided to prevent the premature combustion of the fuel in the auger tube.

A computer driven X-Y probe-positioning table is mounted on top of the combustion chamber. The table holds three probes, one for gas sampling and two for temperature measurement. The gas sampling probe is placed at the center of the combustion chamber. The temperature probes are located on the sides of the gas probe. All three probes are at the same distance from the grate. Two computer-controlled stepper motors are used to position the probes in the combustion chamber. This arrangement allows for very accurate positioning (i.e.,  $\pm 0.0005$  inches) and movement of the probes in the combustion chamber.

Particulate samples are collected on fiber-glass filters using a High Volume Sampler. Type K thermocouples are used for the temperature measurement of under-fire and over-fire air, combustion products, exhaust, and the outside wall of the combustion chamber.

Combustion gas samples are drawn through the gas probe by an Enerac-2000 combustion gas analyzer. A Keithly-500 data acquisition unit and a microcomputer are used to record the data and control the probe positioning. Additional testing and measurement equipment used for the current study and more detailed descriptions of the combustion system have been described by Dadkhah-Nikoo et al. [1988], Haluzak [1989] and Bushnell et al. [1989].

### 1.7 Experiments

There are wide variations in the moisture content, composition, size distribution, and heating values of biomass fuels. Different combustion systems have been designed to accommodate these variations. These systems have different operating conditions and require different levels of fuel preparation and handling [Dadkhah-Nikoo 1985]. To examine the influence of some of the variables affecting the combustion of wood, several experiments were designed and performed. The main fuel for these experiments was Douglas-fir wood in the shape of cubes. In addition, three wood pellet fuels were also used and are denoted by PHC, KMP, and BCCP. PHC is a mixture of the bark and wood of Hemlock fir. KMP is a mixture of wood and bark from red alder and maple. BCCP is wood from the Ponderosa pine. The proximate and ultimate analyses, higher heating values,

and ash fusion temperatures of these fuels are given in Table 1.1.

Table 1.1 Analysis of the experimental fuels.

Ultimate Analysis (% dry basis)				
	Douglas-Fir	BCCP	PHC	KMP
Carbon	51.3	51.20	51.16	50.35
Hydrogen	6.31	6.35	6.09	5.92
Nitrogen	0.048	0.25	0.1	0.27
Sulfur	0.004	0.01	0.01	0.03
Chlorine	0.0	0.01	0.003	0.00
Ash	0.05	0.22	0.96	1.15
Oxygen (by diff.)	42.29	41.97	41.68	42.29
Proximate Analysis (% dry basis)				
Fixed carbon	14.26	16.63	21.06	19.25
Volatile matter	85.69	83.15	77.98	79.6
Ash	0.05	0.22	0.96	1.15
Ash Fusion Temperature (deg. F)				
Initial	2450	2450	2500	2220
Fluid	2480	2510	2550	2240
Higher Heating Value (btu/lb, dry)				
	8775	8968	8787	8688

Experiments were carried out after the system reached a steady-state operating condition. To reach steady-state, a 2.5 hour warm-up period preceded each experiment. Once the experiment was started, the probes moved inside the combustion chamber down toward the grate. Temperature and composition data collection from the thermocouples and gas probe were initiated when the probes were located 24 inches above the grate. From this point to 10 inches above the grate, data was collected at 2-inch intervals. From 10 to 4 inches above the grate, data was collected at 1-inch intervals. From 4 inches to 1 inch above the grate, the data collection interval was 0.5 inches. At each point a wait-

ing period proceeded the data collection to allow for the transient effect of the thermocouples and the combustion gas analysis unit. At each data point, 15 combustion gas samples were analyzed and recorded. Three temperature readings from each thermocouple were recorded.

Particulate samples were collected over a period of 15 minutes. Filters were weighed before and after sampling to determine the amount of particulate. To find the fraction of the combustible in the particulate samples, filters were placed in an oven for three hours at a temperature of 1,000°F. The differences in the weight of the filters before and after placement in the oven represented the quantity of the combustible in the particulate sample.

To determine the location of the over-fire air tube for optimum operation, a series of tests were carried out, using commercial wood pellets as the fuel. The optimum operating condition was determined based on minimizing opacity and particulate emissions and maximizing combustion temperature and efficiency. The results indicated that the optimum location for the over-fire tube was 4 inches above the grate. If the over-fire tube was placed below the optimum location, the over-fire air flow disturbed the particles on the grate and significantly increased emissions of the unburned particulate, which in turn decreased combustion efficiency. If the over-fire tube was above the optimum location, residence time of the pyrolysis products was reduced, as indicated by high opacity readings. High opac-

ity readings were an indication of incomplete combustion of the pyrolysis products and was accompanied by low combustion efficiency.

The statistical validity of the data collection methodology has been determined by Haluzak [1989] and is not considered in detail in the current study.

## CHAPTER 2

### BURNING TIME OF WOOD PARTICLES IN A COMBUSTION CHAMBER

This chapter presents a mathematical model for predicting the burning time of wood particles in a combustion chamber. Wood particles in a combustion chamber experience thermal radiation from high temperature chamber walls and adjacent burning particles. Flames, resulting from combustion of pyrolysis products, provide further thermal radiation to the particles. Wood particles on the grate are subjected to heat transfer from the grate. Heat is also convected from the surrounding combustion air and other gaseous combustion products to the particles.

#### 2.1 Mathematical Modeling of Wood Combustion

Three approaches are used for the mathematical modeling of wood combustion. The first technique is based upon the first law of thermodynamics. This technique treats the combustion chamber (wood particles and their surroundings) as a black box with fuel and air entering the chamber and combustion products exiting [Dadkhah-Nikoo 1987; Bauer 1984; Junge 1980]. This approach is suitable when the fi-



nal temperature and major constituents of the combustion products are required.

The second approach is based upon the first and second laws of thermodynamics. In this method, the composition and temperature of combustion products are determined from application of the principle of chemical equilibrium. This method requires solution of a series of non-linear equations which relate the mole fraction, pressure and equilibrium constants of the species present in combustion products and the energy balance equation [Tillman et al. 1983]. These first two methods are discussed in Chapters 3 and 4.

The third method involves the kinetics of pyrolysis and char combustion. As noted in Chapter 1, wood pyrolysis can be described by an Arrhenius type of decomposition reaction. In the current study, a different method for the prediction of pyrolysis time is used, leading to a closed form solution. Although several assumptions are made to derive the governing equations, the results of this model are in good agreement with previously conducted experimental investigations. This model was first proposed by Kanury [1973] for wood pyrolysis, who provided the governing equations for three geometries (sphere, slab and cylinder). In the current study, the case of the sphere is used for wood particles shaped as cubes and pellets.

After the completion of pyrolysis, the remaining char reacts with the surrounding air. As noted in Chapter 1,

the combustion of char at high temperatures is controlled by the diffusion of oxygen to the surface of the char. The model used to estimate the char combustion time is based on the pseudo steady-state burning of coal particles [Kanury 1977; Welty et al. 1976].

### 2.1.1 Pyrolysis Time

Consider a spherical wood particle of radius  $R$ , with its center at  $r = 0$ , exposed to a constant uniform heat flux  $\dot{q}''$  at the surface ( $r = R$ ). Assuming uniform properties and neglecting the internal convection, moisture migration effects, heterogeneous reaction in the char and fissure formation, the energy conservation equation is given by

$$\frac{K}{r^2} \frac{\partial}{\partial r} \left( r^2 \frac{\partial T}{\partial r} \right) = \rho c \frac{\partial T}{\partial t} + L_p \left( - \frac{\partial \rho}{\partial t} \right) . \quad (2.1)$$

In this equation  $K$ ,  $\rho$ ,  $c$  and  $L_p$  are, respectively, thermal conductivity, density, specific heat and endothermicity of pyrolysis. The temperature of the particle at time  $t$  and location  $r$  is denoted by  $T$ . Pyrolysis rate is given by a kinetic equation in the form of

$$- \frac{\partial \rho}{\partial t} = F(\rho, T) \quad (2.2)$$

with the initial and boundary conditions

$$t < 0 , T = T_0 , \rho = \rho_0 , \quad (2.3)$$

$$r = 0 , \frac{\partial T}{\partial r} = 0 , \quad (2.4)$$

and

$$r = R, \quad K \frac{\partial T}{\partial r} = \dot{q}'' . \quad (2.5)$$

Integrating equation (2.1) with respect to  $r$ , and applying the boundary conditions (2.4) and (2.5) gives

$$\dot{q}'' R^2 = \int_0^R \rho c \frac{\partial T}{\partial t} r^2 \partial r + \int_0^R L_p \left[ - \frac{\partial \rho}{\partial t} \right] r^2 \partial r . \quad (2.6)$$

Equation (2.2) can then be written as

$$\dot{m}'' R^2 = \int_0^R - \left[ \frac{\partial \rho}{\partial t} \right] r^2 \partial r , \quad (2.7)$$

where  $\dot{m}''$  is the outward mass flux of the pyrolysis vapors at the exposed surface.

Assuming a first-order Arrhenius-type rate law for wood pyrolysis requires a numerical solution for equations (2.1) and (2.2). Here, an alternative kinetic hypothesis is chosen such that a solution in closed form for pyrolysis time is obtained. Suppose that upon attaining a characteristics temperature  $T_p$ , pyrolysis of the solid begins at a measurable speed ( $V$ ), and upon reaching a higher characteristic temperature  $T_c$ , pyrolysis is complete and only charred solid remains. One may then imagine a pyrolysis thickness  $\Delta$ , such that its front and back faces are, respectively, at  $r = r_p$  where  $T = T_p$ , and  $r = r_c$  where  $T = T_c$ . A char depth  $r'$  may then be defined as the location of the midpoint of the pyrolysis wave. The pyrolysis speed

$$\left[ V = - \frac{\partial r'}{\partial t} \right]$$

is defined as

$$V(\rho_0 - \rho_C)r'^2 = \dot{m}''R^2, \quad (2.8)$$

where  $\rho_0$  and  $\rho_C$  are virgin wood and char densities, respectively.

The first term on the right hand side of equation (2.6) (the sensible heat integral) can be broken into two parts. The first part is for the virgin solid (from  $r = 0$  to  $r = r'$ ) and the second part is for the charred section (from  $r = r'$  to  $r = R$ ). Equation (2.6) can then be rewritten in the form of

$$\begin{aligned} \dot{q}''R^2 - \int_{r'}^R \rho_C C_C \frac{\partial T_C}{\partial t} r^2 \partial r &= \int_0^{r'} \rho_0 C_0 \frac{\partial T}{\partial t} r^2 \partial r \\ &+ \int_0^R L_p \left[ - \frac{\partial \rho}{\partial t} \right] r^2 \partial r. \end{aligned} \quad (2.9)$$

From Kanury [1977], assuming that the rate of change of char temperature is equal to

$$\frac{\partial T_C}{\partial t} = \frac{3\dot{q}''}{\rho_C C_C R},$$

and is independent of char depth and charring velocity, the left hand side of equation (2.9) reduces to  $\dot{q}''r'^3/R$ . Then, equating equations (2.8) and (2.7) gives

$$\int_0^R L_p \left[ - \frac{\partial \rho}{\partial t} \right] r^2 \partial r = L_p V(\rho_0 - \rho_C)r'^2. \quad (2.10)$$

Equation (2.9) can then be written in the form of

$$\dot{q}'' \left( \frac{r'}{R} \right) = \frac{1}{r'^2} \int_0^{r'} \rho_0 C_0 \frac{\partial T}{\partial t} r^2 dr + L_p V(\rho_0 - \rho_C) . \quad (2.11)$$

Assuming a pure conduction temperature profile for the virgin solid [Carslaw and Jaeger 1965], and neglecting the series term in the solution (this assumption is valid when  $\alpha t/R^2$  is greater than 0.05, i.e. when the char depth exceeds  $0.05R$  [Kanury 1973]), then the temperature profile in the solid is given by

$$T - T_0 = \frac{3\dot{q}''}{\rho_0 C_0 R} t + \frac{\dot{q}'' R}{K} \left[ \frac{1}{2} \left( \frac{r}{R} \right)^2 - \frac{3}{10} \right] . \quad (2.12)$$

From equation (2.12), if  $T_{r=0}$  is the center temperature and  $T_{r'}$  is the temperature at  $r = r'$ , then the following relations can be obtained:

$$\frac{T - T_{r=0}}{T_{r'} - T_{r=0}} = \left( \frac{r}{r'} \right)^2 , \quad (2.13)$$

$$\frac{T - T_{r'}}{T_{r'} - T_{r=0}} = \left( \frac{r}{r'} \right)^2 - 1 \quad (2.14)$$

and

$$\frac{\partial T}{\partial t} = 2V(T_{r'} - T_{r=0}) \frac{r^2}{r'^3} - \left[ \left( \frac{r}{r'} \right)^2 - 1 \right] \frac{\partial T_{r=0}}{\partial t} . \quad (2.15)$$

Using the relations (2.13)-(2.15), the first term on the right hand side of equation (2.11) is obtained as

$$\begin{aligned} & \int_0^{r'} \rho C \frac{\partial T}{\partial t} r^2 dr \frac{2}{5r'^2} \left[ \dot{q}'' \left( \frac{r'}{R} \right) \right. \\ & \left. = + \rho C (T_{r'} - T_0) V + \frac{3}{10} \frac{\dot{q}'' R}{\alpha} V - \frac{3\dot{q}'' t}{R} V \right] , \end{aligned} \quad (2.16)$$

where  $\alpha$  is the thermal diffusivity of the virgin solid.

Substituting in equation (2.11) and simplifying gives

$$r' = 2(C_1 - t)V \quad (2.17)$$

or

$$\frac{\partial r'}{r'} = \frac{\partial t}{2(t - C_1)} \quad (2.18)$$

where

$$C_1 = \left[ \frac{5}{6} \frac{(\rho_0 - \rho_c)L_p}{\dot{q}''} + \frac{\rho_0 C_0 (T_{r'} - T_0)}{3\dot{q}''} \right] R + \frac{1}{10\alpha} R^2 \quad (2.19)$$

Finally, assuming that at time  $t = 0$ ,  $r' = R$  (that is, the charring of the surface starts at  $t = 0$ ), and at time equal to  $t_p$  (pyrolysis time),  $r' = 0$ , the integration of equation (2.18) gives

$$\frac{r'}{R} = \left[ 1 - \frac{t}{t_p} \right]^{\frac{1}{2}} \quad (2.20)$$

where pyrolysis time is calculated as

$$t_p = aR + bR^2 \quad (2.21)$$

In this equation,

$$a = \frac{5}{6} \frac{(\rho_0 - \rho_c)L_p}{\dot{q}''} + \frac{\rho_0 C_0 (T_{r'} - T_0)}{3\dot{q}''} \quad (2.22)$$

and

$$b = \frac{1}{10\alpha} \quad (2.23)$$

(For purposes of calculation,  $R = \frac{1}{2} \sqrt[3]{\text{volume of the cubes.}}$ )

Among the variables in equation (2.22), the value of  $L_p$  (i.e., the heat of pyrolysis) is the subject of much

controversy. Its value has been reported from -4500 cal/g (exothermic) to +300 cal/g (endothermic) [Kanury 1972; Kanury 1970b; Wichman et al. 1987]. For this investigation, it was assumed that pyrolysis is an endothermic process and a value of 180 cal/g was chosen for  $L_p$ . In addition, drying of the moist particles was considered to be a part of the pyrolysis process. In order to account for the additional heat required for drying, the value of the heat necessary to remove the bound and free water in wood [Dadkhah-Nikoo 1985] was added to the heat of pyrolysis. Figure 2.1 shows the heat of pyrolysis as a function of moisture content, as described above, and the effect of moisture content on pyrolysis time as calculated in the model described in this investigation. The values chosen for the calculation of pyrolysis time are:  $\rho_0 = 0.65$  g/cm<sup>3</sup>,  $\rho_c = 0.17$  g/cm<sup>3</sup>,  $\alpha = 0.0012$  cm<sup>2</sup>/sec and  $\dot{q}'' = 2$  cal/cm<sup>2</sup>-sec. These results are in excellent agreement with previous experimental results. For example, Simmons [1983] demonstrated that for a 1 cm cube of red oak, increasing the moisture content from zero (oven-dry) to 50 percent (wet basis) increased the time of pyrolysis by approximately 50 seconds. This increase was approximately 150 seconds for 2 cm particles. The increases in the time of pyrolysis predicted by the model under consideration were 60 and 130 seconds, respectively, for 1 cm and 2 cm particles.

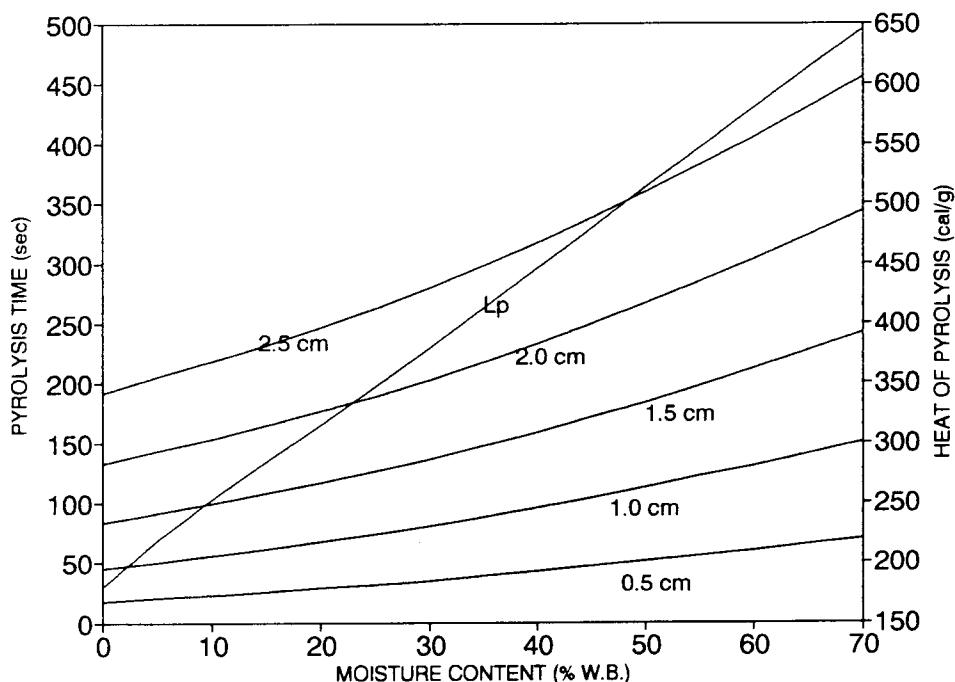


Figure 2.1 Effect of moisture content on endothermicity and time of pyrolysis.

The relative value of  $a/bR$  is an interesting aspect of equation (2.21). If  $a/bR$  is equal to zero or very small (that is, solids with either low pyrolysis endothermicity, specific heat, thermal diffusivity or a large heat flux, or a combination of these variables such that  $a/bR \approx 0$ ), then pyrolysis time will be proportional to  $bR^2$ . On the other hand, if the  $a/bR$  ratio is very large (that is, solids with large thermal diffusivity, pyrolysis endothermicity, specific heat or a small heat flux), then the pyrolysis time will be proportional to  $aR$ . The effects of the relative value of  $a/bR$  (for the case of  $b = 83 \text{ sec/cm}^2$ , or  $\alpha = 0.0012 \text{ cm}^2/\text{sec}$ ) is shown in Figure 2.2, in which the



pyrolysis time of a 1 cm particle changes from approximately 25 to 450 seconds as  $a/bR$  varies from zero to 20. For the experiments considered in this investigation, the lower and upper limits of  $a/bR$  were 0.3 and 10.0, respectively.

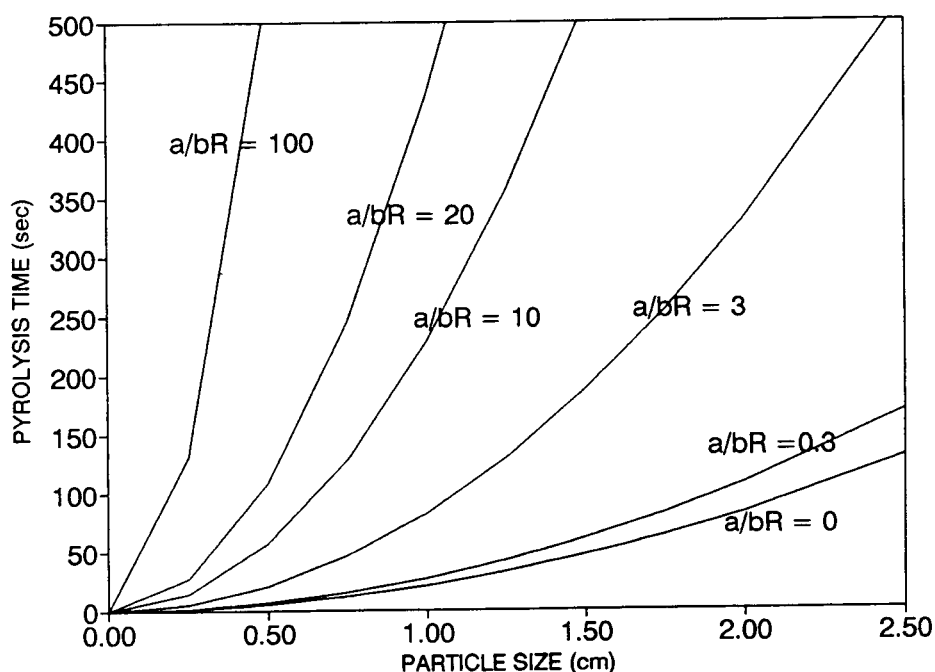


Figure 2.2 Effect of particle size and ratio of  $a/bR$  on pyrolysis time.

#### 2.1.1.2 Char Combustion

When pyrolysis of a wood particle is completed, the remaining residue is a highly carbonaceous char. In this section a model for prediction of char combustion time, resulting from the surface reaction between the char and oxygen, is presented.

Consider a spherical particle of radius  $R$  (diameter =  $d_o$ ) with its surface located at  $r = R$ , that is, placed in an oxidizing atmosphere. Assume that the particle is mainly composed of carbon and that "complete" steady-state combustion takes place at the surface of the sphere. Under conditions imposed on the particle in a combustion chamber, the burning rate of carbon is controlled by the diffusion of oxygen to the surface of the sphere [Kanury 1977]. Since no reaction takes place in the gas phase, the oxygen conservation equation is expressed as a balance between diffusion and convection.

$$\frac{d}{dr} \left[ r^2 \rho_g D_o \frac{dY_o}{dr} \right] - (\dot{w}'' r^2) \frac{dY_o}{dr} = 0 . \quad (2.24)$$

The energy equation in the gas phase is similarly written as

$$\frac{d}{dr} \left[ r^2 K_g \frac{dT}{dr} \right] - (\dot{w}'' r^2) C_g \frac{dT}{dr} = 0 , \quad (2.25)$$

where  $\rho_g$ ,  $K_g$  and  $C_g$  are, respectively, the density, thermal conductivity and specific heat of the gas mixture. The oxygen mass fraction and gas temperature at location  $r$  are denoted by  $Y_o$  and  $T$ , respectively, and  $D_o$  is the oxygen diffusion coefficient. The continuity of mass is given by

$$4\pi(\dot{w}'' r^2) = 4\pi(\dot{w}_w'' R^2) = \text{constant} , \quad (2.26)$$

where  $\dot{w}''$  is the local fuel flux and  $\dot{w}_w''$  is the rate of loss of carbon from the particle at  $r = R$ .

The free stream oxygen concentration is  $Y_o = Y_{o\infty}$ .

The oxygen mass flux at the surface of the particle is

$$\dot{W}_{ow}'' = \rho_g D_o \left. \frac{dY_o}{dr} \right|_w - \dot{W}_w'' Y_{ow} . \quad (2.27)$$

Assuming that each gram of oxygen consumes "f" grams of carbon (fuel), then

$$\dot{W}_{ow}'' = \frac{\dot{W}_w''}{f} . \quad (2.28)$$

Equating equations (2.27) and (2.28) yields

$$\frac{\dot{W}_w''}{f} = \left[ \rho_g D_o \frac{dY_o}{dr} - \dot{W}_w'' Y_o \right]_w . \quad (2.29)$$

Integrating equations (2.25) and (2.28) gives

$$r^2 \rho_g D_o \frac{dY_o}{dr} = \dot{W}_w'' R^2 \left[ Y_o + \frac{1}{f} \right] .$$

and rearranging,

$$\frac{dY_o}{\left[ Y_o + \frac{1}{f} \right]} = \frac{\dot{W}_w'' R^2}{\rho_g D_o} \frac{dr}{r^2} . \quad (2.30)$$

Then, integrating equation (2.30) and applying the boundary condition  $Y_o \rightarrow Y_{o\infty}$  as  $r \rightarrow \infty$  gives

$$\ln \left( \frac{Y_o + \frac{1}{f}}{Y_{o\infty} + \frac{1}{f}} \right) = - \frac{\dot{W}_w'' R^2}{\rho_g D_o} \frac{1}{r} . \quad (2.31)$$

For diffusionally controlled flames, the oxygen concentration at the surface of the particle is nearly zero. Therefore, the application of equation (2.31) at  $r = R$  gives

$$\frac{\dot{W}_w'' R}{\rho_g D_o} = \ln(1 + fY_{O\infty}) = \ln(1 + B) , \quad (2.32)$$

where the mass transfer number is defined as  $B = fY_{O\infty}$ .

From equation (2.32), the time to completely consume a particle of the diameter  $d_0$ , can be deduced from the conservation of mass:

$$4\pi r^2 \left[ -\rho_c \frac{dr}{dt} \right] = 4\pi r^2 \dot{W}_w'' = 4\pi r \left[ \dot{W}_w'' R \right] = \text{constant} , \quad (2.33)$$

where  $\rho_c$  is the carbon density. Substituting for  $\dot{W}_w'' R$  from equation (2.32) gives the differential equation for the time of consumption of the particle as

$$\rho_c r dr = \rho_g D_o \ln(B + 1) dt . \quad (2.34)$$

From equation (2.34), the burning time ( $t_{c0}$ ) of the charred particle placed in air (i.e.,  $Re_d = 0$ ) is calculated as

$$t_{c0} = \frac{\rho_c d_0^2}{8\rho_g D_o \ln(B + 1)} . \quad (2.35)$$

The effect of the flow on burning of the particle is then considered. An experiment conducted by Tu [Tu et al. 1934] indicated that the influence of movement (i.e.,  $Re_d \neq 0$ ) of the oxidizing medium on the burning rate of a carbon particle is the same as for the case of a liquid droplet; that is, the apparent mass transfer coefficient varies with the Reynolds and Schmidt numbers according to

$$\left( \frac{\rho_g D_o}{R} \right)_{app.} = \frac{\rho_g D_o}{d} \left[ 2 + 0.6 Re_d^{1/2} Sc^{1/3} \right] . \quad (2.36)$$

Therefore, the differential equation (2.34) is modified accordingly, becoming

$$d\tau = \frac{-2\delta d\delta}{1 + C_2 \delta^{1/2}} , \quad (2.37)$$

where  $\delta = d/d_{d0}$ ,  $\tau = t/t_{c0}$  and  $C_2 = 0.3(\text{Re}_{d0})^{1/2}(\text{Sc})^{1/3}$ .

A solution for this equation in closed-form can be obtained in two extreme cases, those for zero and for very high Reynolds numbers. In the case of  $\text{Re}_{d0} = 0$  (or  $C_2 \ll 1$ ), the integration of equation (2.37) yields

$$\tau = 1 - \delta^2 . \quad (2.38)$$

The time for the complete consumption of the particle (i.e., the time when  $d = 0$ ) obtained from this equation is identical to the time given in equation (2.35) (i.e.,  $t_c = t_{c0}$ ).

In the case of very high Reynolds numbers (or  $C_2 \gg 1$ ), the differential equation (2.37) can be integrated to give

$$\tau = \frac{4}{3C_2} (1 - \delta^{3/2}) . \quad (2.39)$$

In cases which fall between the two extremes, the numerical integration of equation (2.37) is required. This is the case for the curves established in Figures 2.3 and 2.4 and the calculations for the experiments.

Figures 2.3 and 2.4 show the effect of Reynolds numbers on  $\tau$  as a function of  $\delta$  and  $\delta^2$ , respectively (for  $\text{Sc} = 0.89$ ). As shown in Figure 2.3, increasing the Reynolds number from zero to 1 reduces  $\tau$  from 1 to 0.82 for  $\delta = 0$ , a

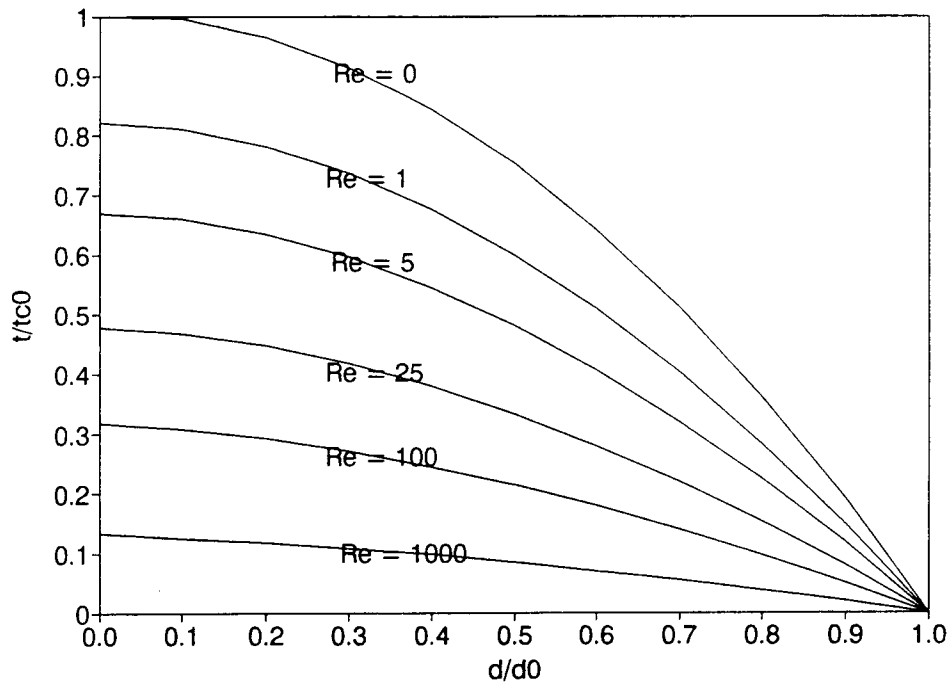


Figure 2.3 Variation of  $\tau$  as a function of  $\delta$  for different Reynolds number values.

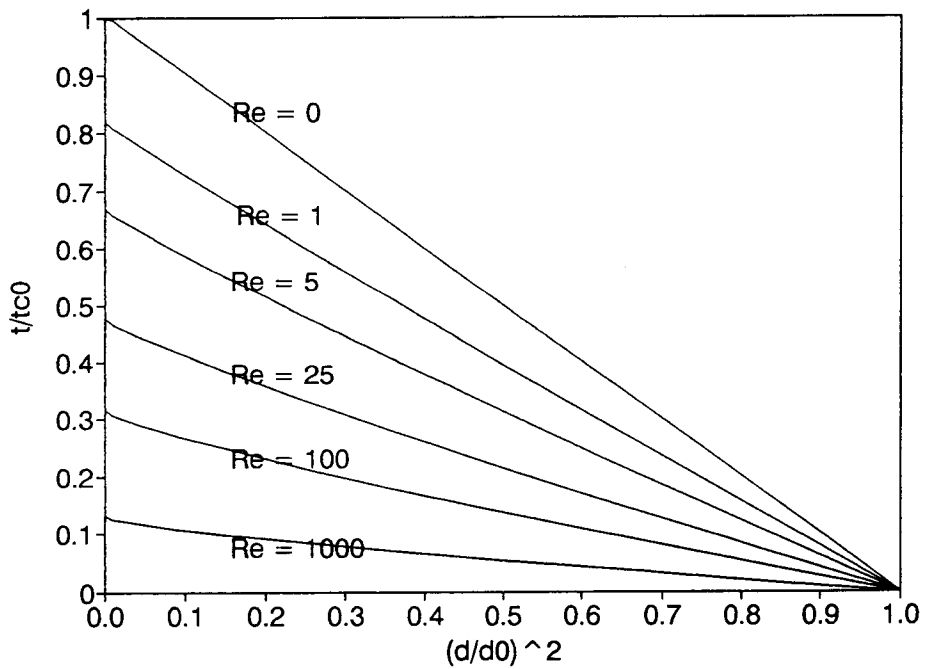


Figure 2.4 Variation of  $\tau$  as a function of  $\delta^2$  for different Reynolds number values.

reduction of 18 percent. For Reynolds numbers equal to 1000, this reduction is from 1 to 0.12. For Reynolds numbers higher than 1000, the curves depart little from the curve for  $Re = 1000$ .

Figure 2.5 presents a comparison of the results obtained from equations (2.37) and (2.39). For  $Re = 100$ , using equation (2.39) in place of equation (2.37) results in an overestimation of  $t_c$  by approximately 30 percent. For Reynolds numbers equal to 500 and 1000, the use of equation (2.39) results in an overestimation of  $t_c$  by 17 and 10 percent, respectively.

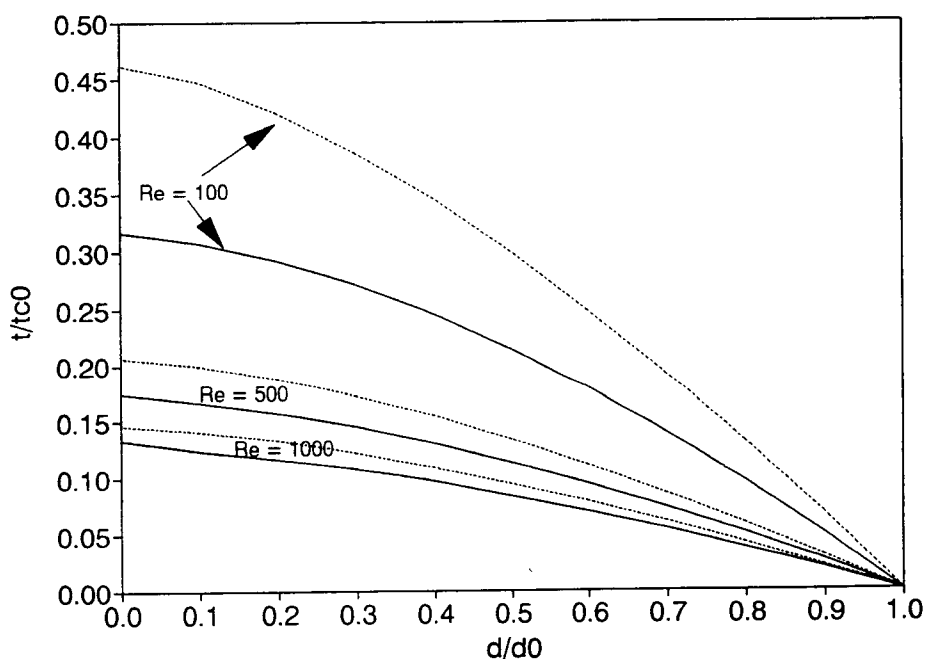


Figure 2.5 Comparison of the results obtained from equations (2.37) and (2.39), calculating  $\tau$  as a function of  $\delta$  for different Reynolds numbers.

Once the pyrolysis and char combustion times for a particle have been calculated, the total combustion time ( $t_t$ ) of the particle can be calculated as  $t_t = t_p + t_c$ .

## 2.2 Experiments

For the current investigation, 17 experiments under steady-state conditions were conducted. Douglas-Fir cubes were used as fuel for 14 of these experiments, while wood pellets were used as fuel for the remaining 3 experiments. The total combustion time for the particles were calculated from measured fuel feed rates and the photographs of the grate taken during the experiments. The net heat transfer ( $\dot{q}''$ ) to wood particles was calculated based upon the assumption that each fresh particle falls on the grate and is surrounded by charring particles. Furthermore, it was assumed that the particles formed a single layer on the grate. Therefore, each fresh particle experienced heat conduction to or from the grate, thermal radiation from the refractory wall, charring particles, and the flame. The location of the flame was assumed to be at the point of the highest temperature in the combustion chamber. Convective heat transfer between the particles and combustion air was neglected since the maximum temperature of combustion air used for these experiments was 480 K, which did not constitute a significant contribution to overall heat transfer to the particles.



### 2.2.1 Radiation Heat Transfer from the Refractory Wall

Since the temperature of the inside wall of the combustion chamber (i.e., ceramic refractory) was not measured during the experiments, using the temperature of the steel casing (outside wall) and heat loss from the chamber, the temperature of the ceramic refractory was calculated.

Heat loss from the combustion chamber was calculated using two methods. First, using the computer program discussed in Chapter 4, the difference between energy input to the combustion chamber and the energy content of the combustion products was calculated. This difference represented heat loss from the combustion chamber, or the sum of convective and radiative heat loss and incomplete fuel combustion.

The second method was to predict convective and radiative heat losses from the chamber, based upon the temperature of the outside wall of the combustion chamber.

1) Convective heat loss from the combustion chamber was estimated according to equation

$$Q_{\text{con}} = hA_{\text{wo}}(T_{\text{wo}} - T_{\text{air}}) . \quad (2.40)$$

In this relation,  $h$  is the average convective heat transfer coefficient,  $A_{\text{wo}}$  is the outside area of the combustion chamber,  $T_{\text{wo}}$  is the average temperature of the combustion chamber outside wall and  $T_{\text{air}}$  is the ambient air temperature. The convective heat transfer coefficient was calculated from the correlation

$$\text{Nu}_L = 0.59(\text{Gr}_L \text{ Pr})^{1/4} . \quad (2.41)$$

Note that this correlation is valid for  $10^4 < Gr_L < 10^9$  [Pitts et al. 1977].

2) Radiation heat loss from the combustion chamber was calculated from the equation

$$Q_{\text{rad}} = \epsilon_s A_{\text{wo}} \sigma (T_{\text{wo}}^4 - T_{\text{air}}^4) , \quad (2.42)$$

where  $\epsilon_s$  is the emissivity of the stainless steel and  $\sigma$  is the Stefan-Boltzmann constant. Refractory temperature was then calculated, based on heat loss from the combustion chamber, according to the equation

$$T_{\text{wi}} = T_{\text{wo}} + Q(R_T) , \quad (2.43)$$

where  $T_{\text{wi}}$  is the refractory temperature,  $Q$  is the total heat loss from the chamber (i.e., the sum of radiative and convective heat losses) and  $R_T$  is the total thermal resistance of the combustion chamber wall, which was calculated from the equation

$$R_T = \frac{1}{2\pi H_s} \left[ \frac{\ln \left( \frac{D_m}{D_i} \right)}{K_C} + \frac{\ln \left( \frac{D_o}{D_m} \right)}{K_s} \right] . \quad (2.44)$$

In equation (2.44),  $H_s$  is the height of the combustion chamber,  $D_o$  is the outside diameter of the chamber,  $D_m$  is the outside diameter of the refractory (i.e., the inside diameter of the stainless steel casing),  $D_i$  is the inside diameter of the refractory,  $k_C$  is the refractory thermal conductivity and  $k_s$  is the thermal conductivity of the stainless steel.

Once the refractory temperature was calculated, radiation heat transfer from the refractory wall to particles on the grate (at  $T_p$ ) was calculated from the equation

$$Q_{W-G} = \frac{\sigma \left[ T_{wi}^4 - T_p^4 \right]}{\frac{1 - \epsilon_p}{\epsilon_p A_G} + \frac{1}{A_{wi} \tau_{gas} F_{W-G}} + \frac{1 - \epsilon_{wi}}{\epsilon_{wi} A_{wi}}}, \quad (2.45)$$

where  $Q_{W-G}$  is the radiation heat transfer from the refractory wall to particles on the grate,  $\epsilon_{wi}$  is refractory emissivity,  $A_G$  is the area of the grate,  $A_{wi}$  is the area of the refractory wall,  $F_{W-G}$  is the wall-to-grate radiation shape factor,  $\tau_{gas}$  is the transmissivity of the combustion products in the chamber and  $\epsilon_p$  is the wood particle emissivity. The radiation shape factor was calculated from the equation [Siegel et al. 1981]

$$F_{W-G} = \frac{A_G}{A_{wi}} \left\{ 1 - \frac{1}{2} \left[ 2 + \left( \frac{H_R}{R_G} \right)^2 - \left( \frac{H_R}{R_G} \right) \sqrt{4 + \left( \frac{H_R}{R_G} \right)^2} \right] \right\}, \quad (2.46)$$

where  $H_R$  is the height of the refractory wall and  $R_G$  is the radius of the grate.

### 2.2.2 Radiation Heat Transfer from Adjacent Particles

When fresh particles reside on the grate they are subjected to radiation heat flux from neighboring particles. Assuming that neighboring particles are at charring temperature (assumed to be 1000°C) [Simmons 1983] and fresh particles are at volatilization temperature (assumed to be 300°C), the net radiation heat transfer from neighboring particles can be estimated according to the equation

$$Q_{p'-p} = \frac{\sigma \left[ T_{p'}^4 - T_p^4 \right]}{\frac{1 - \epsilon_p}{\epsilon_p A_p} + \frac{1}{A_{p'} F_{p'-p}} + \frac{1 - \epsilon_{p'}}{\epsilon_{p'} A_{p'}}}, \quad (2.47)$$

where  $Q_{p'-p}$  is the radiation heat transfer from charring particles to pyrolyzing particles,  $T_{p'}$  is the charring temperature of the wood particles,  $\epsilon_p$  is the emissivity of the fresh particles,  $A_p$  is the area of the particle exposed to neighboring particles,  $F_{p'-p}$  is the radiation shape factor,  $\epsilon_{p'}$  is the emissivity of the charring particle and  $A_{p'}$  is the area of the charring particles. The shape factor (for parallel plates) was calculated from the equation [Siegel et al. 1981]

$$F_{p'-p} = \frac{2}{\pi x^2} \left\{ \ln \left[ \frac{(1 + x^2)}{\sqrt{1 + 2x^2}} \right] + 2x \sqrt{1 + x^2} \tan^{-1} \frac{x}{\sqrt{1 + x^2}} - 2x \tan^{-1} x \right\}, \quad (2.48)$$

where  $x$  is the ratio of the  $R/c$ ,  $R$  is the particle size, and  $c$  is the distance between the particles.

### 2.2.3 Radiation from Flame

Particles on the grate experience radiation heat transfer from the flame. The net radiative heat transfer from the flame to the grate was calculated according to the equation:

$$Q_{f-G} = \frac{\delta \left[ T_f^4 - T_p^4 \right]}{\frac{1 - \epsilon_p}{\epsilon_p A_G} + \frac{1}{A_f F_{f-G} \tau_{gas}} + \frac{1 - \epsilon_f}{\epsilon_f A_f}}, \quad (2.49)$$

where  $Q_{f-G}$  is the net radiation heat transfer from the flame to particles on the grate (at  $T_p$ ),  $T_f$  is the flame temperature,  $A_f$  is the area of the flame and  $\epsilon_f$  is the flame emissivity.  $F_{f-G}$  is the radiation shape factor calculated from equation (2.50) [Siegel et al. 1981]

$$F_{f-G} = \frac{1}{2} \left[ 2 + \left[ \frac{H_f}{R_G} \right]^2 - \left[ \frac{H_f}{R_G} \right] \sqrt{4 + \left[ \frac{H_f}{R_G} \right]^2} \right], \quad (2.50)$$

where  $H_f$  is the distance between the flame and the particles on the grate and  $R_G$  is the radius of the grate. Note that the radii of the flame and the grate are assumed to be equal ( $R_f = R_G$ ).

#### 2.2.4 Heat Conduction to the Grate

The conduction heat transfer between the particles and the grate was calculated from the equation

$$Q_{cond} = k_s (T_G - T_p) A_p / R_p \quad (2.51)$$

where  $Q_{cond}$  is conduction heat transfer to (or from) the grate,  $k_s$  is the grate thermal conductivity,  $T_G$  is the temperature of the grate and  $R_p$  is the size of the particle.

The net heat transfer to the fresh particles is the algebraic sum of the heat transfers calculated in section 2.2.

### 2.2.5 Additional Experiments

In addition to the experiments carried out for this investigation, additional experimental data [Simmons 1983; 1986] were used to test the validity of the model under consideration. These experiments were conducted on red oak and sugar pine samples in the shape of cubes in high temperature convective air flows.

To calculate the heat transfer to particles for Simmons' [1983; 1986] experiments, flame temperature was assumed to be 300 K higher than the combustion air temperature (i.e., a combustion air temperature range from 900 to 1200 K) [Simmons 1983]. The convective heat transfer was calculated using the correlation

$$Nu = 2 + 0.6 Re^{1/2} Pr^{1/3} . \quad (2.52)$$

The temperature of the combustion chamber wall was assumed to be 75 percent of the mainstream temperature [Simmons 1983]. Radiation heat transfer from the wall and flame were calculated in a manner similar to the calculations performed for the current investigation. It was further assumed that the particles were surrounded by flame (i.e., a sphere with a radius 1.5 times the radius of the particle). In both cases of wall and flame radiation, it was assumed that the particle was completely enclosed by the flame and the wall. Computer programs used for calculating the burning times of wood particles are given in Appendix A.

### 2.2.5 Properties

The properties used for the model under consideration were either measured or were chosen from different sources. These properties include:

1) Density: The densities of the dry wood cubes and wood pellets were measured as follows:

Douglas-Fir (cube)	0.561 g/cm <sup>3</sup>
Ponderosa pine (wood only, pellets)	1.302 g/cm <sup>3</sup>
Hemlock Fir (wood and bark mix, pellets)	1.344 g/cm <sup>3</sup>
Red alder (wood and bark mix, pellets)	1.327 g/cm <sup>3</sup>

From Simmons [1983], measurements included:

Oak (cube)	0.69 g/cm <sup>3</sup>
Sugar pine (cube)	0.35 g/cm <sup>3</sup>

The density of moist particles was calculated from equation  $\rho_{\text{wet}} = (1 + M/100)\rho_{\text{dry}}$ , where M is the percent wet basis of the moisture content of the sample. Char density was assumed to be 0.17 g/cm<sup>3</sup> for all samples.

2) Specific heat capacity: The specific heat capacities of the dry wood were calculated from the Dunlap equation [Kanury 1970b]:

$$C_{p\text{-dry}} = 0.266 + 0.00116(T_p - 273) \quad \text{cal/g} - ^\circ\text{C}$$

The effect of moisture content [Siau 1971] was accounted for by:

$$C_{p\text{-wet}} = (C_{p\text{-dry}} + 0.01 \text{ Mdb}) / (1 + 0.01 \text{ Mdb}) ,$$

where Mdb is the percent dry basis of the moisture content of the fuel.

3) Thermal diffusivity: The thermal diffusivities (in  $\text{cm}^2/\text{sec}$ ) were assumed to be [Kanury 1970b]:

Douglas-Fir and pellets	0.00123
Red oak	0.00160
Pine	0.00151

4) Emissivity: The emissivity of the pyrolyzing particle was assumed to be 0.7. For charring particles and the ceramic refractory the emissivity was assumed to be 0.9, while the transmissivity of the flame was assumed to be 0.3 [Pitts et al. 1970; Welty et al. 1976].

5) Combustion air properties: The combustion air properties were calculated as functions of temperature, pressure and the mole fractions of their constituents [Fox 1984].

6) Mass diffusion coefficient: Mass diffusion coefficient were calculated from  $D = D_0(T_{\text{air}}/298)^{1.75}$ , where  $D_0 = 0.42 \text{ cm}^2/\text{sec}$  [Kanury 1977].

### 2.3 Results

Tables 2.1, 2.2A and 2.2B present the variables of interest, the experimental results from this investigation and as provided by Simmons [1983; 1986], and the results of calculations based on the model described in this chapter. In all of the figures included in this section, solid lines



Table 2.1 Experimental conditions, results and model predictions for Douglas-Fir and wood pellets.

EXP. CODE	SAMPLE SPECIES	COMB. AIR TEMP.	Re No.	SAMPLE M.C.	PARTICLE DIAMETER	HEAT FLUX	CALC. PYRO. TIME	CALC. CHAR COMB. TIME	CALC. TOTAL COMB. TIME	EXP. TOTAL COMB. TIME
		K		% W.B.	cm	cal/s-sq.cm	sec	sec	sec	sec
A	D.FIR	300	86	54	0.953	1.860	119	149	269	274
B	D.FIR	300	86	35	0.953	1.916	86	149	235	236
C	D.FIR	300	86	11	0.953	1.893	55	149	204	194
D	D.FIR	300	95	54	0.953	1.894	117	143	261	256
E	D.FIR	300	76	54	0.953	1.920	116	154	270	260
F	D.FIR	480	61	54	0.953	1.989	113	117	230	224
G	D.FIR	480	61	35	0.953	2.099	80	117	197	201
H	D.FIR	300	115	11	1.270	2.332	72	240	313	316
I	D.FIR	300	19	53	0.635	1.650	82	101	183	166
J	D.FIR	300	23	53	0.635	1.666	82	97	178	166
K	D.FIR	300	19	11	0.635	1.734	35	101	136	132
L	D.FIR	300	23	11	0.635	1.685	36	96	132	132
M	D.FIR	370	20	53	0.635	1.670	81	87	168	161
N	D.FIR	480	17	53	0.635	1.667	82	75	156	151
O	PHC	300	42	8	0.839	1.844	98	144	242	232
P	KMP	300	45	7	0.940	1.879	104	176	280	300
Q	BCCP	300	35	8	0.683	1.813	76	101	177	185

Table 2.2A Experimental conditions and calculated heat transfers for red oak and sugar pine. Experimental values from Simmons [1983; 1986].

EXPERIMENT CODE	SAMPLE SPECIES	COMBUSTION AIR TEMPERATURE	Re No.	SAMPLE M.C.	PARTICLE DIAMETER	HEAT FLUX
		UNIT--> K		% W.B.	cm	cal/s-sq.cm
S1	RED OAK	1100	120	0	1	2.175
S2	RED OAK	1100	120	9	1	2.175
S3	RED OAK	1100	120	13	1	2.175
S4	RED OAK	1100	120	20	1	2.175
S5	RED OAK	1100	120	50	1	2.175
S6	RED OAK	1100	120	0	2	1.822
S7	RED OAK	1100	120	9	2	1.822
S8	RED OAK	1100	120	13	2	1.822
S9	RED OAK	1100	120	20	2	1.822
S10	RED OAK	1100	120	50	2	1.822
S11	RED OAK	900	120	0	1	1.113
S12	RED OAK	1200	120	0	1	2.880
S13	RED OAK	900	280	0	2	1.000
S14	RED OAK	1200	280	0	2	2.607
S15	RED OAK	1100	60	0	1	2.021
S16	RED OAK	1100	260	0	1	2.423
S17	RED OAK	1100	280	0	2	1.961
S18	RED OAK	1100	600	0	2	2.147
S19	SUGAR PINE	900	120	0	1	1.113
S20	SUGAR PINE	1100	120	0	1	2.175
S21	SUGAR PINE	1200	120	0	1	2.880
S22	SUGAR PINE	900	280	0	2	1.000
S23	SUGAR PINE	1200	280	0	2	2.607
S24	SUGAR PINE	1100	60	0	1	2.021
S25	SUGAR PINE	1100	120	0	1	2.175
S26	SUGAR PINE	1100	260	0	1	2.423
S27	SUGAR PINE	1100	280	0	2	1.961
S28	SUGAR PINE	1100	600	0	2	2.147
S29	SUGAR PINE	1100	120	9	1	2.175
S30	SUGAR PINE	1100	120	13	1	2.175
S31	SUGAR PINE	1100	120	21	1	2.175
S32	SUGAR PINE	1100	120	67	1	2.175
S33	SUGAR PINE	1100	120	0	0.5	2.880
S34	SUGAR PINE	1100	120	0	1.5	1.940
S35	SUGAR PINE	1100	120	0	2.5	1.752

Table 2.2B Experimental and calculated results for red oak and sugar pine. Experimental values from Simmons [1983; 1986].

EXP. CODE	CALC. PYRO. TIME	EXP. PYRO. TIME	CALC. CHAR. COMB. TIME	EXP. CHAR. COMB. TIME	CALC. TOTAL COMB. TIME	EXP. TOTAL COMB. TIME
	sec	sec	sec	sec	sec	sec
S1	50	58	48	51	98	109
S2	61	59	48	66	109	125
S3	66	60	48	55	114	115
S4	76	64	48	57	123	121
S5	128	105	48	45	176	150
S6	152	165	191	145	343	310
S7	180	185	191	135	370	320
S8	192	210	191	150	383	360
S9	214	210	191	170	405	380
S10	339	340	191	85	530	425
S11	78	62	55	73	133	135
S12	43	46	45	63	87	109
S13	210	176	162	227	372	403
S14	131	129	131	42	262	171
S15	52	53	60	79	112	132
S16	47	42	36	55	83	97
S17	147	165	140	175	287	340
S18	142	124	103	135	245	259
S19	40	47	55	61	95	108
S20	29	38	48	43	76	81
S21	26	31	45	38	70	69
S22	118	131	162	198	280	329
S23	86	100	131	44	217	144
S24	29	39	60	45	89	84
S25	29	38	48	42	76	80
S26	27	27	36	41	63	68
S27	93	113	140	84	232	197
S28	90	84	103	101	193	185
S29	33	60	48	30	81	90
S30	35	65	48	30	83	95
S31	40	75	48	30	88	105
S32	80	120	48	40	127	160
S33	-	-	-	-	21	30
S34	57	95	107	70	165	165
S35	141	220	298	180	439	400

indicate the results of calculations based upon the present model. The error bars show the standard deviation of the experimental results.

Figure 2.6 shows a comparison of pyrolysis time, indicating very good agreement between model predictions and experimental values. Figure 2.7 shows a comparison for char combustion time. The agreement between the model predictions and the experimental results was not as close as for pyrolysis time. The differences between the two comparisons may be attributed to the following:

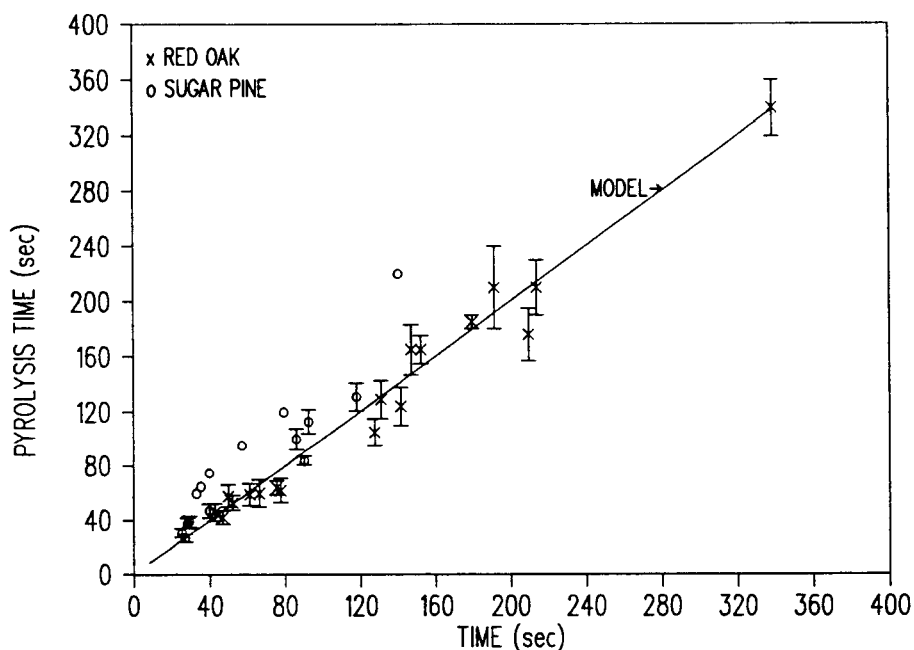


Figure 2.6 Comparisons of model predictions for pyrolysis times of red oak and sugar pine to experimental data [Simmons 1983; 1986].

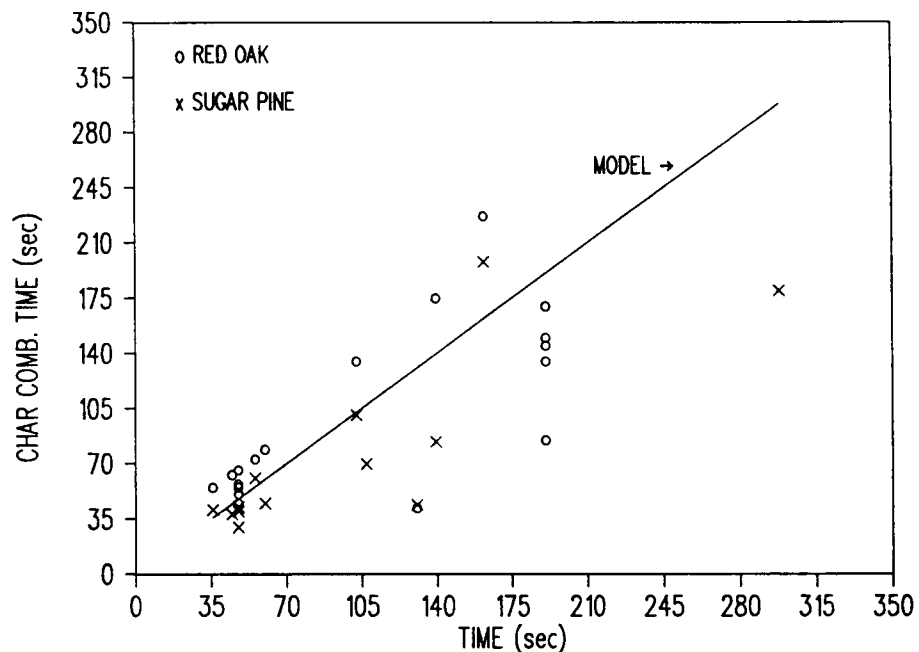


Figure 2.7 Comparison of model predictions of char combustion times for red oak and sugar pine and experimental data [Simmons 1983; 1986].

- 1) For the model, it was assumed that the density of the char was constant ( $0.17 \text{ g/cm}^3$ ) for all samples. However, this was not an accurate assumption. In fact, the density and amount of char remaining after pyrolysis is highly dependent on the physical and chemical properties of the fuel. Moisture content and the size of the wood particles also affects the density and the amount of the remaining char. In addition, the pyrolysis environment and the intensity of the heat flux affect the amount and properties of the char [Kanury 1974; Walker 1982; Antal 1982; Sateyindra 1982].

- 2) The mass diffusion coefficient ( $D_0$ ) used in this model was assumed to be constant for all samples, when in fact it is dependent on the physical properties of the char [Welty et al. 1976].
- 3) For the model, it was assumed that the char remaining after pyrolysis would be the same size as the fresh particles (i.e., the reduction in volume of the sample after pyrolysis is neglected), but the size of the char is also dependent upon the factors noted in (1) above.

In particular, the model overestimated the char combustion time for samples with high pyrolysis time (i.e., high moisture content, large particles or a low heat flux). This is in part due to the fact that in these cases pyrolysis and char combustion tended to occur simultaneously rather than successively.

Figure 2.8 shows a comparison of total combustion time, indicating excellent agreement between the model predictions and the experimental results.

### 2.3.1 Effect of Moisture Content on Particle Burning Times

Figures 2.9-2.11 show the influence of moisture content on pyrolysis and total combustion time for red oak, Douglas-fir and sugar pine samples. The model predictions for red oak and Douglas-fir were in good agreement with the experimental results, but the results for the pyrolysis of

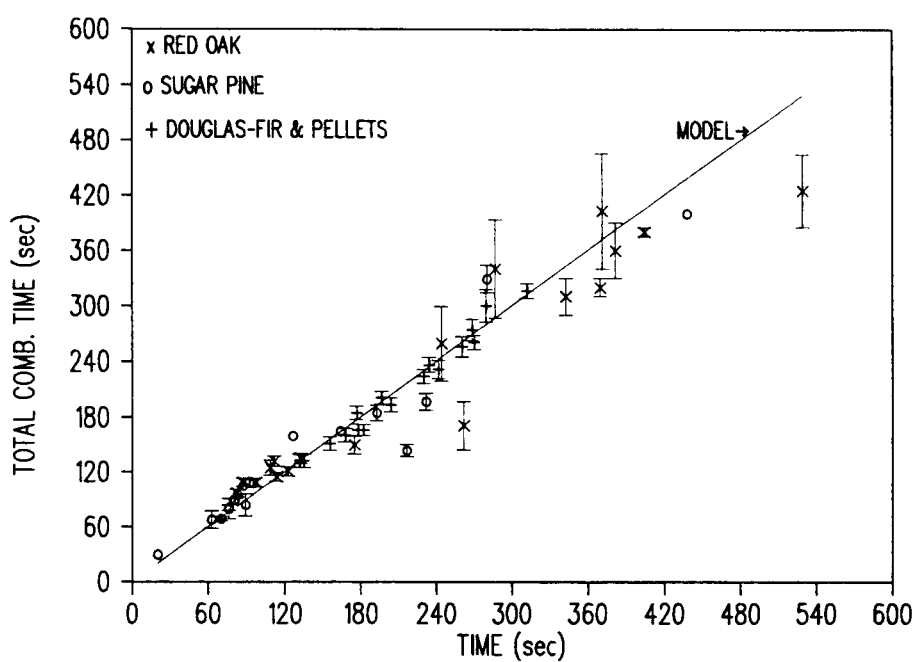


Figure 2.8 Comparison of model predictions of total combustion times for Douglas-Fir, red oak and sugar pine and experimental data for red oak and sugar pine, from Simmons [1983; 1986].

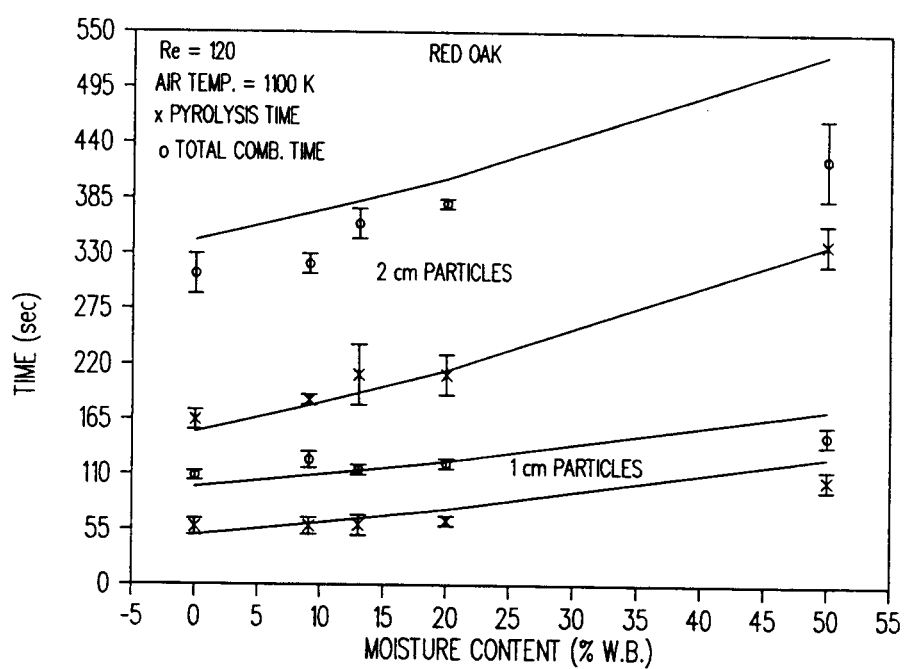


Figure 2.9 Comparison of model predictions and experimental data for pyrolysis and total combustion times of red oak cubes as a function of moisture content. Experimental data from Simmons [1983; 1986].



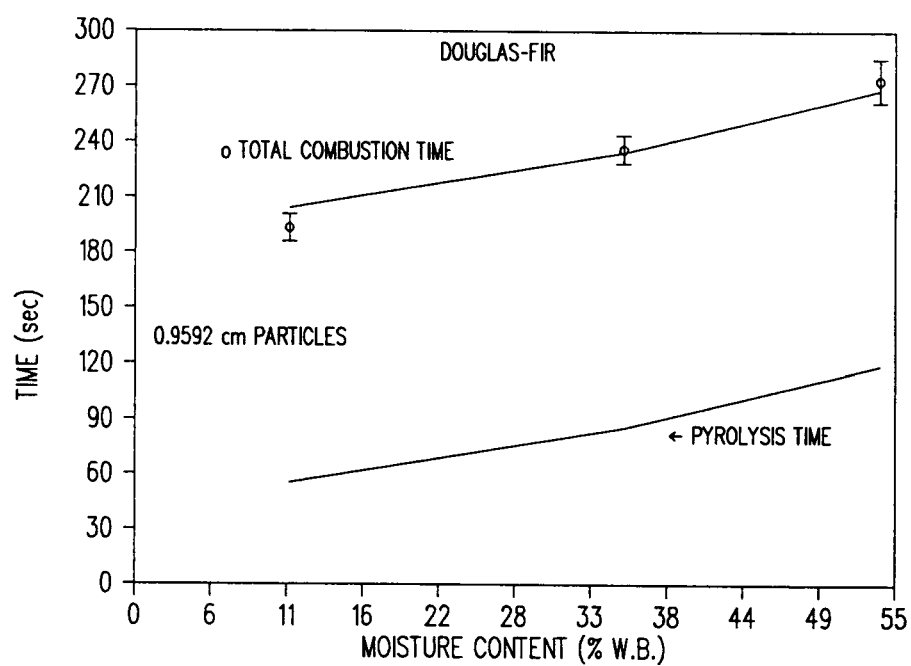


Figure 2.10 Comparison of model predictions and experimental data for total combustion times as a function of moisture content, Douglas-fir.

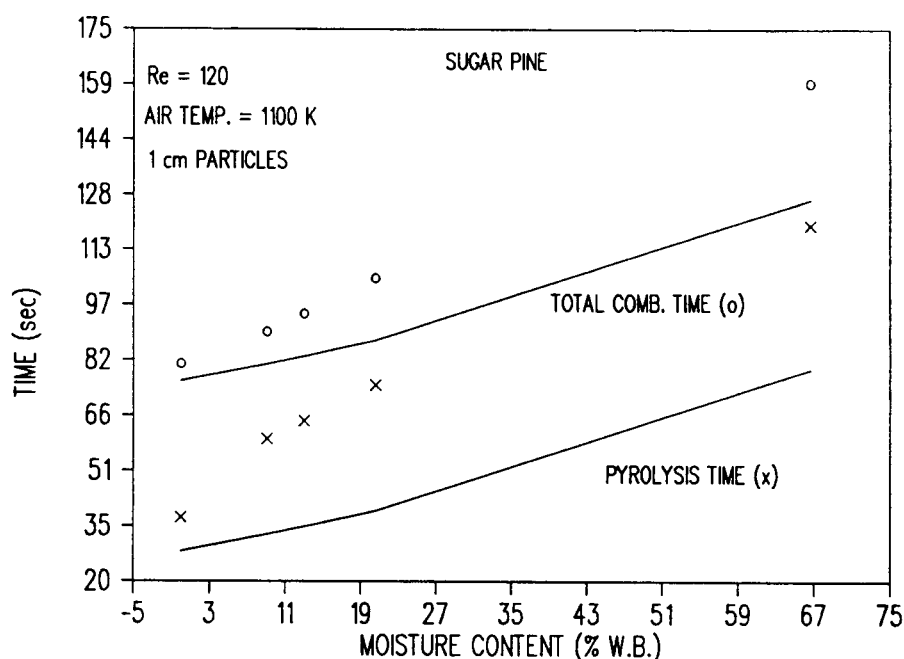


Figure 2.11 Comparison of model predictions of pyrolysis and total combustion times as a function of moisture content, sugar pine, and experimental data [Simmons 1983; 1986].

sugar pine was underestimated by the model. This could be due to a higher value of endothermicity of pyrolysis and the lower char density of the sugar pine.

As shown in Figure 2.9, increasing the moisture content of 1 cm red oak samples by 50 percent (wet basis) increased pyrolysis time from 58 sec to 105 sec. For 2 cm red oak samples, the increase in pyrolysis time over the same range of moisture content was from 165 sec to 340 sec. In other words, a 50 percent increase in moisture content approximately doubled the pyrolysis time for red oak. For Douglas-fir, the model indicated an increase of 64 sec for pyrolysis and total combustion time when moisture content

was increased from 11 to 54 percent. The experimental data showed an increase of 80 sec for total combustion time, in comparison to a 64 sec increase predicted by the model. For sugar pine, increasing the moisture content from zero to 67 percent increased pyrolysis time from 38 sec to 120 sec (i.e., an increase of more than 200%). The model predicted an increase of 180 percent in pyrolysis time.

### 2.3.2 Effect of Reynolds Numbers on Particle Burning Times

Figures 2.12 and 2.13 show the model predictions and experimental data for pyrolysis and total combustion times for 1 and 2 cm red oak and 1 cm sugar pine cubes as functions of Reynolds numbers. As expected from equation (2.21), the change in Reynolds numbers did not significantly change the pyrolysis times. This was also supported by the experimental data (Figs. 2.12-2.13). Increasing the Reynolds number reduced char combustion time, as predicted by equations (2.37) and (2.39) and as demonstrated in Figure 2.3; thus, the total burning time of the particles was reduced accordingly. This was verified by the experimental data (Figs. 2.12-2.13).

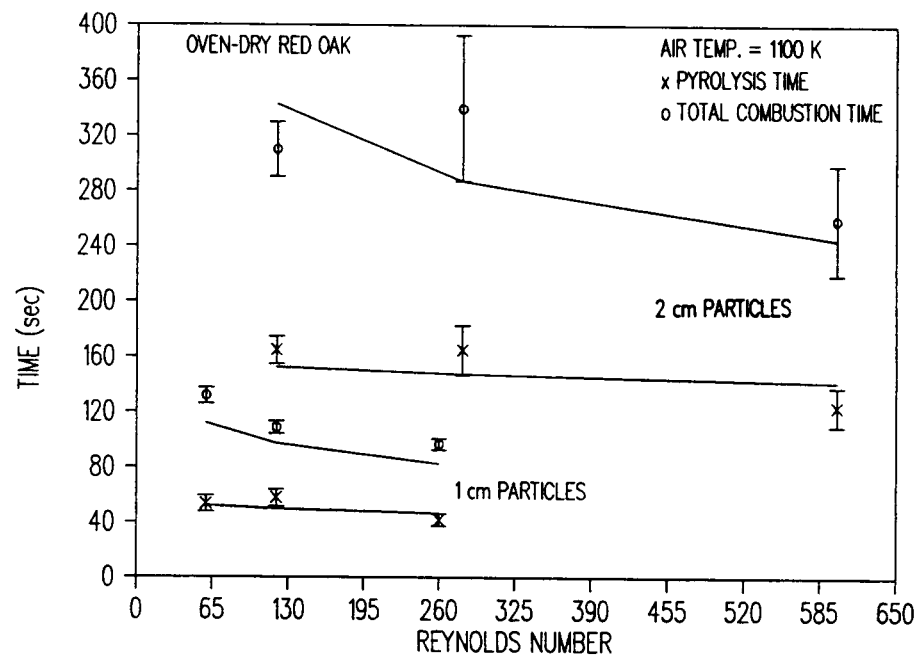


Figure 2.12 Comparison of model predictions of pyrolysis and total combustion times for red oak as a function of Reynolds numbers and experimental data [Simmons1983].

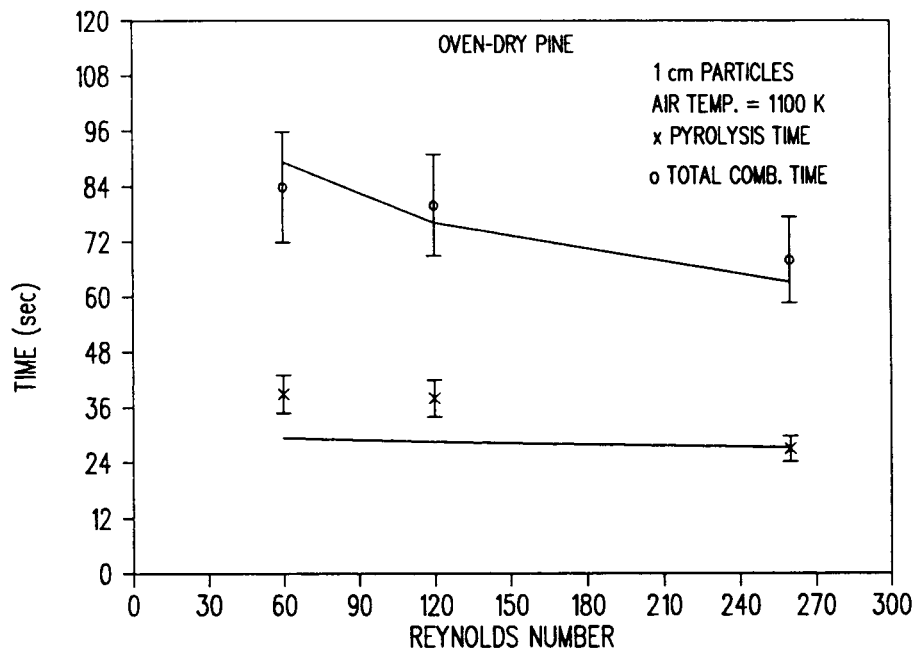


Figure 2.13 Comparison of model predictions of pyrolysis and total combustion times for 1 cm sugar pine as a function of Reynolds numbers and experimental data [Simmons 1983].

### 2.3.3 Effect of Heat Flux on Particle Burning Times

Figures 2.14-2.16 show pyrolysis and total combustion times as functions of heat flux for, respectively, red oak, sugar pine and Douglas-fir. It is clear that increasing the heat flux intensity reduced pyrolysis time, as predicted by equation (2.21) and verified by experimental data.

### 2.3.4 Effect of Size on Particle Burning Times

Figure 2.17 shows a comparison for oven-dry sugar pine samples as a function of particle size, indicating excellent agreement between the experimental values and the

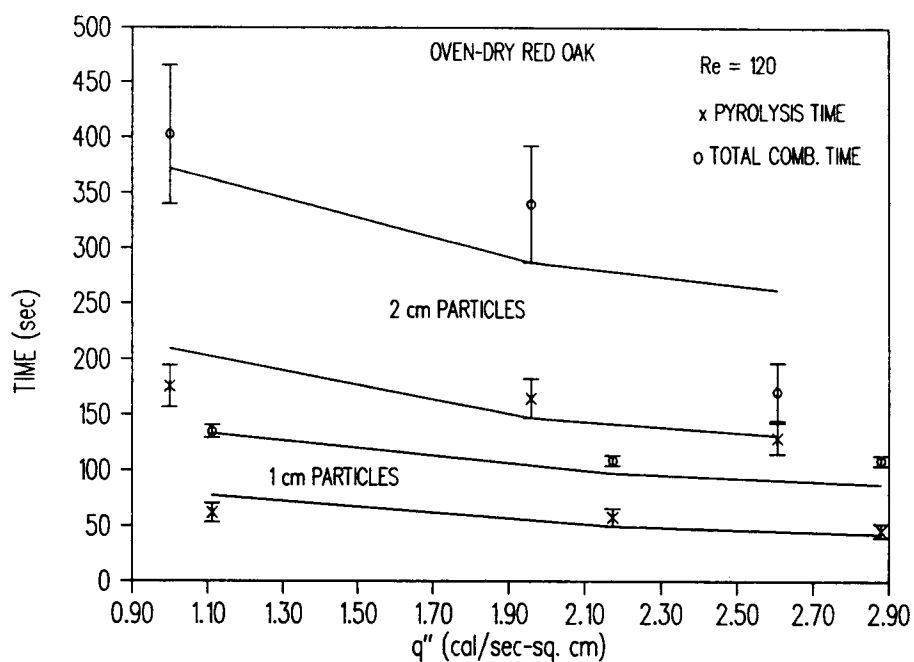


Figure 2.14 Comparison of model predictions of pyrolysis and total combustion times for red oak as a function of heat flux and experimental data [Simmons 1983].

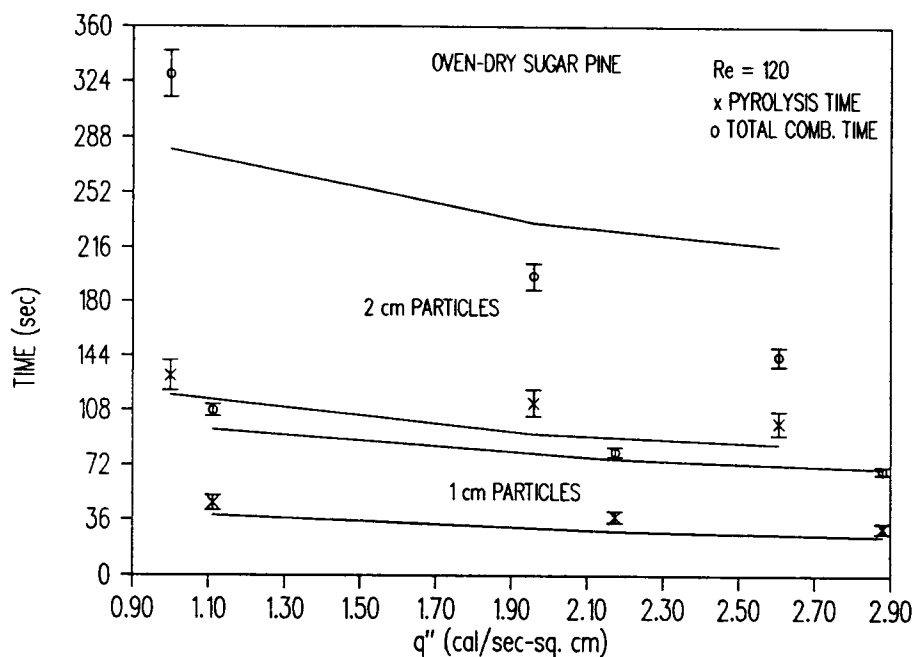


Figure 2.15 Comparison of model predictions of pyrolysis and total combustion times for sugar pine as a function of heat flux and experimental data [Simmons 1983].

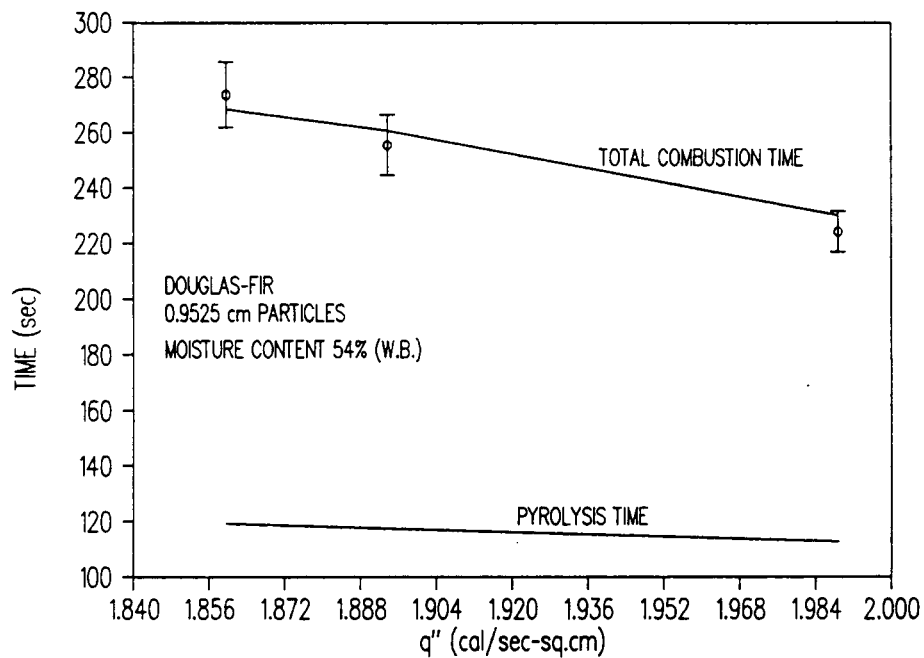


Figure 2.16 Comparison of model predictions of total combustion times for Douglas-fir as a function of heat flux and experimental data.

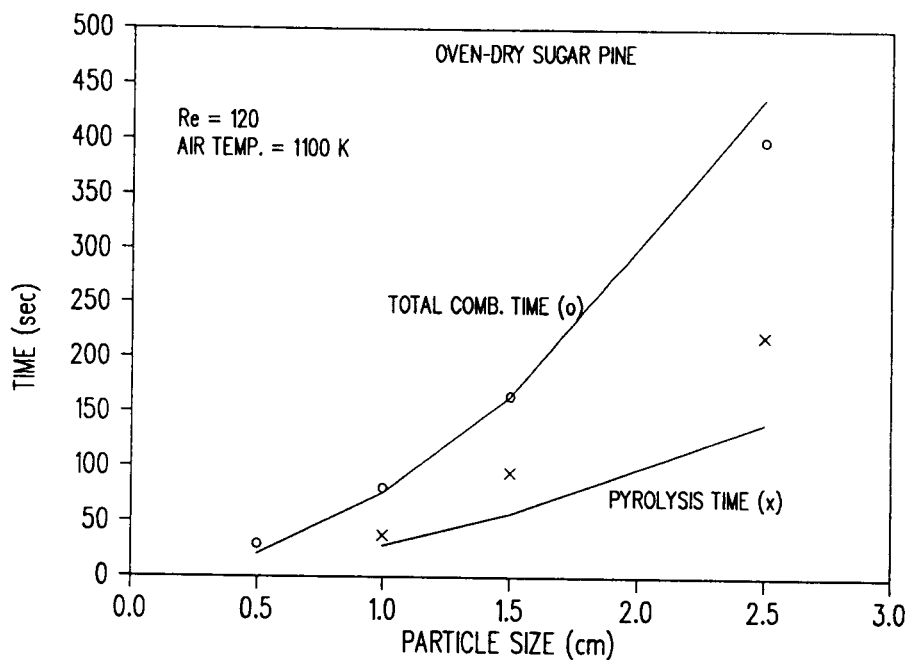


Figure 2.17 Comparison of model predictions for pyrolysis and total combustion times as function of particle size for sugar pine and experimental data [Simmons 1986].

model predictions for total burning time. The agreement between pyrolysis times was not as good as total burning time. In the case of sugar pine samples, although the pyrolysis and char combustion times were not in close agreement with the model predictions, the total combustion time was in good agreement with the model. This is because when pyrolysis time is underestimated by the model (due to higher values of endothermicity of pyrolysis or higher char densities), char combustion time is overestimated (due to lower densities and higher diffusion coefficients). These two effects cancel each other, thus the results for total combustion time were in close agreement with the experimental values. Therefore, even when the assumption of constant values for diffusion coefficients, char densities and endothermicities of pyrolysis are seemingly too simplistic, then the calculation of the model predictions for pyrolysis and char combustion times cancel the effects of the assumption.

#### 2.3.5 Effect of Combustion Air Temperature on Particle Burning Times

Increasing combustion air temperatures affected the burning time of wood samples in different ways. Equation (2.35) predicted that char combustion time would be inversely proportional to combustion air temperature to the power of 0.75. In diffusionally controlled regimes, the burning rate of coal particles is weakly dependent upon



temperature ( $T^{0.5-1.0}$ ) and strongly dependent upon particle size [Kanury 1977]. These two observations seem to be in agreement with the model predictions and the experimental results considered in this investigation.

Pyrolysis time is also dependent upon combustion air temperature. Convective heat transfers to particles increases as combustion air temperature increases. Increased combustion air temperature increases the temperature of the flame and the combustion chamber wall. The overall results were increased  $\dot{q}''$ , reducing pyrolysis time. Tables 2.1 and 2.2 show that an increase in combustion air temperatures from 900 K to 1200 K decreased the total combustion times for 1 cm oak cubes from 135 sec to 109 sec and from 403 sec to 171 sec for 2 cm cubes. The decrease for sugar pine under similar conditions was from 108 sec to 69 sec for 1 cm samples and from 329 sec to 144 sec for 2 cm samples. For Douglas-fir, an increase of 177 K (from 300 K to 477 K) in combustion temperature decreased the total combustion time from 236 to 200 sec.

#### 2.4. Conclusion

In this chapter, a mathematical model with a closed-form solution for the prediction of pyrolysis times of wood particles was presented. For char combustion, the model provided two closed-form solutions for the cases of very low and very high Reynolds numbers. For intermediate

Reynolds numbers, char combustion time was provided by the simple numerical integration of equation (2.37). Although several simplifying assumption were made for the derivation of the model equations, the model predictions were in very good agreement with the experiment results.

Further improvements in the model could be achieved if the amount, density and porosity of the char remaining after pyrolysis could be determined with greater accuracy. In addition, the means to provide a more accurate determination of the pyrolysis endothermicity values for different species, together with the relationship between virgin solid density and char density, could significantly enhance the results of this model.

### CHAPTER 3

#### TEMPERATURE AND COMPOSITION PROFILES IN THE COMBUSTION CHAMBER

#### 3.1 Combustion Profile

A brief, qualitative description of the temperature and composition profiles in the fuel bed was given in Chapter 1. In this chapter, the temperature and composition profiles for the gas phase above the fuel bed are discussed.

##### 3.1.1 Temperature Profile

Neglecting the variation in temperature and the composition of the gas mixture in a radial direction, a one-dimensional model was developed for the prediction of the temperature of the mixture in the combustion chamber. Consider a cylindrical control volume at a distance of  $x$  from the grate with a diameter equal to the combustion chamber inside diameter ( $D_{cer}$ ) and the thickness  $\Delta x$ . If the cross-sectional area and perimeter of the chamber are, respectively, denoted by  $A_{cer}$  and  $P_{cer}$ , then the energy balance for this control volume can be written as:

$$\begin{aligned} & \rho_g U_g A_{cer} C_{Pg} T|_{x+\Delta x} - \rho_g U_g A_{cer} C_{Pg} T|_x \\ & + \dot{q}''_{cer} \cdot P_{cer} \cdot \Delta x - \dot{S}''' \cdot A_{cer} \cdot \Delta x = 0, \quad (3.1) \end{aligned}$$

where  $T$  is temperature,  $\rho_g$  is density,  $C_{pg}$  is specific heat, and  $U_g$  is the velocity of the gas mixture. The rate of heat loss from the control volume to the ceramic wall in the chamber is denoted by  $\dot{q}''_{cer}$ . The volumetric energy generation rate due to combustion reactions in the control volume is indicated by  $\dot{S}'''$ .

Under steady-state conditions, the heat loss from the control volume in the radial direction is equal to the heat loss from the combustion chamber outer wall. The heat loss from the control volume to the ceramic wall is then related to the steel wall heat loss according to:

$$\dot{q}''_{cer} \cdot P_{cer} \cdot \Delta x = \dot{q}''_{st} \cdot P_{st} \cdot \Delta x , \quad (3.2)$$

where  $\dot{q}''_{st}$  is heat loss from the steel wall and  $P_{st}$  is the perimeter of the steel wall. Furthermore, the product  $\rho_g U_g A_{cer}$  is equal to the mass flow rate of the gas ( $\dot{m}_g$ ) in the combustion chamber. Introducing the non-dimensional distance  $X = x/L$ , where  $L$  is the height of the combustion chamber, Equation (3.1) can then be written as:

$$d(\dot{m}_g C_{pg} T) + L \dot{q}''_{st} P_{st} dX - \dot{S}''' \cdot A_{cer} \cdot L dX = 0 . \quad (3.4)$$

The volumetric energy generation rate  $\dot{S}'''$  for a gaseous mixture of fuel and oxidant is expressed in the form [Kanury 1977]:

$$\dot{S}''' = \Delta H_C \cdot K_n \cdot C_O^{n-j} \cdot C_f^j \cdot e^{-E/RT} , \quad (3.5)$$

where  $\Delta H_C$  is the heat of combustion,  $C_O$  is the oxidant concentration,  $C_f$  is the fuel concentration,  $n$  is the overall

order of reaction,  $j$  is the order of reaction with respect to the fuel,  $E$  is activation energy,  $K_n$  is the specific reaction rate constant, and  $R$  is the universal gas constant. Using  $\dot{S}'''$ , as given in equation (3.5) requires knowledge of the fuel and oxidant concentrations. From Kanury [1977], the use of the conservation of species for reactive gas mixtures provides the two additional equations required for the numerical solution of the set of equations. For the current investigation, a different approach was chosen such that the temperature of the combustion products in the chamber could be obtained independently of the species conservation equations.

Assume that  $\dot{S}'''$  can be expressed as:

$$\dot{S}''' = \frac{\dot{m}_f \cdot \text{LHV2}}{A_{\text{cer}} \cdot L} (D_1 e^{D_2 X}) \quad , \quad (3.6)$$

where  $\dot{m}_f$  is the mass flow rate of the fuel, LHV2 is the net heating value of the fuel (Chapter 4), and  $D_1$  and  $D_2$  are constants. Determination of the values of  $D_1$  and  $D_2$  is based upon the assumption that from the surface of the grate to 5 cm above the grate (i.e., half-way between the grate and the over-fire air port), 75% of the fuel is consumed, while the remaining 25% is consumed 5 cm from the grate to the location where fuel is introduced into the chamber (i.e., 61 cm above the grate). Note that the combustion of the char takes place only on the grate. Furthermore, the under-fire air supply is usually greater than

the amount required for the combustion of char. Thus, a major portion of the flaming combustion takes place very close to the grate.

Substituting the value of  $\dot{S}'''$ , given by equation (3.6), into equation (3.4) and integrating, based upon the boundary condition on the grate (i.e. at  $X = 0$ ,  $T = T_0$ ), results in the solution for the temperature in the combustion chamber:

$$T = \frac{\dot{m}_{ufa} \cdot C_{Pufa}}{\dot{m}_g \cdot C_{Pg}} T_0 + \frac{\dot{m}_f \cdot LHV2}{\dot{m}_g \cdot C_{Pg}} \left[ \frac{D_1}{D_2} \right] (e^{D_2 X} - 1) - \frac{Q_{st}}{\dot{m}_g \cdot C_{Pg}}, \quad (3.7)$$

where  $\dot{m}_{ufa}$  and  $C_{Pufa}$  are, respectively, the mass flow rate and specific heat capacity of the under-fire air and  $Q_{st}$  is the heat loss,  $X = 0$  to  $X$ , from the combustion chamber.

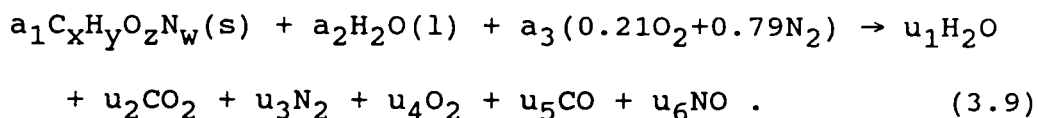
Injection of the over-fire air at a temperature lower than the combustion product temperature will result in cooling of the mixture. The effect of cooling is accounted for by a correction term added to equation (3.7). Therefore, the temperature profile in the combustion chamber is given by equation:

$$T = \frac{\dot{m}_{ufa} \cdot C_{Pufa}}{\dot{m}_g \cdot C_{Pg}} T_0 - \frac{\dot{m}_{ofa} \cdot C_{Pofa}}{\dot{m}_g \cdot C_{Pg}} T_{ofa} + \frac{\dot{m}_f \cdot LHV2}{\dot{m}_g \cdot C_{Pg}} \left[ \frac{D_1}{D_2} \right] (e^{D_2 X} - 1) - \frac{Q_{st}}{\dot{m}_g \cdot C_{Pg}}, \quad (3.8)$$

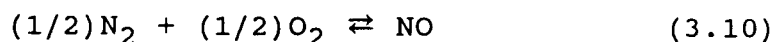
where  $\dot{m}_{ofa}$ ,  $T_{ofa}$  and  $C_{pofa}$  are, respectively, the mass flow rate, temperature and specific heat capacity of the over-fire air.

### 3.1.2 Composition Profile

Once the temperature of the combustion product has been calculated, the composition of the gas mixture can be estimated from a chemical equilibrium model. From the ultimate analysis of the fuel (Table 1.1), an empirical formula for wood in the form of  $C_xH_yO_zN_w$  can then be calculated. Moreover, it is assumed that the combustion products consist of  $H_2O$ ,  $CO_2$ ,  $N_2$ ,  $O_2$ ,  $CO$  and  $NO$ . Therefore the combustion reaction can be written as:



In equation (3.9),  $a_1$ ,  $a_2$  and  $a_3$  are, respectively, the moles of fuel, moisture in the fuel and combustion air; the coefficients  $u_1$  through  $u_6$  must be determined. The balance between the C, H, N and O atoms provides four equations, while two additional equations are obtained from the following dissociation reactions:



and



Using the temperature calculated from equation (3.8), the values of the equilibrium constant  $K_p$  [Kanury 1977] for re-

actions (3.10) and (3.11) can be determined. The equilibrium constants and the mole fractions of the constituents of the reactions are related as

$$K_{pNO} = \left[ \frac{Y_{NO}}{(Y_{O_2} Y_{N_2})^{1/2}} \right] \quad (3.13)$$

and

$$K_{pCO_2} = \left[ \frac{Y_{CO} (Y_{O_2})^{1/2}}{Y_{CO_2}} \right], \quad (3.14)$$

where  $Y$  is the mole fraction of the particular specie. Solution of the six equations mentioned above will give the composition of the combustion products.

### 3.2 Experiments

Seventeen experiments were carried out for the measurement of combustion product temperature and composition profiles. The measurements were taken from 61 cm above the grate to 1 cm above the grate (see Chapters 1 and 2). The conditions for these experiments are given in Table 3.1.

The First Law efficiency (denoted by EFF11) of the overall process is also given in Table 3.1. This efficiency is defined as the energy content of the combustion products (upon leaving the combustion chamber) divided by the energy input to the combustion chamber. Therefore, EFF11 accounts for the heat loss from the combustion chamber wall, as well as losses resulting from incomplete com-



Table 3.1 Experimental test conditions.

EXP. CODE	EXP. NO. (see APP.)	FUEL	FUEL FEED RATE (dry Kg/hr)	U.F. AIR TEMP. (deg. C)	FUEL M.C W.B.%	EXCESS AIR percent	U.F. AIR FRACTION percent	EFF11 percent
A	3	D.FIR	1.82	28	54	117	50	71
B	6	D.FIR	1.85	29	35	113	50	61
C	9	D.FIR	1.89	28	11	108	50	55
D	12	D.FIR	1.95	31	54	123	50	76
E	13	D.FIR	1.95	32	54	78	50	68
F	14	D.FIR	1.95	207	54	63	50	63
G	15	D.FIR	2.08	207	35	53	50	51
H	17	D.FIR	2.10	30	11	87	50	52
I	20	D.FIR	1.03	35	53	83	35	55
J	21	D.FIR	1.03	32	53	119	35	60
K	22	D.FIR	1.17	33	11	62	35	40
L	23	D.FIR	1.17	34	11	91	35	46
M	24	D.FIR	1.13	96	53	88	35	58
N	25	D.FIR	1.13	207	53	75	35	54
O	26	PHC	1.94	33	8	68	35	54
P	27	KMP	1.88	32	7	74	35	49
Q	28	BCCP	1.90	31	8	71	35	52

bustion of the fuel and the emission of unburned particulate. In Chapter 4, a detailed discussion of the efficiency of the overall combustion process and a comparison between the actual and the adiabatic composition of the combustion products are given.

### 3.3 Experimental Results

#### 3.3.1 Temperature Profile

The temperature profile predicted from equation (3.8) is based upon the assumption of the complete combustion of the fuel. For the experiments listed in Table 3.1, as indicated by the given efficiencies, the actual combustion of the fuel was less than complete. In fact, one of the shortcomings of the method described in section 3.1.1 is that it does not account for the factors that affect emis-

sions of the unburned particulate or the conversion of carbon to CO rather than to CO<sub>2</sub>. For purposes of calculation, it was assumed that 95% of the heating value of the fuel was consumed, and the remaining 5 percent was not utilized due to emissions of unburned particulate and the conversion of carbon to CO. For purposes of comparison, selected experimental temperature profiles for the case of 85% conversion are also presented. For most wood combustion systems, the conversion rate is reported to range from 92 to 98 percent [Tillman et al. 1989].

Figure 3.1 shows the temperature profile in the combustion chamber for experiment A, indicating excellent agreement between the model and the experimental results. The sudden drop in temperature at about 10 cm above the grate was due to introduction of over-fire air at temperature below that of the combustion products in the chamber. The over-fire tube was placed in the combustion chamber (Fig. 1.3), therefore the temperature of the over-fire air was increased substantially due to heat transfer from the combustion gases. The precise temperature was not measured for each experiment. However, previous experiments indicated that the over-fire air temperature was approximately 200°C lower than the temperature of the combustion products when they exit the over-fire air tube. Therefore, in equation (3.8) it was assumed that the over-fire air temperature was 200°C lower than the combustion temperature. However, it should be emphasized that this temperature

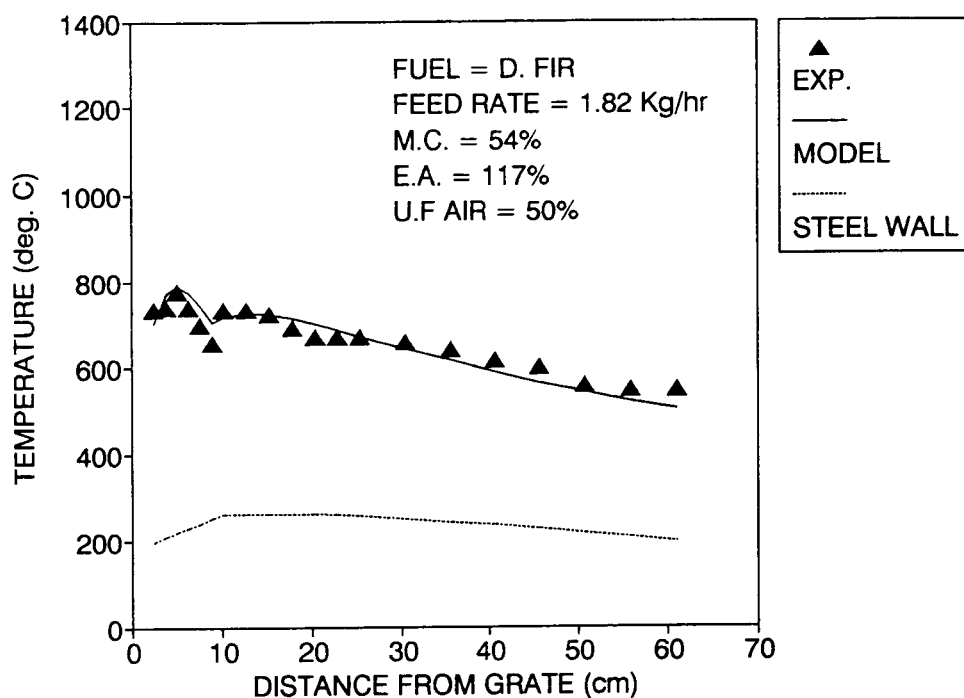


Figure 3.1 Temperature profile for experiment A.

differential can only be approximated. The precise temperature of the over-fire air as it exits the over-fire tube is dependent upon the amount of over-fire air and the combustion temperature.

Figure 3.2 shows the temperature profile for experiment B. For this experiment, temperatures were calculated for conversion rate cases of 95% and 85%. Note that the model prediction (95% conversion) was very close to the results given for this experiment, up to 10 cm above the grate. However, the temperature predicted by the model for distances approximately 15 cm above the grate or higher was consistently lower than the experimental measurements. In fact, the temperature above the over-fire air was much

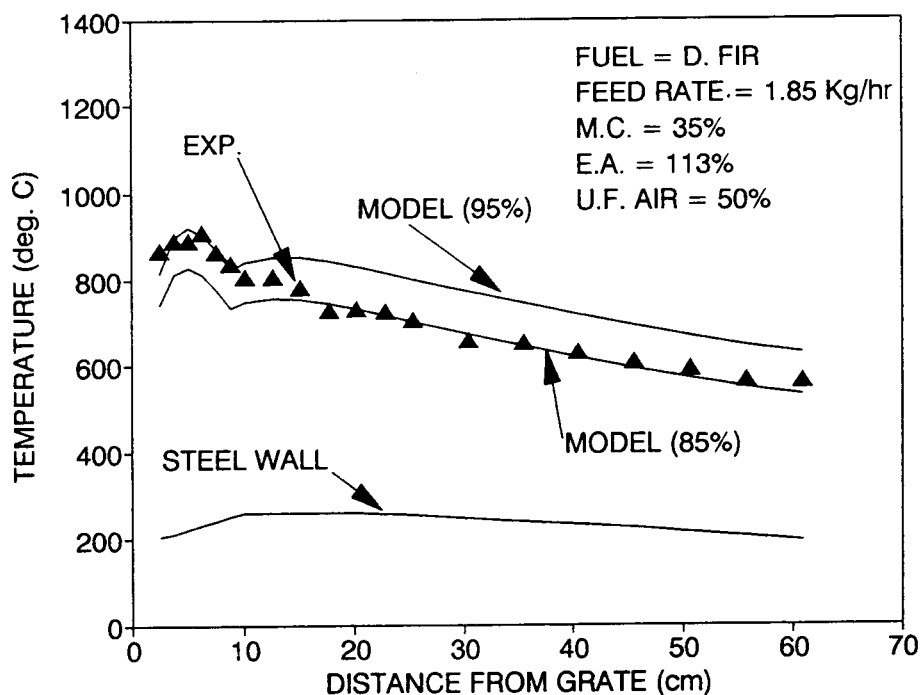


Figure 3.2 Temperature profile for experiment B.

closer to that for the 85 percent conversion rate. This was due to the introduction of low temperature over-fire air. For this experiment, note that the lower moisture content of the fuel resulted in higher combustion temperatures before the introduction of the over-fire air. Therefore, for this case, the assumption of a 200°C difference between the temperatures of the over-fire air and the combustion product would seem to be inaccurate. Furthermore, the introduction of low temperature over-fire air served to substantially reduce the overall efficiency of combustion. Junge [1975] recommended the use of the highest possible temperatures for over-fire air, and this re-

commendation has been substantiated by the present experiments.

Figures 3.3 and 3.4 show results for experiments C and F which were similar to the results for experiment B. As indicated in Table 3.1, the fuel moisture contents for experiments A and F, experiment B and experiment C were, respectively, 54%, 35% and 11%. The combustion of fuels with lower moisture contents resulted in higher temperatures for the combustion products prior to the introduction of the over-fire air. Therefore, the difference between the temperature of the combustion products and the over-fire air increased (experiments C and B) as fuel moisture content increased. Similar results were achieved by preheating the under-fire air (experiment F).

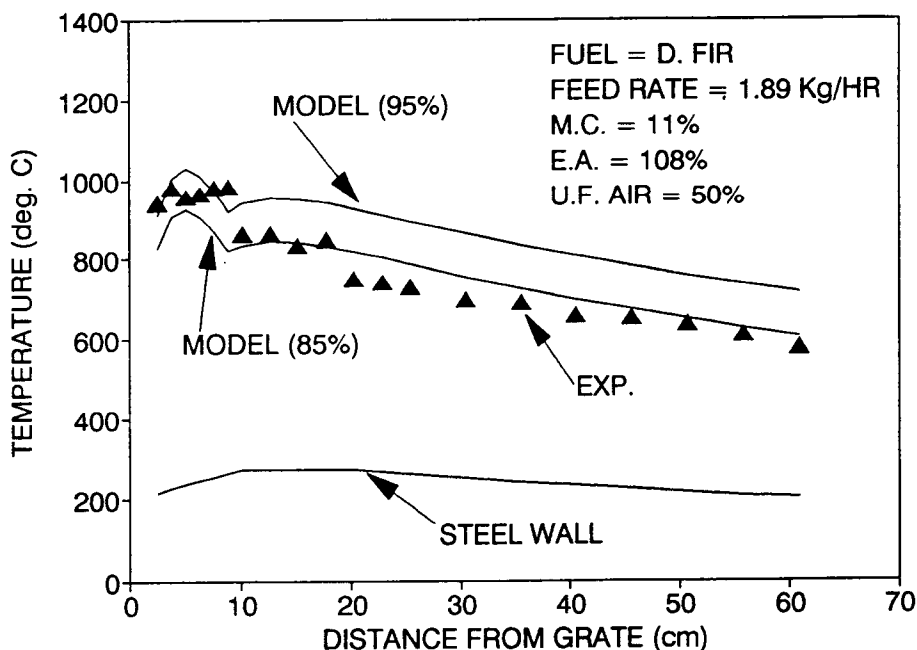


Figure 3.3 Temperature profile for experiment C.

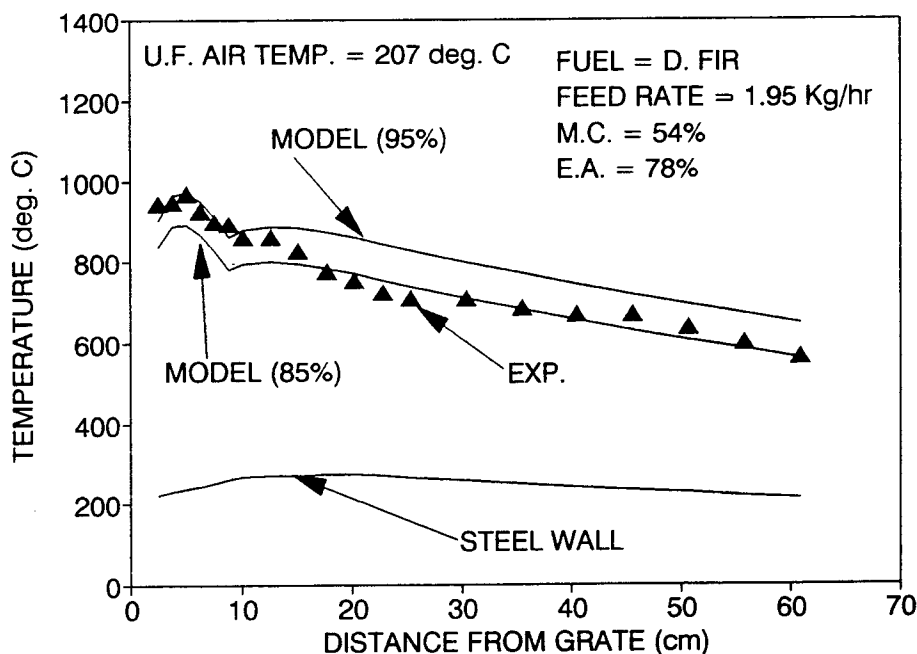


Figure 3.4 Temperature profile for experiment F.

The conversion rate for experiment D, shown in Figure 3.5, was higher than 95 percent. This may be attributed to the use of a higher fuel feed rate than was used in experiment A, resulting in an improvement in the conversion rate, as will be demonstrated in Chapter 4.

For experiments operated at off-design (part-load) conditions, similar results were obtained. The results for experiment L are shown in Figure 3.6. The off-design experiments (i.e., experiments I through N) were accompanied by periods of flare-up, particularly in cases where high moisture content fuels were used. This resulted in lower

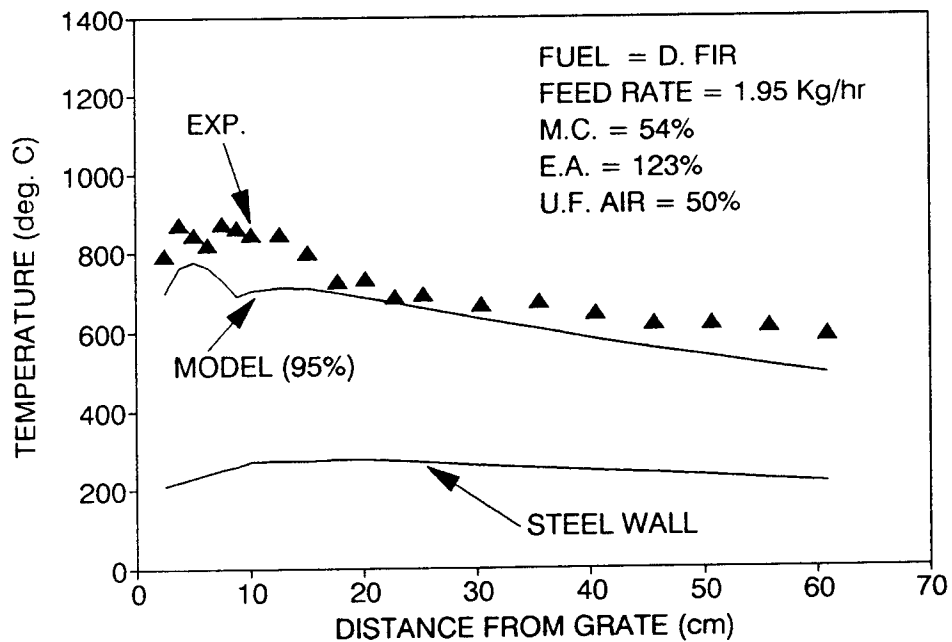


Figure 3.5 Temperature profile for experiment D.

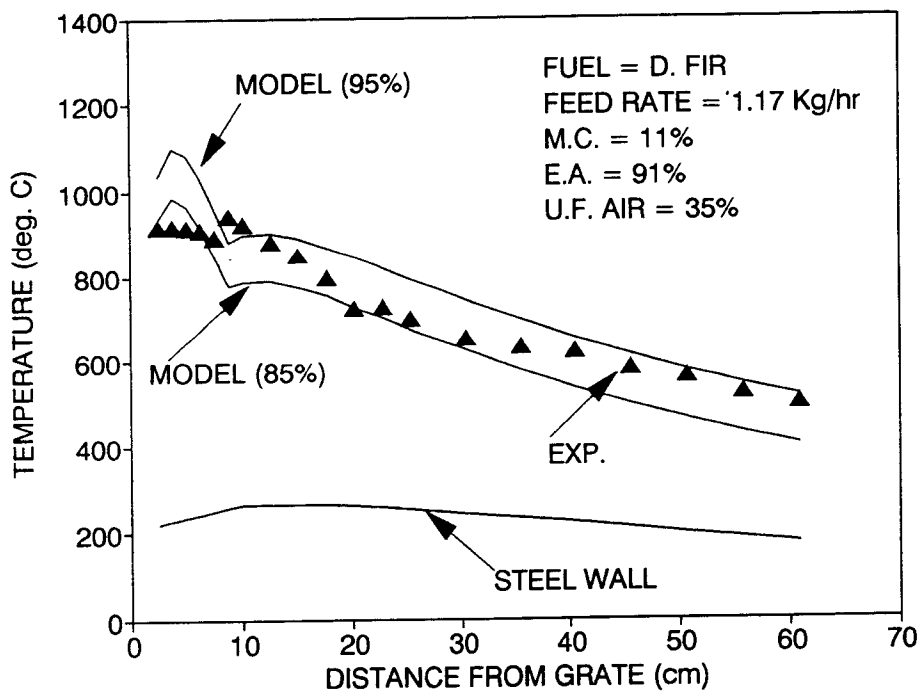


Figure 3.6 Temperature profile for experiment L.

combustion efficiencies and inconsistent temperature and composition readings.

The temperature profiles for pelletized fuels, used in experiments O, P and Q, are shown in Figures 3.7-3.9. The First Law efficiencies for these experiments were, respectively, 54%, 49% and 52%. At the 85% conversion rate, it was expected that the temperature profiles for these experiments would be close to the model predictions. This would have been principally due to higher levels of unburned particulate emissions resulting from the high percentage of fines in pelletized fuels.

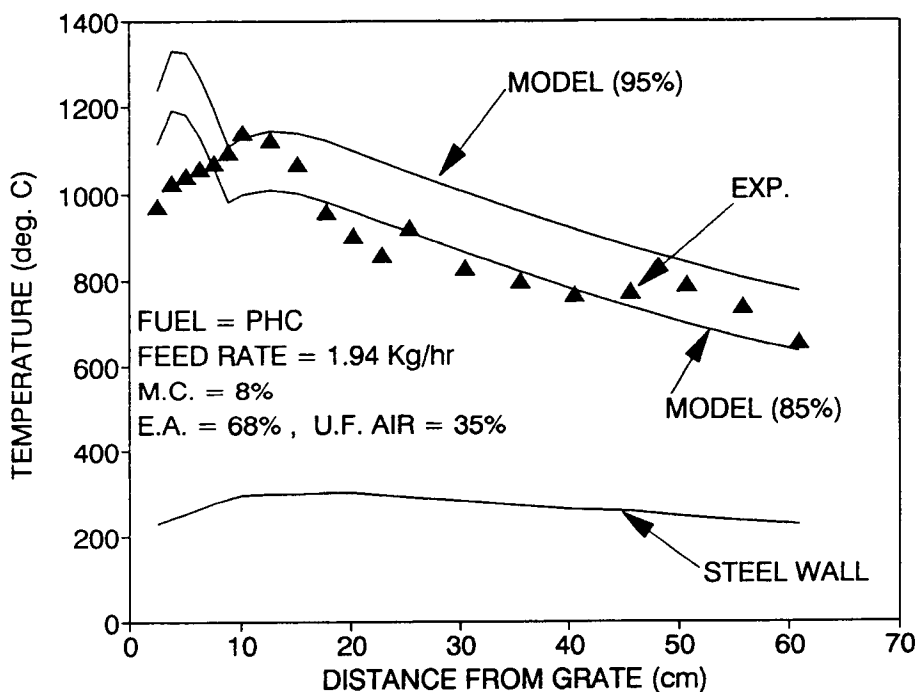


Figure 3.7 Temperature profile for experiment O.



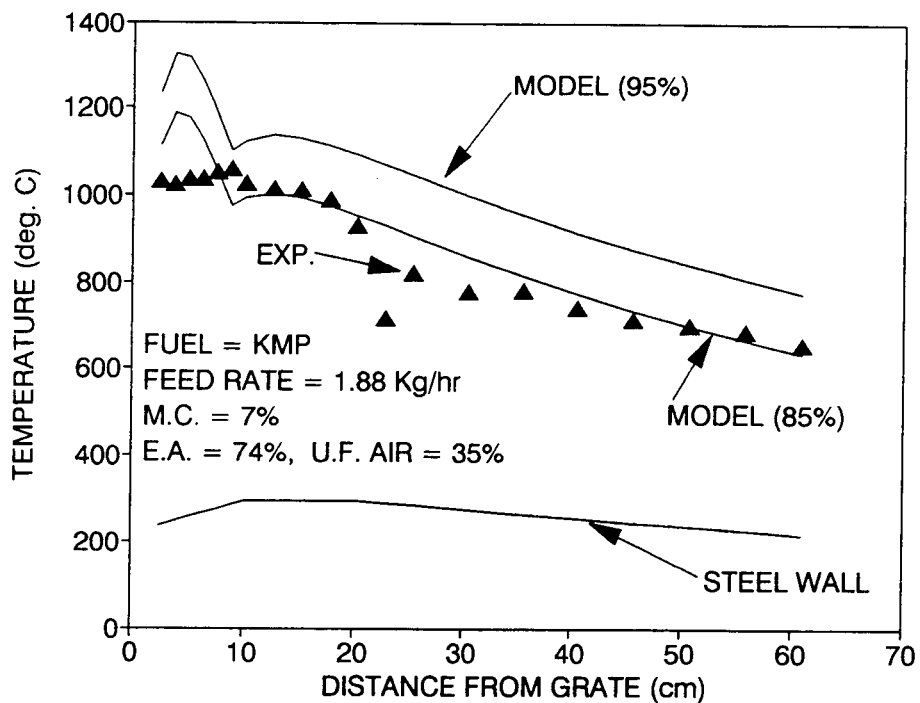


Figure 3.8 Temperature profile for experiment P.

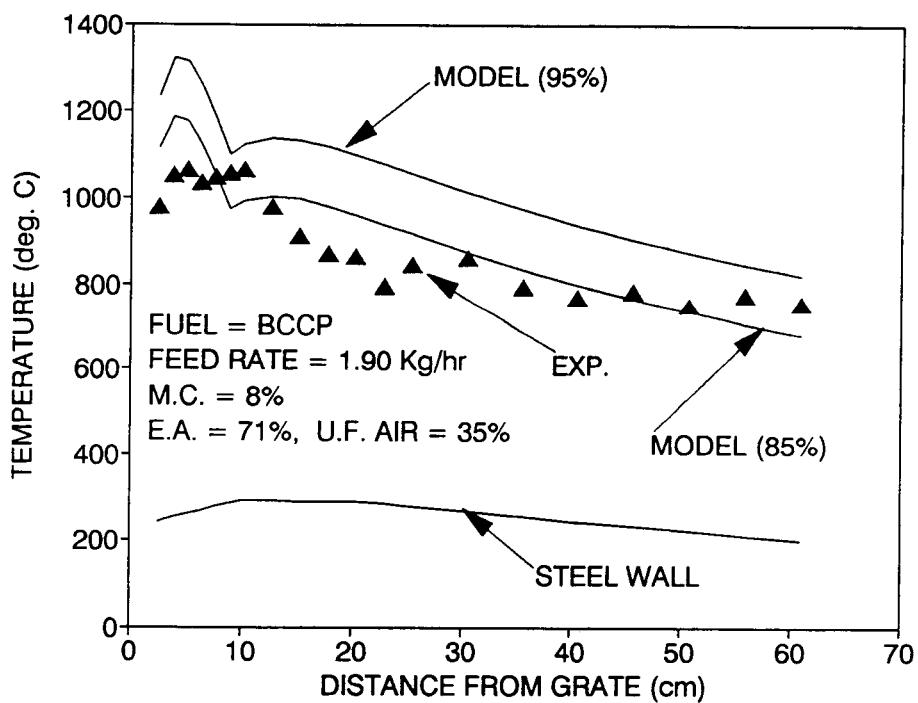


Figure 3.9 Temperature profile for experiment Q.

Although the temperature profiles above the over-fire air were relatively well predicted by the model at the 85 percent conversion rate, the profiles for the space below the over-fire tube was distinctly different from that of Douglas-fir. It should be pointed out that the pelletized fuels have a much higher density and lower porosity than wood. As discussed in Chapter 2, differences in density and porosity exercise a significant effect upon the rate of pyrolysis and the char combustion of the pellets. Furthermore, the amount of excess air and the fraction of under-fire air was less than the required amount for the complete combustion of the fuel on the grate. This was contrary to the calculation assumptions for the constants given in equation (3.6).

### 3.3.2 Composition

For prediction of the composition of the combustion products it was also assumed that 5% of the fuel leaving the combustion chamber would remain unburned. Similar to the results obtained for the temperature profiles, the amount of the unburned fuel was in some cases shown to be higher than 5%. This could be predicted to have a considerable effect upon the values of the constituents of the combustion products.

#### 3.3.2.1 **NO<sub>x</sub> and CO Content**

In Chapter 1, it was noted that the major portion of the NO<sub>x</sub> generated from combustion of wood is due to the ni-

trogen content of the fuel and not to the fixation of nitrogen in the combustion air [Howlett et al. 1977; Tillman et al. 1989]. In order to predict the amount of  $\text{NO}_x$  and CO generated from the combustion of hogged fuel, Junge [1979] recommended using an emission factor of 2.67 lbs of  $\text{NO}_x$  and 2 lbs of CO per ton of fuel. In general, it should be noted that hogged fuels contain higher amounts of nitrogen content than the Douglas-fir samples used in experiments A through N, and combustion of fuels with higher nitrogen contents results in higher levels of  $\text{NO}_x$  emissions.

The model described in this chapter predicted the emission of  $\text{NO}_x$  and CO based solely upon the temperature of combustion. To compare the results of  $\text{NO}_x$  and CO emissions based on the model and those recommended by Junge [1979], fuel-generated  $\text{NO}_x$  and CO was also calculated. The emission factor chosen for  $\text{NO}_x$  and CO were, respectively, 1.34 and 2 lbs per ton of fuel burned.

Figures 3.10-3.13 show the  $\text{NO}_x$  contents for combustion products calculated by the chemical equilibrium model, fuel-bound nitrogen and  $\text{NO}_x$  measured experimentally. The overall pattern for the equilibrium model was the same as for temperature, which was the expected result. However, the equilibrium model grossly underestimated the final  $\text{NO}_x$  content of the combustion products. Note that the temperature used to determine  $\text{NO}_x$  was calculated from equation (3.8) (i.e., based on a 95% conversion rate). Therefore,

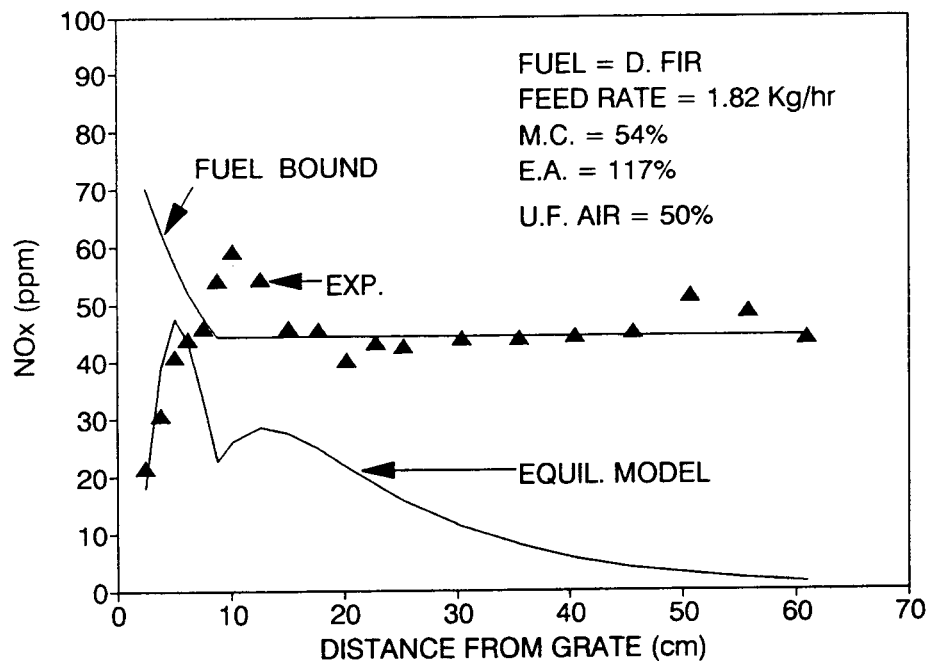


Figure 3.10  $\text{NO}_x$  profile for experiment A.

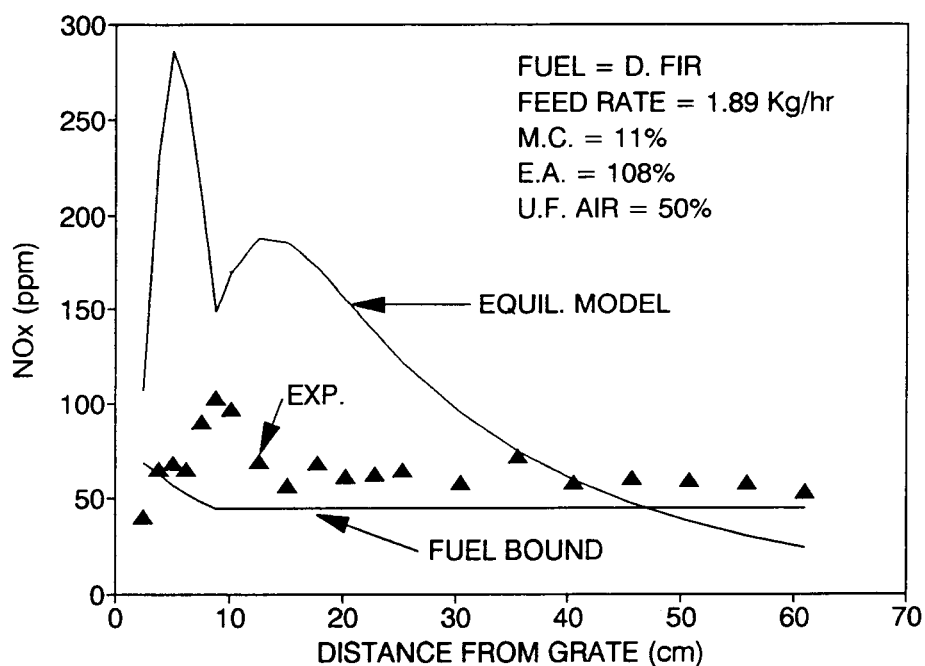


Figure 3.11  $\text{NO}_x$  profile for experiment C.

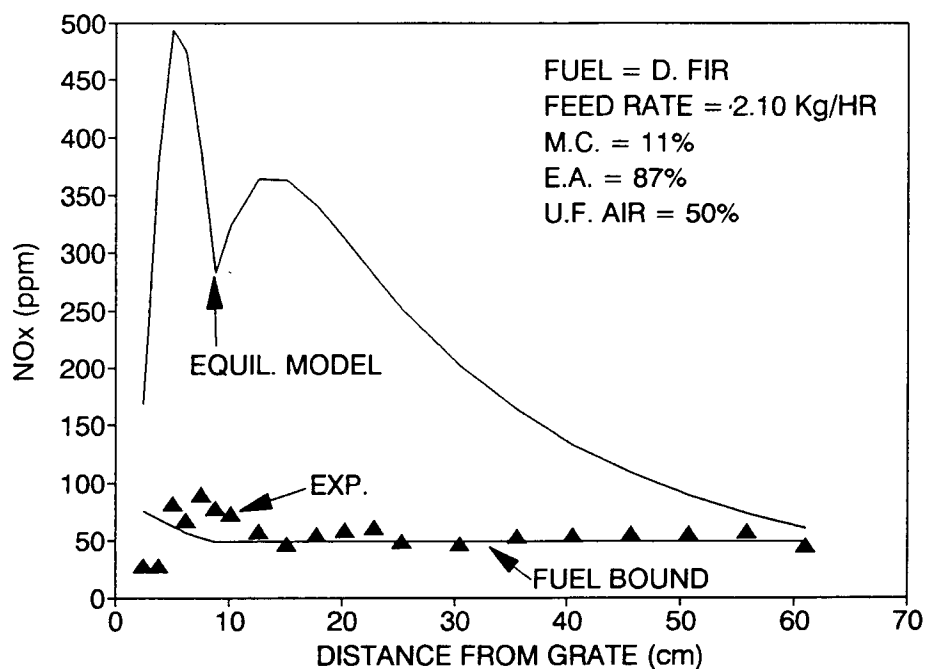


Figure 3.12 NO<sub>x</sub> profile for experiment H.

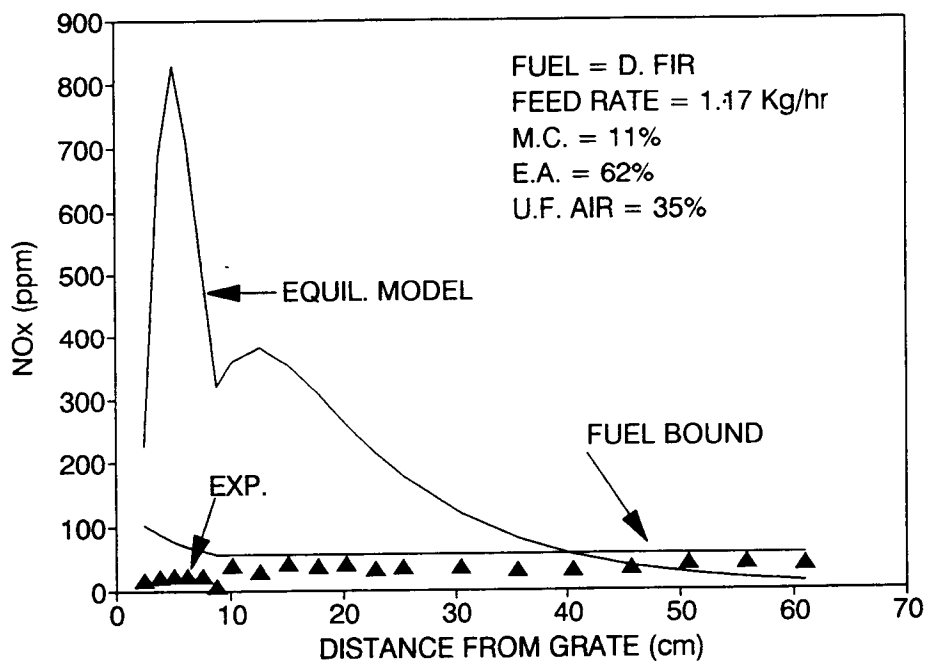


Figure 3.13 NO<sub>x</sub> profile for experiment K.

when the temperatures were overestimated, so was the  $\text{NO}_x$  content. However,  $\text{NO}_x$  calculations based on fuel-bound nitrogen seemingly predict the final  $\text{NO}_x$  contents of the combustion products very well.

Figures 3.14-3.16 show the  $\text{NO}_x$  profile in the combustion chamber for experiments O, P and Q. The  $\text{NO}_x$  contents for these three experiments were substantially higher than those for the Douglas-fir experiments. This was due to the higher nitrogen contents of these fuels (Table 1.1). For these three experiments, note that the temperatures were overestimated by equation (3.8). Therefore, if actual experimental temperatures had been used, the model would have underestimated the  $\text{NO}_x$  content of the combustion products to an even greater extent.

The chemical equilibrium model presented in this chapter predicted zero CO content for all experiments. However, CO content calculations, based on an emission factor of 2 lbs of CO per ton of fuel, predicted the CO profile reasonably well. The results for experiments A, H and Q are shown, respectively, in Figures 3.17-3.19. It should be noted that CO readings by the combustion gas analyzer showed a high degree of sensitivity to the occurrence of disturbances during the conduct of the experiments. For the experiments with low excess air, the amount of CO present in the combustion products prior to the introduction of over-fire air exceeded the limit of the combustion gas

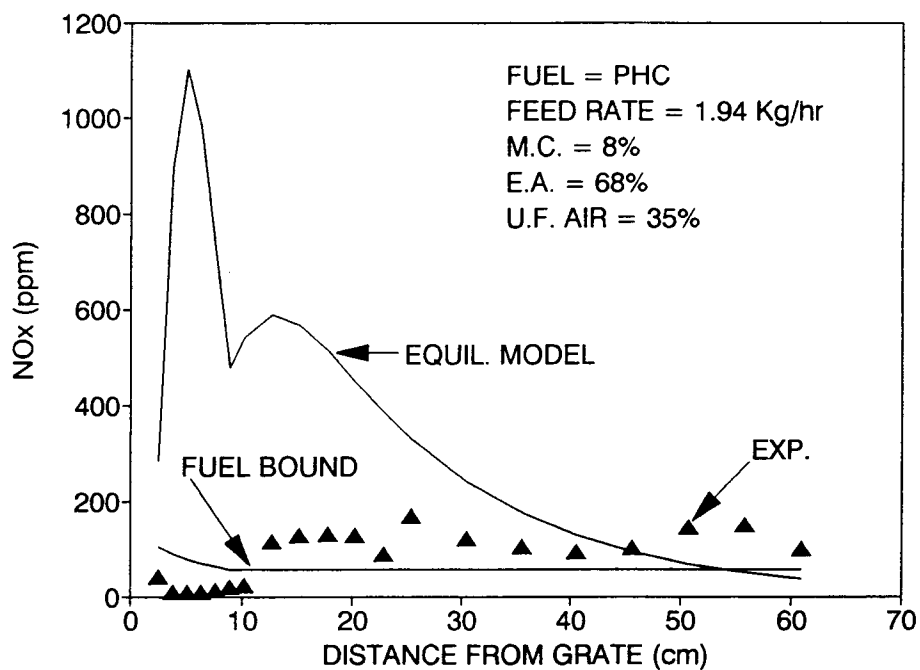


Figure 3.14 NO<sub>x</sub> profile for experiment O.

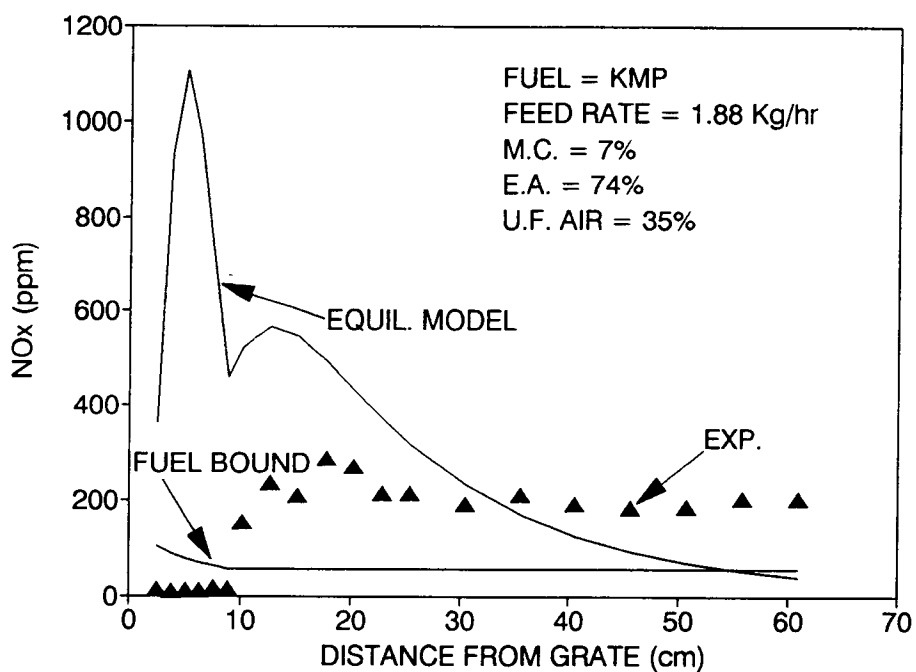


Figure 3.15 NO<sub>x</sub> profile for experiment P.

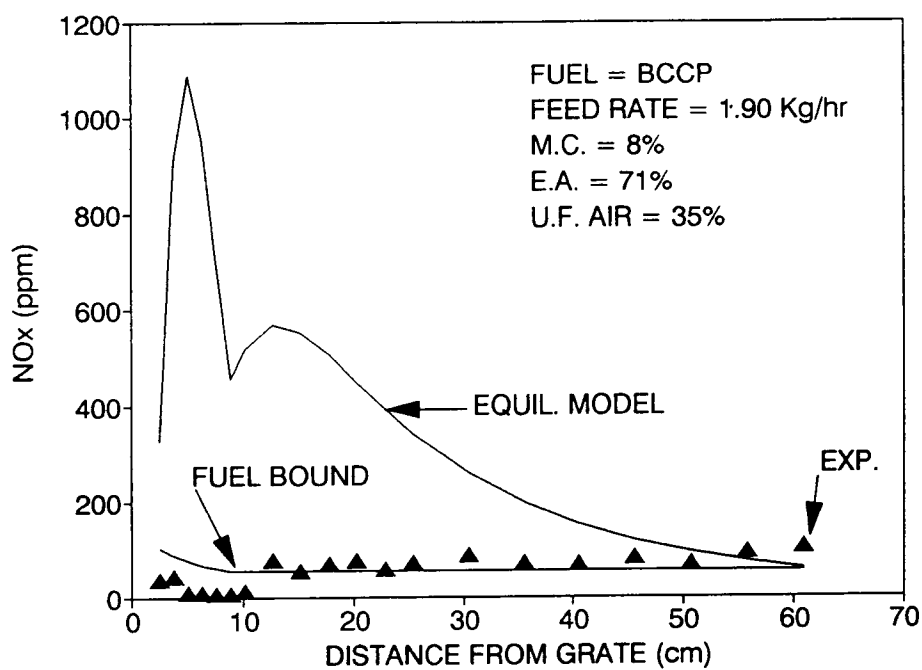


Figure 3.16 NO<sub>x</sub> profile for experiment Q.

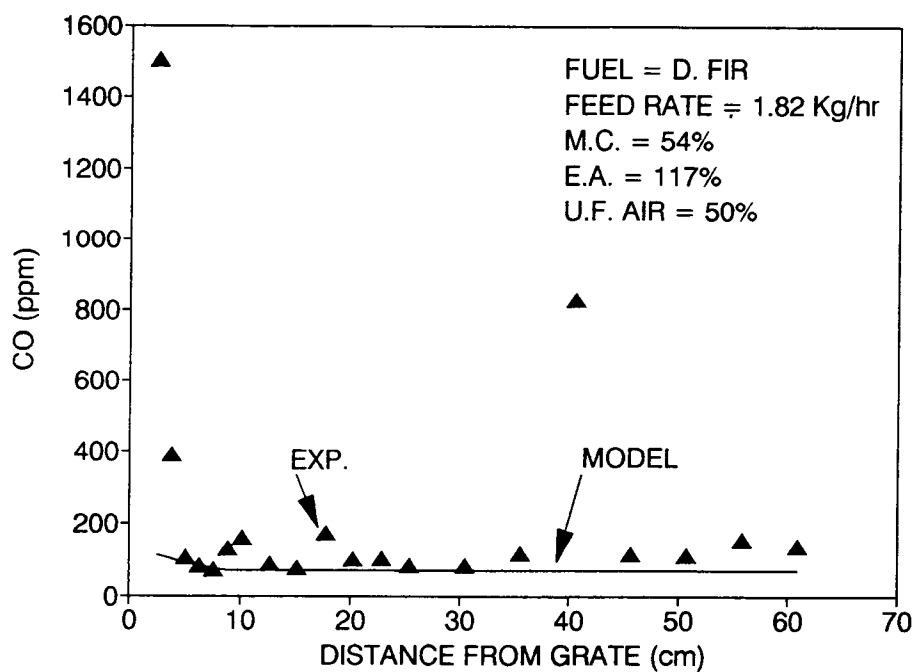


Figure 3.17 CO profile for experiment A.



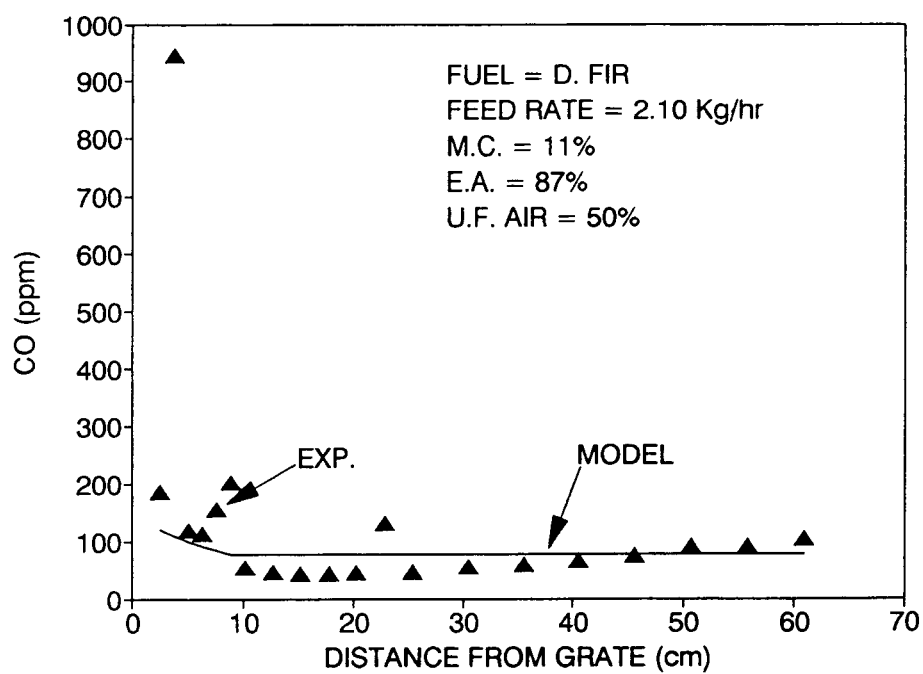


Figure 3.18 CO profile for experiment H.

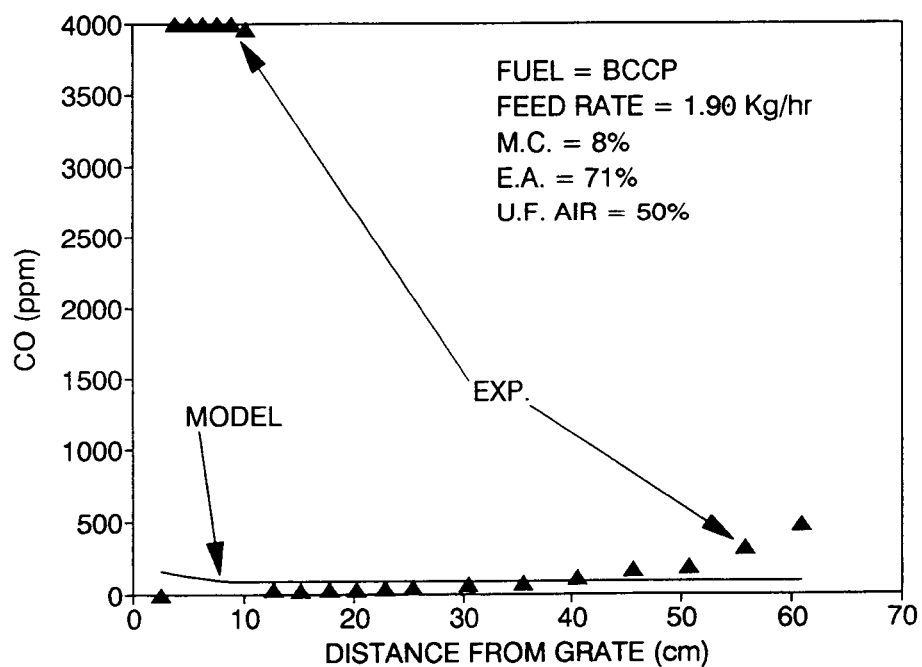


Figure 3.19 CO profile for experiment Q.

analyzer. In such a case (i.e., Fig. 3.19) the maximum reading of the gas analyzer was reported.

#### 3.3.2.2 O<sub>2</sub> and CO<sub>2</sub> Profiles

Comparison of the O<sub>2</sub> and CO<sub>2</sub> profiles predicted by the model and the experimental measurements for experiments A, B and K are presented in Figures 3.20-3.22, respectively. The model predictions for the above over-fire air tube seems to be in fair agreement with the experimental measurements. However, the model predictions for below the over-fire tube do not follow the same patterns as the experimental results. This was in part due to presence of other constituents in the gas mixture, such as hydrocarbons resulting from fuel pyrolysis, which were not considered in the model. Lack of mixing was another contributing factor to differences between the experimental readings and the model predictions.

### 3.4 Conclusion

In this chapter an analytical model was presented for the prediction of temperature profiles in the combustion chamber. This model used the temperature of the outer wall of the combustion chamber (for calculation of heat losses) and fuel and air inputs to the chamber to predict temperatures inside the combustion chamber. The results of the model were in good agreement with the experimental results.

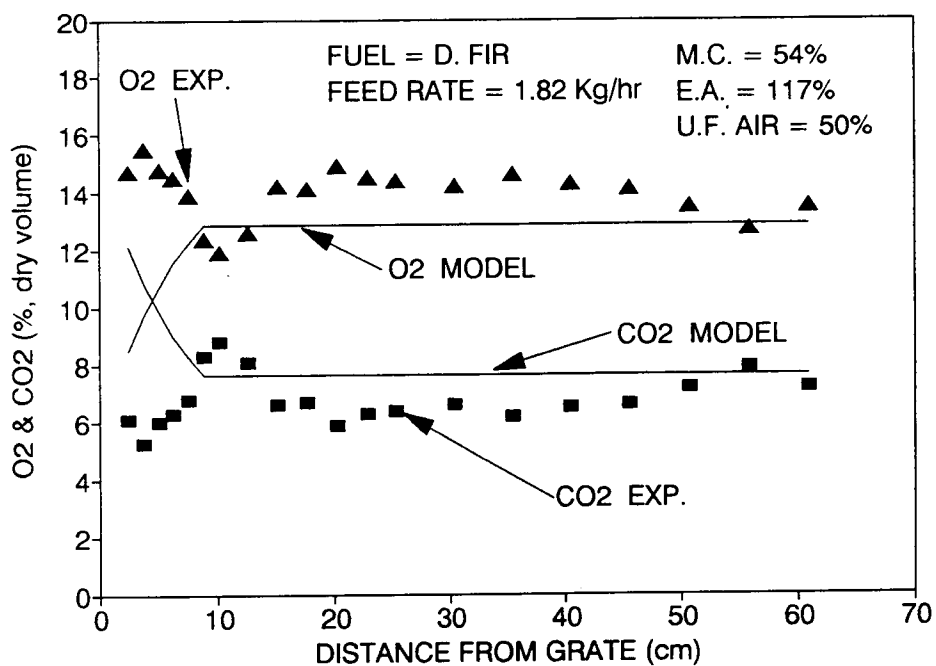


Figure 3.20 O<sub>2</sub> and CO<sub>2</sub> profiles for experiment A.

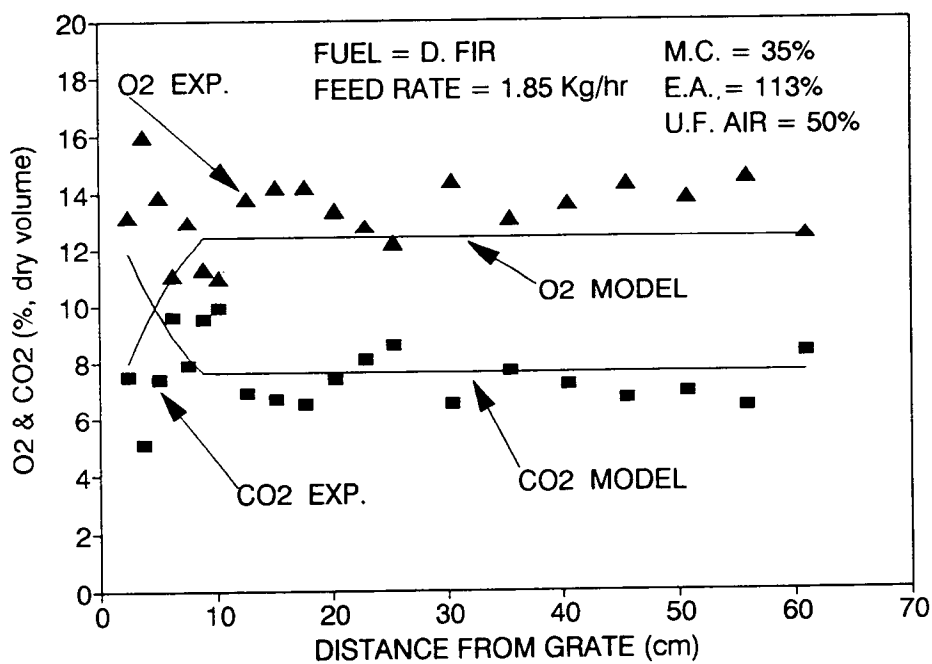


Figure 3.21 O<sub>2</sub> and CO<sub>2</sub> profiles for experiment B.

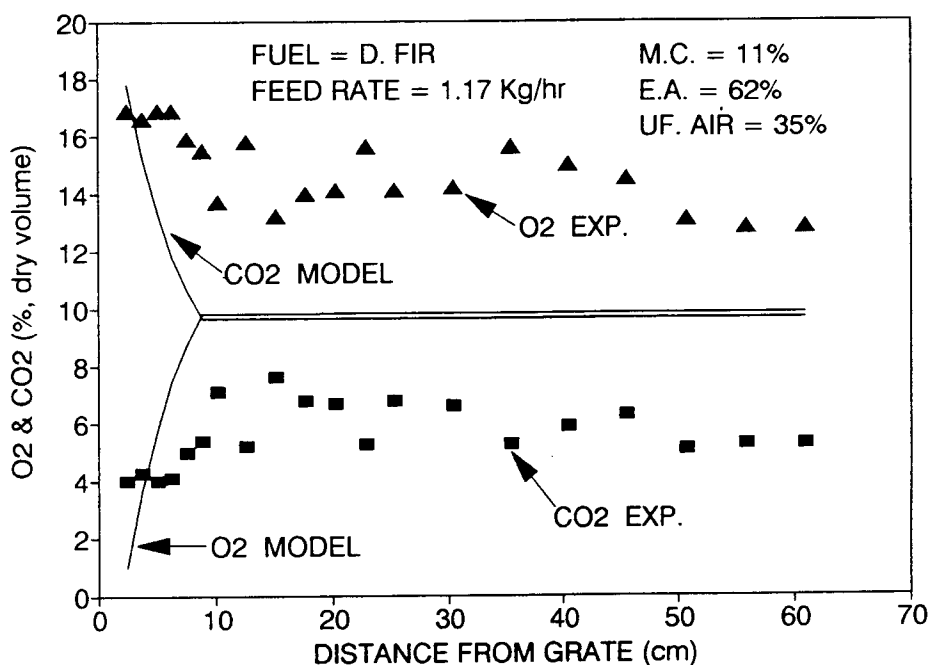


Figure 3.22 O<sub>2</sub> and CO<sub>2</sub> profiles for experiment K.

However, the model could be significantly improved if precise over-fire air temperatures and the final fuel conversion rates (i.e., the CO<sub>2</sub> content of the exhaust) were known.

A chemical equilibrium model was used for the estimation of composition profiles within the combustion chamber. This model predicted O<sub>2</sub> and CO<sub>2</sub> profiles for the above over-fire air port reasonably well. Just as for the temperature profile model, however, further improvements could be realized if the final conversion rates of the fuel were known. In addition, the chemical equilibrium failed to predict NO<sub>x</sub> and CO profiles. This leads to the conclusion

that the  $\text{NO}_x$  generated from the combustion of wood is largely dependent upon fuel-bound nitrogen, particularly in low efficiency combustion units operated at low temperatures. The CO and  $\text{NO}_x$  predictions, for modified conversion factors, recommended by Junge [1979] seem to be in general agreement with the experimental results.

The models for the temperature and composition profiles failed to account for factors that increased the emissions of particulate. However, if overall efficiency (i.e., the conversion of fuel carbon to  $\text{CO}_2$ ) were known, the  $\text{O}_2$ ,  $\text{CO}_2$  and temperature profiles could have been predicted with greater accuracy.

## CHAPTER 4

### PERFORMANCE OF THE COMBUSTION SYSTEM

This chapter presents the results from an experimental investigation of the performance of the combustion unit described in Chapter 1. The objective of the investigation was to identify and highlight the relationships between the variables affecting the combustion process and the performance of the combustion unit. The variables related to fuel include moisture content and the size of the fuel particles. Variables related to the control of the combustion system include the amount of excess air, the ratio of under-fire to over-fire air and the temperature of under-fire air. To examine the off-design (part-load) performance of the combustion unit, a range of different fuel feed rates from full-load to half-load were selected for experimentation.

The data collected from these experiments was used in a linear regression program to generate sets of regression coefficients. These coefficients enabled the prediction of combustion products and combustion system performance over a wide range of variables. A computer model was used to predict the composition and temperature of the combustion products for each experiment under adiabatic conditions, and to calculate combustion process efficiencies with adia-

batic counterparts for each experiment. The resultant efficiencies provided a tool for the comparison of experimental results with ideal cases.

#### 4.1 Adiabatic Combustion Model, Experiments and Regression Analysis

A computer model for wood combustion [Dadkhah-Nikoo 1987; 1985] was used to predict the results of experiments under adiabatic conditions.

##### 4.1.1 Adiabatic Combustion Model

For model development, different efficiencies were defined to emphasize the significance of moisture and exhaust losses. Two efficiencies were defined based on the First Law of thermodynamics, allowing the analysis of the combustion process based upon the energy content of the fuel. Three efficiencies were defined based on the Second Law of Thermodynamics, allowing the analysis of the combustion process based on the exergy of the fuel. Exergy (or availability) is defined as "a property which measures the maximum work which can be obtained from the system when it is allowed to come into equilibrium with the atmosphere" [Reistad 1970]. First Law efficiencies are denoted by EFF11 and EFF12 and Second Law efficiencies are denoted by EFF21, EFF22 and EFF23.

EFF11 is defined as:

$$\frac{\text{enthalpy of combustion products}}{\text{energy input to combustion units}} .$$

The heat of vaporization of the moisture in wood is included in the enthalpies used in this definition as well as those subsequently discussed in this chapter. Moreover, energy input to the system is the sum of the energy content of the combustion air as well as the higher heating value of the fuel. In turn, EFF12 is defined as:

$$\frac{\text{enthalpy of combustion products} - \text{enthalpy of exhaust gases}}{\text{energy input to combustion unit}} .$$

The difference between EFF11 and EFF12 represents the exhaust loss. This loss results from exhausting the combustion products at high temperatures. For most applications, the exhaust temperature is sufficiently high to keep the water in exhaust gases in vapor or superheated vapor form. For this experimental investigation, since the combustion products were not used in any process, an exhaust temperature of 250°F was assumed.

EFF21 and EFF22 are defined as:

$$\frac{\text{exergy of combustion products}}{\text{exergy of fuel} + \text{exergy of combustion air}} .$$

The calculation of EFF21 was based on the higher heating values of the fuel rather than exergy [Dadkhah-Nikoo 1985]; EFF22 and EFF23 were calculated based on the exergy of the fuel.

EFF23 is defined as:

$$\frac{\text{exergy of combustion products} - \text{exergy of exhaust gases}}{\text{exergy of fuel} + \text{exergy of combustion air}} .$$



The gas properties used for the adiabatic cases were based on compositions predicted by the adiabatic model. For the experiments the properties were calculated according to the compositions measured for each experiment.

#### 4.1.2 Experiments

As noted in Chapter 1, there is a wide variation in wood fuel moisture content, composition, and size distribution. To investigate the influence of selected variables, several experiments were designed and carried out. The fuel used for these experiments was Douglas-fir, the proximate and ultimate analyses, higher heating values, and ash fusion temperatures for which are given in Chapter 1.

To examine the effect of fuel particle size variations, samples in cubed form were prepared in three sizes, 1/4, 3/8, and 1/2 inches. Moisture levels were controlled at 11, 35 and 53 percent (wet basis), and various levels of excess air, fractions of under-fire air and under-fire air temperatures were selected. To study the off-design (part-load) performance of the combustion unit, a range of different fuel feed rates, from full-load (4 lb/hr) to half-load (2 lbs/hr), were chosen for the experiments. Table 4.1 presents the actual test settings for the experiments.

To reflect the collective characteristics of each experiment, temperature and composition data were collected at distances ranging from 16 to 24 inches from the grate at 2-inch intervals within the combustion chamber. At each

Table 4.1 Experimental settings for the experiments and independent variables for regression analysis.

Exp. No.	Fuel Feed Rate dry lb/hr	Fuel M.C. W.B. %	Excess Air %	U.F. Air %	U.F. Air Temp. deg. F	Fuel Size sq. in.
1	4.01	54	116	35	84	0.84375
2	4.01	54	117	65	82	0.84375
3	4.01	54	117	50	82	0.84375
4	4.07	35	114	65	82	0.84375
5	4.07	35	113	35	84	0.84375
6	4.07	35	113	50	84	0.84375
7	4.17	11	108	65	83	0.84375
8	4.17	11	108	35	81	0.84375
9	4.17	11	108	50	83	0.84375
10	4.43	35	72	50	89	0.84375
11	4.43	35	116	50	88	0.84375
12	4.29	54	123	50	87	0.84375
13	4.29	54	78	50	89	0.84375
14	4.29	54	63	50	405	0.84375
15	4.59	35	53	50	405	0.84375
16	4.99	11	40	50	408	0.84375
17	4.62	11	87	50	84	1.5
18	4.62	11	108	50	85	1.5
19	4.62	11	66	50	88	1.5
20	2.26	53	83	35	96	0.375
21	2.26	53	119	35	91	0.375
22	2.58	11	62	35	90	0.375
23	2.58	11	92	35	93	0.375
24	2.49	53	88	35	206	0.375
25	2.49	53	75	35	406	0.375

data point, 15 combustion gas samples were analyzed and recorded. Two temperature probes, located at the same distance from the grate and equidistant from the gas probe, were used to record three temperature readings of the combustion products from each probe. Therefore, 15 gas composition and 6 temperature readings were collected at each point. Each experiment was represented by a single temperature and a single composition (that is, an average of 30 temperature measurements and an average of 80 composition measurements). The compositions were specified by the

amounts of  $O_2$ ,  $CO_2$  and the combustibles ( $CH_4$ ),  $CO$ ,  $NO_x$ ,  $SO_2$ , and  $H_2S$ . Since the  $SO_2$ ,  $H_2S$  and combustible measurement values were not significant, these values are not reported in the current investigation.

It should be noted that the particulate sampler used for these experiments was designed for larger exhaust flow rates; therefore, for these experiments the particulate sampler was operated near its lower limit. In addition, since a significant amount of cooling air was introduced into the exhaust stream (to protect the opacity meter), the test results were not adjusted to 12 percent  $CO_2$ . On average, exhaust compositions at the point of particulate sampling for all tests contained approximately 3.5 percent  $CO_2$ . For the reasons cited above, experimental results pertaining to particulate samples should be interpreted with caution.

The results of the experiments are presented in Tables 4.2A and 4.2B. Table 4.3 shows the results of the adiabatic model for the operating conditions specified in Table 4.1.

#### 4.1.3 Regression Model

A linear regression model was used to generate sets of regression coefficients to investigate the effects of individual variables on combustion unit performance. The independent variables for the model are given in Table 4.1; the dependent variables include combustion product tempera-

Table 4.2A Experimental results.

Exp. No.	Comb. Temp. deg. F	O2 dry vol. %	CO2 dry vol. %	NOx dry vol. ppm	CO dry vol. ppm	Particulate darin/dscf	Combustible in part. %
1	1045	14	7	46	187	0.0077	42
2	1057	13	7	51	432	0.0079	34
3	1067	14	7	47	272	0.0068	33
4	1091	14	7	51	95	0.0056	17
5	1091	14	7	48	105	0.0057	20
6	1097	14	7	49	68	0.0035	20
7	1180	12	8	58	336	0.0128	13
8	1179	12	8	59	151	0.0071	7
9	1160	13	8	57	82	0.0037	4
10	1210	12	9	59	87	0.0051	24
11	1149	14	6	42	87	0.0054	0
12	1140	14	7	49	120	0.0074	0
13	1154	12	8	54	112	0.0057	0
14	1162	17	4	28	169	0.0061	8
15	1189	18	3	20	54	0.0051	0
16	1260	13	8	54	103	0.0071	0
17	1188	12	9	54	87	0.0078	0
18	1186	15	6	33	172	0.0103	0
19	1276	12	9	55	61	0.0068	11
20	892	15	5	25	792	0.0359	87
21	872	15	4	32	1694	0.0869	94
22	1023	14	6	38	119	0.0092	10
23	1039	18	3	17	83	0.0115	23
24	945	17	4	22	1084	0.0289	74
25	914	14	6	32	542	0.0512	91

Table 4.2B Experimental results (continued).

Exp. No.	EFF11 %	EFF12 %	EFF21 %	EFF22 %	EFF23 %	Heat Loss btu/hr
1	70	40	26	25	20	10661
2	71	41	27	25	20	10351
3	71	41	27	26	20	10145
4	61	39	25	24	19	14067
5	60	39	25	23	19	14179
6	61	39	25	24	20	14070
7	56	41	26	24	21	16108
8	56	41	26	25	21	16048
9	55	40	25	24	20	16442
10	58	38	25	24	20	16372
11	64	43	27	25	21	14126
12	76	46	30	29	23	9047
13	68	40	27	25	20	12067
14	63	36	24	23	19	14342
15	51	32	21	20	17	20288
16	44	31	20	19	16	25463
17	52	37	24	23	19	19379
18	56	41	25	24	21	17763
19	51	37	24	23	19	19823
20	55	28	18	17	13	8845
21	60	31	19	19	14	7981
22	40	27	16	15	13	13677
23	46	32	18	18	15	12185
24	58	31	20	19	15	9235
25	54	27	18	17	13	10264

Table 4.3 Adiabatic model results for the experimental settings.

Exp. No.	Comb. Temp. deg. F	O2 dry vol. %	CO2 dry vol. %	EFF11 %	EFF12 %	EFF21 %	EFF22 %	EFF23 %
1	1593	11	9	100	70	48	46	40
2	1588	11	9	100	70	48	46	40
3	1587	11	9	100	70	48	46	40
4	1853	11	9	100	79	54	51	47
5	1861	11	9	100	79	54	52	47
6	1861	11	9	100	79	54	52	47
7	2087	11	10	100	85	59	56	52
8	2080	11	10	100	84	59	56	52
9	2086	11	10	100	85	59	56	52
10	2161	9	12	100	80	57	55	50
11	1844	11	9	100	79	54	52	47
12	1563	12	9	100	70	48	45	40
13	1813	9	11	100	72	51	48	42
14	1988	8	12	100	73	54	52	46
15	2426	7	13	100	81	61	58	54
16	2876	6	14	100	87	67	64	60
17	2258	10	11	100	85	61	58	54
18	2089	11	10	100	85	59	56	52
19	2477	8	12	100	86	63	60	55
20	1809	10	11	100	73	51	49	43
21	1604	12	9	100	71	49	46	41
22	2546	8	12	100	86	63	60	56
23	2228	10	11	100	85	61	58	54
24	1798	10	11	100	73	51	49	43
25	1912	9	12	100	73	53	51	45

tures and compositions ( $O_2$ ,  $CO_2$ ,  $NO_x$ , and  $CO$ ), particulate emissions, the amounts of combustibles in the particulate, efficiencies, and heat losses. The results of the regression model (regression coefficients) are presented in Table 4.4.

Each dependent variable could be predicted using the coefficients provided in Table 4.4. In addition, standard errors and multiple coefficients of determination ( $R^2$ ) are also given. The multiple coefficients of determination, in a range from one (perfect correlation) to zero (no correla-

Table 4.4 Table of regression coefficients.

Variable (Y)	Unit	Constant	COEFFICIENTS						R**2	Standard Err. of Y
			Fuel Feed lb/hr	Moisture Content % W.B.	Excess Air %	U.F. AIR %	U.F. Air Temp. deg. F	Surface Area sq. in.		
Comb. Temp.	deg. F	841.6141	117.2459	-1.4243	-1.1325	0.1337	-0.1253	-32.2997	0.9591	25.6217
O2	%	14.9190	-0.9789	-0.0018	0.0209	-0.0110	0.0097	0.2560	0.4407	1.5544
CO2	%	4.1521	1.2361	0.0048	-0.0180	0.0113	-0.0087	-0.1176	0.5041	1.5054
NOx	ppm	13.7301	13.2059	-0.0406	-0.0555	0.1210	-0.0600	-14.8735	0.5864	9.8406
CO	ppm	893.5249	-439.7121	4.5404	3.4949	3.5030	0.7676	415.6050	0.5977	282.1554
Particulate	gr/dscf	0.1491	-0.0683	0.0003	0.0006	0.0000	0.0002	0.0754	0.6283	0.0387
Combustible	%	95.3295	-35.5112	0.5258	0.1623	-0.0321	0.0565	33.0666	0.8006	15.5545
EFF11	%	16.2632	4.4907	0.3640	0.1422	0.0100	-0.0103	0.0661	0.9557	2.1024
EFF12	%	7.2182	5.0743	0.0459	0.1107	0.0083	-0.0093	-1.3429	0.9372	1.5369
EFF21	%	3.6079	3.5186	0.0582	0.0560	0.0094	-0.0062	-0.6325	0.9216	1.1322
EFF22	%	3.4449	3.3511	0.0555	0.0531	0.0091	-0.0059	-0.6028	0.9217	1.0768
EFF23	%	2.1253	3.1779	0.0133	0.0481	0.0054	-0.0041	-0.8033	0.9235	0.9466
Heat Loss	btu/hr	11865.30	2443.20	-124.97	-44.62	-4.09	7.34	450.06	0.95	1085.63

tion), are defined as "explained variation divided by total variation." As indicated in the table,  $R^2$  for this range of experiments varied from 0.4407 to 0.9591. When the value of  $R^2$  was close to one, it was indicated that the linear regression model could be used to predict the variable with a high degree of accuracy over the range considered in the model; when the value of  $R^2$  was low, the non-linearity of the variable or the lack of correlation between the chosen variables was indicated.

The results of the adiabatic and regression models for experimental combustion temperatures are given in Figure 4.1. As shown in this figure, and indicated by the  $R^2$  value given in Table 4.4 for combustion temperatures, the regression model results were close approximations of the experimental measurements. However, the results of the adiabatic model were significantly different from the results of experimental measurements.

The  $O_2$  contents of the combustion products are shown in Figure 4.2. As indicated, agreement between the results of the regression model and the experiments was not as close as the results given in Figure 4.1. Nonetheless, the regression model provided significantly better approximations of the experimental values than did the adiabatic model.



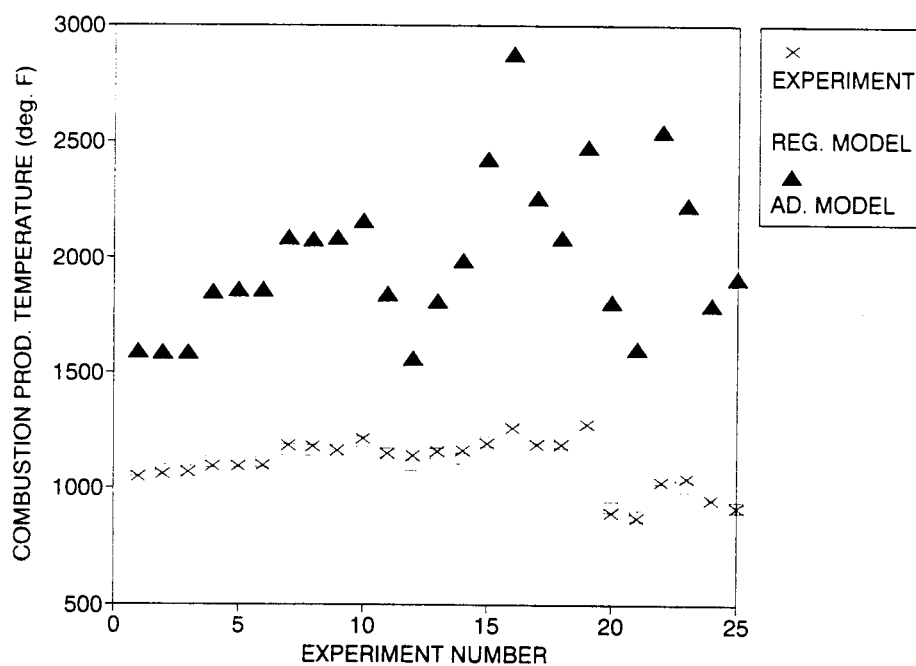


Figure 4.1 Comparison of the results for the adiabatic model, the experiments, and regression models for combustion temperatures.

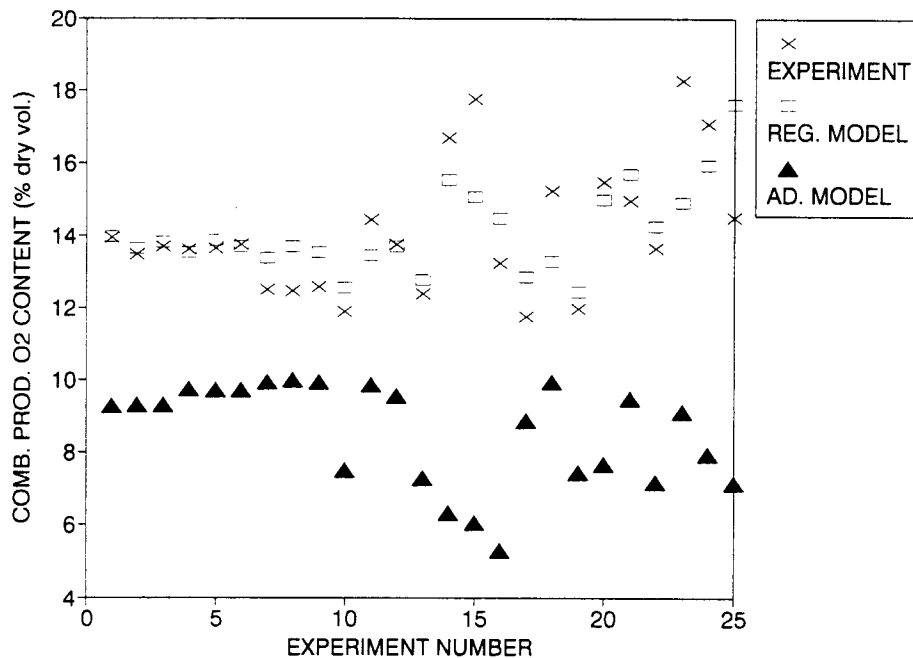


Figure 4.2 Comparison of the results for the adiabatic model, the experiments, and regression models oxygen content of combustion products.

#### 4.2 Experimental Results

For purposes of analysis, the term "heat loss" refers to the difference in energy input to the combustion chamber and the energy content of the combustion products. In this sense, heat loss is a combination of convective and radiative heat loss from the combustion chamber, incomplete combustion of the fuel (that is, conversion of carbon to CO rather than CO<sub>2</sub>), and emissions of unburned particulate. A significant portion of the "heat loss" was contributed by radiation and convection losses. The typical average temperature of the combustion chamber outside wall for the experiments was 400°F. Convective and radiative heat losses

at this temperature were estimated to be between 30 to 40 percent of the energy input (at full-load) to the combustion chamber.

#### 4.2.1 Part-Load Operation (Off-Design)

Figure 4.3 shows the effect of variations in the fuel feed rate on combustion temperatures for three levels of excess air. Increasing the fuel feed rate from 2 lbs/hr (half-load) to 4 lbs/hr (full-load) increased the combustion temperature by approximately 200°F. The adiabatic temperature for identical operating conditions was approximately 1,000°F higher than the experimental temperatures.

The increase in combustion temperatures resulted from increased energy input into the combustion unit. Because of the increased energy input, radiation and convection heat losses from the combustion chamber's outer wall also increased, but were not directly proportional to energy inputs.

Combustion temperature increases could have been significantly higher if the outer wall of the chamber had been insulated. This would have decreased heat loss fractions as the fuel feed rates (energy inputs) were increased. Although adiabatic conditions could not be achieved under this condition, the insulation of the chamber would have brought the actual combustion temperatures considerably closer to adiabatic temperatures. However, the insulation of the outer chamber was intentionally avoided for the

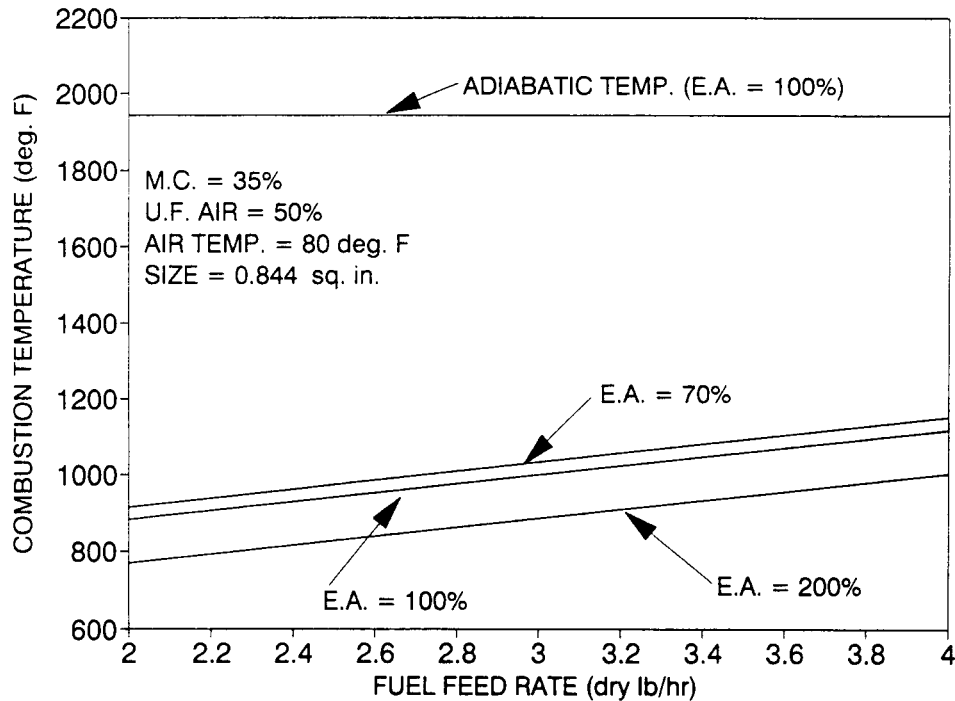


Figure 4.3 Combustion temperature vs. fuel feed rate.

experiments considered in order to prolong the life of the chamber casing and the instruments within the chamber.

Figure 4.4 shows the  $O_2$  and  $CO_2$  contents of the combustion products. Note that  $CO_2$  is a calculated quantity, whereas  $O_2$  was measured by the combustion gas analyzer.

The increase in fuel feed rate from half-load to full-load decreased the  $O_2$  content of combustion products from 15.5 to 14 percent (for the case indicated). The decrease in  $O_2$  content was accompanied by an increase in  $CO_2$  content, implying that at a full-load feed rate, or closer to the design condition of the burner, combustion would be more complete than at half-load.

Similarly, Figure 4.5 shows the CO and  $NO_x$  contents of combustion products as the fuel feed was increased. Higher

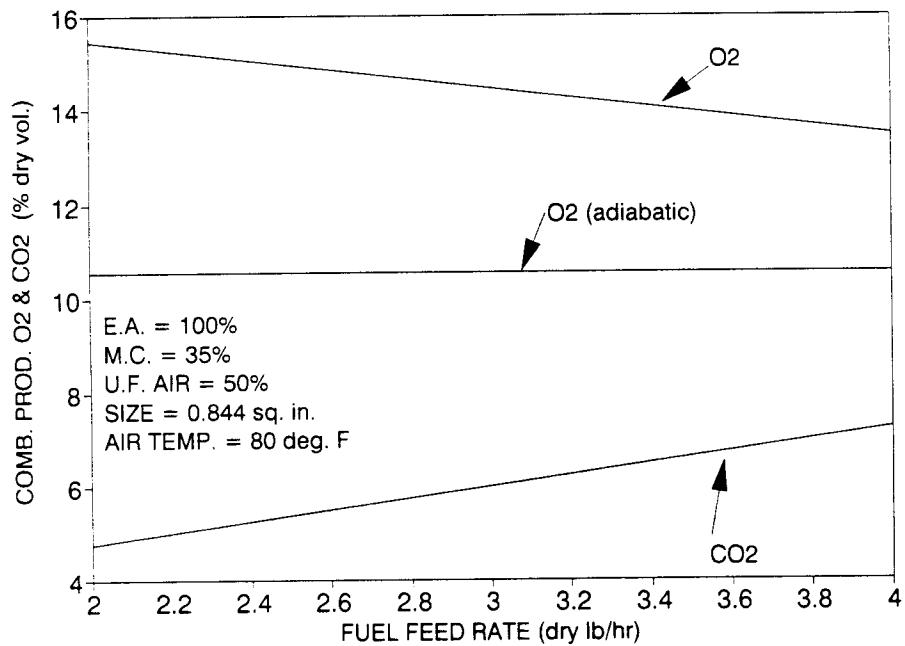


Figure 4.4 Oxygen and carbon dioxide content of combustion products vs. fuel feed rate.

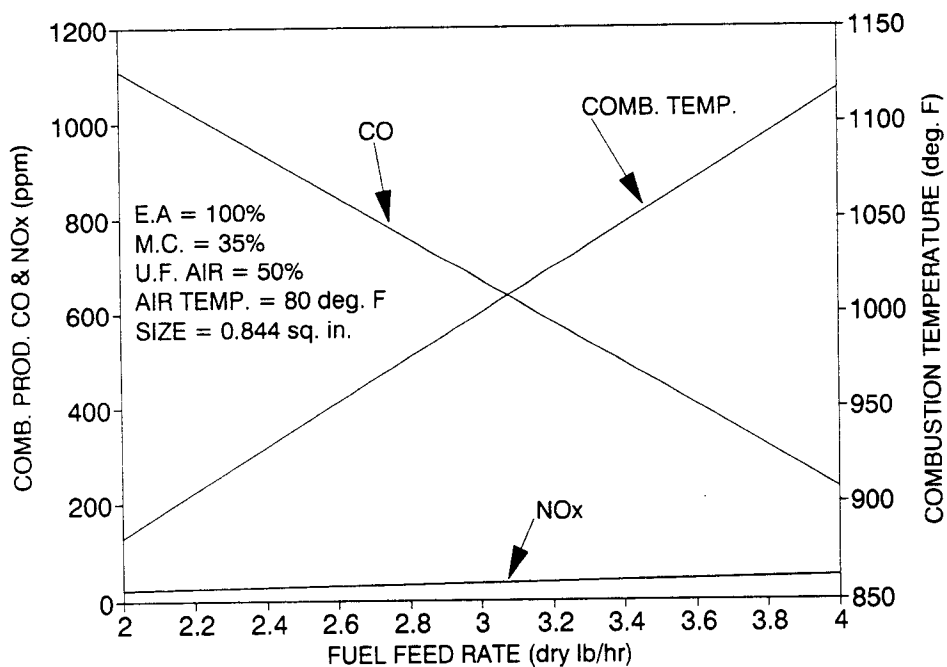


Figure 4.5 CO and NO<sub>x</sub> content of the combustion products as a function of fuel feed rate.

fuel feed rates resulted in lower CO content (from 1,150 ppm at half-load to 250 ppm at full-load), while the NO<sub>x</sub> content of the combustion products was subject to a slight increase. The decrease in CO content is an indication of more complete combustion. It should be noted that NO<sub>x</sub> generated during the combustion of wood is mainly due to the nitrogen content of the fuel (wood) and cannot be related to the fixation of atmospheric nitrogen [Howlett et al. 1977; Tillman et al. 1989]. Typically, wood combustion takes place at substantially lower temperatures than the fixation temperature of atmospheric nitrogen (3,000°F). Therefore, mainly fuel-bound nitrogen generated nitrogen oxides at temperatures below 3,000°F [Babcock and Wilcox 1978].

It should be emphasized that the combustion gases were sampled within the combustion chamber and not from the exhaust gases. Furthermore no air pollution control device preceded the sampling point. So, these values (CO, CO<sub>2</sub>, NO<sub>x</sub>) should be viewed as relative measures of the completeness of combustion and not as pollutants.

Figure 4.6 shows particulate emissions and the amount of combustibles in the particulate. The decrease in both variables suggests that the fuel feed rate had a significant effect on these variables. It should be noted that at low fuel feed rate levels, which are accompanied by lower combustion temperatures, unstable combustion resulted in flare-ups which contributed to higher particulate and com-

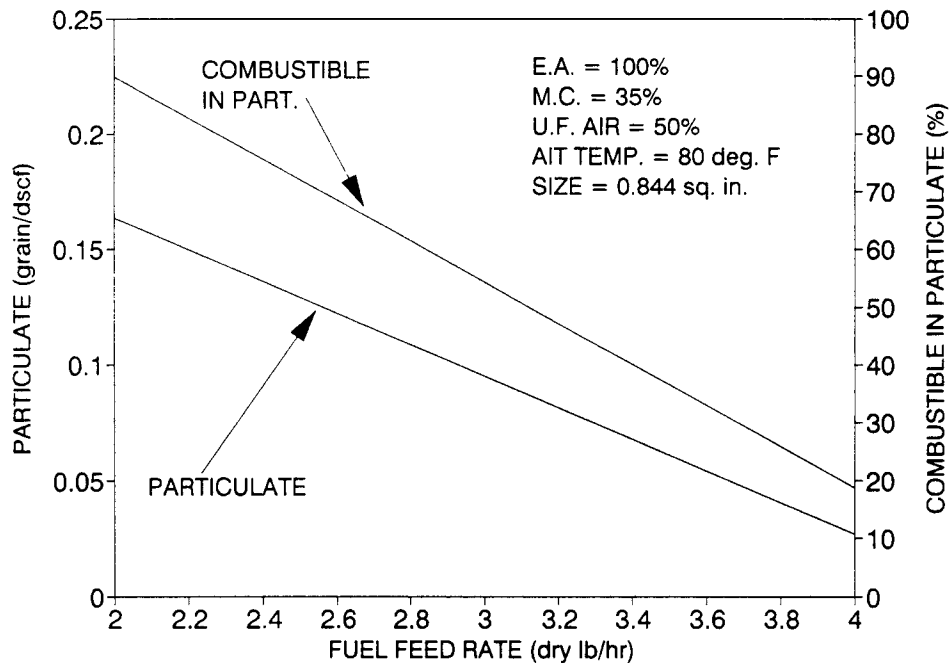


Figure 4.6 Particulate emissions and combustibles in the particulate as a function of fuel feed rate.

bustible emissions. This was particularly pronounced for fuels with high moisture contents, which burned at low levels of under-fire air.

Figure 4.7 shows efficiencies as a function of fuel feed rate. Note that EFF21 was approximately one percent higher than EFF22. The difference is attributed to the application of higher fuel heating values in place of fuel exergies. Since all of the EFF21 values show close similarities to those for EFF22 (that is, EFF21 always exceeded EFF22 by one percent), only the results for EFF22 are given and considered. As fuel feed was increased from 2 to 4 lbs/hr, EFF11 and EFF12 showed nearly a 9 percent increase. This increase was due to increased combustion temperatures,

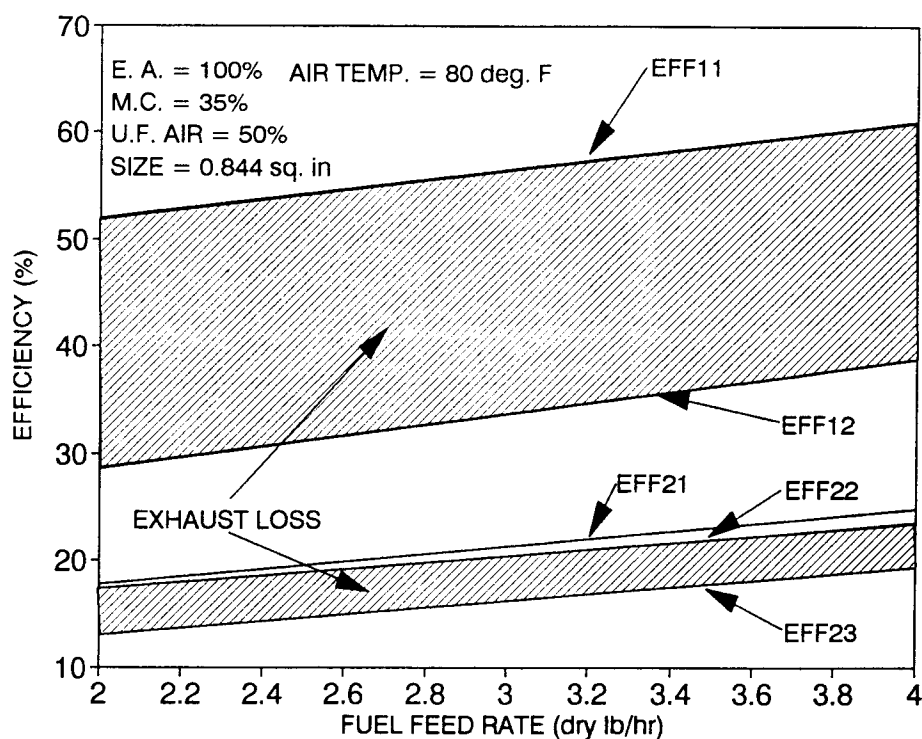


Figure 4.7 Efficiencies vs. fuel feed rate.

changes in the composition of the combustion products, and a decrease in the heat losses (i.e., the "fraction" of heat loss decreased as energy input increases).

There was approximately a 25 percent difference between EFF11 and EFF12, indicating a significant reduction in the efficiency of the process due to exhaustion of the combustion products at a high temperature (in this case, 250°F). For oil- and gas-fired boilers (which lack moisture in the fuel), exhaust losses range from 10 to 40 percent as exhaust temperatures increase from 100°F to 800°F [KVB, Inc. 1980].

The EFF22 and EFF23 efficiencies showed an increase of nearly 6 percent over the range of fuel feed variations,



the difference indicating exhaust losses. The low values of the Second Law efficiencies indicated significant losses of exergies in this process, resulting from the conversion of high exergy fuels to low exergy combustion products and from heat losses.

#### 4.2.2 Moisture Content

Figure 4.8 shows the effect of moisture content on combustion temperatures for three levels of excess air. Increasing the moisture content from 11 to 55 percent (wet basis) decreased the combustion temperature by nearly 70°F, whereas the decrease for the adiabatic temperature was 470°F. The small decline in experimental combustion temperature was because the fraction of heat used in the vaporization of the additional moisture was relatively small in comparison to total heat loss. For the adiabatic case, the additional heat of vaporization was the main source of energy consumed, serving to reduce the combustion temperature.

Figure 4.9 presents  $O_2$  and  $CO_2$  contents of the combustion products as a function of moisture content on a dry volume basis. There were no significant changes in either the  $O_2$  or  $CO_2$  contents of the combustion products.

Figure 4.10 shows  $CO$ ,  $NO_x$  contents and combustion temperatures. There were no significant changes in  $NO_x$  as the moisture content was increased, but  $CO$  contents increased by 200 ppm. This increase was due to reduction of combus-

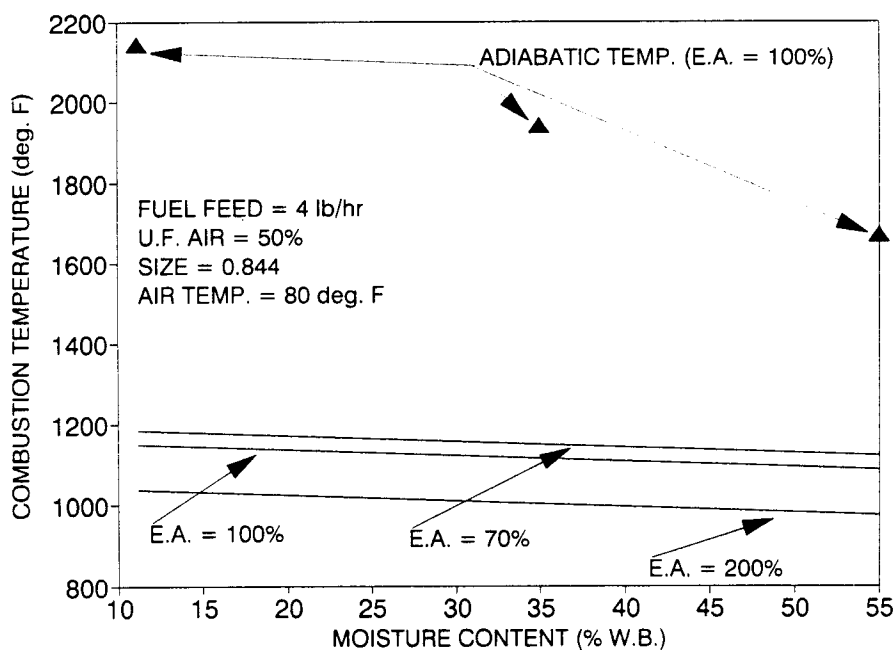


Figure 4.8 Combustion temperature as a function of fuel moisture content.

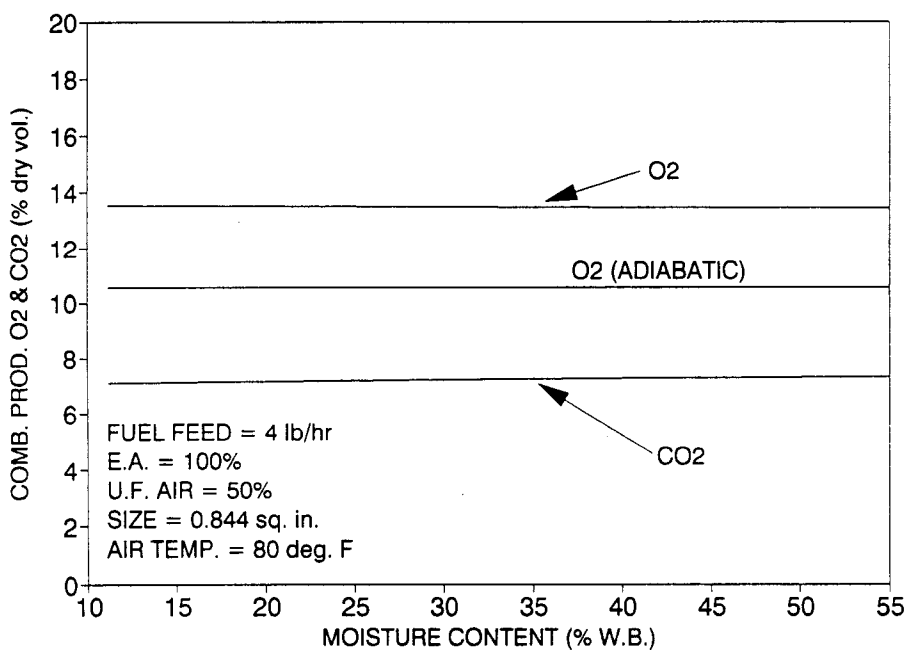


Figure 4.9 Combustion products oxygen and carbon dioxide content as a function of fuel moisture content.

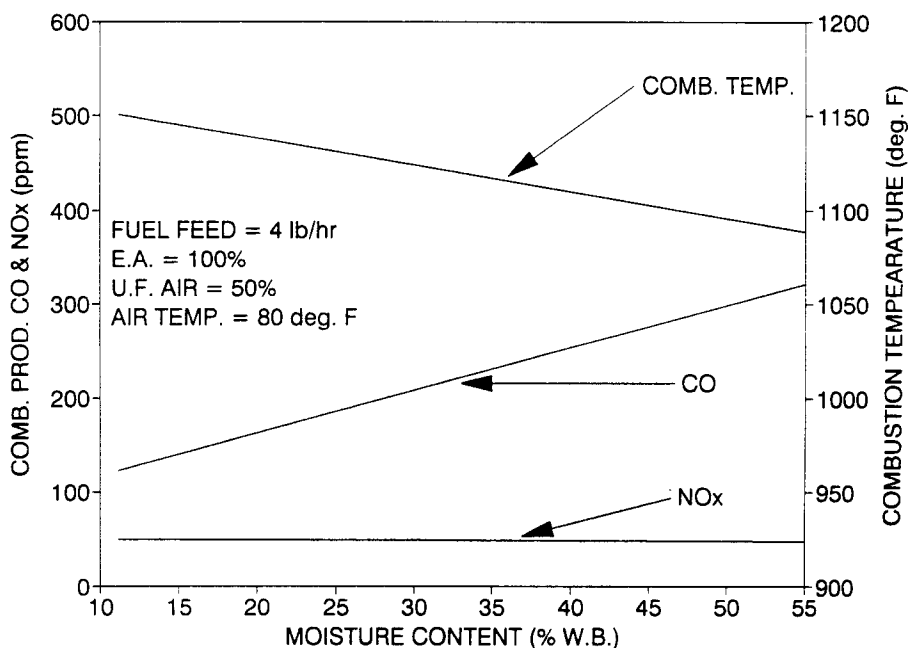


Figure 4.10 Combustion products CO and NO<sub>x</sub> content as a function of fuel moisture content.

tion temperatures and higher gas velocities caused by the increased volume of combustion gases in the chamber. The higher gas velocities in the chamber resulted in shorter residence times for the combustion products. Except for CO content, the increase in moisture content did not affect the composition of the combustion products.

Figure 4.11 presents particulate emissions and the combustible content of the particulate as a function of moisture content. Increasing the moisture content from 11 to 55 percent increased the particulate from 0.02 to 0.033 grains/dscf, and the combustibles in the particulate increased from 5 to 27 percent over the same range. The increase in particulate emissions was caused by the higher

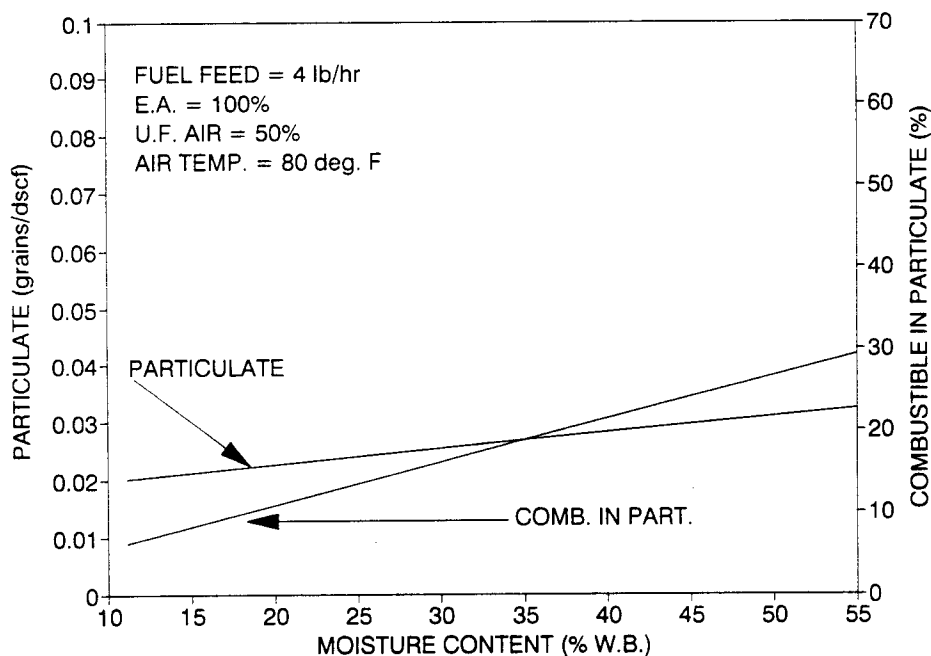


Figure 4.11 Particulate and combustibles in particulate as a function of fuel moisture content.

velocities of the combustion products, which reduced residence time and increased the drag on small particles within the chamber. In turn, reduced residence times and lower combustion temperatures induced a higher percentage of combustibles in the particulate.

Figure 4.12 shows efficiencies as a function of moisture content. Increasing the moisture content of the fuel increased the flow rate of the combustion products. This increase, in conjunction with the decrease in heat loss through the chamber wall shown in Figure 4.13 (due to reduced combustion temperatures), resulted in an increase in EFF11. As shown in Figure 4.12, EFF11 increased by nearly 16 percent, in contrast to an EFF12 increase of only 2 per-

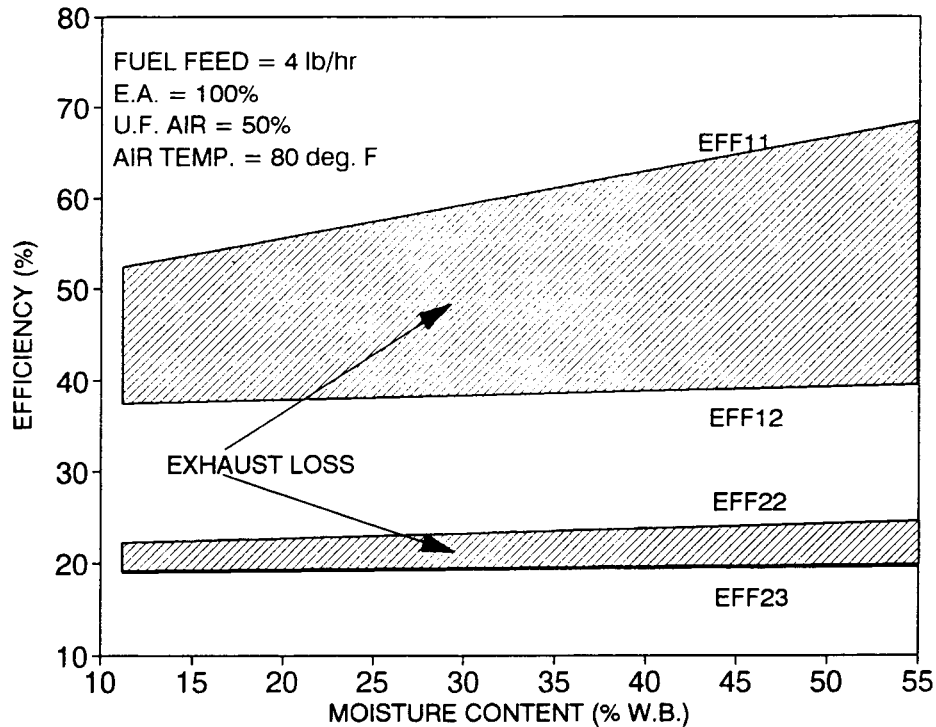


Figure 4.12 Efficiencies as a function of fuel moisture content.

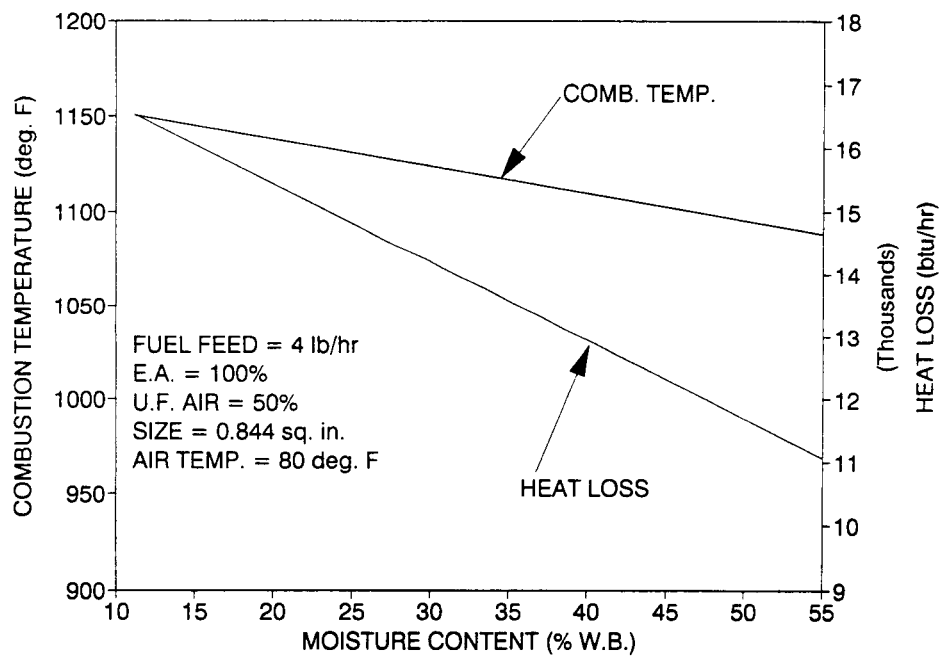


Figure 4.13 Combustion temperature and heat loss as a function of fuel moisture content.

cent. The EFF11 increase was due to a higher mass rate of combustion products and lower heat losses, whereas the EFF12 increase was due only to reduced heat losses. The difference between EFF11 and EFF12 increased by 14 percent in exhaust heat losses as the moisture content was increased from 11 to 55 percent.

Second Law efficiencies failed to show significant changes as a result of adjustment of the moisture content of the fuel.

#### 4.2.3 Excess Air

Figure 4.14 indicates a 150°F drop in combustion temperature when excess air was increased from 70 to 200 percent. The comparable decrease for adiabatic combustion temperature was 740°F.

Figure 4.15 shows an NO<sub>x</sub> decrease due to the increase of other combustion product constituents, including oxygen and nitrogen. The decrease in combustion temperature could also be a factor in the marginal decline of the NO<sub>x</sub> content of the combustion products.

Reduction of the combustion temperatures and the shorter residence times of the gases within the combustion chamber (due to introduction of a higher volume of combustion air) contributed to the increase in CO in combustion products. A similar increase in CO content in the exhaust products, resulting from increased excess air, has been reported for oil- and gas-fired boilers [KVB, Inc. 1980].

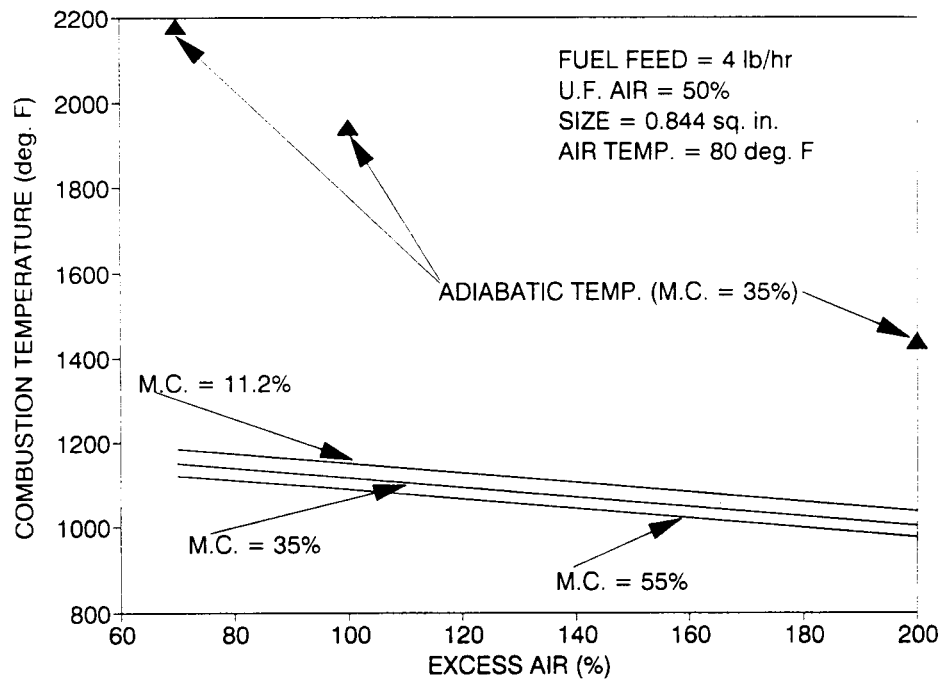


Figure 4.14 Combustion temperature as a function of excess air.

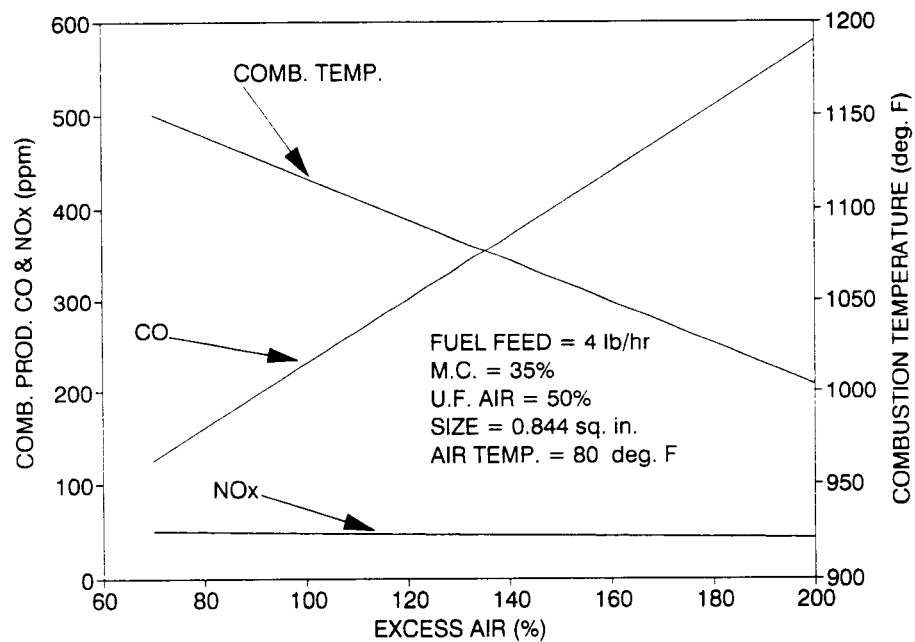


Figure 4.15 Temperature, CO, and NO<sub>x</sub> content of combustion products as a function of excess air.

Figure 4.16 shows an increase in particulate emissions from less than 0.01 to 0.09 grains/dscf over the range of excess air considered. The increase in both particulate and combustibles may be attributed to shorter residence times, higher gas velocities, and lower combustion temperatures.

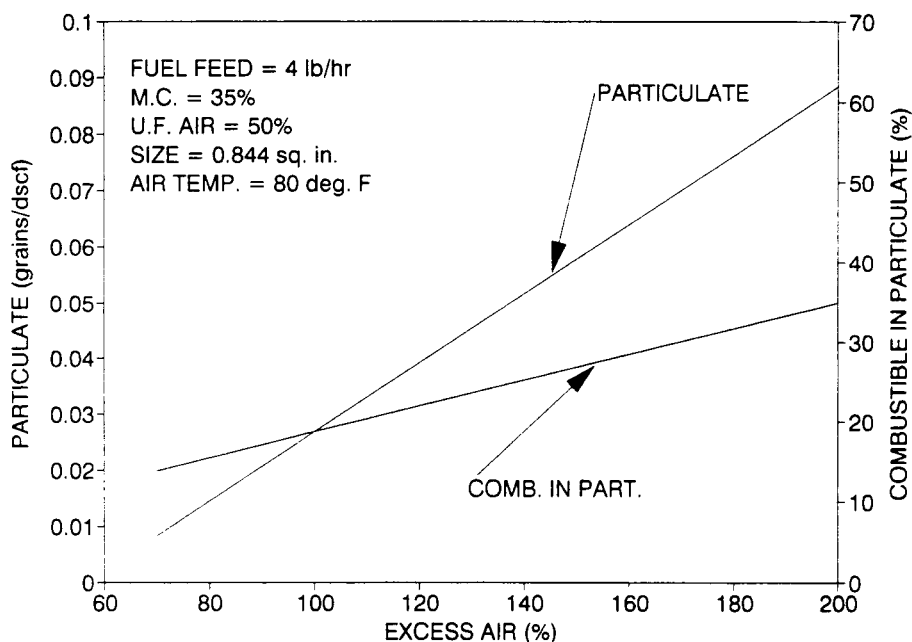


Figure 4.16 Particulate emissions and combustibles in particulate as a function of excess air.

Figure 4.17 shows that all efficiencies improved as excess air was increased. This increase was nearly 20 percent for EFF11 and approximately 14 percent for EFF12; EFF22 and EFF23 increased by 7 percent. These improvements were due to the increased flow rate of the combustion products and to reduced heat losses from the combustion chamber (in turn, due to lower combustion temperatures). Heat loss



was reduced by approximately 35 percent over the range of excess air considered for these experiments.

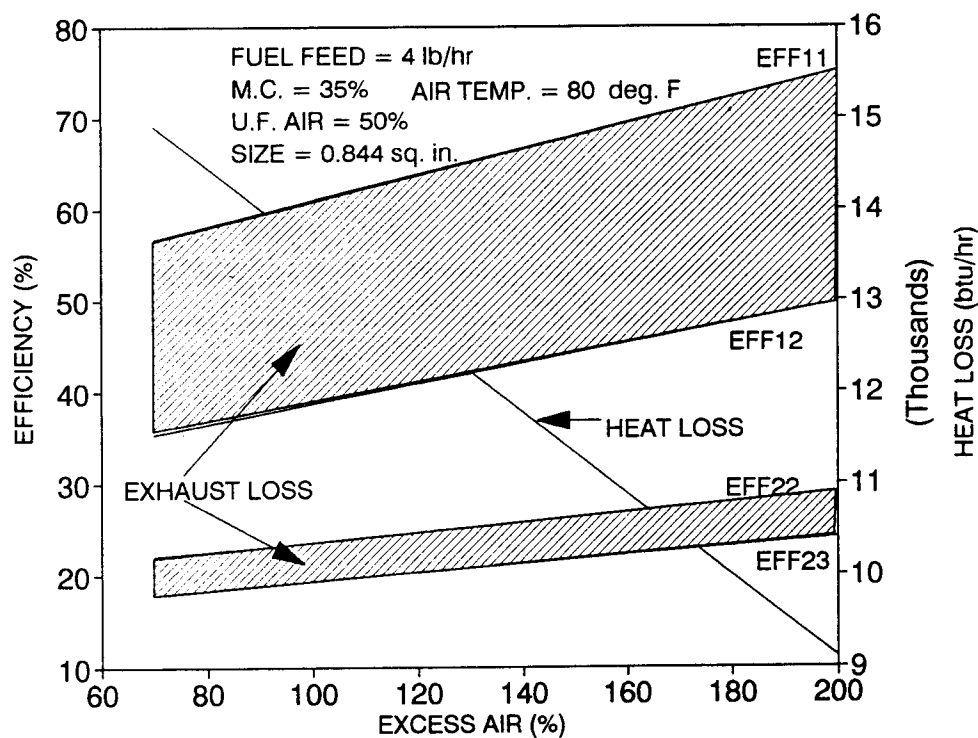


Figure 4.17 Efficiencies as a function of excess air.

#### 4.2.4 Under-Fire Air

Figures 4.18 and 4.19 show temperature, heat loss, and efficiency as percentages of under-fire air increases. The results of regression analyses indicated that changing the ratio of under-fire air to total combustion air would not affect most of the parameters considered in this experimental investigation. However, higher levels of under-fire air were required to maintain stable operation for high moisture content fuels.

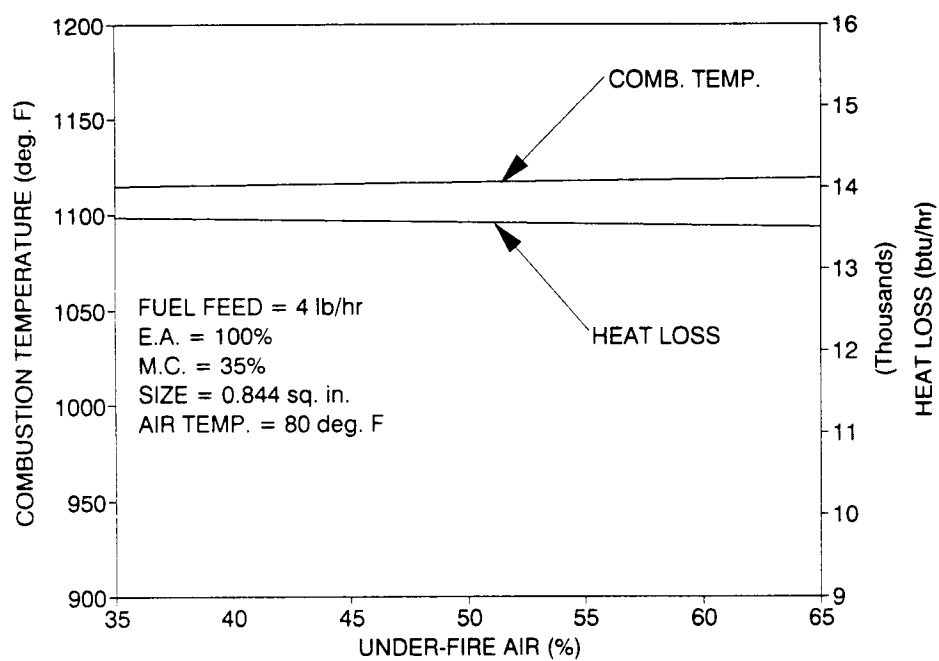


Figure 4.18 Combustion temperature and heat loss as a function of under-fire air.

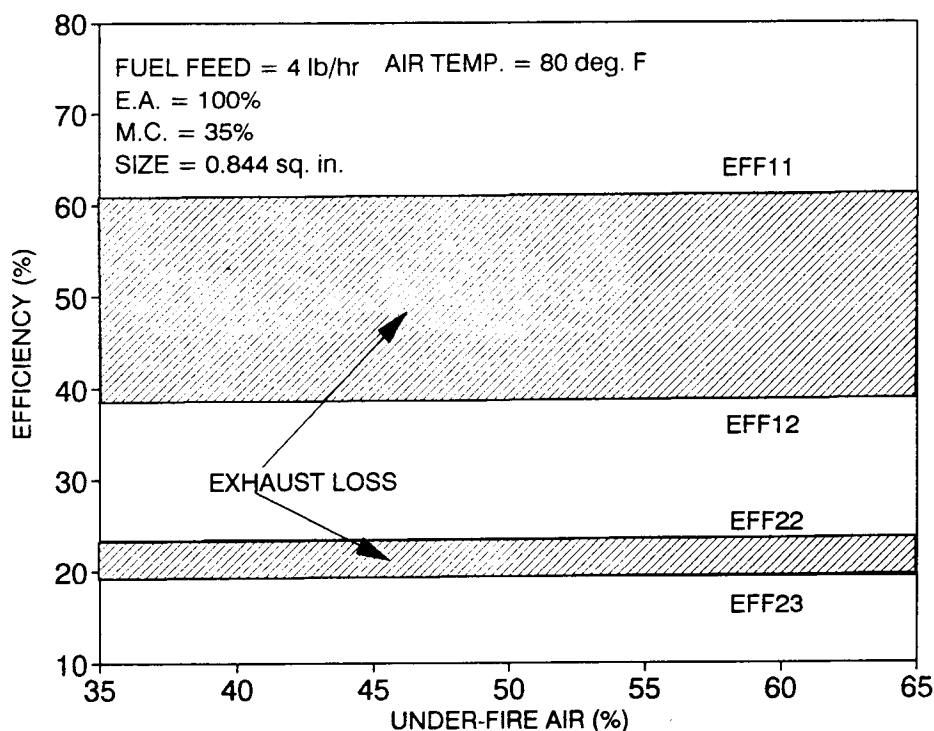


Figure 4.19 Efficiency as a function of under-fire air.

#### 4.2.5 Fuel Particle Size

In Figure 4.20, the  $\text{NO}_x$  and CO content of the combustion products are given for combustion temperatures as the size (surface area) of the fuel particles was increased. When the surface area of the fuel particles was increased from 0.844 to 1.500 in<sup>2</sup>, combustion temperatures decreased by approximately 21°F. Useful conclusions are difficult to determine from these results since the decreases were within the limits of allowable error in the regression model.

A significant increase was also indicated in the CO content of the combustion products. This was an expected

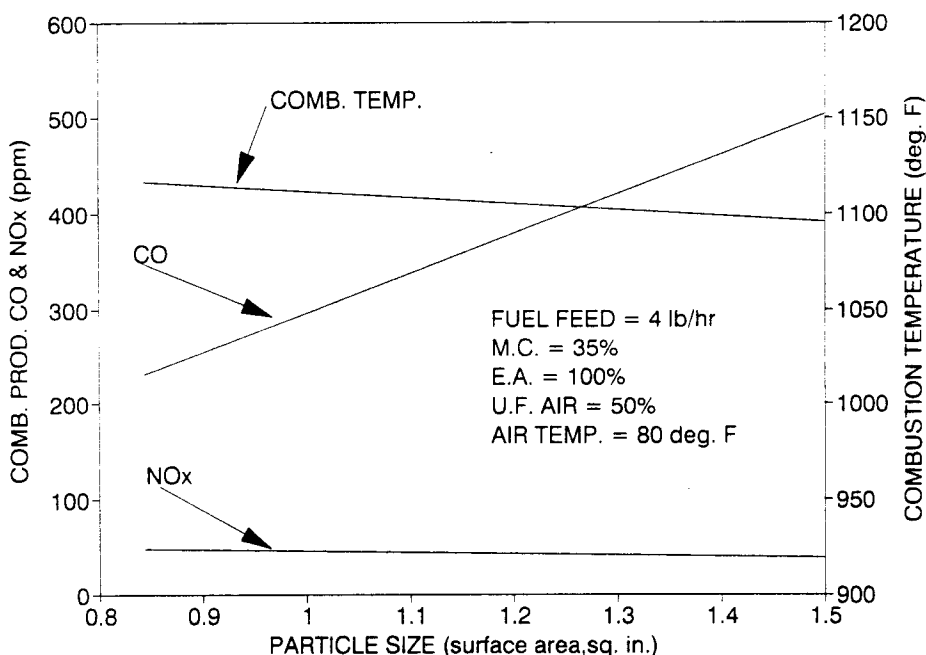


Figure 4.20 Temperature, CO and NO<sub>x</sub> content of combustion products as a function of particle size.

result since larger particles burn at slower rates. (Thus, larger particles require longer residence times, see Chapter 2.) Therefore, the drop in combustion temperatures was validated by the indication of higher CO content (i.e., a lower conversion rate of carbon to CO<sub>2</sub>). The NO<sub>x</sub> content of the combustion products showed no significant changes over the same range.

Figure 4.21 shows particulate emissions and combustible contents of the particulate. There was no substantial change in the combustible contents of the particulate. This is not surprising since there was no change in the residence times of the fly ash within the combustion chamber. The particulate emissions, however, showed an in-

crease of 0.05 grains/dscf as the surface area of the particles was increased.

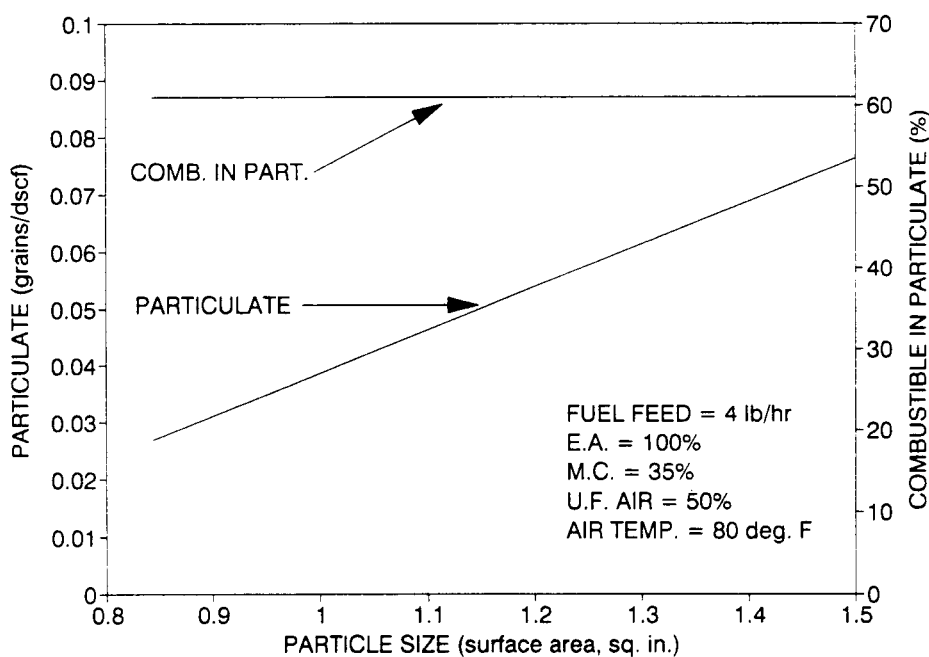


Figure 4.21 Particulate emissions and combustibles in particulate as a function of particle size.

Efficiencies and heat losses are shown in Figure 4.22. Since there was only a small change in combustion temperature, the heat losses and efficiencies did not change appreciably.

For typical industrial wood-fired boilers, fuel particle size has a wide range of variation. In these boilers, fines in the feed substantially increase particulate emissions and  $\text{NO}_x$  generation, while reducing the efficiency of the process [Tillman et al. 1989].

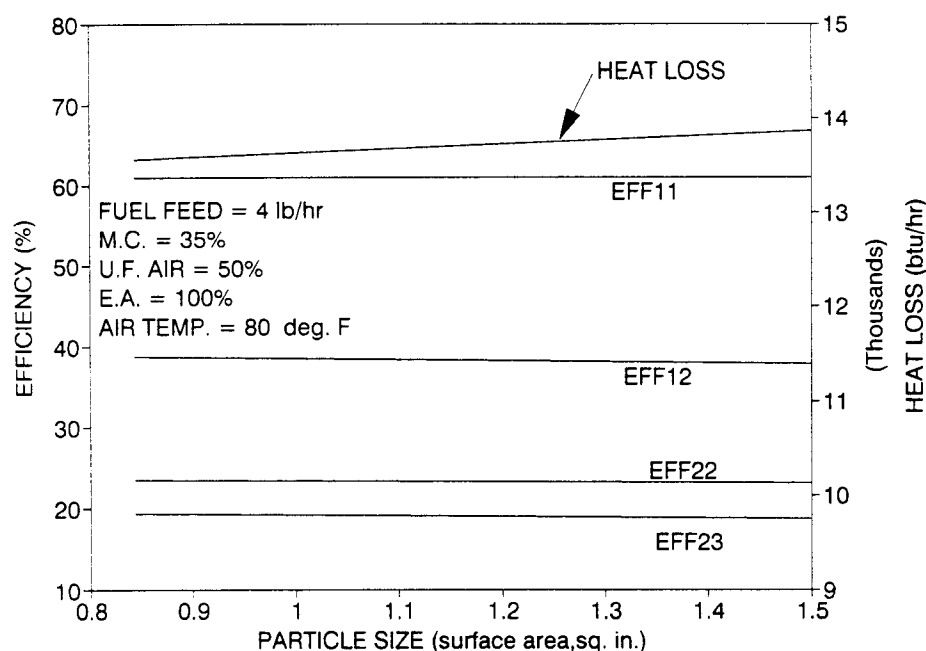


Figure 4.22 Efficiency and heat loss as a function of particle size.

#### 4.2.6 Under-Fire Air Temperature

To enhance the combustion process it is common practice to preheat the combustion air. When the moisture content of the fuel is high, preheated combustion air provides a faster rate of drying and combustion [Simmons 1983]. Increasing the combustion air temperature is accompanied by an increase in the volume of air, a factor which could offset some of the benefits of preheating the air.

For the experiments under consideration, preheating the combustion air from 80°F to 400°F increased combustion air volume by approximately 60 percent, which in turn increased combustion gas velocity while reducing residence time for the suspended particulate. As shown in Figure

4.23, combustion temperature showed a decrease of approximately 15°F as under-fire air temperature was increased by 320°F. Initially, this was a surprising result. However, when the increase in gas velocity and the reduction in residence time were noted, it was possible to conclude that the combustion process was deteriorated rather than enhanced.

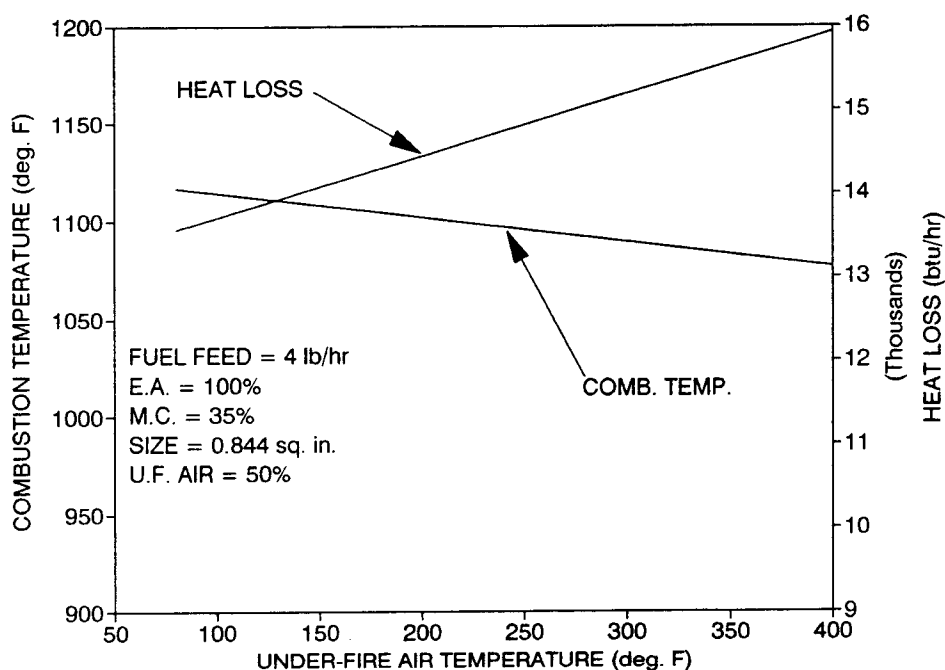


Figure 4.23 Heat loss and combustion temperature as functions of under-fire temperature.

Particulate emissions and combustibles in the particulate also showed an increase over the range of increased air temperature, as indicated in Figure 4.24. Figure 4.25 shows that efficiency decreased as combustion temperatures were increased. Note that the energy used to heat the air was accounted for in the calculation of the efficiencies.

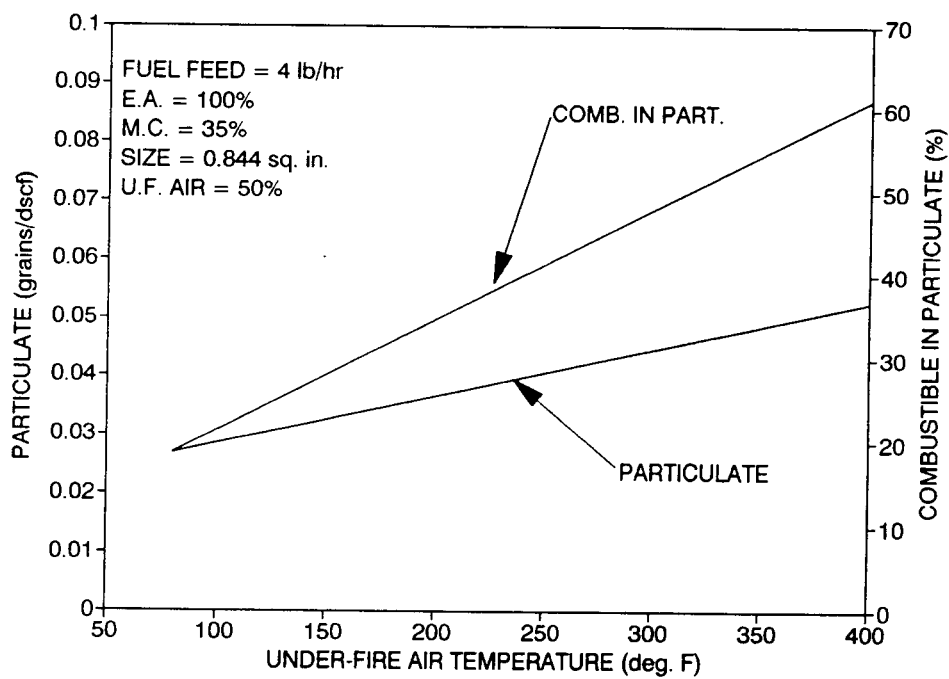


Figure 4.24 Particulate emissions and combustibles in particulate as functions of under-fire air temperature.



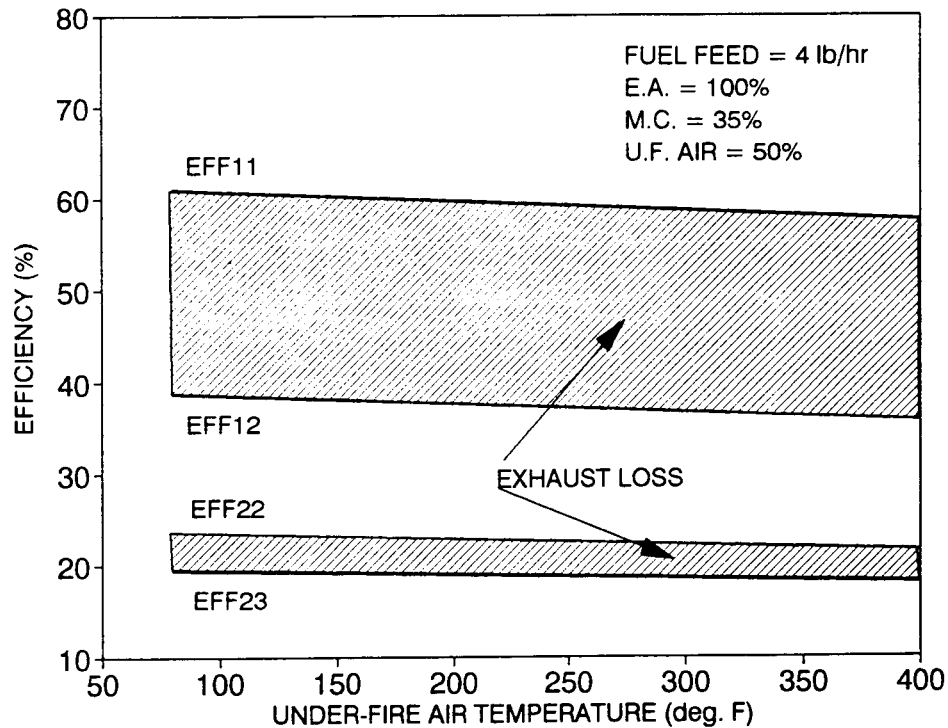


Figure 4.25 Efficiencies as functions of under-fire air temperature.

Earlier experiments with wood pellets [Bushnell et al. 1989] also support these results.

For industrial hogged-fuel boilers burning fuels with high moisture contents, it has been demonstrated that the highest possible combustion air temperatures should be applied [Junge 1978b]. In addition, increased combustion air temperatures have been shown to improve the efficiency of oil- and gas-fired boilers [KVB Inc. 1980]. These results are in contradiction with the results of the present investigation and the investigation performed by Haluzak [1988]. This is because the system used for the present experiments had a substantially smaller combustion chamber than those

used for the industrial applications. The smaller combustion chamber makes the combustion process extremely sensitive to any changes that result in the reduction of the residence time of the combustion products (for example, preheated combustion air, moisture content, or excess air). These sensitivities are not as crucial in the case of industrial boilers.

#### 4.3 Conclusions

From the discussion of the experimental results, based upon regression analysis, it is possible to conclude the following:

- 1) Convective and radiative heat loss from the combustion chamber were the dominant factors related to combustion temperatures and efficiencies.
- 2) The variables that increased the volume of combustion products (and their velocity, which in turn decreased the residence time of the combustion products) adversely affected combustion temperatures and conversion rates while increasing particulate emissions. These variables include higher excess air, higher fuel moisture content, and higher combustion air temperature.
- 3) The variation in the ratio of under-fire to total combustion air had no significant effect upon combustion performance over the range of variables

considered in this study. Previous experiments on wood pellets and hogged fuel boilers resulted in the recommendation of different operating conditions for highest efficiencies [Junge 1975; 1978a; 1978b; Haluzak 1989]. Therefore, it is concluded that the optimum ratio of the under-fire air is dependent upon the type of fuel, fuel moisture content and the combustion system in utilization. In addition, when the combustion unit was operated at a lower fuel feed rate than its design specification, higher under-fire air was required to prevent black-out in the chamber. This was particularly more pronounced for high moisture content fuels.

- 4) Operating the combustion unit at fuel feed rates lower than the design conditions contributes to lower efficiency, lower combustion temperature, higher CO, higher particulate emissions, and higher combustible content of the particulate.
- 5) Although, with the exception of CO content, moisture content did not affect the composition of combustion products, it adversely affected combustion temperatures, particulate emissions and the combustible contents of the particulate, while increasing exhaust heat losses.
- 6) Increasing excess air above 70 percent decreased the combustion temperatures, while increasing par-

ticulate emissions, combustibles in the particulate, and CO production. Due to the higher flow rate of combustion products, all of the efficiencies investigated indicated improvements as excess air was increased. Previous investigations have shown that 60 percent excess air is the optimum excess air rate for wood pellets. (Note that wood pellets have a substantially lower moisture content than other wood products.)

- 7) Increased fuel particle size (surface area) increased CO production and particulate emissions, while decreasing combustion temperatures and efficiencies.

Finally, no opacity was observed during the conduct of experimental testing, other than flare-ups occurring at low fuel feed rates or at the start-up of the unit.

## CHAPTER 5

### CONCLUSION AND RECOMMENDATIONS

#### 5.1 Conclusion

For this study, an experimental investigation of wood combustion was carried out and presented. Experiments were conducted using the Biomass Combustion Facility at Oregon State University, Corvallis, Oregon. The variables selected for investigation were fuel feed rate, fuel moisture content, fuel particle size, excess air, and the fraction and temperature of the under-fire air. The experimental data obtained was used for the calculation of the combustion times of the wood particles, the temperatures and composition profiles of the combustion products within the combustion chamber and the overall performance of the combustion unit.

Most of the models developed for the pyrolytic analysis of wood and for char combustion require numerical solutions, whereas the model developed for the current investigation was used to generate sets of closed form solutions. Despite the simplifying assumptions applied in the model development, the results of model predictions showed excellent agreement with the experimental measurements.

In Chapter 3, an analytical solution to the problem of predicting the temperature profiles of combustion products within the combustion chamber was presented. The results obtained with this model were in good agreement with the experimental data. Analysis of the experimental data and the model predictions indicated that increasing the temperature of the over-fire air can serve to substantially increase combustion temperature and efficiency.

A chemical equilibrium model was used to predict the composition profiles of the combustion products within the combustion chamber. Although the model predicted the oxygen and carbon dioxide contents of the combustion products with reasonable accuracy, the results for  $\text{NO}_x$  and CO proved to be inaccurate. This was in agreement with previous experimental findings. In Chapter 3, model modifications were suggested for the estimation of the  $\text{NO}_x$  and CO contents of the combustion products, thus closing the gap between experimental results and the predictive capacity of the chemical equilibrium model.

Combustion system overall performance was considered in Chapter 4. Over the range of variables considered, it was concluded that combustion efficiency and particulate emissions are most influenced by the factors that increase the volume of the combustion products in the combustion chamber. These variables include excess air, the moisture content of the fuel and the temperature of the under-fire air. Fuel particle size and the fraction of under-fire air

did not significantly affect combustion efficiency or particulate emissions. It was also concluded that the off-design (part-load) operation of the combustion unit resulted in higher particulate emissions and lower combustion efficiency.

## 5.2 Recommendations

In Chapter 2, it was observed that further research would be required to determine the value of the endothermicity of pyrolysis for different species of wood. Furthermore, the relation between moisture content and the size of the fuel particles, and the amount and density of the char remaining following pyrolysis, are areas of investigation which require further research. This information will be essential for accurate modeling of pyrolysis rates and combustion char.

Combustion products near the fuel bed consist of species that were not measured for this study. Further investigation is required to identify these constituents. Similarly, further information on temperature and composition profiles within the fuel bed for wood combustion systems would be of assistance in improved understanding of the burning processes in and near the fuel bed. Acquisition of this type of information could lead to improvements in the design and operation of combustion systems.

## REFERENCES

- Antal, M. J. Jr., "A Review of the Vapor Phase Pyrolysis of Biomass Derived Volatile Matter," in "Fundamentals of Thermochemical Biomass Conversion," eds. Overend, R. P., Milne, T. A., and Mudge, L. K., Elsevier Applied Science Publisher, 1982.
- Babcock and Wilcox, "Steam/Its Generation and Use," Babcock and Wilcox company, New York, N.Y., 1978.
- Barriga, A., and Essenhig, R.H., "A Mathematical Model of a Combustion Pot: Comparison of Theory and Experiment," Proc. ASME Winter Annual Meeting, November 16-21, Chicago, Ill., 1980.
- Bauer, T. L., "Investigation of Combustor and Fuel Preparation Requirements for a Combined-Cycle Wood Fired Power Plants," M.S. Thesis, Oregon State University, Corvallis, OR, 1984.
- Benson, H. K, "Chemical Utilization of Wood," U.S. Department of Commerce, United state Government Printing Office, Washington D.C., 1932.
- Biomass Energy Technology Research Program Summary, prepared by Technical Information Branch Solar Energy Research Institute, Prepared for U.S. Department of Energy. DOE/CE-0032/1, FY 1983.
- Britten, J. A., "Recession of a Coal Face Exposed to a High Temperature," Int. J. Heat Mass Transfer, Vol. 29, No. 7, p.965-978, 1986.
- Browne, F. L., "Theories of the Combustion of Wood and its Control a Survey of the Literature," U.S. Forest Products Laboratory Report No. 2136, Forest Products Laboratory Madison, WI, 1958.
- Bushnell, D. J., Haluzak, C. and Dadkhah-Nikoo, A., "Biomass Fuel Characterization: Testing and Evaluating the Combustion Characteristics of Selected Biomass Fuels," Final Report, Contract No. DE-A179-88BP39 643, September 1989.
- Carslaw, H. S., and Jaeger, J. C., "Conduction of Heat in Solids," Oxford University Press, 1965.



- Dadkhah-Nikoo, A., "Analysis of Wood Combustion and Combustion Systems for a Combined-Cycle Wood Fired Power Plant," M.S. thesis, Oregon State University, Corvallis, Ore, 1985.
- Dadkhah-Nikoo, A. and Bushnell, D. J., "Analysis of Wood Combustion Based on the First and Second Laws of Thermodynamics," Journal of Energy Resources Technology, Vol. 109, September 1987, pp. 129-141.
- Dadkhah-Nikoo, A., and Bushnell, D. J., "Design, Construction and Characterization of a Biomass Fuel Testing and Combustion Unit," Combined Cycle Biomass Research Project Final Report, Task 1, Part 10, prepared for USDA, June 1988.
- Daw, C. S., and Krishnan, R. P., "Direct Combustion of Solid Carbonaceous Fuels: The Diffusionally Controlled Regime," in "Combustion of Tomorrow's Fuels," The American Society of Mechanical Engineers, 1988.
- Dosanjh, S. S., and Pagni, P. J., "Forced Countercurrent Smoldering Combustion," Proc. 1987 ASME/JSME Thermal Engineering Joint Conference, eds. Marto, P. J., and Tanasawa, I., p. 165, Honolulu, Hawaii, March 22-27, 1987.
- Drucker, S. J. et al., "The Industrial Wood Energy Handbook," New York, Van Nostrand Reinhold Co., 1984.
- Eapen, T., Blackadar, R., and Essenhight, R. H., "Kinetics of Theory and Experiment in a Combustion pot: A Comparison of Theory and Experiment," Sixteenth Symposium (International) on Combustion, p. 515-522, The Combustion Institute, Pittsburgh, Pa., 1976.
- Fox, S.J., "Computer Simulation of a Combined-Cycle Biomass-Fueled Power Plant," M.S. Thesis, Oregon State University, Corvallis, OR, 1984.
- Gullett, B. K., and Smith, P., "Thermogravimetric Study of Decomposition of Pelletized Cellulose at 315 deg. C-800 deg. C," combustion and Flame Vol. 67, p. 143, 1987.
- Haluzak, C., "Experimental Combustion Analysis and Development of Representative Fuel Specifications for Selected Wood and Refuse Derived Fuel Pellets from the Pacific Northwest," M.S. thesis, Oregon State University, Corvallis, Ore., 1989.

- Howlett, K., and Gamache, A. "Forest and Mill Residues as Potential Sources of Biomass," Silvicultural Biomass Farms, vol. VI, Georgia-Pacific Corporation, May 1977.
- Johnson, R. E., "Some Aspects of Wood Waste Preparation for Use as Fuel," in "Wood and Bark Residues for Energy," Compiled by S.E. Corder, School of Forestry, Oregon State University, Corvallis, OR, 1975.
- Junge, D. C., "Boilers Fired with Wood and Bark Residues," Res. Bull. Forest Research Laboratory, Oregon State University, Corvallis, OR, 17, Nov. 1975.
- Junge, D. C., "The Combustion Characteristics of Pelletized Douglas Fir," technical progress report No. 12, prepared for the U.S. Department of Energy, contract No. EY-76-C-06-2227 task No. 22, Oregon State University, Corvallis, Ore, December 1979.
- Junge, D. C., "The Combustion Characteristics of Ponderosa Pine," Technical Progress Report No. 7, prepared for the U.S. Department of Energy, contract No. EY-76-C-06-2227 task No. 22, Oregon State University, Corvallis, Ore, December 1978a.
- Junge, D.C., "The Combustion Characteristics of Red Alder Bark," Technical Progress Report No. 6, prepared for the U.S. Department of Energy, contract No. EY-76-C-06-2227 task No. 22, Oregon State University, Corvallis, Ore, December 1978b.
- Junge, D. C., and Oswald, K. D., "Drying Wood and Bark Fuels With Boiler Exhaust Gases," Energy Research Development Institute, Oregon State University, Corvallis, OR, 1980.
- Kailasanath, K., and Zinn, B. T., "a Theoretical Investigation of the Smoldering Combustion of Porous Solids," in "Fluid Mechanics of Combustion Systems", eds. Morel, T., Lohmann, R. P., and Rackley, J. M., The American Society of Mechanical Engineers, 1981.
- Kamke, F. A., "Engineering Analysis of a Rotary Dryer: Drying of Wood Particles," Ph.D. Thesis, Oregon State University, Corvallis, OR, 1984.
- Kansa, E. J., Perlee, H. E., and Chaiken, R. F., "Mathematical Model of Wood Pyrolysis Including Internal Forced Convection," Combustion and Flame Vol. 29, p. 311, 1977.
- Kanury, A. M., "Introduction to Combustion Phenomena," Gordon and Breach Science Publisher, 1977.

- Kanury, A. M., "Mass Regression in the Pyrolysis of Pine Wood Macrocyllinders in a Nitrogen Atmosphere-An Experimental Study," Combustion Science and Technology, Vol. 9, p. 31, 1974.
- Kanury, A. M., "Rate of Burning of Wood," Combustion Science and Technology, Vol. 5, p. 135, 1972.
- Kanury, A. M., "Rate of Charring Combustion in a Fire," Fourteenth Symposium (International) on Combustion, p. 1131, The Combustion Institute, 1973.
- Kanury, A. M., and Blackshear, P. L. Jr., "On the Combustion of Wood II: The Influence of Internal Convection on the Transient Pyrolysis of Cellulose," Combustion Science and Technology, Vol. 2, p. 5, 1970a.
- Kanury, A. M., and Blackshear, P. L. Jr., "Some Considerations Pertaining to the Problem of Wood-Burning," Combustion Science and Technology, Vol. 1, p. 339, 1970b.
- Klass, Donald L., "Energy from Biomass and Waste: 1979 Update," in "Energy From Biomass and Waste IV," Produced by White J. W., McGrew W., Sutton M.R., Institute of Gas Technology, January 1980.
- Kung, H. C., "A Mathematical Model of Wood Pyrolysis," Combustion and Flame, Vol. 18, p. 185, 1972.
- KVB, Inc., "Boiler Efficiency Manual," prepared for Energy Conservation Clearinghouse for Commerce and Industry Oregon Department of Energy, for presentation at: Boiler Efficiency Workshop Series, August 1980.
- Malte, P. C., Dorri, B., Emery, A. F., Cox, R. W., and Robertus, R. J., "Drying of Small Wood Particles," Drying Technology Vol. 1, No. 1, p. 83, 1983-84.
- Martin, W., and Koenigshofer, D. R., "Development and Testing of a Small Wood Combustion System," in Fuels from Biomass and Wastes, Eds. Klass D.L., and Emert, G.H., p.567-581, 1980.
- Mujumdar, A. S., "Advances in Drying," Vol. 1, Hemisphere Publishing Corporation, 1980.
- Mujumdar, A. S., "Advances in Drying," Vol. 2, Hemisphere Publishing Corporation, 1983.
- Mujumdar, A. S., "Advances in Drying," Vol. 3, Hemisphere Publishing Corporation, 1984.
- Mujumdar, A. S., "Advances in Drying," Vol. 4, Hemisphere Publishing Corporation, 1987.

- Mujumdar, A. S., "Advances in Drying," Vol. 5, Hemisphere Publishing Corporation, 1990.
- Pitts, D. R., and Sissom, L. E., "Schaum's Outline Series Theory and Problems of Heat Transfer," McGraw-Hill Book Company, 1977.
- Reistad, G. M., "Availability: Concepts and Applications," Ph.D. thesis, University of Wisconsin, 1970.
- Roberts, F. A., "A Review of Kinetics Data for the Pyrolysis of Wood and Related substances," Combustion and Flame, Vol. 14, p. 261, 1970.
- Satyendra, P. N., and Onischak, M., "Gasification of Char Obtained from Maple and Jack Pine Woods," in "Fundamentals of Thermochemical Biomass Conversion," eds. Overend, R. P., Milne, T. A., and Mudge, L. K., Elsevier Applied Science Publisher, 1982.
- Shafizadeh, F., "Fuels from Wood Waste," Fuels from Waste, eds., L. L. Anderson and D. A. Tillman, Academic Press, 1977.
- Siau, J.F., "Flow in Wood," Syracuse University Press, 1971.
- Siegel, R., and Howell, J. R., "Thermal Radiation Heat Transfer," Second Edition, Hemisphere Publishing Corporation, 1981.
- Simmons, W. W., "Analysis of Single Particle Wood Combustion in Convective Flow," Ph.D. Thesis, The University of Wisconsin, Madison, 1983.
- Simmons, W. W., and Ragland, K. W., "Burning Rate of Millimeter Sized Wood Particles in a Furnace," Combustion Science and Technology, Vol. 46, p. 1, 1986.
- Simpson, W. T., "Drying Wood: A review - Part I," Drying Technology, Vol. 2, No. 2, p. 235, 1983-84.
- Simpson, W. T., "Drying Wood: A Review - Part II," Drying Technology, Vol. 2, No. 3, p. 353, 1983-84.
- Tillman, D. A., and Anderson, L. L., "Computer Modeling of Wood Combustion with Emphasis on Adiabatic Flame Temperature," Journal of Applied Polymer Science: Applied Polymer Symposium 37, p. 761, 1983.
- Tillman, D.A., Meagher, M., and Wegehaupt T., "Modeling the Combustion of Low Value Solid and Waste Fuels in Grate Fired Systems to Estimate Flame Temperature and Prod-

- ucts of Combustion," presented at: the American Flame Research Committee 1989 International Symposium on Combustion in Industrial Furnaces and Boilers, Short Hills, New Jersey, September 25-27, 1989.
- Tu, C. M., Davis, H., and Hottel, H. C., "Combustion Rate of Carbon Sphere in Flowing Gas Streams," Ind. and Eng. Chem. Vol. 26, p. 749, 1934.
- Tuttle, K.L., "Combustion Mechanism in Wood Fired Boilers," Ph.D. Thesis, Dept. of Mechanical Engineering, Oregon State University, Corvallis, OR, 1977.
- Walker P. L. Jr., "Char Properties and Gasification", in "Fundamentals of Thermochemical Biomass Conversion", eds. Overend, R. P., Milne, T. A., and Mudge, L. K., Elsevier Applied Science Publisher, 1982.
- Welty, J. R., Wicks, C. E., and Wilson, R. E., "Fundamental of Momentum, Heat, and Mass Transfer, Second Edition, John Wiley and Sons, 1976.
- Wichman, I. S., and Atreya, A., "A Simplified Model for Pyrolysis of Charring Material," Combustion and Flame Vol. 68, p. 231, 1987.
- Winslow, A.M., "Numerical Model of Coal Gasification in a Packed Bed," Sixteenth Symposium (International) on Combustion, The Combustion Institute, p. 1131, 1976.
- Wise, L.E., and Jahn, E.C., "Wood Chemistry," Second Edition, Vol. 2, Reinhold Publishing Corporation, 1952.

## APPENDICES

## APPENDIX A

### COMPUTER PROGRAMS

#### A.1 Program for Calculation of the Gas Properties

```

$debug
c ----- Enthalpy of gas, HGAST(T,yCO2,yH2O,...,yCO) -----
c
c This function calculates the enthalpy of a gas as a function
c of temperature and mole fractions. The equations for Cp are
c from "Fundamentals of Classical Thermodynamics", G.J. Van Wylen
c and R.E. Sonntag, pp. 683 - 684. Cp for argon is assumed to be
c constant: 5.005 btu/lbmole R. Maximum error for air was
c around 0.5 %.
c
c function HGAST (T,yCO2,yH2O,yO2,yN2,yAr,yCO)
c
c common /DS/Tds,Pds,YdsCO2,YdsH2O,YdsO2,YdsN2,YdsAr,YdsCO
c real Mm,mO2,mN2,mCO2,mH2O,mAr,mCO
c data R /1.9858/
c data a1,a2,a3,a4 /9.3355,-122.56,256.38,-196.08/
c data b1,b2,b3,b4 /8.9465,4.8044E-03,-42.679,56.615/
c data c1,c2,c3,c4 /-.89286,7.2967,-.98074,5.7835E-03/
c data d1,d2,d3,d4 /34.190,-43.868,19.778,-0.88407/
c data e1,e2,e3,e4 /16.526,-0.16841,-47.985,42.246/
c data mO2,mCO2,mN2,mH2O,mAr /32.,44.01,28.016,18.016,39.944/
c data mCO /28.01/
c
c Q = (T+459.67)/180.
c Qref= (Tds+459.67)/180.
c
c hN2=(a1*(Q-Qref)-a2*2.*(1./sqrt(Q)-1./sqrt(Qref))-a3*(1./Q-
> 1./Qref)-a4*.5*(1./Q**2-1./Qref**2))*180.
c hO2=(b1*(Q-Qref)+b2*.4*(Q**2.5-Qref**2.5)-b3*2.*(1./sqrt(Q)-
> 1./sqrt(Qref))-b4*(1./Q-1./Qref))*180.
c hCO2=(c1*(Q-Qref)+c2/1.5*(Q**1.5-Qref**1.5)+c3*.5*(Q**2-
Qref**2)
> +c4/3.*(Q**3-Qref**3))*180.
c hH2O=(d1*(Q-Qref)+d2/1.25*(Q**1.25-Qref**1.25)+d3/1.5*(Q**1.5-
> Qref**1.5)+d4*.5*(Q**2-Qref**2))*180.
c hCO=(e1*(Q-Qref)+e2/1.75*(Q**1.75-Qref**1.75)+e3*2.*(sqrt(Q)-
> sqrt(Qref))+e4*4.*(Q**.25-Qref**.25))*180
c hAr=5.005*(Q-Qref)*180.
c
c Mm=yN2*mN2+yO2*mO2+yCO2*mCO2+yH2O*mH2O+yAr*mAr+yCO*mCO
c
c HGAST=(yN2*hN2+yO2*hO2+yCO2*hCO2+yH2O*hH2O+yAr*hAr+yCO*hCO)/Mm
c
c end
c
c ----- Entropy, SGASTP(T,P,yCO2,...,yCO) -----
c
c This function calculates the entropy of a gas as a function
c of temperature, pressure and mole fractions. The equations for
c Cp are from "Fundamentals of Classical Thermodynamics",
c G.J. Van Wylen and R.E. Sonntag, pp. 683 - 684. Maximum error
c for air was around 0.5 %.
c

```

```

function SGASTP (T,P,yCO2,yH2O,yO2,yN2,yAr,yCO)

common /DS/Tds,Pds,YdsCO2,YdsH2O,YdsO2,YdsN2,YdsAr,YdsCO
real Mm,mO2,mN2,mCO2,mH2O,mAr,mCO
data R /1.9858/
data a1,a2,a3,a4 /9.3355,-122.56,256.38,-196.08/
data b1,b2,b3,b4 /8.9465,4.8044E-03,-42.679,56.615/
data c1,c2,c3,c4 /-.89286,7.2967,-.98074,5.7835E-03/
data d1,d2,d3,d4 /34.190,-43.868,19.778,-0.88407/
data e1,e2,e3,e4 /16.526,-0.16841,-47.985,42.246/
data mO2,mCO2,mN2,mH2O,mAr /32.,44.01,28.016,18.016,39.944/
data mCO /28.01/

Q = (T+459.67)/180.
Qref= (Tds+459.67)/180.
sO2 =0.
sN2 =0.
sCO2=0.
sH2O=0.
sCO =0.
sAr =0.

if (yO2 .ne. 0.0) then
  sO2=b1*log(Q/Qref)+b2/1.5*(Q**1.5-Qref**1.5)-b3/1.5*
    (Q**(-1.5)-Qref**(-1.5))-b4*.5*(Q**(-2)-Qref**(-2))
  -R*log(yO2*P/ydsO2/Pds)
endif
if (yN2 .ne. 0.0) then
  sN2=a1*log(Q/Qref)-a2/1.5*(Q**(-1.5)-Qref**(-1.5))-
    a3*.5*(Q**(-2)-Qref**(-2))-a4/3.*(Q**(-3)-Qref**(-3))
  -R*log(yN2*P/ydsN2/Pds)
endif
if (yCO2 .ne. 0.0) then
  sCO2=c1*log(Q/Qref)+c2*2.*(sqrt(Q)-sqrt(Qref))+
    c3*(Q-Qref)+c4*.5*(Q**2-Qref**2)
  -R*log(yCO2*P/ydsCO2/Pds)
endif
if (yH2O .ne. 0.0) then
  sH2O=d1*log(Q/Qref)+d2*4.*(Q**.25-Qref**.25)+
    d3*2.*(sqrt(Q)-sqrt(Qref))+d4*(Q-Qref)
  -R*log(yH2O*P/ydsH2O/Pds)
endif
if (yCO .ne. 0.0) then
  sCO=e1*log(Q/Qref)+e2/.75*(Q**.75-Qref**.75)-e3/.5*(1.
    /sqrt(Q)-1./sqrt(Qref))-e4/.75*(Q**(-.75)-Qref**(-.75))
  -R*log(yCO*P/ydsCO/Pds)
endif
if (yAr .ne. 0.0) then
  sAr=5.005*log(Q/Qref)-R*log(yAr*P/ydsAr/Pds)
endif

Mm=yN2*mN2+yO2*mO2+yCO2*mCO2+yH2O*mH2O+yAr*mAr+yCO*mCO
SGASTP=(yN2*sN2+yO2*sO2+yCO2*sCO2+yH2O*sH2O+yAr*sAr+yCO*sCO)/Mm
end

----- Temperature of gas, TGASH (H,yCO2,...) -----

This program calculates the temperature of gas as a
function of the enthalpy, Tref and mole fractions. It uses
the function HGAST and iterates. 3-5 iterations are needed
for air. For low temperatures, it only takes 2-3.

```



```

c      function TGASH(H,yCO2,yH2O,yO2,yN2,yAr,yCO)
c
c      common /DS/Tds,Pds,YdsCO2,YdsH2O,YdsO2,YdsN2,YdsAr,YdsCO
c      T1=Tds
c      H1=0.
c      T2=Tds+50.
c      H2=HGAST(T2,yCO2,yH2O,yO2,yN2,yAr,yCO)
c
c...   Iteration:
c
c      DO 10 I=1,20
c          T=T2-(H2-H)*(T2-T1)/(H2-H1)
c          IF(ABS(T/T2-1.).LT.0.0005)GO TO 20
c          T1=T2
c          H1=H2
c          T2=T
c          H2=HGAST(T2,yCO2,yH2O,yO2,yN2,yAr,yCO)
10      CONTINUE
20      TGASH=T
c
c      END
c
c      ----- Temperature of gas, f(S,Pds,yCO2,...,yCO) -----
c
c      This program calculates the temperature of gas as a
c      function of the entropy, P, Tds, Pds and mole fractions. It
c      uses the function SGASTP and iterates. 4-6 iterations are
c      needed for air. For low temperatures, it only takes 2-4.
c
c      FUNCTION TGASS(S,P,yCO2,yH2O,yO2,yN2,yAr,yCO)
c
c      common /DS/Tds,Pds,YdsCO2,YdsH2O,YdsO2,YdsN2,YdsAr,YdsCO
c      T1=Tds
c      S1=SGASTP(T1,P,yCO2,yH2O,yO2,yN2,yAr,yCO)
c      T2=Tds+50.
c      S2=SGASTP(T2,P,yCO2,yH2O,yO2,yN2,yAr,yCO)
c
c...   Iteration:
c
c      DO 10 I=1,20
c          T=T2-(S2-S)*(T2-T1)/(S2-S1)
c          IF(ABS(T/T2-1.).LT.0.0005)GO TO 20
c          T1=T2
c          S1=S2
c          T2=T
c          S2=SGASTP(T2,P,yCO2,yH2O,yO2,yN2,yAr,yCO)
10      CONTINUE
20      TGASS=T
c
c      END
c
c      ----- Mole fractions -----
c
c      This function calculates the mole fractions after
c      mixing two gas streams. The mole fractions of the mixing gases
c      and mass flows are input to the program. It then returns the
c      mass flow, mole fractions and molar mass of the new mixture.
c      ynO2,ynN2,... are number of moles pr. lb of "dry" gas.

```

```

c      subroutine MOLFRC (MRi1,yi1CO2,yi1H2O,yi1O2,yi1N2,yi1Ar,yi1CO,
>          Mi1,MRi2,yi2CO2,yi2H2O,yi2O2,yi2N2,yi2Ar,yi2CO,Mi2,
>          MRO,yoCO2,yoH2O,yoO2,yoN2,yoAr,yoCO,Mo)
c      real MRi1,MRi2,MRO,mO2,mN2,mCO2,mH2O,mAr,mCO,MOLi1,MOLi2,MOLo
c      real Mi1,Mi2,Mo
c      data mO2,mCO2,mN2,mH2O,mAr /32.,44.01,28.016,18.016,39.944/
c      data mCO /28.01/
c
c...    molar mass of inlet streams:
c
c      Mi1=yi1O2*mO2+yi1N2*mN2+yi1CO2*mCO2+yi1Ar*mAr+yi1H2O*mH2O+
>          yi1CO*mCO
c      Mi2=yi2O2*mO2+yi2N2*mN2+yi2CO2*mCO2+yi2Ar*mAr+yi2H2O*mH2O+
>          yi2CO*mCO
c
c...    number of moles (pr.sec):
c
c      MOLi1=MRi1/Mi1
c      MOLi2=MRi2/Mi2
c      MOLo=MOLi1+MOLi2
c
c      yoCO2=(yi1CO2*MOLi1+yi2CO2*MOLi2)/MOLo
c      yoH2O=(yi1H2O*MOLi1+yi2H2O*MOLi2)/MOLo
c      yoO2=(yi1O2*MOLi1+yi2O2*MOLi2)/MOLo
c      yoN2=(yi1N2*MOLi1+yi2N2*MOLi2)/MOLo
c      yoAr=(yi1Ar*MOLi1+yi2Ar*MOLi2)/MOLo
c      yoCO=(yi1CO*MOLi1+yi2CO*MOLi2)/MOLo
c
c      MRO=MRi1+MRi2
c      Mo=yoO2*mO2+yoN2*mN2+yoCO2*mCO2+yoAr*mAr+yoH2O*mH2O+yoCO*mCO
c
c      end
c
c      ----- Viscosity, MUGAST (T,yCO2,...,yAr) -----
c
c      This function calculates the dynamic viscosity of
c      gas. It uses semiempirical formula recommended by
c      Frank M. White, "Viscous Fluid Flow", pp. 25-38.
c
c          y1 = yCO2      y2 = yH2O
c          y3 = yO2       y4 = yN2
c          y5 = yAr       y6 = yCO
c
c      real function MUGAST (T,yCO2,yH2O,yO2,yN2,yAr,yCO)
c
c      real mu(6),y(6),M(6),T0(6),S(6),mu0(6)
c      data M /44.01,18.016,32.,28.016,39.944,28.01/
c      data T0 /491.6,750.,491.6,491.6,491.6,491.6/
c      data S /400.,1550.,250.,192.,260.,245./
c      data mu0 /.1370,.1703,.1919,.1663,.2125,.1657/
c
c      y(1)= yCO2
c      y(2)= yH2O
c      y(3)= yO2
c      y(4)= yN2
c      y(5)= yAr
c      y(6)= yCO
c      Tabs=T+459.67
c
c      do 10 i=1,6
c          mu(i)=mu0(i)*(Tabs/T0(i))**1.5*(T0(i)+S(i))/(Tabs+S(i))
10      continue

```

```

c
temp=0.
do 20 i=1,6
    temp1=0.
    do 30 j=1,6
        temp2=1.+sqrt(mu(i)/mu(j))*(M(j)/M(i))**.25
        temp3=sqrt(8.+8.*M(i)/M(j))
        temp1=temp1+temp2**2/temp3*y(j)
30    continue
    temp=temp+mu(i)*y(i)/temp1
20    continue
c
MUGAST=temp*1.E-3/14.882
c
end
c
----- Conductivity, KGAST (T,yCO2,...,yAr) -----
c
    This function calculates the thermal conductivity of
c    gas. It uses semiempirical formula recommended by
c    Frank M. White, "Viscous Fluid Flow", pp.30 - 36. It is not
c    accurate for high temperatures. (approx 4-5 % for T > 1000. F)
c
c        y1 = yCO2      y2 = yH2O
c        y3 = yO2       y4 = yN2
c        y5 = yAr       y6 = yCO
c
real function KGAST (T,yCO2,yH2O,yO2,yN2,yAr,yCO)
c
real k(6),y(6),M(6),T0(6),S(6),k0(6)
data M /44.01,18.016,32.,28.016,39.944,28.01/
data T0 /491.6,491.6,491.6,491.6,491.6,491.6/
data S /4000.,2300.,400.,300.,270.,320./
data k0 /.008407,.01036,.01419,.0140,.009444,.01342/
c
y(1)= yCO2
y(2)= yH2O
y(3)= yO2
y(4)= yN2
y(5)= yAr
y(6)= yCO
Tabs=T+459.67
c
do 10 i=1,6
    k(i)=k0(i)*(Tabs/T0(i))**1.5*(T0(i)+S(i))/(Tabs+S(i))
10    continue
c
temp=0.
do 20 i=1,6
    temp1=0.
    do 30 j=1,6
        temp2=1.+sqrt(k(i)/k(j))*(M(j)/M(i))**.25
        temp3=sqrt(8.+8.*M(i)/M(j))
        temp1=temp1+temp2**2/temp3*y(j)
30    continue
    temp=temp+k(i)*y(i)/temp1
20    continue
c
KGAST=temp
c
end
c
----- Density, f(T,P,yCO2,yH2O,yO2,yN2,yAr,yCO) -----
-

```

```

c
c      This function calculates the density according to the ideal
c      gas law. Temperature in F, pressure in psia and density in
c      lbm/cu.ft
c
c      function ROGAS (T,P,yCO2,yH2O,yO2,yN2,yAr,yCO)
c
c      real Mm,mO2,mN2,mCO2,mH2O,mAr,mCO
c      data mO2,mCO2,mN2,mH2O,mAr /32.,44.01,28.016,18.016,39.944/
c      data mCO /28.01/
c
c      Mm=yN2*mN2+yO2*mO2+yCO2*mCO2+yH2O*mH2O+yAr*mAr+yCO*mCO
c      ROGAS =Mm/10.73/(T+459.67)*P
c
c      end
c
c      ----- Prandtl number, f(T,yCO2,yH2O,yO2,yN2,yAr,yCO) -----
c
c      This function calculate the Prandtl number of a gas as a
c      function of temperature. But since the thermal conductivity
c      is not accurate for high temperatures, the Prandtl number is
c      assumed constant. That is just as accurate.
c
c      function PrGAST (T,yCO2,yH2O,yO2,yN2,yAr,yCO)
c      end

```

## A.2 Computer Programs for Chapter 2

```

$title: 'pyrolysis'
$storage:2
      implicit real (a-z)
      integer NN,I,J
      character*8 test
      common /DS/Tds,Pds,ydsCO2,ydsH2O,ydsO2,ydsN2,ydsAr,ydsCO
c.....
c
c          PROGRAM TO CALCULATE THE COMBUSTION TIME
c          FOR DOUGLUS FIR PARTICLES IN OSU BIOMASS
c          COMBUSTION TEST UNIT.
c
c..... dead state properties .....
c
      Tds    = 59.0
      Pds    = 14.696
      ydsCO2 = 0.0002999
      ydsH2O = 0.0111
      ydsO2  = 0.2072
      ydsN2  = 0.7722
      ydsAr  = 0.0092
      ydsCO  = 0.0000001
c
c..... properties of comb. air.....
c
      Pair   = 14.7
      yCO2a  = 0.000296
      yH2Oa  = 0.011129
      yO2a   = 0.20717
      yN2a   = 0.77221
      yAra   = 0.009196
      yCOa   = 0.0000008
c
c..... higher heating value of the fuel (Btu/lb dry).....
c
      HHV    = 8775.21
c
c..... amb. and fuel initial temp. (deg.F) .....
c
      TambF  = 80.0
      TambR  = TambF + 460.0
      TambC  = (TambF - 32.0)*5./9.
      TambK  = TambC + 273.0
c
      TpK    = 570.0
      TpC    = TpK - 273.0
      TpF    = (TpC + 17.78)*1.8
      TpR    = TpF + 460.0
c
      TplF   = 1832.0
      TplR   = TplF + 460.0
      TplC   = (TplF - 32.0)*5./9.
      TplK   = TplC + 273.0

```

```

C
write(*,*)'input the following values'
write(*,*)'TEST CODE'
read(*, '(a8)') test
write(*,*)'VOLUME FLOW RATE OF UNDER-FIRE AIR (scfh)'
read(*,*)Vair
write(*,*)'TEMPERATURE OF UNDER-FIRE AIR (deg. F)'
read(*,*)TaF

C
TaR  = TaF + 460.0
TaC  = (TaF - 32)*5./9.
Tak  = TaC + 273.0

C
write(*,*)'MASS FLOW RATE OF THE FUEL (lb/hr dry)'
read(*,*)mf
write(*,*)'TOTAL HEAT LOSS FROM ADIABATIC MODEL (Btu/hr)'
read(*,*)Q1
write(*,*)'MOISTURE CONTENT OF THE FUEL (percent WB)'
read(*,*)mc

C
mcdb = 100.0*mc/(100.0 - mc)

C
write(*,*)'SIZE OF PARTICLE (inches)'
read(*,*)Dp

C
Dpcgs = Dp*2.54

C
write(*,*)'AVERAGE TEMPERATURE OF OUTSIDE WALL (deg F)'
read(*,*)TstF

C
TstR  = TstF + 460.0
TstC  = (TstF - 32.0)*5./9.
TstK  = TstC + 273.0

C
write(*,*)'GARTE TEMPERATUE (deg. F)'
read(*,*)TgF

C
TgR  = TgF + 460.
TgC  = (TgF - 32.0)*5./9.
TgK  = TgC + 273.0

C
write(*,*)'FLAME TEMPERATURE (deg F)'
read(*,*)TfF

C
TfR  = TfF + 460.0
TfC  = (TfF - 32.0)*5./9.
TfK  = TfC + 273.0
write(*,*)'DISTANCE OF THE FLAME FROM GRATE (in.)'
read(*,*)Hf

C
write(*,*)'NUMBER OF PARTICLES PER GRATE NNPGL-NNPG-NNPGH'
read(*,*)NNpgL
read(*,*)NNpg
read(*,*)NNpgH

C
ROpdcgs = 0.5613
ROpcgs  = (1. + mc/100.0)*ROpdcgs
ROccgs  = 0.17
ROc     = ROccgs*62.428
ROp     = ROpcgs*62.428
ROpd    = ROpdcgs*62.428

C
c.....mass of the particle & exp. time of combustion .....

```

```

c
mp      = ROpdcgs*(Dpcgs**3.)
texp    = ((NNpg*mp/453.59)/mf)*3600.
texpL   = ((NNpgL*mp/453.59)/mf)*3600.
texpH   = ((NNpgH*mp/453.59)/mf)*3600.
meant   = (texp + texpL + texpH)/3.
var = ((meant-texp)**2+(meant-texpL)**2+(meant-texpH)**2)/3
STD     = (var)**0.5

c..... diffusion coef. ....
c
CONST   = 0.4248
POWER   = 1.75
Diffgas = CONST*((Tak/298.16)**POWER)

c
Cpcgsd  = 0.266 + 0.00116*(Tpk - 273.)
Cpcgs   = (Cpcgsd + 0.01*mcdb)/(1. + 0.01*mcdb)

c
c..... thermal diffusivity .....
c
alpha   = 0.001235

c
c..... heat of volatilization .....
c
Ldry    = 180.0
if (mc .LT. 23.08)then
    x = mc
else
    x =23.08
endif

c
QbH2o   = (1.0/x)*(467.94*x - 32.314*x**2 + 1.040787*x**3
> + 0.046801*x**4 - 0.006588*x**5 + 2.56985E-4*x**6
> - 3.48937E-6*x**7)
LH2O    = (QbH2O + 1059.)*mc/(100.0*1.8)
Lcgs    = Ldry + LH2O

c
c..... constants (English units) .....
c
PI       = 3.14159265
sigma    = 0.173E-8

c
c..... (INCHES) .....
c
Dcer     = 6.50
Dcs      = 12.25
Dg       = 6.50
Dst      = 12.75

c
Hcer     = 36.0
Hst      = 36.0
Hp       = 0.03125

c..... AREA (SQUARE FEET) .....
c
Acer     = PI*Dcer*Hcer/144.
Ag       = PI*Dcer*Dcer/(4.*144.)
Ap       = Dp*Dp/144.
Ast      = PI*Dst*Hst/144.

c..... emisivity and transmisivity .....
c
Ec       = 0.95
Ecer     = 0.90
Ef       = 0.70
Ep       = 0.90
Est      = 0.95
Taug     = 0.30

```

```

c..... bed volume .....
    Bvol    = NNpg*(Dp**3.0)
    Bh      = NNpg*(Dp**3.0)/(Ag*144.)
    Bvolcgs = Bvol*16.39
    Bhcgs   = Bh*2.54
c..... conductivity (Eng. units) .....
    Kcer = (5.0/12.0)*(Dcs -Dcer)/2.0
    Kp   = (0.45*(1.39+2.8*mc/100.) + 0.165)/12.
    kst  = 10.9
c..... convective heat trans. coeff. (Btu/hr-F-sq. ft) .....
    hcon = 1.0
c..... ReDp, B, C, Sc .....
c
    ROastd = ROGAS(Tds,Pds,ydsCO2,ydsH2O,ydsO2,ydsN2,ydsAr,ydsCO)
    mair   = Vair*ROastd
    ROair  = ROGAS(TaF,Pair,yCO2a,yH2Oa,yO2a,yN2a,yAra,yCOa)
    ROgcgs = ROair*0.0160185
    MUair  = MUGAST(TaF,yCO2a,yH2Oa,yO2a,yN2a,yAra,yCOa)
    Uair   = (mair/(ROair*Ag))/3600.0
    ReDp   = (ROair*Uair*(Dp/12.))/(MUair)
    Sc     = 0.89
    C      = 0.3*((ReDp)**(0.5))*(Sc**(1./3.))
    B      = 0.087
c
c..... heat trans. to particles .....
c
c..... ceramic wall temp. ....
c
    Qcon = hcon*Ast*(TstR - TambR)
    Qrad = Est*Ast*sigma*(TstR**4. - TambR**4.)
    Q2    = Qcon + Qrad
    Rt    = (1./(2.*PI*Hst/12.))*(alog(Dcs/Dcer)/Kcer+alog(Dst/Dcs)/Kst)
    TcerR = TstR + Q1*Rt
    TcerF = TcerR - 460.0
    TcerC = (TcerF - 32.0)*5./9.
    TcerK = TcerC + 273.0
    Q2cgs=Q2*(0.07)
    Q1cgs=Q1*(0.07)
c
c..... raddiation from ceramic wall to grate .....
c
    D1 = Hcer/(Dg/2.0)
    Fcerg=(Ag/Acer)*(1.-0.5*(2.+D1**2.-D1*((4.+D1**2.)*(1./2.))))
    D2 = (1.-Ecer)/(Ecer*Acer)
    D3 = 1./(Acer*Fcerg*Taug)
    D4 = (1.-Ep)/(Ep*Ag)
    qcer=(1./Ag)*(sigma)*(TcerR**4. - TpR**4.)*(1./(D2+D3+D4))
c
c..... radiation from flame to grate .....
c
    D5 = (Hf - Bh*12.)/(Dg/2.)
    Ffg = 0.5*(2.+D5**2 - D5*((4.+D5**2)*(1./2.)))
    D6 = (1.-Ep)/Ep
    D7 = 1./(Ffg*Taug)
    D8 = (1.-Ef)/Ef
    qf  = sigma*(TfR**4. - TpR**4.)*(1./(D6+D7+D8))
c
c..... radiation from charing particles .....

```



```

C
  D9 = Dp/Hp
  D10 = (1.+D9**2.)
  D11 = D10**0.5
  D12 = (1.+2.*D9**2.)**0.5
  Fpp = (2./(pi*D9**2.))*(alog(D10/D12) +2.*D9*D11*atan(D9/D11)
>      - 2.*D9*atan(D9))
  D13 = (1.-Ep)/Ep
  D14 = 1./Fpp
  D15 = (1.-Ec)/Ec
  qc = sigma*(Tp1R**4. - TpR**4.)*(1./(D13+D14+D15))
C
C..... conduction from grate .....
C
  qg = (Kp/(Dp/12.))*(TgF - TpF)
C
C..... NET HEAT TRANSFER TO VIRGIN PARTICLE .....
C
  q      = (qcer + qf + 4*qc + qg)/6.0
  FRqf   = 100.0*qf/(q*6.0)
  FRqcer = 100.0*qcer/(q*6.0)
  FRqc   = 100.0*4.0*qc/(q*6.0)
  FRqg   = 100.0*qg/(q*6.0)
C
C..... convert to CGS units .....
C
  qcercgs = qcer*(0.00007535)
  qfcgs   = qf*(0.00007535)
  qccgs   = qc*(0.00007535)
  qgcgs   = qg*(0.00007535)
  qcgs    = q*(0.00007535)
  q0cgs   = q0*(0.00007535)
C
C
C
C
C
C***** pyrolysis time *****
C
  D16 = (5./6.)*(ROpcgs - ROccgs)*Lcgs/qcgs
  D17 = ROpcgs*Cpcgs*(350.)/(3.*qcgs)
  AA  = D16+D17
  BB  = 1./(10.*alpha)
  tpp = AA*(Dpcgs/2.) + BB*((Dpcgs/2.)**2.)
C
C***** CHAR COMBUSTION *****
C
  tc0 = (ROccgs*(Dpcgs**2.))/(8.*ROgcgs*Diffgas*alog(B+1))
C
  x1   = 0.0
  sum1 = 0.0
  x2   = 0.0
  sum2 = 0.0
  NN   = 100
C
  do 10 I=1,NN,2
    x1 = I*(1.0/NN)
    sum1 = sum1 + 2.*x1/(1. + c*(x1**0.5))
10  continue

```

```

C
  NN      = 100
  do 20 J=2,NN-1,2
    x2      = J*(1./NN)
    sum2     = sum2 + 2.*x2/(1. + c*(x2**0.5))
20    continue
C
  tc = tc0*(1./(3.*NN))*(2./(1.+c) + 4.*sum1 + 2.*sum2)
C
C*****
C..... fuel feed rate (calculated) .....
C
  mfcalc = (((NNpg*mp)/(tpp + tc))*3600.)/453.59
C
C..... error .....
C
  ERR1 = 100*(texp - (tpp + tc))/texp
  ERR2 = 100*(mf - mfcalc)/mf
C
C..... convert values for output .....
C
  Qin      = mf*HHV
  Qincgs   = Qin*(0.07)
  m1cgs    = mfcalc*0.125997
  m2cgs    = mf*0.125997
  RODcgs   = ROgcgs*Diffgas
  macgs    = mair*0.1259972
  Uacgs    = Uair*30.48
  Leng1    = Lcgs/0.555478
C
C
C
C..... print the results .....
C
  write(4,*)'
  write(4,19)'TEST CODE:',TEST
  write(4,17)'-----'
>-----'
C
  write(4,4)'q to particle (cal/sec-cm2, Btu/hr-ft2) =',qcgs,q
  write(4,2)'Frac. of heat trans. from wall      (%) =',FRqcer
  write(4,2)'Frac. of heat trans. from falme      (%) =',FRqf
  write(4,2)'Frac. of heat trans. from grate      (%) =',FRqg
  write(4,2)'Frac. of heat trans. from char. part.(%) =',FRqc
  write(4,*)' ..... '
  write(4,2)'Pyrolysis time                        (sec) =',tpp
  write(4,2)'Char comb.time at Re=0.0              (sec) =',tc0
  write(4,2)'Actual char comb. time                (sec) =',tc
  write(4,2)'Total comb. time (calculated)          (sec) =',tpp+tc
  write(4,2)'Total comb. time (experimental)        (sec) =',texp
  write(4,2)'Standard deviation of exp. time        (sec) =',STD
  write(4,2)'Error in time of comb.                 (%) =',ERR1
  write(4,*)' ..... '
  write(4,4)'Calc. fuel feed rate                    (g/sec, lb/hr)
=',m1cgs,mfcalc
  write(4,4)'Exp. fuel feed rate                    (g/sec, lb/hr) =',m2cgs,mf
  write(4,2)'Error in fuel feed rate                 (%) =',ERR2
  write(4,*)' ..... '
  write(4,2)'Values of "a" in pyrolysis equation    =',AA
  write(4,2)'Values of "b" in pyrolysis equation    =',BB
  write(4,*)' ..... '
  write(4,2)'Renolds No. based on part. dia.        =',ReDp
  write(4,4)'Coeff. C (in char comb. eq.)          =',C

```

```

        write(4,*)' ..... '
        write(4,1)'Dry part. density (g/cm3, lb/ft3)
=,ROpdcgs,ROpd
        write(4,1)'Wet part. density (g/cm3, lb/ft3) =,ROpcgs,ROp
        write(4,1)'Char density (g/cm3, lb/ft3) =,ROccgs,ROC
        write(4,5)'Comb. air density (g/cm3, lb/ft3)
=,ROgcgs,ROair
        write(4,*)' ..... '
        write(4,5)'Bed volume (cm3, in3)
=,Bvolcgs,Bvol
        write(4,5)'Bed height (cm, in) =,Bhcgcs,bh
        write(4,2)'No. pf particles on the grate =,NNpg
        write(4,1)'Moisture content of the part.(% WB, DB) =,mc,mcdb
        write(4,5)'Size of the particles (cm, in) =,Dpcgs,Dp
        write(4,*)' ..... '
        write(4,1)'Comb. air flow rate (g/sec, lb/hr) =,macgs,mair
        write(4,5)'Comb. air velocity (cm/sec, ft/sec) =,Uacgs,Uair
        write(4,*)' ..... '
        write(4,1)'Heat of vol. wet (cal/g, Btu/lb) =,Lcgs,Lengl
        write(4,*)' ..... '
        write(4,1)'Average flame temp. (deg. C,F) =,TfC,TfF
        write(4,1)'Average ceramic wall temp. (deg. C,F) =,TcerC,TcerF
        write(4,1)'Average steel wall temp. (deg. C,F) =,TstC,TstF
        write(4,1)'Average grate temp. (deg. C,F) =,TgC,TgF
        write(4,*)' ..... '
        write(4,1)'Energy input (cal/sec, Btu/hr) =,Qincgs,Qin
        write(4,1)'Heat loss ad. model (cal/sec, Btu/hr) =,Qlcs,Ql
        write(4,1)'Heat loss wall temp. (cal/sec, Btu/hr) =,Q2cgs,Q2
        write(4,*)' ..... '
        write(4,5)'Gas diffusivity (cm2/sec) =,Diffgas
        write(4,5)'prod. of density and diff. (g/cm-sec) =,RODcgs
        write(4,17)'-----'
>-----'

```

```

c
1      format(5x,a,f11.2,5x,f11.2)
4      format(5x,a,f11.4,5x,f11.2)
5      format(5x,a,f11.5,5x,f11.5)
2      format(5x,a,f11.2)
17     format(5x,a)
19     format(25x,a,10x,(a8))
      end
$title: 'pyrolysis'
$storage:2
      implicit real (a-z)
      integer NN,I,J
      character*8 test
      common /DS/Tds,Pds,ydsCO2,ydsH2O,ydsO2,ydsN2,ydsAr,ydsCO
c.....
c
c      PROGRAM TO CALCULATE THE COMBUSTION TIME
c      FOR WOOD-PELLET PARTICLES IN OSU BIOMASS
c      COMBUSTION TEST UNIT.
c.....
c      dead state properties .....
c
      Tds = 59.0
      Pds = 14.696
      ydsCO2 = 0.0002999
      ydsH2O = 0.0111
      ydsO2 = 0.2072
      ydsN2 = 0.7722
      ydsAr = 0.0092
      ydsCO = 0.0000001
c

```

```

c..... properties of comb. air.....
c
    Pair    = 14.7
    yCO2a   = 0.000296
    yH2Oa   = 0.011129
    yO2a    = 0.20717
    yN2a    = 0.77221
    yAra    = 0.009196
    yCOa    = 0.0000008
c
c
c..... amb. and fuel initial temp. (deg.F) .....
c
    TambF   = 80.0
    TambR   = TambF + 460.0
    TambC   = (TambF - 32.0)*5./9.
    TambK   = TambC + 273.0
c
    TpK     = 570.0
    TpC     = TpK - 273.0
    TpF     = (TpC + 17.78)*1.8
    TpR     = TpF + 460.0
c
    TplF    = 1832.0
    TplR    = TplF + 460.0
    TplC    = (TplF - 32.0)*5./9.
    TplK    = TplC + 273.0
c
c.....
c
    write(*,*)'input the following values'
    write(*,*)'TEST CODE'
    read(*, '(a8)') test
    write(*,*)'VOLUME FLOW RATE OF UNDER-FIRE AIR (scfh)'
    read(*,*)Vair
c
    write(*,*)'TEMPERATURE OF UNDER-FIRE AIR (deg. F)'
    read(*,*)TaF
    TaR     = TaF + 460.0
    TaC     = (TaF - 32)*5./9.
    Tak     = TaC + 273.0
c
    write(*,*)'MASS FLOW RATE OF THE FUEL (lb/hr dry)'
    read(*,*)mf
    WRITE(*,*)'HIGHER HEATING VALUE OF THE FUEL'
    read(*,*)HHV
    write(*,*)'TOTAL HEAT LOSS FROM ADIABATIC MODEL (Btu/hr)'
    read(*,*)Ql
c
    write(*,*)'MOISTURE CONTENT OF THE FUEL (percent WB)'
    read(*,*)mc
    mcdb    = 100.0*mc/(100.0 - mc)
c
    write(*,*)'SIZE OF PARTICLE (inches)'
    read(*,*)Dp
    Dpcgs   = Dp*2.54
c
    write(*,*)'AVERAGE TEMPERATURE OF OUTSIDE WALL (deg F)'
    read(*,*)TstF
    TstR    = TstF + 460.0
    TstC    = (TstF - 32.0)*5./9.
    TstK    = TstC + 273.0

```

```

C      write(*,*)'GARTE TEMPERATUE (deg. F)'
      read(*,*)TgF
      TgR      = TgF      + 460.
      TgC      = (TgF - 32.0)*5./9.
      TgK      = TgC + 273.0

C      write(*,*)'FLAME TEMPERATURE (deg F)'
      read(*,*)TfF
      TfR      = TfF + 460.0
      TfC      = (TfF - 32.0)*5./9.
      TfK      = TfC + 273.0

C      write(*,*)'DISTANCE OF THE FLAME FROM GRATE (in.)'
      read(*,*)Hf

C      write(*,*)'NUMBER OF PARTICLES PER GRATE NNPGL-NNPG-NNPGH'
      read(*,*)NNpgL
      read(*,*)NNpg
      read(*,*)NNpgH
      write(*,*)'VOLUME OF THE PARTICLE (cub. cm)'
      read(*,*)VOLp
      write(*,*)'DENSITY OF PARTICLES (lb/cub. ft)'
      read(*,*)ROpd

C      ROpcgs = ROpd/62.428
      ROp     = (1. + mc/100.0)*ROpd
      ROpcgs  = ROp/62.428
      ROccgs  = 0.17
      ROc     = ROccgs*62.428

C
C..... constants (English units) .....
C
      PI      = 3.14159265
      sigma   = 0.173E-8

C
C..... (INCHES) .....
C
      Dcer    = 6.50
      Dcs     = 12.25
      Dg      = 6.50
      Dst     = 12.75

C
      Hcer    = 36.0
      Hst     = 36.0
      Hp      = 0.03125

C
C..... AREA (SQUARE FEET) .....
C
      Acer    = PI*Dcer*Hcer/144
      Ag      = PI*Dcer*Dcer/(4*144)
      Ap      = Dp*Dp/144
      Ast     = PI*Dst*Hst/144

C
C..... emisivity and transmisivity .....
C
      Ec      = 0.95
      Ecer    = 0.90
      Ef      = 0.70
      Ep      = 0.90
      Est     = 0.95
      Taug    = 0.30
C

```

```

c..... experimental time of combustion & bed height .....
c
    mp      = ROpdcgs*(VOLp)
    texp    = ((NNpg*mp/453.59)/mf)*3600.
    texpL   = ((NNpgL*mp/453.59)/mf)*3600.
    texpH   = ((NNpgH*mp/453.59)/mf)*3600.
    meant   = (texp + texpL + texpH)/3.
    var     = ((texp-meant)**2+(texpL-meant)**2+(texpH-meant)**2)/3
    STD     = (var)**0.5
c
    bvolcgs = NNpg*Volp
    bvol    = bvolcgs/16.39
    bh      = bvol/(Ag*144.0)
    bhcgs   = bh*2.54
c
c..... volume and diameter reduction after pyrolysis .....
c
    mchar    = ROccgs*(Volp)
    mstar    = 1. - mchar/mp
    vv0      = 1.0 + 0.03182*mstar - 0.7687*(mstar**2.0)
    dd0      = vv0**(1./3.)
c
c..... diffusion coef. ....
c
    CONST    = 0.4248
    POWER    = 1.75
    Diffgas  = CONST*((Tak/298.16)**POWER)
c
    Cpcgsd   = 0.266 + 0.00116*(Tpk - 273)
    Cpcgs    = (Cpcgsd + 0.01*mcdb)/(1. + 0.01*mcdb)
c
c..... thermal diffusivity & conductivity .....
c
    if (mcdb .LE. 30.0) then
        ROG = ROpdcgs - (mcdb/30.)*0.15
    else
        ROG = ROpdcgs - 0.15
    endif
c
    if (mcdb .lt. 40.0)then
        alpha = (-11.3*(1. - ROG*(0.667 + 0.01*mcdb))**0.5
>          +12.2)/(ROG*(0.01*mcdb + 0.324)*10000.0)
        Kt    = (ROG*(4.8 + 0.090*mcdb) + 0.57)/10000.0
    else
        Vat   = 1.0 - (0.685*ROG + 0.01*mcdb)
        Kt    = (ROG*(5.18 + 0.131*mcdb) + 0.57*Vat)/10000.
        alpha = Kt/(ROG*(0.01*mcdb + 0.324))
    endif
    Kpcgs    = 1.75*Kt
    alpha    = 0.001235
c..... heat of volatilization .....
c
    Ldry     = 180.0
    if (mc .LT. 23.08)then
        x = mc
    else
        x =23.08
    endif
c
    QbH2o    = (1.0/x)*(467.94*x - 32.314*x**2 + 1.040787*x**3
>    + 0.046801*x**4 - 0.006588*x**5 + 2.56985E-4*x**6
>    - 3.48937E-6*x**7)
    LH2O     = (QbH2O + 1059.)*mc/(100.0*1.8)
    Lcgs     = Ldry + LH2O

```

```

c
c..... conductivity (Eng. units) .....
c
      Kcer = (5.0/12.0)*(Dcs -Dcer)/2.0
      Kp   = (0.45*(1.39+2.8*mc/100) + 0.165)/12
      kst   = 10.9
c
c..... convective heat trans. coeff. (Btu/hr-F-sq. ft) .....
c
      hcon = 1.0
c
c..... ReDp, B, C, Sc .....
c
      ROastd = ROGAS(Tds,Pds,ydsCO2,ydsH2O,ydsO2,ydsN2,ydsAr,ydsCO)
      mair   = Vair*ROastd
      ROair  = ROGAS(TaF,Pair,yCO2a,yH2Oa,yO2a,yN2a,yAra,yCOa)
      ROGcgs = ROair*0.0160185
      MUair  = MUGAST(TaF,yCO2a,yH2Oa,yO2a,yN2a,yAra,yCOa)
      Uair   = (mair/(ROair*Ag))/3600.0
      ReDp   = (ROair*Uair*(Dp/12.))/(MUair)
      Sc     = 0.89
      C      = 0.3*((ReDp)**(0.5))*(Sc**(1./3.))
      B      = 0.087
c
c..... heat trans. to particles .....
c
c..... ceramic wall temp. ....
c
      Qcon = hcon*Ast*(TstR - TambR)
      Qrad = Est*Ast*sigma*(TstR**4 - TambR**4)
      Q2    = Qcon + Qrad
      Rt=(1/(2.0*PI*Hst/12.))*(          alog(Dcs/Dcer)/Kcer          +
alog(Dst/Dcs)/Kst)
      TcerR = TstR + Q1*Rt
      TcerF = TcerR - 460.0
      TcerC = (TcerF - 32.0)*5./9.
      TcerK = TcerC + 273.0
      Q2cgs=Q2*(0.07)
      Q1cgs=Q1*(0.07)
c
c..... raddiation from ceramic wall to grate .....
c
      D1 = Hcer/(Dg/2.0)
      Fcerg = (Ag/Acer)*(1-0.5*(2.+D1**2.-D1*((4+D1**2.)*(1./2.))))
      D2 = (1.-Ecer)/(Ecer*Acer)
      D3 = 1./(Acer*Fcerg*Taug)
      D4 = (1.-Ep)/(Ep*Ag)
      qcer=(1./Ag)*(sigma)*(TcerR**4. - TpR**4.)*(1./(D2+D3+D4))
c
c..... radiation from flame to grate .....
c
      D5 = (Hf - Bh*12.)/(Dg/2.0)
      Ffg = 0.5*(2+D5**2-D5*((4+D5**2)**0.5))
      D6 = (1.-Ep)/Ep
      D7 = 1./(Ffg*Taug)
      D8 = (1.-Ef)/Ef
      qf = sigma*(TfR**4. - TpR**4.)*(1./(D6+D7+D8))
c
c..... radiation from charing particles .....

```

```

C
  D9 = Dp/Hp
  D10= (1.+D9**2.)
  D11 = D10**0.5
  D12 = (1.+2.*D9**2.)**0.5
  Fpp = (2./(pi*D9**2.))*(alog(D10/D12) +2.*D9*D11*atan(D9/D11)
>    - 2.*D9*atan(D9))
  D13 = (1.-Ep)/Ep
  D14 = 1./Fpp
  D15 = (1.-Ec)/Ec
  qc = sigma*(Tp1R**4 - TpR**4)*(1./(D13+D14+D15))
C
C..... conduction from grate .....
C
  qq = (Kp/(Dp/12))*(TgF - TpF)
C
C..... NET HEAT TRANSFER TO VIRGIN PARTICLE .....
C
  q      = (qcer + qf + 4*qc + qq)/6.0
  FRqf   = 100.0*qf/(q*6.0)
  FRqcer = 100.0*qcer/(q*6.0)
  FRqc   = 100.0*4.0*qc/(q*6.0)
  FRqq   = 100.0*qq/(q*6.0)
C
C..... convert to CGS units .....
C
  qcercgs = qcer*(0.00007535)
  qfcgs   = qf*(0.00007535)
  qccgs   = qc*(0.00007535)
  qgcgs   = qq*(0.00007535)
  qcgs    = q*(0.00007535)
  q0cgs   = q0*(0.00007535)
C
C***** pyrolysis time *****
C
  D16 = (5./6.)*(ROpcgs - ROccgs)*Lcgs/qcgs
  D17 = ROpcgs*Cpcgs*(350.0)/(3*qcgs)
  AA  = D16+D17
  BB  = 1./(10.0*alpha)
  tpp = AA*Dpcgs/2. + BB*((Dpcgs/2. )**2.)
C
C***** CHAR COMBUSTION *****
C
  tc0 = (ROccgs*(Dpcgs**2.))/(8.*ROgcgs*Diffgas*alog(B+1))
C
  x1   = 0.0
  sum1 = 0.0
  x2   = 0.0
  sum2 = 0.0
  NN   = 100
C
  do 10 I=1,NN,2
    x1   = I*(1.0/NN)
    sum1 = sum1 + 2.*x1/(1. + c*(x1**0.5))
10    continue
C
  do 20 J=2,NN-1,2
    x2   = J*(1./NN)
    sum2 = sum2 + 2.*x2/(1. + c*(x2**0.5))
20    continue
C
  tc = tc0*(1./(3.*NN))*(2./(1.+c) + 4.*sum1 + 2.*sum2)
C
C*****

```



```

C
C..... fuel feed rate (calculated) .....
C
      mfcalc = (((NNpg*mp)/(tpp + tc))*3600.)/453.59
C
C..... error .....
C
      ERR1 = 100*(texp - (tpp + tc))/texp
      ERR2 = 100*(mf - mfcalc)/mf
C
C..... convert values for output .....
C
      Qin      = mf*HHV
      Qincgs    = Qin*(0.07)
C
      m1cgs     = mfcalc*0.125997
      m2cgs     = mf*0.125997
C
      RODcgs    = ROgcgs*Diffgas
C
      macgs     = mair*0.1259972
      Uacgs     = Uair*30.48
      Leng1     = Lcgs/0.555478
C
C..... print the results .....
C
      write(4,*)'
      write(4,19)'TEST CODE:',TEST
      write(4,17)'-----'
      >-----'
C
      write(4,4)'q to particle (cal/sec-cm2, Btu/hr-ft2) =',qcgs,q
      write(4,2)'Frac. of heat trans. from wall      (%) =',FRqcer
      write(4,2)'Frac. of heat trans. from falme      (%) =',FRqf
      write(4,2)'Frac. of heat trans. from grate      (%) =',FRqg
      write(4,2)'Frac. of heat trans. from char. part.(%) =',FRqc
      write(4,*)' ..... '
      write(4,2)'Pyrolysis time                        (sec) =',tpp
      write(4,2)'Char comb.time at Re=0.0              (sec) =',tc0
      write(4,2)'Actual char comb. time                (sec) =',tc
      write(4,2)'Total comb. time (calculated)          (sec) =',tpp+tc
      write(4,2)'Total comb. time (experimental)        (sec) =',texp
      write(4,2)'Standard deviation of exp. time        (sec) =',STD
      write(4,2)'Error in time of comb.                 (%) =',ERR1
      write(4,*)' ..... '
      write(4,4)'Calc. fuel feed rate                    (g/sec, lb/hr)
= ',m1cgs,mfcalc
      write(4,4)'Exp. fuel feed rate                    (g/sec, lb/hr) = ',m2cgs,mf
      write(4,2)'Error in fuel feed rate                (%) = ',ERR2
      write(4,*)' ..... '
      write(4,2)'Values of "a" in pyrolysis equation    = ',AA
      write(4,2)'Values of "b" in pyrolysis equation    = ',BB
      write(4,*)' ..... '
      write(4,2)'Renolds No. based on part. dia.        = ',ReDp
      write(4,4)'Coeff. C (in char comb. eq.)           = ',C
      write(4,*)' ..... '
      write(4,1)'Dry part. density                      (g/cm3, lb/ft3)
= ',ROpdcgs,ROpd
      write(4,1)'Wet part. density                      (g/cm3, lb/ft3) = ',ROpcgs,ROp
      write(4,1)'Char density                          (g/cm3, lb/ft3) = ',ROccgs,ROC
      write(4,5)'Comb. air density                      (g/cm3, lb/ft3)
= ',ROgcgs,ROair
      write(4,*)' ..... '

```

```

      write(4,5)'Bed volume                                     (cm3, in3)
=','Bvolcgs,Bvol
      write(4,5)'Bed height                                     (cm, in) =','Bhcgsg,bh
      write(4,2)'No. pf particles on the grate                =','NNpg
      write(4,1)'Moisture content of the part.(% WB, DB) =','mc,mcdb
      write(4,5)'Size of the particles                         (cm, in) =','Dpcgs,Dp
      write(4,*)' .....
      write(4,1)'Comb. air flow rate                           (g/sec, lb/hr) =','macgs,mair
      write(4,5)'Comb. air velocity                           (cm/sec, ft/sec) =','Uacgs,Uair
      write(4,*)' .....
      write(4,1)'Heat of vol. wet                             (cal/g, Btu/lb) =','Lcgs,Lengl
      write(4,*)' .....
      write(4,1)'Average flame temp.                         (deg. C,F) =','TfC,TfF
      write(4,1)'Average ceramic wall temp.                 (deg. C,F) =','TcerC,TcerF
      write(4,1)'Average steel wall temp.                   (deg. C,F) =','TstC,TstF
      write(4,1)'Average grate temp.                         (deg. C,F) =','TgC,TgF
      write(4,*)' .....
      write(4,1)'Energy input                                 (cal/sec, Btu/hr) =','Qincgs,Qin
      write(4,1)'Heat loss ad. model                         (cal/sec, Btu/hr) =','Ql1cgs,Q1
      write(4,1)'Heat loss wall temp.                       (cal/sec, Btu/hr) =','Q2cgs,Q2
      write(4,*)' .....
      write(4,5)'Gas diffusivity                             (cm2/sec) =','Diffgas
      write(4,5)'prod. of density and diff.                 (g/cm-sec) =','RODcgs
      write(4,17)'-----
>-----'

c
1      format(5x,a,f11.2,5x,f11.2)
4      format(5x,a,f11.4,5x,f11.2)
5      format(5x,a,f11.5,5x,f11.5)
2      format(5x,a,f11.2)
17     format(5x,a)
19     format(25x,a,10x,(a8))
      end
$title: 'pyrolysis'
$storage:2
c.....
c
c      THIS PROGRAM CALCULATES THE PYROLYSIS AND
c      TOTAL COMBUSTION TIME FOR A SINGLE PARTICLE
c      OF WOOD IN CONVECTIVE AIR FLOW FOR RED OAK AND
c      SUGAR PINE. EXPERIMENTAL DATA OF SIMMONS [1983]
c.....
c
      implicit real (a-z)
      integer NN,I,J,II
      character*8 test
      common /DS/Tds,Pds,ydsCO2,ydsH2O,ydsO2,ydsN2,ydsAr,ydsCO

c
c..... dead state properties .....
c
      Tds = 59.0
      Pds = 14.696
      ydsCO2 = 0.0002999
      ydsH2O = 0.0111
      ydsO2 = 0.2072
      ydsN2 = 0.7722
      ydsAr = 0.0092
      ydsCO = 0.0000001
c

```

```

c..... properties of comb. air.....
c
    Pair = 14.7
    yCO2a= 0.000296
    yH2Oa= 0.011129
    yO2a = 0.20717
    yN2a = 0.77221
    yAra = 0.009196
    yCOa = 0.0000008
c
    Ep    = 0.9
    Ef    = 0.7
    Taug  = 0.3
    sigma = 5.672E-8
    PI    = 3.141592654
c
c..... INPUT .....
c
    write(*,*)'input the following values'
    write(*,*)'TEST CODE'
    read(*, '(a8)') test
    write(*,*)'ENTER THE Re NO.'
    read(*,*)Redp
    write(*,*)'EXPERIMENTAL PYR. TIME & STD'
    read(*,*)tpexp
    read(*,*)stdp
    write(*,*)'TOTAL EXP. COMBUSTION TIME & STD'
    read(*,*)texp
    read(*,*)stdt
    write(*,*)'TEMPERATURE OF COMB. AIR (deg. K)'
    read(*,*)Tak
    write(*,*)'MOISTURE CONTENT OF THE FUEL (percent DB)'
    read(*,*)mcdb
c
    mc = (100.0*mcdb)/(100.0 + mcdb)
c
    write(*,*)'SIZE OF PARTICLE (cm)'
    read(*,*)Dpcgs
    Dp = dpcgs/2.54
    write(*,*)'ENTER (1) IF OAK, (2) IF PINE'
    read(*,*)II
    if(II .eq. 1)then
        ROpcgs = 0.69
        FRACC  = 0.25
        ALPHA  = 0.00121
        TfK    = Tak + 300.0
    else
        ROpcgs = 0.35
        FRACC  = 0.30
        ALPHA  = 0.00151
        TfK    = Tak + 300.0
    endif
c
    if (mcdb .GT. 0.5) then
        ROpcgs = (1. + mc/100.0)*ROpcgs
    else
        ROpcgs = ROpcgs
    endif
    ROpd  = ROpcgs*62.428
    ROp   = ROpcgs*62.428
c
    ROccgs = 0.17
    ROC    = ROccgs*62.428
c

```

```

      mp      = ROp*(Dp**3.)
c
      Tpk     = 570.0
      Ldry    = 180.0
      tcexp   = texp - tpexp
c
c..... heat transfer to particles .....
c
      Ap      = (Dpcgs**2.)*6./10000.0
      Af      = PI*((Dpcgs + Dpcgs/2. )**2.0)/10000
      D1      = (1. - Ep)/Ep
      D2      = 1.0/Taug
      D3      = (1.0 - Ef)*Ap/(Af*Ef)
      qfmks   = sigma*(Tfk**4.0 - Tpk**4.0)/(D1 + D2 + D3)
      qfcgs   = qfmks*2.388444E-5
c
      Pr      = 0.7
      Nud     = 2.0 + 0.6*(Redp**0.5)*(Pr**(1./3.))
      Kacgs   = (543.305E-9)*(Tak**0.8202638)
      h       = Nud*Kacgs/dpcgs
      qacgs   = h*(Tak - Tpk)
c
      qwmks   = sigma*((Tak*0.75)**4.0 - Tpk**4.)/(D1 + D2)
      qwcgs   = qwmks*2.388444E-5
c
      qcgs    = (qacgs + qfcgs + qwcgs)
c
c..... heat of volatilization (wet) .....
c
      Cpcgsd  = 0.266 + 0.00116*(Tpk -273.)
      Cpcgs   = (Cpcgsd +0.01*mcdb)/(1. + 0.01*mcdb)
c
      if (mc .EQ. 0.0)then
         LH2O = 0.0
         goto 111
      endif
c
      if (mc .LT. 23.08)then
         x = mc
      else
         x =23.08
      endif
c
      QbH2o   = (1.0/x)*(467.94*x - 32.314*x**2 + 1.040787*x**3
> + 0.046801*x**4 - 0.006588*x**5 + 2.56985E-4*x**6
> - 3.48937E-6*x**7)
      LH2O    = (QbH2O + 1059.)*mc/(100.0*1.8)
111 Lcgs     = Ldry + LH2O
c
c***** pyrolysis time *****
c
      D16     = (5./6.)*(ROpcgs - ROccgs)*Lcgs/qcgs
      D17     = ROpcgs*Cpcgs*(350.0)/(3.*qcgs)
      AA      = D16+D17
      BB      = 1./(10.0*alpha)
      tpp     = AA*(Dpcgs/2.) + BB*((Dpcgs/2. )**2.)
c

```

C\*\*\*\*\* CHAR COMBUSTION \*\*\*\*\*

```

C
  CONST  = 0.4248
  POWER  = 1.75
  Diffgas = CONST*((Tak/273.16)**POWER)
  TaF    = ((TaK - 273.15) +17.78)*1.8
  ROa    = ROGAS(TaF,Pair,yCO2a,yH2Oa,yO2a,yN2a,yAra,yCOa)
  ROacgs = ROa/62.428
  B      = 0.087
  Sc     = 0.89
  C      = 0.3*(ReDp**(0.5))*(Sc**(1./3.))

C
  tc0 = (ROccgs*(Dpcgs**2.))/(8.*ROacgs*Diffgas*log(B+1))

C
  x1  = 0.0
  sum1 = 0.0
  x2  = 0.0
  sum2 = 0.0
  NN  = 100

C
  do 10 I=1,NN,2
    x1  = I*(1.0/NN)
    sum1 = sum1 + 2.*x1/(1. + c*(x1**0.5))
10    continue

C
  NN  = 100
  do 20 J=2,NN-1,2
    x2  = J*(1./NN)
    sum2 = sum2 + 2.*x2/(1. + c*(x2**0.5))
20    continue

C
  tc = tc0*(1./(3.*NN))*(2./(1.+c) + 4.*sum1 + 2.*sum2)

C
C..... error .....
C
  ERR1 = 100*(tpexp - tpp)/tpexp
  ERR2 = 100*(tcexp - tc)/tcexp
  ERR3 = 100*(texp - (tpp + tc))/texp

C
C..... convert values for output .....
C
  RODcgs = ROgcgs*Diffgas
  Leng1  = Lcgs/0.555478
  q      = qcgs/(0.00007535)

C
C..... print the results .....
C
  write(4,19)'TEST CODE:',TEST
  write(4,17)'-----
>-----'
  write(4,4)'q to particle (cal/sec-cm2, Btu/hr-ft2) =',qcgs,q
  write(4,*)'.....'
  write(4,2)'Pyrolysis time (calculated) (sec) =',tpp
  write(4,2)'Pyrolysis time (experimental) (sec) =',tpexp
  write(4,2)'Standard deviation in pyr. time (sec) =',stdp
  write(4,2)'Error in time of comb. (%) =',ERR1
  write(4,*)'.....'
  write(4,2)'Char comb.time at Re=0.0 (calc.) (sec) =',tc0
  write(4,2)'Actual char comb. time (calc.) (sec) =',tc
  write(4,2)'Cha combustion time (experimental)(sec) =',tcexp
  write(4,2)'Error in time of char comb. (%) =',ERR2
  write(4,*)'.....'
  write(4,2)'Total comb. time (calculated) (sec) =',tpp+tc
  write(4,2)'Total comb. time (experimental) (sec) =',texp

```

```

write(4,2)'Standard deviation tot.comb. time (sec) =' ,stdt
write(4,2)'Error in time of comb.                (%) =' ,ERR3
write(4,*)' .....
write(4,2)'Values of "a" in pyrolysis equation    =' ,AA
write(4,1)'Values of "b" in pyrolysis equation    =' ,BB
write(4,*)' .....
write(4,2)'Renolds No. based on part. dia.        =' ,ReDp
write(4,4)'Coeff. C  (in char comb. eq.)          =' ,C
write(4,*)' .....
write(4,1)'Dry  part.  density                      (g/cm3,  lb/ft3)
=',' ,ROpdcgs,ROpd
write(4,1)'Wet part. density                      (g/cm3,  lb/ft3) =' ,ROpcgs,ROp
write(4,1)'Char density                          (g/cm3,  lb/ft3) =' ,ROccgs,ROC
write(4,5)'Comb. air density                      (g/cm3,  lb/ft3) =' ,ROacgs,ROa
write(4,*)' .....
write(4,1)'Moisture content of the part. (% WB, DB)=' ,mc,mcdb
write(4,5)'Size of the particles                  (cm, in) =' ,Dpcgs,Dp
write(4,*)' .....
write(4,1)'Heat of vol. wet                      (cal/g,  Btu/lb) =' ,Lcgs,Lengl
write(4,17)'-----
>-----'

C
1      format(5x,a,f11.2,5x,f11.2)
4      format(5x,a,f11.4,5x,f11.2)
5      format(5x,a,f11.5,5x,f11.5)
2      format(5x,a,f11.2)
17     format(5x,a)
19     format(25x,a,10x,(a8))
end

```

### A.3 Computer Programs for Chapter 3

```

$title: 'PROFILE'
$storage:2
    implicit real (a-z)
    integer I,J,K
    dimension X(25),Ts(25),Qloss(25),TfF(25),TfC(25),GG(25),HH(25),
>HH2(25)
    character*8 test
    common /DS/Tds,Pds,ydsCO2,ydsH2O,ydsO2,ydsN2,ydsAr,ydsCO
c
c.....
c
c          PROGRAM TO CALCULATE THE COMBUSTION PROFILE
c          IN THE COMBUSTION CHAMBER.
c
c..... dead state properties .....
c
    Tds    = 59.0
    Pds    = 14.696
    ydsCO2 = 0.0002999
    ydsH2O = 0.0111
    ydsO2  = 0.2072
    ydsN2  = 0.7722
    ydsAr  = 0.0092
    ydsCO  = 0.0000001
c
c..... properties of comb. air.....
c
    Pair   = 14.7
    yCO2a  = 0.000296
    yH2Oa  = 0.011129
    yO2a   = 0.20717
    yN2a   = 0.77221
    yAra   = 0.009196
    yCOa   = 0.0000008
c
c..... amb. and fuel initial temp. ....
c
    TambF  = 85.0
    TambR  = TambF + 460.0
    TambC  = (TambF - 32.0)*5./9.
    TambK  = TambC + 273.0
c
c..... constants (English units) .....
c
    PI     = 3.14159265
    sigma  = 0.173E-8
c
c..... molecular weights .....
c
    MWf    = 100.0
    MWair  = 28.97
    MWH2O  = 18.016
c
c..... (INCHES) .....
c
    Dcer   = 6.50
    Dcs    = 12.25
    Dst    = 12.75
    Hst    = 36.0

```

```

C
C..... AREA (SQUARE FEET) .....
C
      Ag  = PI*Dcer*Dcer/(4.*144.)
      Ast = PI*Dst*Hst/144.
      Pcer = PI*Dcer/12.0
C
C..... emisivity and transmisivity .....
C
      Ecer = 0.90
      Ef   = 0.70
      Est  = 0.95
      Taug = 0.30
C
C..... conductivity (Eng. units) .....
C
      Kcer = (5.0/12.0)*(Dcs -Dcer)/2.0
      kst  = 10.9
C
C..... X(I) .....
C
      X(1)  = 0.0
      X(2)  = 1.0
      X(3)  = 1.5
      X(4)  = 2.0
      X(5)  = 2.5
      X(6)  = 3.0
      X(7)  = 3.5
      X(8)  = 4.0
      X(9)  = 5.0
      X(10) = 6.0
      X(11) = 7.0
      X(12) = 8.0
      X(13) = 9.0
      X(14) = 10.0
      X(15) = 12.0
      X(16) = 14.0
      X(17) = 16.0
      X(18) = 18.0
      X(19) = 20.0
      X(20) = 22.0
      X(21) = 24.0
C
C.....READ THE DATA .....
C
      read(6,'(a8)') test
      read(6,*)Vair
      read(6,*)FRACuf
      read(6,*)mf
      read(6,*)mc
      read(6,*)LHV2
      read(6,*)HHV
      read(6,*)TufaF
      read(6,*)xC
      read(6,*)xO
      read(6,*)xN
      read(6,*)xH
      DO 55 J=1, 21
         read(6,*)Ts(J)
55      CONTINUE

```



```

C
  Cx = xC
  Ox = xO
  Hx = xH
  Nx = xN
  write(4,19)'TEST CODE:',TEST
  write(4,20)'      X---Ts-----Tf1---Tf2---O2---CO2---COT---NOT---NOf---
Cof'
  write(4,20)'      cm---C-----C-----C-----%-----%-----ppm---ppm---ppm---
ppm'
C
C.....
C
  ROastd = ROGAS(50.0,Pds,ydsCO2,ydsH2O,ydsO2,ydsN2,ydsAr,ydsCO)
  mufa   = Vair*FRACuf*ROastd
  mofa   = Vair*(1. - FRACuf)*ROastd
C
  mcdb   = 100.0*mc/(100.0 - mc)
  mH2O   = mf*mcdb/100.0
  molH2O = mH2O/MWH2O
  b      = molH2O
  a      = mf/MWf
  a0     = mf/MWf
  c0     = (mufa + mofa)/MWair
C
C.....steel wall heat loss Q2(I) & TcerF(I).....
C
  DO 10 I=2, 21
  Ls      = x(I) - x(I-1)
  TsC     = Ts(I)
  TsF     = (TsC + 17.78)*1.8
  TsR     = TsF + 460.0
  Ast     = PI*Dst*Ls/144.0
  hs      = 1.4
  Qcon    = hs*Ast*(TsR - TambR)
  Qrad    = Est*Ast*sigma*(TsR**4. - TambR**4.)
  Q2      = Qcon + Qrad
  Qloss(I) = Q2
10  continue
C
C.....          under-fire          air          heat          loss
C.....
C
  DO 11 J=2, 21
  IF (X(J) .LT. 3.5) THEN
    mair = mufa + (X(J)/3.5)*mofa
  ELSE
    mair = mufa + mofa
  ENDIF
  c      = mair/MWair
  mg     = mf + mH2O + mair
  Cpg    = 0.27
C
C.....          COOLING DUE TO OVER-FIRE AIR .....
C
  Tcool = 400.0*(mair - mufa)/mg
C
C.....          calculate HH and GG .....
C
  Q = 0.0
  DO 44 K=2,J
    Q = Q + Qloss(K)
44  CONTINUE

```

```

C
  GG(J) = Q/(mg*Cpg)
  HH(J) = (0.95*mf*LHV2)/(mg*Cpg)
  HH2(J) = (0.85*mf*LHV2)/(mg*Cpg)
C
C..... T(J) .....
C
  AA = 16.635532
  BB = -16.635532
C
C..... assume at X=0, T=Tambf .....
C
  T1F = ((mufa+mf+mH2O)/mg)*(((Ts(1)+17.78)*1.8) +TufaF)
  Tff(J) = T1F - (HH(J))*(EXP(BB*X(J)/24.)-1.0) - GG(J) - Tcool
  Tfc(J) = (Tff(J) - 32.0)*5./9.
  Tfk = Tfc(J) + 273.0
  a = 0.95*mf/MWf
  totN1 = (mf + mH2O + mair)/28.0
C
  CALL COMPOS (Tfk,a,b,c,ydO2,ydCO2,ppmdCO,ppmdNO,Cx,Ox,Nx,Hx,
>totNd,totN1,a0)
  Xnther = 0.5*(2.67/2000.0)*(mf/30.0)
  Xcther = (2.0/2000.0)*(mf/28.0)
  NOxF = Xnther*1000000.0/totNd
  COF = Xcther*1000000.0/totNd
  xx = X(J)*2.54
C
  Tff2 = T1F - (HH2(J))*(EXP(BB*X(J)/24.)-1.0) - GG(J) - Tcool
  Tfc2 = (Tff2 - 32.0)*5./9.
C
  write(4,30)xx,Ts(J),Tfc(J),Tfc2,ydO2,ydCO2,ppmdCO,ppmdNO,NOxF,COF
11  continue
C
19  format(25x,a,10x,(a8))
20  format(2x,a)
30  format(2x,f4.1,1x,f5.1,1x,f6.1,1x,f6.1,1x,f5.2,1x,f5.2,4(1x,f6.1))
31  format(5x,f7.2,3x,f7.2)
  end
$TITLE: 'EQUATION'
c$STORAGE:8
  subroutine COMPOS(Tfk,a,b,c,ydO2,ydCO2,ppmdCO,ppmdNO,Cx,Ox,Nx,Hx,
>totNd,totN1,a0)
  implicit real (a-z)
  common/DS/Tds,Pds,ydsCO2,ydsH2O,ydsO2,ydsN2,ydsAr,ydsCO
C.....
C
c  subroutine to calculate the composition for program PROFILE
C.....
C
  p1 = -31.7035+(0.0854312*Tfk)-(1.11734E-4)*(Tfk**2)
> +7.70827E-8*(Tfk**3)-2.68315E-11*(Tfk**4)+3.70942E-15*(Tfk**5)
C
  p2 = -81.492+(0.200159*Tfk)-(2.37933E-4*(Tfk**2))+(1.52047E-
> 7*(Tfk**3))-(4.92742E-11*(Tfk**4))+(6.26376E-15*(Tfk**5))
C
  Kp1 = (10.0**p1)
  Kp2 = (10.0**p2)
C
  x = Cx
  y = Hx
  z = Ox
  w = Nx
C
  X3 = a0 - a

```

```

c      x1  = 0.00000001
      x2  = 0.00000001
c
100  R    = x1
      S    = x2
c
      U1  = 0.5*a*y + b - 0.5*y*X3
      U2  = X2
      U3  = a*X - X1 - x*X3
      U4  = 0.5*a*w + 0.79*c - 0.5*X2 - 0.5*X3*w
      U5  = a*(-0.25*y - x + 0.5*z) + 0.21*c + 0.5*X1 - 0.5*X2 +
>0.5*X3*(2.0*x + 0.5*y - z)
      U6  = X1
      U7  = X3
      totN = totN1
      totNd = totN - U1
c
      x1  = x2*(Kp2/Kp1)*(U3/U5)*((totN/U4)**0.5)
      x2  = Kp1*((U5*U4)**0.5)
c
      TEST1 = ABS(100.0*(X1 - R)/R)
      TEST2 = ABS(100.0*(X2 - S)/S)
c
      IF(TEST1 .LT. 0.00001 .AND. TEST2 .LT. 0.00001)THEN
          GOTO 200
      ELSE
          GOTO 100
      ENDIF
c
200  ydO2   = U5*100.0/totNd
      ydCO2  = U3*100.0/totNd
      ppmdCO = U6*1000000.0/totNd
      ppmdNO = U2*1000000.0/totNd
c
      return
      end

```

#### A.4 Computer Programs for Chapter 4

```

$title: 'test of burner'
$storage:2
    implicit real (a-z)
    logical print*2
    common/DS/Tds,Pds,Ydsco2,Ydsh2o,Ydso2,Ydsn2,Ydsar,Ydsco
C
C.....
C  MAIN      PROGRAM TO CALCULATE THE PERFORMANCE OF THE
C              OSU COMBUSTION UNIT FOR THE ACTUAL TESTS AND
C              ADIABATIC CONDITIONS
C.....
C
    Tds=59.0
    Pds=14.696
    ydsco2=0.0003
    ydsh2o=0.0111
    ydso2=0.2072
    ydsn2=0.7722
    ydsar=0.0092
    ydsco=0.000001
    xash=0.008
    xdir=0.0
    xc=0.523
    xH2=0.063
    xn2=0.001
    xo2=0.405
    xcco=0.01
    dpburn=8.0
    yco2in=0.000296
    yh2oin=0.011129
    yo2in=0.20717
    yn2in=0.77221
    yarin=0.009196
    ycoin=0.0000008
    Pair=26.0
    Tamb=60.
    write(*,*) ' ENTER THE FOLLWING VALUES : '
    write(*,*) ' MASS RATE OF FUEL (MRWDIN) IN LB/HR '
    read(*,*) MRwdinH
    MRwdin = MRwdinH/3600.
    write(*,*) ' RADIATION AND CONVECTION HEAT LOSS (BTU/SEC) '
    read(*,*) radlos
    write(*,*) ' FRACTION OF UNBURNED CARBON (XUNBC) '
    READ(*,*) unbcbn
    write(*,*) ' FRACTION OF CARBON BURNED TO CO (XCCO) '
    read(*,*) XCCO
    write(*,*) ' HHV '
    read(*,*) HHV
    write(*,*) ' MASS RATE OF AIR IN SCFH '
    read(*,*) SCFH
    XMra = SCFH*(0.075/3600)
    write(*,*) ' AIR TEMP. '
    READ(*,*) Tair
    write(*,*) ' FRACTION OF MOISTURE CONTENT xH2O (o.1 for 10%) '
    read(*,*) xH2O
    print=.true.
C
    call burner(HHV,radlos,xash,xdir,xc,xh2,xn2,xo2,xh2o,unbcbn,
<          xcco,AFrat,yco2in,yh2oin,yo2in,yn2in,yarin,ycoin,

```

```

Pair,dpburn,Tair,xMRa,Tamb,yeco2,yeh2o,yeo2,
yen2,year,yeco,LHV1,LHV2,MRwdin,MRbdwd,Metot,
Tadflm,PfgeX,Qrel2,IRRbrn,print)
c
stop
end

$title: 'COMBUSTOR'
$storage:2
$debug
subroutine BURNER (HHV,radlos,xash,xdirT,xC,xH2,xN2,xO2,
> xH2O,xunbc,xCCO,AF,yCO2a,yH2Oa,yO2a,
> yN2a,yARa,yCOa,Pa,dpburn,Ta,MRA,Tamb,
> yCO2c,yH2Oc,yO2c,yN2c,yARc,yCOc,LHV1,
> LHV2,MRwdin,MRbdwd,MRC,Tc,Pc,Qwd,IRRbrn,
> print)
c
c
ccccccccccccccccccccccccccccccccccccccccccccccccccccccccccccccccc
c
c This program calculates the temp., mass flow rate, composition, and c
c pressure of products of the combustion. It also calculates first c
c and second law efficiencies, lower heating values of the fuel, c
c mass rate of solid discharge, theoretical and actual air-fuel c
c ratios, theoretical mass flow rate of air, and heat generated c
c in the combustor. c
c Input of this program includes higher heating value of the fuel, c
c radiation heat loss, mass rate of air to the combustor, mass rate c
c of bone-dry fuel, temperature and pressure of the air, pressure c
c drop of the combustor, ambient air temperature , dead state temp., c
c pressure and mole fractions, fuel composition, fraction of c
c unburned carbon, and fraction of carbon burned to CO. c
c
c METHOD OF CALCULATION: c
c
c From fuel composition mass flow rates of carbon, hydrogen, oxygen, c
c nitrogen, ash, dirt, water, carbon burned to CO, and unburned c
c carbon are calculated. It is assumed that all the nitrogen c
c remains unchanged, all the hydrogen will form water, and carbon c
c will form CO, CO2 or remains unburned as specified. From these c
c mass flow rates, mole rates of the constituents are determined. c
c Also mole rates of the constituents in the combustion air is c
c calculated. From mass balance of these streams, final composition c
c and mass flow rate of flue gas is determined. c
c To determine the flue gas temperature, an energy balance of the c
c energy input, energy output, and heat losses is done. Second law c
c is used to calculate the availabilities, irreversibility, and c
c second law efficiencies. c
c
c..NOMENCLATURE: c
c
c...Substance or Stream Abbreviations: c
c
c a or air.....air c
c AR.....argon c
c ash.....ash in the fuel c
c b.....biomass (wood) c
c c.....combustion products c
c C or cbn.....carbon c
c CO.....carbon monoxide c
c CO2.....carbone dioxide c
c dirt.....dirt in the fuel c
c ds.....dead state c
c e.....exhaust c

```



```

c
  implicit real (a-z)
  logical print*2
  common /DS/Tds,Pds,ydsCO2,ydsH2O,ydsO2,ydsN2,ydsAR,ydsCO
  data MWC02,MWH2O,MWO2,MWN2,MWAR,MWCO,MWC,MWH2/44.01,18.016,
>    32.0,28.016,39.944,28.01,12.011,2.016/
  write(*,*)'from the sub'

c
  eps      = 0.000001
  CpH2O    = 1.0
  Paabs    = 14.696 + 0.03613*Pa
  Pc       = Pa - dpburn
  Pcabs    = 14.696 + 0.03613*Pc

c
c.....calculate air-fuel ratio, mass rate of
c          constituents in fuel, and total mass of
c          biomass fuel to the combustor.(stream b)
c
c          NOTE THIS VERSION OF THE COMBUSTION
c          PROGRAM ASSUMES NO DIRT IN THE FUEL
c
  AFrat    = MRa/MRwdin
  MRH2O    = xH2o*MRwdin
  MRbdwd   = MRwdin - MRH2O
  MRdirt   = xdirty*MRbdwd
  MRash    = xash*MRbdwd
  MRCbn    = xC*MRbdwd
  MRCCO    = xCCO*MRCbn
  MRunbC   = xunbC*MRCbn
  MRCCO2   = MRCbn - MRunbC - MRCCO
  MRO2     = xO2*MRbdwd
  MRH2     = xH2*MRbdwd
  MRN2     = xN2*MRbdwd

c
c.....convert to mole basis ( stream "b" )
c
  MLH2b    = MRH2/MWH2
  MLH2Ob   = MRH2O/MWH2O + MLH2b
  MLCb     = MRCbn/MWC
  MLCOb    = MRCCO/MWC
  MLunbC   = MRunbC/MWC
  MLO2b    = MRO2/MWO2
  MLN2b    = MRN2/MWN2
  MLCO2b   = MRCCO2/MWC
  MLARb    = 0.0

c
c.....calculate molecular weight of combustion air
c          and moles of constituents in combustion air.
c          ( stream "a" )
c
  MWa      = yARa*MWAR + yCOa*MWCO + yCO2a*MWC02 +
>    yH2Oa*MWH2O + yN2a*MWN2 + yO2a*MWO2
  MLARa    = MRa*yARa/MWa
  MLC0a    = MRa*yCOa/MWa
  MLCO2a   = MRa*yCO2a/MWa
  MLN2a    = MRa*yN2a/MWa
  MLH2Oa   = MRa*yH2Oa/MWa
  MLO2a    = MRa*yO2a/MWa

c
c.....calculate moles of constituents in
c          products of combustion.(stream "c")

```

```

c
  MLARc = MLARa + MLARb
  MLCOc = MLCOa + MLCOb
  MLCO2c = MLCO2a + MLCO2b
  MLN2c = MLN2a + MLN2b
  MLH2Oc = MLH2Oa + MLH2Ob
  MLO2c = MLO2a + MLO2b - (MLCOb/2. + MLCO2b + MLH2b/2.)
c
c.....calculate molefractions of the product
c              of combustion.
c
  sumMLc = MLH2Oc + MLCOc + MLCO2c + MLN2c + MLO2c + MLARc
  yH2Oc = MLH2Oc/sumMLc
  yCOc = MLCOc/sumMLc
  yCO2c = MLCO2c/sumMLc
  yN2c = MLN2c/sumMLc
  yO2c = MLO2c/sumMLc
  yARc = MLARc/sumMLc
c
c.....calculate molecular weight and mass rate
c              of products of combustion. ( MWcp )
c
  MWcp = yARc*MWAR + yCOc*MWCO + yCO2c*MWCO2 +
>      yH2Oc*MWH2O + yN2c*MWN2 + yO2c*MWO2
  MRc = sumMLc*MWcp
c
c..... calculate the dry basis mole fractions
c
  dMLc = sumMLc - MLH2Oc
  dyCOc = MLCOc/dMLc
  dyCO2c = MLCO2c/dMLc
  dyN2c = MLN2c/dMLc
  dyO2c = MLO2c/dMLc
  dyARc = MLARc/dMLc
c
c.....ENERGY BALANCE
c
c
c initial guess for Tc
c
  Tc = Ta + 100.0
c
c.....energy into the combustor.
c
c a) Energy of wood
c
  Qwd = HHV*MRbdwd
c
c b) Energy of air in
c
  Ha = HGASt(Ta,yCO2a,yH2Oa,yO2a,yN2a,yARa,yCOa)
  Hrefa = HGASt(Tamb,yCO2a,yH2Oa,yO2a,yN2a,yARa,yCOa)
  Qa = MRa*( Ha - Hrefa )
c
c.....total energy into the combustor.
c
  Qin = Qwd + Qa
c
c.....energy losses
c
c a) due to radiation loss
c
  Qrad = radlos
  Frad = Qrad/Qin

```



```

c
c b) due to unburned carbon
c
c      QunbC = MRunbC*14086.
c
c c) due to co generation
c
c      QCCO  = MLCOb*MWCO*4343.6
c
c d) due to formation of H2O from H2 in wood ( at 60 F )
c
c      QH2   =MLH2b*MWH2O*1059.
c
c e) due to vaporization of h2o in wood
c
c 1) To vaporize the free water ( at 60 F )
c
c      Qfw   = MRH2O*1059.
c
c 2) additional energy for bound water
c
c      if ( xH2O .ge. .2308 ) then
c          MC = 23.08
c      else
c          MC = xH2O*100.
c      endif
c      MRbw  = MC*MRwcf/100.
c      Hbw   = (1./MC)*(4.679415E2*MC - 3.2314115E1*(MC**2) +
>      1.040786667*(MC**3) + 4.680145E-2*(MC**4) -
>      6.588278E-3*(MC**5) + 2.569851667E-4*(MC**6) -
>      3.48937E-6*(MC**7))
c      Qbw   = MRbw*Hbw
c
c      total energy to vaporize the water
c
c      Qvap  = QH2 + Qfw + Qbw
c
c f) due to heating of the dirt
c
c 111  Qdirt = MRdirt*0.2*(Tc - Tamb)
c
c.....sum of the heat losses
c
c      Note that although QH2, Qfw, and Qw are treated as loss
c      here ( in order to find Tc ), however, these values are
c      not lost but absorbed by flue gas. In other words these values
c      can be recovered if condensation takes place.
c
c
c      Qloss = Qrad + QunbC + QCCO + Qvap + Qdirt
c
c.....energy out
c
c      Hc    = HGAST(Tc,yCO2c,yH2Oc,yO2c,yN2c,yARc,yCOc)
c      Hrefc  = HGAST(Tamb,yCO2c,yH2Oc,yO2c,yN2c,yARc,yCOc)
c      Qc     = MRc*(Hc - Hrefc)
c
c.....check the root

```

```

c
  check = ABS((Qin - Qloss - Qc)/Qc)
  if ( check .ge. eps ) then
    Hc = Hrefc + (Qin - Qloss)/ MRc
    Tc = TGASH(Hc,yCO2c,yH2Oc,yO2c,yN2c,yARc,yCOc)
    go to 111
  endif
c
c Total energy transfer to flue gas
c
  Qflue = Qc + Qvap
c
c.....calculate theo. amont of air
c          and excess air
c
  MLO2th = MLCb + MLH2b/2. - MLO2b
  MLath = MLO2th/yO2a
  MRath = MLath*MWa
  EA = (MRa - MRath)/MRath*100.0
  thAF = MRath/MRbdwd
c
c.....calculate lower heating values
c
  LHV1 = HHV - QH2/MRbdwd
  LHV2 = LHV1 - (Qbw/MRbw + 1059.)*xH2O/(1. - xH2O)
  if ( print ) then
c
c.....secnd law analysis
c
c a) Avail. of wood in
c
c 1) dry wood ( 1: based on HHV, 2: based on impirical formula)
c
  Abdwd1 = MRbdwd*HHV
  Abdwd2 = MRbdwd*((340.124*xC + 5.25*xN2 - 5996.25*xH2 +
> 1062.45*xO2 - 51.139*xash ) *1.7997732 + HHV )
c
c 2) availability of bound water, based on EMC of 11% (wb)
c
  FDG = 54.3714 - ( 2.924894E2 - 4.284346E1*MC +
> 5.039131*(MC**2) - 5.740694E-1*(MC**3) +
> 3.584556E-2*(MC**4) - 8.335498E-4*(MC**5) -
> 9.477914E-6*(MC**6) + 1.095668E-6*(MC**7) -
> 4.493423E-8*(MC**8) + 8.533094E-10*(MC**9) )
  Abw = MRbw*ABS(FDG)
c
c Avail. of wet fuel
c
  Awdin1 = Abdwd1 + Abw
  Awdin2 = Abdwd2 + Abw
c
c b) Avail of air in
c
  Tdsabs = Tds + 459.67
  Sa = SGASTP(Ta,Paabs,yCO2a,yH2Oa,yO2a,yN2a,yARa,yCOa)
  Sds = SGASTP(Tds,Pds,ydsCO2,ydsH2O,ydsO2,ydsN2,
> ydsAR,ydsCO)
  Hds = HGASt(Tds,ydsCO2,ydsH2O,ydsO2,ydsN2,ydsAR,ydsCO)

  Aa = MRa*((Ha - Hds) - Tdsabs*(Sa - Sds))
c

```

```

c c)Avail. of flue gas exiting
c
  Hc = HGASt(Tc,yCO2c,yH2Oc,yO2c,yN2c,yARc,yCOc)
  Sc = SGASTP(Tc,Pcabs,yCO2c,yH2Oc,yO2c,yN2c,yARc,yCOc)
  Ac = MRC*((Hc - Hds) - Tdsabs*(Sc - Sds))
c
c.....calculate the properties at an assumed
c          exhaust temperature of 350
c
  He = HGASt(350.,yCO2c,yH2Oc,yO2c,yN2c,yARc,yCOc)
  Se = SGASTP(350.,Pcabs,yCO2c,yH2Oc,yO2c,yN2c,yARc,yCOc)
  Ae = MRC*((He - Hds) - Tdsabs*(Se - Sds))
  Qe = MRC*(He - Hrefc) + Qvap
c
c.....calculate irreversibility of the processes
c          and eff.
  IRR1 = Awdin1 + Aa - Ac
  IRR2 = Awdin2 + Aa - Ac
  EFF21= 100.*Ac/(Awdin1 + Aa)
  EFF22= 100.*Ac/(Awdin2 + Aa)
  EFF23= 100.*(Ac - Ae)/(Awdin2 + Aa)
  EFF1 = 100.*(Qflue - Qa)/Qwd
  EFF12= 100.*(Qflue - Qa - Qe)/Qwd
c
c.....convert to SI, and calc. total mass of solid
c          and total mass in
c
  IRRbrn = IRR2*1.0552
  MRsld = MRash + MRdirt + MRunbc
c
c.....write the results
c
  write(8,10)'----- COMBUSTOR -----'
,
  write(8,10)'
  write(8,11)'Theor. Air-Fuel ratio(dry wood)           :',thAF
  write(8,11)'Theor. mass rate of air, lb/sec           :',MRath
  write(8,11)'Actual Air-Fuel ratio(dry wood)           :',AFrat
  write(8,11)'Excess Air, percent                       :',EA
  write(8,10)'
  write(8,11)'HHV, Btu/lb (dry basis)                   :',HHV
  write(8,11)'LHV1, Btu/lb (dry basis)                  :',LHV1
  write(8,11)'LHV2, Btu/lb (dry basis)                  :',LHV2
  write(8,10)'
  write(8,11)'Mass rate of fuel, lb/sec (bone-dry)      :',MRbdwd
  write(8,11)'Mass rate of fuel, lb/sec (wet dirty)     :',MRwdin
  write(8,11)'Mass rate of water in the fuel, lb/sec    :',MRH2O
  write(8,11)'Mass rate of combustion air, lb/sec      :',MRa
  write(8,11)'Mass rate of solid discharge, lb/sec     :',MRsld
  write(8,11)'Mass rate of flue gas out, lb/sec        :',MRC
  write(8,10)'
  write(8,11)'Energy input of fuel, Btu/sec             :',Qwd
  write(8,11)'Energy input of Comb. air, Btu/sec       :',Qa
  write(8,11)'Energy trans. to flue gas, Btu/sec       :',Qflue
  write(8,10)'
  write(8,11)'Heat loss due to unburned C, Btu/sec      :',QunbC
  write(8,11)'Heat loss due to CO gen., Btu/sec        :',QCCO
  write(8,11)'Heat loss due to dirt, Btu/sec           :',Qdirt
  write(8,11)'Rad. heat loss, Btu/sec                  :',Qrad
  write(8,11)'Energy used for vap. of water, Btu/sec    :',Qvap
  write(8,10)'
  write(8,11)'Frac. of unburned carbon                  :',xunbC
  write(8,11)'Frac. radiation loss                     :',Frad
  write(8,11)'Frac. of carbon burned to CO              :',xCCO

```

```

write(8,10)'
write(8,11)'Temp. of combustion air, deg. F      : ',Ta
write(8,11)'Temp. of flue gas exiting, deg. F    : ',Tc
write(8,10)'
write(8,11)'Avail. of dry wood (HHV), Btu/sec     : ',Abdwd1
write(8,11)'Avail. of dry wood (emp.), Btu/sec    : ',Abdwd2
write(8,11)'Avail. of bound water, Btu/sec       : ',Abw
write(8,11)'Avail. of wet wood (HHV), Btu/sec    : ',Awdin1
write(8,11)'Avail. of wet wood (emp.), Btu/sec   : ',Awdin2
write(8,11)'Avail. of comustion air, Btu/sec      : ',Aa
write(8,11)'Avail. of flue gas, Btu/sec          : ',Ac
write(8,10)'
write(8,11)'Irreversibility of comb. (HHV), Btu/sec : ',IRR1
write(8,11)'Irreversibility of comb. (emp.), Btu/sec: ',IRR2
write(8,10)'
write(8,11)'First law efficiency, percent        : ',EFF1
write(8,11)'1st law eff. compared to 350 exh.    : ',EFF12
write(8,11)'Sec. law eff. ( based on HHV), percent : ',EFF21
write(8,11)'Sec. law eff. (empirical eq.), percent : ',EFF22
write(8,11)'2nd law eff. emp. eq. comp. to 350 exh. : ',EFF23

c
10  format(11x,a)
11  format(11x,a,f10.4)
c
c..... WRITE FOR QUATTRO OUTPUT
c
write(8,*)'MRwdin (lb/hr)          = ',MRwdin
write(8,*)'EXCESS AIR (percent) = ',EA
write(8,*)'comb. temp. (deg. F) = ',Tc
write(8,*)'percent CO2 (dry basis) = ', dyco2c*100.
write(8,*)'Percent O2 (dry basis) = ', dyO2*100
endif
return
end

```

## APPENDIX B

## COMBUSTION PROFILES FOR EXPERIMENTS, CHAPTER 2

Results for Chapter 2

X = DISTANCE FROM GRATE (cm)  
 Ts = STEEL WALL TEMP. (deg. C)  
 Tf1 = COMBUSTION TEMPERATURE (95% conversion, deg. C)  
 Tf2 = COMBUSTION TEMPERATURE (85% conversion, deg. C)  
 O2 = OXYGEN (% , dry basis)  
 CO2 = CARBON DIOXIDE (% , dry basis)  
 COT = THERMAL CO (ppm, dry basis)  
 NOT = THERMAL NOx (ppm, dry basis)  
 Nof = FUEL GENERATED NOx (ppm, dry basis)  
 Cof = FUEL GENERATED CO (ppm, dry basis)

TEST CODE:						TEST A			
X----	Ts-----	Tf1----	Tf2----	O2-----	CO2-----	COT-----	NOT----	Nof----	Cof
2.5	198.0	701.6	640.9	8.49	12.12	.0	18.0	70.2	112.6
3.8	209.0	771.6	699.6	9.72	10.85	.0	38.8	62.8	100.9
5.1	219.0	788.5	711.3	10.72	9.83	.0	47.5	56.9	91.3
6.3	230.0	774.8	696.1	11.55	8.98	.0	43.4	52.0	83.4
7.6	240.0	744.2	666.2	12.24	8.27	.0	33.3	47.8	76.8
8.9	251.0	704.8	628.5	12.84	7.66	.0	22.7	44.3	71.1
10.2	261.0	717.5	639.0	12.84	7.66	.0	26.0	44.3	71.1
12.7	261.5	726.5	645.4	12.84	7.66	.0	28.5	44.3	71.1
15.2	262.0	723.0	640.6	12.84	7.66	.0	27.5	44.3	71.1
17.8	262.5	713.2	630.2	12.84	7.66	.0	24.8	44.3	71.1
20.3	263.0	700.3	616.9	12.84	7.66	.0	21.6	44.3	71.1
22.9	260.0	686.1	602.6	12.84	7.66	.0	18.5	44.3	71.1
25.4	257.0	671.5	587.9	12.84	7.66	.0	15.7	44.3	71.1
30.5	250.0	642.8	559.2	12.84	7.66	.0	11.2	44.3	71.1
35.6	243.0	615.2	531.5	12.84	7.66	.0	7.9	44.3	71.1
40.6	236.0	588.9	505.2	12.84	7.66	.0	5.5	44.3	71.1
45.7	226.0	564.5	480.8	12.84	7.66	.0	3.8	44.3	71.1
50.8	216.0	542.0	458.3	12.84	7.66	.0	2.7	44.3	71.1
55.9	206.0	521.2	437.5	12.84	7.66	.0	1.9	44.3	71.1
61.0	196.0	502.1	418.4	12.84	7.66	.0	1.4	44.3	71.1
TEST CODE:						TEST B			
X----	Ts-----	Tf1----	Tf2----	O2-----	CO2-----	COT-----	NOT----	Nof----	Cof
2.5	204.0	813.2	740.9	7.96	11.87	.0	50.3	68.7	110.2
3.8	213.0	897.7	812.4	9.21	10.67	.0	108.7	61.8	99.1
5.1	223.0	918.6	827.5	10.22	9.69	.0	134.5	56.1	90.0
6.3	233.0	903.5	810.9	11.07	8.88	.0	124.6	51.4	82.5
7.6	242.0	868.6	777.0	11.78	8.19	.0	97.5	47.4	76.1
8.9	251.0	823.6	734.3	12.40	7.60	.0	68.6	44.0	70.6
10.2	260.0	839.5	747.7	12.40	7.60	.0	78.6	44.0	70.6
12.7	260.0	852.3	757.4	12.39	7.60	.0	87.5	44.0	70.6
15.2	260.0	850.6	754.1	12.39	7.60	.0	86.2	44.0	70.6
17.8	260.0	841.5	744.3	12.40	7.60	.0	80.0	44.0	70.6
20.3	260.0	828.9	731.3	12.40	7.60	.0	71.8	44.0	70.6
22.9	257.0	814.8	717.0	12.40	7.60	.0	63.6	44.0	70.6
25.4	254.0	800.1	702.2	12.40	7.60	.0	55.8	44.0	70.6
30.5	247.0	771.1	673.1	12.40	7.60	.0	42.8	44.0	70.6
35.6	240.0	743.1	645.1	12.40	7.60	.0	32.7	44.0	70.6
40.6	233.0	716.4	618.4	12.40	7.60	.0	24.9	44.0	70.6
45.7	224.0	691.5	593.5	12.40	7.60	.0	19.1	44.0	70.6
50.8	214.0	668.5	570.5	12.40	7.60	.0	14.7	44.0	70.6
55.9	204.0	647.3	549.3	12.40	7.60	.0	11.5	44.0	70.6

61.0	195.0	627.7	529.7	12.40	7.60	.0	9.0	44.0	70.6
TEST CODE:						TEST C			
2.5	218.0	910.8	828.8	7.44	11.86	.0	106.9	68.7	110.2
3.8	228.0	1006.1	909.6	8.70	10.69	.0	230.8	61.9	99.3
5.1	237.0	1029.3	926.6	9.74	9.73	.1	285.9	56.3	90.4
6.3	246.0	1012.0	907.8	10.61	8.93	.0	265.6	51.7	83.0
7.6	255.0	972.6	869.7	11.35	8.25	.0	208.8	47.8	76.7
8.9	264.0	922.0	822.0	11.98	7.67	.0	148.1	44.4	71.2
10.2	273.0	939.9	837.0	11.98	7.67	.0	169.3	44.4	71.2
12.7	273.0	954.2	847.8	11.98	7.67	.0	188.0	44.4	71.2
15.2	273.0	952.2	844.1	11.98	7.67	.0	185.3	44.4	71.2
17.8	273.0	942.0	833.1	11.98	7.67	.0	172.0	44.4	71.2
20.3	273.0	927.8	818.5	11.98	7.67	.0	154.7	44.4	71.2
22.9	268.0	912.2	802.6	11.98	7.67	.0	137.4	44.4	71.2
25.4	263.0	896.1	786.4	11.99	7.67	.0	121.3	44.4	71.2
30.5	253.0	865.1	755.3	11.99	7.67	.0	94.8	44.4	71.2
35.6	242.0	836.0	726.2	11.99	7.67	.0	74.4	44.4	71.2
40.6	232.0	808.8	699.0	11.99	7.67	.0	58.8	44.4	71.2
45.7	225.0	783.1	673.3	11.99	7.67	.0	46.6	44.4	71.2
50.8	218.0	758.7	648.9	11.99	7.67	.0	37.1	44.4	71.2
55.9	210.0	735.9	626.1	11.99	7.67	.0	29.6	44.4	71.2
61.0	203.0	714.3	604.6	11.99	7.67	.0	23.8	44.4	71.2
TEST CODE:						TEST D			
2.5	212.0	698.8	639.8	8.93	11.66	.0	17.9	67.5	108.4
3.8	222.0	763.8	694.0	10.12	10.45	.0	36.7	60.5	97.1
5.1	231.0	777.8	703.0	11.08	9.46	.0	43.7	54.8	87.9
6.3	241.0	762.6	686.3	11.87	8.65	.0	39.2	50.0	80.3
7.6	251.0	731.3	655.6	12.54	7.96	.0	29.6	46.1	74.0
8.9	260.0	691.7	617.8	13.11	7.37	.0	19.9	42.7	68.5
10.2	270.0	704.0	628.0	13.11	7.37	.0	22.7	42.7	68.5
12.7	272.0	712.7	634.1	13.11	7.37	.0	24.9	42.7	68.5
15.2	274.0	709.0	629.2	13.11	7.37	.0	24.0	42.7	68.5
17.8	275.0	699.3	618.8	13.11	7.37	.0	21.6	42.7	68.5
20.3	277.0	686.3	605.5	13.11	7.37	.0	18.7	42.7	68.5
22.9	273.0	672.2	591.3	13.11	7.37	.0	16.0	42.7	68.5
25.4	269.0	657.9	576.9	13.11	7.37	.0	13.5	42.7	68.5
30.5	261.0	629.8	548.8	13.11	7.37	.0	9.6	42.7	68.5
35.6	252.0	603.1	522.1	13.11	7.37	.0	6.8	42.7	68.5
40.6	244.0	577.8	496.8	13.11	7.37	.0	4.7	42.7	68.5
45.7	237.0	553.8	472.8	13.11	7.37	.0	3.3	42.7	68.5
50.8	230.0	531.1	450.0	13.11	7.37	.0	2.3	42.7	68.5
55.9	222.0	509.7	428.6	13.11	7.37	.0	1.6	42.7	68.5
61.0	215.0	489.5	408.4	13.11	7.37	.0	1.1	42.7	68.5
TEST CODE:						TEST E			
2.5	208.0	807.8	737.4	5.92	14.75	.0	42.4	85.4	137.1
3.8	218.0	896.2	812.4	7.43	13.20	.0	98.6	76.4	122.6
5.1	227.0	922.0	832.0	8.66	11.94	.0	129.5	69.1	111.0
6.3	237.0	911.5	819.5	9.67	10.90	.0	126.1	63.1	101.3
7.6	246.0	880.5	789.0	10.52	10.03	.0	103.0	58.1	93.2
8.9	255.0	838.5	749.0	11.25	9.29	.0	75.4	53.8	86.3
10.2	264.0	853.8	761.7	11.25	9.29	.0	85.7	53.8	86.3
12.7	266.0	865.0	769.9	11.24	9.29	.0	93.9	53.8	86.3
15.2	268.0	861.4	764.7	11.24	9.29	.0	91.2	53.8	86.3
17.8	270.0	850.2	752.8	11.25	9.29	.0	83.2	53.8	86.3
20.3	271.0	835.3	737.4	11.25	9.29	.0	73.4	53.8	86.3
22.9	267.0	819.0	721.0	11.25	9.29	.0	63.8	53.8	86.3
25.4	263.0	802.3	704.2	11.25	9.29	.0	55.1	53.8	86.3
30.5	255.0	769.8	671.6	11.25	9.29	.0	40.9	53.8	86.3
35.6	247.0	738.6	640.4	11.25	9.29	.0	30.2	53.8	86.3
40.6	238.0	709.3	611.1	11.25	9.29	.0	22.4	53.8	86.3
45.7	232.0	681.3	583.1	11.25	9.29	.0	16.5	53.8	86.3
50.8	225.0	654.8	556.6	11.25	9.29	.0	12.1	53.8	86.3
55.9	218.0	629.7	531.4	11.25	9.29	.0	8.9	53.8	86.3
61.0	211.0	606.0	507.7	11.25	9.29	.0	6.5	53.8	86.3

TEST CODE:						TEST F		
2.5	221.0	903.6	839.5	7.60	13.03	.0	105.6	75.4 121.1
3.8	229.0	966.0	889.8	8.92	11.66	.0	181.8	67.5 108.4
5.1	237.0	974.0	892.3	10.00	10.56	.0	203.4	61.1 98.1
6.3	245.0	951.3	867.9	10.89	9.64	.0	179.8	55.8 89.6
7.6	252.0	911.9	829.1	11.64	8.88	.0	138.2	51.4 82.5
8.9	260.0	864.1	783.1	12.28	8.22	.0	97.2	47.6 76.4
10.2	268.0	877.7	794.4	12.28	8.22	.0	108.5	47.6 76.4
12.7	270.0	887.4	801.3	12.28	8.22	.0	117.2	47.6 76.4
15.2	271.0	883.7	796.3	12.28	8.22	.0	113.9	47.6 76.4
17.8	273.0	873.3	785.2	12.28	8.22	.0	104.7	47.6 76.4
20.3	274.0	859.4	770.9	12.28	8.22	.0	93.6	47.6 76.4
22.9	270.0	844.4	755.7	12.28	8.22	.0	82.6	47.6 76.4
25.4	266.0	829.0	740.2	12.28	8.22	.0	72.5	47.6 76.4
30.5	257.0	799.1	710.3	12.29	8.22	.0	55.8	47.6 76.4
35.6	249.0	770.5	681.7	12.29	8.22	.0	42.9	47.6 76.4
40.6	240.0	743.6	654.8	12.29	8.22	.0	33.1	47.6 76.4
45.7	234.0	717.9	629.1	12.29	8.22	.0	25.5	47.6 76.4
50.8	227.0	693.5	604.7	12.29	8.22	.0	19.7	47.6 76.4
55.9	220.0	670.5	581.6	12.29	8.22	.0	15.2	47.6 76.4
61.0	214.0	648.5	559.6	12.29	8.22	.0	11.7	47.6 76.4
TEST CODE:						TEST G		
2.5	229.0	1054.1	974.1	6.37	13.38	.2	275.6	77.5 124.4
3.8	236.0	1138.0	1043.5	7.77	12.03	.6	510.0	69.7 111.8
5.1	243.0	1153.4	1052.3	8.91	10.93	.6	596.6	63.3 101.5
6.3	250.0	1130.1	1027.3	9.87	10.01	.4	548.3	57.9 93.0
7.6	256.0	1085.9	984.0	10.68	9.23	.1	436.0	53.5 85.8
8.9	263.0	1031.2	931.8	11.37	8.57	.0	316.1	49.6 79.6
10.2	270.0	1049.4	947.2	11.37	8.57	.1	356.4	49.6 79.6
12.7	272.0	1064.3	958.6	11.37	8.57	.1	392.3	49.6 79.6
15.2	273.0	1062.8	955.5	11.37	8.57	.1	388.7	49.6 79.6
17.8	274.0	1053.2	945.0	11.37	8.57	.1	365.2	49.6 79.6
20.3	275.0	1039.3	930.7	11.37	8.57	.1	333.6	49.6 79.6
22.9	271.0	1024.0	915.2	11.38	8.57	.0	301.2	49.6 79.6
25.4	267.0	1008.1	899.2	11.38	8.57	.0	270.4	49.6 79.6
30.5	258.0	977.1	868.1	11.38	8.57	.0	217.9	49.6 79.6
35.6	250.0	947.3	838.3	11.38	8.57	.0	175.8	49.6 79.6
40.6	241.0	919.4	810.3	11.38	8.57	.0	142.7	49.6 79.6
45.7	234.0	892.8	783.7	11.38	8.57	.0	116.2	49.6 79.6
50.8	228.0	867.4	758.3	11.39	8.57	.0	94.9	49.6 79.6
55.9	221.0	843.3	734.3	11.39	8.57	.0	77.8	49.6 79.6
61.0	215.0	820.4	711.4	11.39	8.57	.0	64.0	49.6 79.6
TEST CODE:						TEST H		
2.5	220.0	986.5	896.9	6.11	13.09	.0	168.5	75.8 121.6
3.8	229.0	1095.6	990.1	7.49	11.80	.3	383.4	68.3 109.7
5.1	238.0	1125.3	1012.9	8.63	10.75	.4	492.9	62.2 99.8
6.3	247.0	1110.0	995.9	9.59	9.86	.2	474.3	57.1 91.6
7.6	255.0	1070.1	957.4	10.41	9.11	.1	385.9	52.7 84.7
8.9	264.0	1017.6	907.8	11.11	8.47	.0	282.5	49.0 78.7
10.2	273.0	1038.1	925.3	11.11	8.47	.0	324.1	49.0 78.7
12.7	273.5	1055.7	939.0	11.11	8.47	.1	363.4	49.0 78.7
15.2	274.0	1055.3	936.7	11.11	8.47	.1	362.5	49.0 78.7
17.8	274.5	1045.9	926.4	11.11	8.47	.1	341.0	49.0 78.7
20.3	275.0	1031.9	912.0	11.11	8.47	.0	311.0	49.0 78.7
22.9	270.0	1016.4	896.2	11.11	8.47	.0	280.2	49.0 78.7
25.4	265.0	1000.3	880.0	11.11	8.47	.0	251.0	49.0 78.7
30.5	254.0	969.4	849.0	11.11	8.47	.0	202.0	49.0 78.7
35.6	244.0	940.1	819.7	11.12	8.47	.0	163.2	49.0 78.7
40.6	234.0	912.7	792.3	11.12	8.47	.0	132.8	49.0 78.7
45.7	227.0	886.8	766.4	11.12	8.47	.0	108.6	49.0 78.7
50.8	220.0	862.2	741.8	11.12	8.47	.0	89.1	49.0 78.7
55.9	214.0	838.8	718.4	11.12	8.47	.0	73.4	49.0 78.7
61.0	207.0	816.7	696.3	11.12	8.47	.0	60.7	49.0 78.7

TEST CODE:					TEST I			
2.5	214.0	839.9	760.3	3.62 17.01	.0	43.8	98.5	158.1
3.8	222.0	892.4	801.4	6.21 14.36	.0	87.6	83.1	133.4
5.1	230.0	881.5	787.0	8.11 12.43	.0	91.5	71.9	115.5
6.3	238.0	838.9	744.9	9.56 10.95	.0	69.8	63.4	101.8
7.6	246.0	781.5	690.2	10.70 9.79	.0	44.4	56.7	91.0
8.9	254.0	718.5	631.0	11.62 8.85	.0	25.0	51.2	82.2
10.2	262.0	726.1	636.1	11.62 8.85	.0	27.0	51.2	82.2
12.7	263.0	722.3	629.3	11.62 8.85	.0	26.0	51.2	82.2
15.2	264.0	704.0	609.6	11.62 8.85	.0	21.4	51.2	82.2
17.8	265.0	678.4	583.2	11.62 8.85	.0	16.2	51.2	82.2
20.3	265.0	649.2	553.6	11.62 8.85	.0	11.5	51.2	82.2
22.9	260.0	619.4	523.6	11.62 8.85	.0	7.9	51.2	82.2
25.4	255.0	589.8	493.9	11.62 8.85	.0	5.3	51.2	82.2
30.5	245.0	533.8	437.8	11.62 8.85	.0	2.3	51.2	82.2
35.6	235.0	481.3	385.3	11.62 8.85	.0	.9	51.2	82.2
40.6	225.0	432.6	336.7	11.62 8.85	.0	.3	51.2	82.2
45.7	213.0	388.4	292.4	11.62 8.85	.0	.1	51.2	82.2
50.8	202.0	348.0	252.0	11.62 8.85	.0	.0	51.2	82.2
55.9	191.0	311.3	215.3	11.62 8.85	.0	.0	51.2	82.2
61.0	180.0	278.0	182.1	11.62 8.85	.0	.0	51.2	82.2
TEST CODE:					TEST J			
2.5	190.0	733.1	663.4	6.38 14.20	.0	21.7	82.2	131.9
3.8	199.0	774.0	694.7	8.52 12.01	.0	37.1	69.5	111.6
5.1	207.0	760.6	678.5	10.10 10.40	.0	35.5	60.2	96.7
6.3	215.0	720.6	639.2	11.30 9.17	.0	25.2	53.1	85.2
7.6	223.0	668.7	589.8	12.25 8.21	.0	14.8	47.5	76.3
8.9	232.0	612.5	537.0	13.02 7.42	.0	7.6	43.0	69.0
10.2	240.0	621.1	543.5	13.02 7.42	.0	8.5	43.0	69.0
12.7	241.0	622.0	541.7	13.02 7.42	.0	8.6	43.0	69.0
15.2	241.0	610.5	529.0	13.02 7.42	.0	7.4	43.0	69.0
17.8	241.0	593.0	510.8	13.02 7.42	.0	5.8	43.0	69.0
20.3	244.0	571.8	489.3	13.02 7.42	.0	4.3	43.0	69.0
22.9	240.0	549.8	467.1	13.02 7.42	.0	3.1	43.0	69.0
25.4	235.0	527.9	445.2	13.02 7.42	.0	2.2	43.0	69.0
30.5	227.0	485.8	403.1	13.02 7.42	.0	1.0	43.0	69.0
35.6	218.0	446.3	363.5	13.02 7.42	.0	.5	43.0	69.0
40.6	210.0	409.1	326.3	13.02 7.42	.0	.2	43.0	69.0
45.7	200.0	374.9	292.1	13.02 7.42	.0	.1	43.0	69.0
50.8	190.0	343.5	260.7	13.02 7.42	.0	.0	43.0	69.0
55.9	180.0	314.9	232.1	13.02 7.42	.0	.0	43.0	69.0
61.0	170.0	288.9	206.1	13.02 7.42	.0	.0	43.0	69.0
TEST CODE:					TEST K			
2.5	208.0	1179.6	1062.2	.98 17.82	4.5	225.2	103.2	165.6
3.8	215.0	1266.4	1133.9	3.75 15.24	6.6	688.4	88.2	141.6
5.1	222.0	1258.6	1122.2	5.83 13.31	4.2	828.2	77.1	123.7
6.3	230.0	1204.4	1069.8	7.46 11.82	1.5	713.1	68.4	109.8
7.6	237.0	1129.0	999.2	8.76 10.63	.4	507.6	61.5	98.7
8.9	244.0	1046.1	922.2	9.82 9.65	.1	320.8	55.9	89.7
10.2	252.0	1063.7	936.3	9.82 9.65	.1	359.6	55.9	89.7
12.7	251.0	1072.6	941.0	9.82 9.65	.1	380.7	55.9	89.7
15.2	251.0	1061.4	927.6	9.82 9.65	.1	354.4	55.9	89.7
17.8	250.0	1040.3	905.5	9.82 9.65	.1	309.0	55.9	89.7
20.3	250.0	1014.2	878.8	9.83 9.65	.0	259.4	55.9	89.7
22.9	245.0	986.7	851.0	9.83 9.65	.0	214.5	55.9	89.7
25.4	240.0	959.0	823.2	9.83 9.65	.0	176.1	55.9	89.7
30.5	230.0	906.3	770.4	9.83 9.65	.0	118.8	55.9	89.7
35.6	220.0	856.9	721.0	9.84 9.65	.0	80.1	55.9	89.7
40.6	210.0	811.2	675.3	9.84 9.65	.0	54.3	55.9	89.7
45.7	200.0	769.1	633.2	9.84 9.65	.0	37.0	55.9	89.7
50.8	190.0	730.5	594.6	9.84 9.65	.0	25.4	55.9	89.7
55.9	179.0	695.6	559.7	9.84 9.65	.0	17.6	55.9	89.7
61.0	169.0	663.9	528.0	9.84 9.65	.0	12.3	55.9	89.7



TEST CODE:						TEST L		
2.5	220.0	1036.2	934.7	3.95	15.08	.1	190.0	87.3 140.1
3.8	228.0	1099.1	984.9	6.31	12.89	.3	359.3	74.6 119.8
5.1	235.0	1082.9	965.7	8.08	11.26	.2	368.2	65.2 104.6
6.3	242.0	1028.9	913.5	9.46	9.99	.1	281.1	57.8 92.8
7.6	250.0	958.3	847.1	10.56	8.98	.0	181.7	52.0 83.4
8.9	258.0	882.2	776.2	11.46	8.15	.0	106.3	47.2 75.8
10.2	265.0	896.0	787.0	11.46	8.15	.0	118.5	47.2 75.8
12.7	264.0	901.0	788.4	11.46	8.15	.0	123.3	47.2 75.8
15.2	264.0	888.9	774.4	11.46	8.15	.0	112.1	47.2 75.8
17.8	264.0	868.1	752.7	11.46	8.15	.0	94.9	47.2 75.8
20.3	263.0	843.1	727.3	11.46	8.15	.0	77.3	47.2 75.8
22.9	258.0	817.1	701.0	11.46	8.15	.0	61.8	47.2 75.8
25.4	253.0	790.9	674.8	11.46	8.15	.0	49.0	47.2 75.8
30.5	242.0	741.5	625.3	11.46	8.15	.0	30.7	47.2 75.8
35.6	231.0	695.5	579.2	11.46	8.15	.0	19.0	47.2 75.8
40.6	221.0	652.8	536.5	11.46	8.15	.0	11.7	47.2 75.8
45.7	210.0	613.7	497.4	11.46	8.15	.0	7.1	47.2 75.8
50.8	198.0	578.4	462.1	11.46	8.15	.0	4.4	47.2 75.8
55.9	186.0	546.6	430.3	11.46	8.15	.0	2.7	47.2 75.8
61.0	175.0	517.9	401.6	11.46	8.15	.0	1.7	47.2 75.8
TEST CODE:						TEST M		
2.5	197.0	916.4	841.4	4.96	15.64	.0	94.4	90.6 145.3
3.8	205.0	950.2	864.8	7.33	13.22	.0	147.2	76.5 122.8
5.1	214.0	927.9	839.3	9.07	11.44	.0	138.2	66.2 106.3
6.3	223.0	878.2	790.2	10.40	10.09	.0	100.5	58.4 93.7
7.6	232.0	816.5	731.2	11.45	9.02	.0	62.9	52.2 83.8
8.9	240.0	751.2	669.4	12.30	8.16	.0	35.6	47.2 75.8
10.2	249.0	760.8	676.7	12.30	8.16	.0	39.1	47.2 75.8
12.7	249.0	762.5	675.7	12.30	8.16	.0	39.8	47.2 75.8
15.2	249.0	751.0	662.7	12.30	8.16	.0	35.6	47.2 75.8
17.8	249.0	732.8	643.8	12.30	8.16	.0	29.7	47.2 75.8
20.3	249.0	711.2	621.9	12.30	8.16	.0	23.8	47.2 75.8
22.9	245.0	688.8	599.3	12.30	8.16	.0	18.7	47.2 75.8
25.4	240.0	666.3	576.8	12.30	8.16	.0	14.5	47.2 75.8
30.5	232.0	623.2	533.5	12.30	8.16	.0	8.5	47.2 75.8
35.6	223.0	582.5	492.8	12.30	8.16	.0	4.9	47.2 75.8
40.6	215.0	544.2	454.6	12.30	8.16	.0	2.7	47.2 75.8
45.7	204.0	509.3	419.6	12.30	8.16	.0	1.5	47.2 75.8
50.8	192.0	477.7	388.1	12.30	8.16	.0	.8	47.2 75.8
55.9	181.0	449.2	359.5	12.30	8.16	.0	.5	47.2 75.8
61.0	170.0	423.4	333.8	12.30	8.16	.0	.3	47.2 75.8
TEST CODE:						TEST N		
2.5	216.0	844.8	769.8	4.93	15.68	.0	53.2	90.7 145.7
3.8	224.0	885.4	799.8	7.31	13.25	.0	89.7	76.7 123.1
5.1	233.0	868.1	779.4	9.05	11.47	.0	86.6	66.4 106.5
6.3	242.0	822.4	734.3	10.38	10.11	.0	63.1	58.5 93.9
7.6	250.0	764.0	678.6	11.43	9.04	.0	39.0	52.3 84.0
8.9	259.0	701.2	619.3	12.28	8.17	.0	21.4	47.3 75.9
10.2	268.0	709.1	624.9	12.28	8.17	.0	23.2	47.3 75.9
12.7	268.0	707.3	620.3	12.28	8.17	.0	22.8	47.3 75.9
15.2	267.0	692.4	604.0	12.28	8.17	.0	19.4	47.3 75.9
17.8	267.0	670.8	581.7	12.28	8.17	.0	15.2	47.3 75.9
20.3	266.0	646.1	556.6	12.28	8.17	.0	11.4	47.3 75.9
22.9	261.0	620.6	531.0	12.28	8.17	.0	8.3	47.3 75.9
25.4	257.0	595.1	505.4	12.28	8.17	.0	5.9	47.3 75.9
30.5	247.0	546.8	457.0	12.28	8.17	.0	2.9	47.3 75.9
35.6	237.0	501.4	411.6	12.28	8.17	.0	1.3	47.3 75.9
40.6	227.0	459.4	369.5	12.28	8.17	.0	.6	47.3 75.9
45.7	214.0	421.4	331.6	12.28	8.17	.0	.3	47.3 75.9
50.8	201.0	387.3	297.5	12.28	8.17	.0	.1	47.3 75.9
55.9	189.0	356.6	266.8	12.28	8.17	.0	.0	47.3 75.9
61.0	176.0	329.4	239.5	12.28	8.17	.0	.0	47.3 75.9

TEST CODE:						TEST P		
2.5	236.0	1234.7	1113.9	1.43	17.63	8.2	361.8	104.0 166.9
3.8	246.0	1325.3	1189.0	4.10	15.11	12.2	931.4	89.1 143.0
5.1	256.0	1318.2	1178.0	6.11	13.22	8.0	1105.6	78.0 125.1
6.3	266.0	1263.3	1125.0	7.69	11.75	3.4	969.2	69.3 111.2
7.6	275.0	1186.6	1053.3	8.96	10.57	1.0	708.8	62.4 100.1
8.9	285.0	1102.0	974.8	10.00	9.61	.2	459.7	56.7 91.0
10.2	295.0	1122.8	992.0	10.00	9.61	.3	521.1	56.7 91.0
12.7	295.0	1137.2	1002.0	10.00	9.61	.4	567.1	56.7 91.0
15.2	296.0	1130.6	993.2	10.00	9.61	.3	545.8	56.7 91.0
17.8	296.0	1113.7	975.3	10.00	9.61	.2	493.6	56.7 91.0
20.3	296.0	1091.7	952.6	10.00	9.61	.2	431.4	56.7 91.0
22.9	291.0	1067.9	928.6	10.01	9.61	.1	371.5	56.7 91.0
25.4	285.0	1043.8	904.4	10.01	9.61	.1	318.0	56.7 91.0
30.5	275.0	997.4	857.9	10.01	9.61	.0	232.5	56.7 91.0
35.6	264.0	953.7	814.2	10.02	9.61	.0	170.5	56.7 91.0
40.6	254.0	912.9	773.4	10.02	9.61	.0	125.7	56.7 91.0
45.7	245.0	874.6	735.1	10.02	9.61	.0	93.1	56.7 91.0
50.8	236.0	838.8	699.3	10.02	9.61	.0	69.4	56.7 91.0
55.9	227.0	805.4	665.9	10.02	9.61	.0	51.9	56.7 91.0
61.0	218.0	774.3	634.7	10.02	9.61	.0	39.1	56.7 91.0

TEST CODE:						TEST O		
2.5	230.0	1237.4	1116.1	.87	18.02	11.2	285.5	104.6 167.9
3.8	242.0	1330.4	1193.5	3.63	15.43	14.0	896.7	89.6 143.8
5.1	253.0	1324.9	1184.0	5.70	13.49	9.1	1100.7	78.3 125.7
6.3	265.0	1270.8	1131.8	7.33	11.99	3.9	982.1	69.6 111.7
7.6	276.0	1194.5	1060.3	8.64	10.78	1.1	727.1	62.6 100.5
8.9	287.0	1109.9	981.9	9.72	9.80	.2	476.1	56.9 91.3
10.2	298.0	1131.1	999.5	9.71	9.80	.3	540.0	56.9 91.3
12.7	299.0	1145.8	1009.8	9.71	9.80	.4	588.4	56.9 91.3
15.2	301.0	1139.4	1001.2	9.71	9.80	.4	566.9	56.9 91.3
17.8	302.0	1122.3	983.1	9.71	9.80	.3	512.9	56.9 91.3
20.3	303.0	1099.9	960.1	9.72	9.80	.2	447.9	56.9 91.3
22.9	298.0	1075.8	935.7	9.72	9.80	.1	385.5	56.9 91.3
25.4	293.0	1051.2	910.9	9.72	9.80	.1	329.3	56.9 91.3
30.5	283.0	1003.7	863.3	9.73	9.80	.0	239.6	56.9 91.3
35.6	273.0	958.6	818.3	9.73	9.80	.0	174.4	56.9 91.3
40.6	263.0	916.5	776.1	9.73	9.80	.0	127.5	56.9 91.3
45.7	256.0	876.3	735.9	9.74	9.80	.0	93.2	56.9 91.3
50.8	244.0	839.5	699.1	9.74	9.80	.0	68.8	56.9 91.3
55.9	235.0	805.0	664.7	9.74	9.80	.0	51.1	56.9 91.3
61.0	226.0	772.9	632.6	9.74	9.80	.0	38.1	56.9 91.3

TEST CODE:						TEST Q		
2.5	243.0	1235.5	1115.2	1.14	17.56	9.3	326.4	101.9 163.5
3.8	251.0	1324.4	1188.8	3.88	15.02	12.4	907.2	87.1 139.9
5.1	259.0	1316.6	1177.0	5.94	13.13	8.0	1086.9	76.1 122.2
6.3	268.0	1261.4	1123.8	7.55	11.66	3.3	955.3	67.6 108.5
7.6	276.0	1184.8	1052.1	8.84	10.48	.9	699.5	60.8 97.6
8.9	284.0	1100.6	974.0	9.90	9.52	.2	454.8	55.2 88.6
10.2	292.0	1122.0	991.8	9.90	9.52	.3	517.5	55.2 88.6
12.7	292.0	1137.7	1003.2	9.89	9.52	.4	567.8	55.2 88.6
15.2	291.0	1133.0	996.3	9.89	9.52	.3	552.4	55.2 88.6
17.8	290.0	1118.2	980.4	9.90	9.52	.3	505.9	55.2 88.6
20.3	290.0	1098.2	959.9	9.90	9.52	.2	448.2	55.2 88.6
22.9	284.0	1076.6	938.0	9.90	9.52	.1	391.9	55.2 88.6
25.4	278.0	1054.7	915.9	9.91	9.52	.1	340.6	55.2 88.6
30.5	266.0	1012.9	874.1	9.91	9.52	.0	258.1	55.2 88.6
35.6	254.0	973.9	835.0	9.91	9.52	.0	196.7	55.2 88.6
40.6	242.0	938.0	799.1	9.91	9.52	.0	151.6	55.2 88.6
45.7	231.0	905.0	766.1	9.92	9.52	.0	118.0	55.2 88.6
50.8	221.0	874.4	735.5	9.92	9.52	.0	92.8	55.2 88.6
55.9	210.0	846.4	707.5	9.92	9.52	.0	73.8	55.2 88.6
61.0	200.0	820.6	681.8	9.92	9.52	.0	59.3	55.2 88.6

**APPENDIX C**  
**EXPERIMENTAL CODE AND DATA**

### C.1 Experimental Code

TEST NO.	TEST CODE	TEST CODE
CH 3&4	CH2&3	APP.
1		DFM501
2		DFM502
3	A	DFM503
4		DFM304
5		DFM305
6	B	DFM306
7		MDMLC1
8		MDMHC2
9	C	MDMMC3
10		MMLMC7
11		MMHMC8
12	D	MWHMC9
13	E	MWLMC10
14	F	MWMMH11
15	G	MMMMH12
16		MDMMH13
17	H	LDMMC4
18		LDHMC5
19		LDLMC6
20	I	DFSW1
21	J	DFSW2
22	K	DFSD3
23	L	DFSD4
24	M	DFSW5
25	N	DFSW6
26	O	PHC3
27	P	KMP2
28	Q	BCCP161

TC11 : PROBE TEMP.

TC12 : PROBE TEMP.

LOC : LOCATION IN THE COMB. CH

Tavg : AVERAGE TEMP. OF TWO TP

Twavg : AVERAGE TEMP. OF STEEL

Taavg : AVERAGE TEMP. OF U.F. AIR

C.2 Experimental Data

TEST CODE AND DATE: DFM501 6/16/89									
M.C. (WB%)= 53.920									
FUEL FEED (WET, DRY lb/hr)= 8.694 4.006									
E.A. (%)= 124.650									
TOTAL AIR (scfh)= 748.800									
U.F. AIR (%)= 35.000									
O.F. AIR (%)= 65.000									
LOC in	T12 C	T11 C	O2 percent	CO2 percent	NOx ppm	CO ppm	COMB. percent		
24.000	537.043	512.217	14.278	6.589	41.667	415.778	0.000		
22.000	557.277	545.060	13.522	7.311	45.000	102.778	0.000		
20.000	560.387	560.007	14.300	6.544	45.000	190.444	0.000		
18.000	586.807	594.447	13.111	7.722	52.333	124.889	0.000		
16.000	585.313	587.607	14.556	6.322	44.333	99.111	0.000		
LOC cm	LOC in	Tavg C	Tavg F	WALL in	LOC cm	Tavg C	Tavg F	Taavg C	Taavg F
60.960	24.000	524.630	976.338	0.000	0.000	194.686	382.439	28.955	84.124
55.880	22.000	551.168	1024.107	4.000	10.160	279.660	535.392		
50.800	20.000	560.197	1040.358	8.000	20.320	281.401	538.526		
45.720	18.000	590.627	1095.132	16.000	40.640	247.991	478.388		
40.640	16.000	586.460	1087.632	24.000	60.960	198.034	388.465		
Tcavg C	Tcavg F	O2avg percent	CO2avg percent	NOxavg ppm	COavg ppm	COMBavg percent	PART. g	COMB% in part.	ASH% in part.
562.616	1044.713	13.953	6.898	45.667	186.600	0.000	0.022	41.500	58.500

TEST CODE AND DATE: DFM502 6/16/89  
 M.C. (WB $\frac{1}{2}$ )= 53.920  
 FUEL FEED (WET, DRY lb/hr)= 8.694 4.006  
 E.A. ( $\frac{1}{2}$ )= 124.650  
 TOTAL AIR (scfh)= 748.800  
 U.F. AIR ( $\frac{1}{2}$ )= 65.000  
 O.F. AIR ( $\frac{1}{2}$ )= 35.000

LOC in	T12 C	T11 C	O2 percent	CO2 percent	NOx ppm	CO ppm	COMB. percent		
24.000	547.233	527.003	13.333	7.522	52.222	190.778	0.000		
22.000	556.493	547.323	13.544	7.278	48.000	268.444	0.000		
20.000	593.190	582.483	12.167	8.622	59.333	108.444	0.000		
18.000	597.013	590.890	13.433	7.400	51.667	224.333	0.000		
16.000	579.857	572.967	14.867	5.978	43.333	1369.222	0.000		
LOC cm	LOC in	Tavg C	Tavg F	WALL LOC in	WALL LOC cm	Twavg C	Twavg F	Taavg C	Taavg F
60.960	24.000	537.118	998.817	0.000	0.000	178.616	353.513	27.905	82.232
55.880	22.000	551.908	1025.439	4.000	10.160	264.501	508.106		
50.800	20.000	587.837	1090.110	8.000	20.320	269.355	516.844		
45.720	18.000	593.952	1101.117	16.000	40.640	241.739	467.134		
40.640	16.000	576.412	1069.545	24.000	60.960	198.599	389.483		
Tcavg C	Tcavg F	O2avg percent	CO2avg percent	NOxavg ppm	COavg ppm	COMBavg percent	PART. g	COMB $\frac{1}{2}$ in part.	ASH $\frac{1}{2}$ in part.
569.445	1057.006	13.469	7.360	50.911	432.244	0.000	0.023	33.900	66.100

TEST CODE AND DATE: DFM503 6/16/89  
 H.C. (WB)= 53.920  
 FUEL FEED (WET, DRY lb/hr) 8.694 4.006  
 E.A. (%)= 124.650  
 TOTAL AIR= 748.800  
 U.F. AIR (%)= 50.000  
 O.F. AIR (%)= 50.000

LOC in	T12 C	T11 C	O2 percent	CO2 percent	NOx ppm	CO ppm	COMB. percent
24.0	552.8	545.9	13.6	7.2	44.0	140.3	0.0
22.0	550.1	545.9	12.8	8.0	48.7	156.6	0.0
20.0	558.5	560.8	13.6	7.3	51.3	114.3	0.0
18.0	595.9	604.4	14.2	6.7	45.0	115.3	0.0
16.0	615.5	620.5	14.3	6.5	44.3	831.6	0.0
14.0	640.4	640.4	14.6	6.3	44.0	118.1	0.0
12.0	661.6	655.8	14.3	6.6	44.0	85.9	0.0
10.0	675.9	668.2	14.4	6.5	42.7	85.0	0.0
9.0	675.1	666.6	14.5	6.3	43.3	103.4	0.0
8.0	676.3	665.1	14.9	6.0	40.3	101.0	0.0
7.0	701.1	680.9	14.2	6.7	45.7	174.0	0.0
6.0	741.3	710.4	14.2	6.7	46.0	80.0	0.0
5.0	733.9	734.2	12.7	8.2	54.4	89.4	0.0
4.0	733.9	734.2	11.9	8.9	59.2	161.1	0.0
3.5	650.5	662.4	12.4	8.4	54.3	130.4	0.0
3.0	691.8	706.6	13.9	6.8	46.0	73.0	0.0
2.5	691.5	789.3	14.5	6.3	44.0	85.3	0.0
2.0	710.1	842.8	14.8	6.0	41.0	107.4	0.0
1.5	656.7	822.8	15.5	5.4	30.8	390.8	0.0
1.0	657.4	814.4	14.7	6.1	21.7	1504.9	1.1

LOC cm	LOC in	Tavg C	Tavg F	WALL in	LOC cm	WALL cm	LOC C	Twavg C	Twavg F	Taavg C	Taavg F
61.0	24.0	549.3	1020.8	0.0	0.0	176.9	350.4	27.6	81.6		
55.9	22.0	548.0	1018.4	4.0	10.2	261.4	502.6				
50.8	20.0	559.6	1039.4	8.0	20.3	263.4	506.1				
45.7	18.0	600.2	1112.3	16.0	40.6	236.1	457.0				
40.6	16.0	618.0	1144.4	24.0	61.0	195.8	384.5				
35.6	14.0	640.4	1184.8								
30.5	12.0	658.7	1217.7								
25.4	10.0	672.0	1241.7								
22.9	9.0	670.9	1239.6								
20.3	8.0	670.7	1239.3								
17.8	7.0	691.0	1275.8								
15.2	6.0	725.8	1338.5								
12.7	5.0	734.1	1353.3								
10.2	4.0	734.1	1353.3								
8.9	3.5	656.5	1213.6								
7.6	3.0	699.2	1290.6								
6.4	2.5	740.4	1364.7								
5.1	2.0	776.4	1429.6								
3.8	1.5	739.7	1363.5								
2.5	1.0	735.9	1356.6								

PART. g	COMB% in part.	ASH% in part.
0.020	32.660	67.340

TEST CODE AND DATE: DFM304 6/16/89  
 M.C. (WB)= 35.359  
 FUEL FEED (WET, DRY lb/hr)= 6.300 4.072  
 E.A. (%)= 121.500  
 TOTAL AIR= 748.800  
 U.P. AIR (%)= 65.000  
 O.P. AIR (%)= 35.000

LOC in	T12 C	T11 C	O2 percent	CO2 percent	NOx ppm	CO ppm	COMB. percent		
24.000	558.190	541.393	13.489	7.367	47.667	61.889	0.000		
22.000	568.900	558.590	14.056	6.767	45.000	67.667	0.000		
20.000	601.387	596.040	12.822	7.989	55.000	57.111	0.000		
18.000	605.617	600.637	14.144	6.756	49.222	204.556	0.000		
16.000	631.307	623.250	13.522	7.311	56.778	85.333	0.000		
LOC cm	LOC in	Tavg C	Tavg F	WALL LOC in	WALL LOC cm	Twavg C	Twavg F	Taavg C	Taavg F
60.960	24.000	549.792	1021.629	0.000	0.000	174.491	346.087	27.535	81.566
55.880	22.000	563.745	1046.745	4.000	10.160	256.567	493.824		
50.800	20.000	598.713	1109.688	8.000	20.320	259.525	499.148		
45.720	18.000	603.127	1117.632	16.000	40.640	235.346	455.627		
40.640	16.000	627.278	1161.105	24.000	60.960	197.320	387.180		
Tcavg C	Tcavg F	O2avg percent	CO2avg percent	NOxavg ppm	COavg ppm	COMBavg percent	PART. g	COMB% in part.	ASH% in part.
588.531	1091.360	13.607	7.238	50.733	95.311	0.000	0.016	16.670	83.330



TEST CODE AND DATE: DFW305 6/16/89  
 M.C. (WB%)= 35.359  
 FUEL FEED (WET, DRY lb/hr)= 6.300 4.072  
 E.A. (%)= 121.500  
 TOTAL AIR (scfh)= 748.800  
 U.F. AIR (%)= 35.000  
 O.F. AIR (%)= 65.000

LOC in	T12 C	T11 C	O2 percent	CO2 percent	NOx ppm	CO ppm	COMB. percent		
24.000	563.647	539.593	13.011	7.822	50.333	121.333	0.000		
22.000	572.473	563.693	13.489	7.356	47.000	87.778	0.000		
20.000	570.580	574.023	14.744	6.089	41.000	102.778	0.000		
18.000	592.387	603.107	14.533	6.344	44.333	91.333	0.000		
16.000	646.110	656.120	12.367	8.456	55.444	123.000	0.000		
LOC cm	LOC in	Tavg C	Tavg F	WALL LOC in	WALL LOC cm	Tavg C	Tavg F	Taavg C	Taavg F
60.960	24.000	551.620	1024.920	0.000	0.000	174.657	346.387	28.900	84.024
55.880	22.000	568.083	1054.554	4.000	10.160	256.962	494.536		
50.800	20.000	572.302	1062.147	8.000	20.320	258.241	496.837		
45.720	18.000	597.747	1107.948	16.000	40.640	233.666	452.603		
40.640	16.000	651.115	1204.011	24.000	60.960	196.262	385.276		
Tcavg C	Tcavg F	O2avg percent	CO2avg percent	NOxavg ppm	COavg ppm	COMBavg percent	PART. g	COMB% in part.	ASH% in part.
588.173	1090.716	13.629	7.213	47.622	105.244	0.000	0.017	19.880	80.120

TEST CODE AND DATE: DFM306 6/16/89  
 M.C. (WBt)=  
 FUEL FEED (WET, DRY lb/hr)= 6.300 4.072  
 E.A. (t)= 121.500  
 TOTAL AIR (scfh)= 748.800  
 U.F. AIR (t)= 50.000  
 O.F. AIR (t)= 50.000

LOC in	T12 C	T11 C	O2 percent	CO2 percent	NOx ppm	CO ppm	COMB. percent
24.00	563.79	561.88	12.52	8.31	50.67	60.00	0.00
22.00	563.04	568.76	14.49	6.38	41.33	68.44	0.00
20.00	585.59	598.58	13.82	6.93	49.00	65.56	0.00
18.00	602.02	613.13	14.29	6.67	48.67	69.00	0.00
16.00	627.36	632.74	13.57	7.24	53.00	75.33	0.00
14.00	655.06	653.90	13.12	7.72	53.11	79.67	0.00
12.00	660.82	656.57	14.44	6.49	48.00	94.11	0.00
10.00	712.35	698.76	12.18	8.64	57.00	65.56	0.00
9.00	734.61	718.98	12.78	8.09	56.00	59.33	0.00
8.00	740.51	720.97	13.38	7.37	52.67	55.00	0.00
7.00	741.69	717.87	14.24	6.53	47.67	57.44	0.00
6.00	803.25	759.77	14.18	6.70	46.67	56.33	0.00
5.00	814.00	798.08	13.82	6.94	49.67	60.00	0.00
4.00	814.00	798.08	10.98	9.86	65.33	62.89	0.00
3.50	925.22	847.28	11.28	9.47	71.00	161.33	0.00
3.00	909.77	817.26	12.97	7.86	56.56	64.22	0.00
2.50	947.02	872.70	11.13	9.57	64.89	204.11	0.00
2.00	920.75	859.35	13.86	7.39	48.22	78.67	0.00
1.50	910.55	868.26	15.99	5.06	41.33	85.33	0.00
1.00	893.00	842.52	13.20	7.52	36.44	347.22	0.03

LOC cm	LOC in	Tavg C	Tavg F	WALL LOC in	WALL LOC cm	Twavg C	Twavg F	Taavg C	Taavg F
60.96	24.00	562.84	1045.11	0.00	0.00	184.60	364.29	29.30	84.74
55.88	22.00	565.90	1050.62	4.00	10.16	259.70	499.46		
50.80	20.00	592.09	1097.76	8.00	20.32	260.14	500.25		
45.72	18.00	607.57	1125.63	16.00	40.64	233.26	451.88		
40.64	16.00	630.05	1166.09	24.00	60.96	195.12	383.22		
35.56	14.00	654.48	1210.06						
30.48	12.00	658.70	1217.66						
25.40	10.00	705.55	1302.00						
22.86	9.00	726.80	1340.24						
20.32	8.00	730.74	1347.34						
17.78	7.00	729.78	1345.60						
15.24	6.00	781.51	1438.73						
12.70	5.00	806.04	1482.88						
10.16	4.00	806.04	1482.88						
8.89	3.50	886.25	1627.25						
7.62	3.00	863.52	1586.33						
6.35	2.50	909.86	1669.76						
5.08	2.00	890.05	1634.09						
3.81	1.50	889.40	1632.93						
2.54	1.00	867.76	1593.97						

PART. COMBt ASHt  
 g in part. in part.  
 -----  
 0.01 19.61 80.39  
 -----

TEST CODE AND DATE: MDMLC1 6/21/89  
M.C. (WB%)=  
FUEL FEED (WET, DRY lb/hr)= 4.700 4.177  
E.A. (%)=  
TOTAL AIR (scfh)= 748.800  
U.F. AIR (%)=  
O.F. AIR (%)= 65.000  
35.000

LOC in	T12 C	T11 C	O2 percent	CO2 percent	NOx ppm	CO ppm	COMB. percent		
24.000	608.403	579.330	12.811	7.989	54.000	499.111	0.000		
22.000	626.123	606.190	12.622	8.233	54.778	382.333	0.000		
20.000	650.797	645.797	11.967	8.867	62.778	276.444	0.000		
18.000	664.703	665.093	12.444	8.333	63.111	266.111	0.000		
16.000	667.450	664.363	12.622	8.044	55.333	256.222	0.000		
LOC cm	LOC in	Tavg C	Tavg F	WALL in	LOC cm	Tavg C	Tavg F	Taavg C	Taavg F
60.960	24.000	593.867	1100.964	0.000	0.000	200.845	393.526	28.261	82.874
55.880	22.000	616.157	1141.086	4.000	10.160	264.400	507.924		
50.800	20.000	648.297	1198.938	8.000	20.320	258.979	498.166		
45.720	18.000	664.898	1228.821	16.000	40.640	212.085	413.756		
40.640	16.000	665.907	1230.636	24.000	60.960	179.966	355.943		
Tcavg C	Tcavg F	O2avg percent	CO2avg percent	NOxavg ppm	COavg ppm	COMBavg percent	PART. g	COMB% in part.	ASH% in part.
637.825	1180.089	12.493	8.293	58.000	336.044	0.000	0.037	13.100	86.900

TEST CODE AND DATE: MDHHC2 6/21/89  
 M.C. (WB%)= 11.200  
 FUEL FEED (WET, DRY lb/hr)= 4.700 4.177  
 E.A. (%)= 115.860  
 TOTAL AIR (scfh)= 748.800  
 U.F. AIR (%)= 35.000  
 O.F. AIR (%)= 65.000

LOC in	T12 C	T11 C	O2 percent	CO2 percent	NOx ppm	CO ppm	COMB. percent		
24.000	598.053	564.030	12.200	8.589	55.444	105.889	0.000		
22.000	633.757	605.000	11.511	9.278	61.667	105.556	0.000		
20.000	661.490	643.773	11.611	9.200	66.333	106.000	0.000		
18.000	651.147	637.677	15.033	5.856	46.667	307.222	0.000		
16.000	698.337	680.500	12.022	8.733	67.000	129.667	0.000		
LOC cm	LOC in	Tavg C	Tavg F	WALL LOC in	WALL LOC cm	Twavg C	Twavg F	Taavg C	Taavg F
60.960	24.000	581.042	1077.879	0.000	0.000	201.587	394.861	27.307	81.156
55.880	22.000	619.378	1146.885	4.000	10.160	272.031	521.659		
50.800	20.000	652.632	1206.741	8.000	20.320	268.055	514.502		
45.720	18.000	644.412	1191.945	16.000	40.640	224.175	435.518		
40.640	16.000	689.418	1272.957	24.000	60.960	193.429	380.177		
Tcavg C	Tcavg F	O2avg percent	CO2avg percent	NOxavg ppm	COavg ppm	COMBavg percent	PART. g	COMB% in part.	ASH% in part.
637.376	1179.281	12.476	8.331	59.422	150.867	0.000	0.021	7.210	92.790

TEST CODE AND DATE: MDMHC3 6/21/89

H.C. (WB%)= 11.200

FUEL FEED (WET, DRY lb/hr) 4.700 4.177

E.A. (%)= 115.86

TOTAL AIR (scfh)= 748.80

U.F. AIR (%)= 50.000

O.F. AIR (%)= 50.000

LOC in	T12 C	T11 C	O2 percent	CO2 percent	NOx ppm	CO ppm	COMB. percent
24.0	588.0	565.5	12.5	8.3	52.7	88.1	0.0
22.0	614.9	604.1	12.4	8.5	57.8	82.4	0.0
20.0	636.0	636.0	12.0	8.8	59.4	80.3	0.0
18.0	652.6	652.9	12.5	8.2	59.8	78.3	0.0
16.0	661.9	655.7	13.5	7.4	57.0	81.6	0.0
14.0	697.9	684.7	11.9	8.9	72.3	86.7	0.0
12.0	707.6	689.4	13.5	7.4	58.4	79.6	0.0
10.0	740.8	719.3	12.5	8.3	64.3	69.4	0.0
9.0	752.5	732.2	13.1	7.8	62.4	66.9	0.0
8.0	760.1	739.3	13.2	7.6	60.8	62.9	0.0
7.0	869.3	832.3	10.8	10.0	68.0	79.0	0.0
6.0	850.8	821.5	13.9	6.9	56.2	64.2	0.0
5.0	868.0	861.8	11.6	9.2	68.7	65.6	0.0
4.0	868.0	861.8	6.1	14.6	97.0	81.8	0.0
3.5	1045.2	920.7	6.1	14.6	102.9	79.1	0.0
3.0	1035.5	926.1	8.2	12.4	89.9	77.2	0.0
2.5	1000.0	927.6	11.8	9.0	65.4	83.2	0.0
2.0	1000.1	916.4	9.6	11.1	67.7	118.4	0.0
1.5	1006.6	954.7	11.6	9.1	64.6	260.7	0.0
1.0	994.1	891.5	15.4	5.4	40.0	203.3	0.0

LOC cm	LOC in	Tavg C	Tavg F	WALL in	LOC cm	WALL cm	LOC C	Twavg F	Twavg C	Taavg C	Taavg F
61.0	24.0	576.8	1070.2	0.0	0.0	200.5	392.8	28.5	83.3		
55.9	22.0	609.5	1129.1	4.0	10.2	273.5	524.3				
50.8	20.0	636.0	1176.8	8.0	20.3	272.8	523.1				
45.7	18.0	652.8	1207.0	16.0	40.6	232.1	449.9				
40.6	16.0	658.8	1217.8	24.0	61.0	202.5	396.6				
35.6	14.0	691.3	1276.3								
30.5	12.0	698.5	1289.3								
25.4	10.0	730.0	1346.0								
22.9	9.0	742.4	1368.2								
20.3	8.0	749.7	1381.4								
17.8	7.0	850.8	1563.5								
15.2	6.0	836.2	1537.1								
12.7	5.0	864.9	1588.8								
10.2	4.0	864.9	1588.8								
8.9	3.5	983.0	1801.3								
7.6	3.0	980.8	1797.4								
6.4	2.5	963.8	1766.8								
5.1	2.0	958.3	1756.9								
3.8	1.5	980.7	1797.2								
2.5	1.0	942.8	1729.0								

PART. COMB% ASH%  
g in part in part.

0.011 4.440 95.560

TEST CODE AND DATE: MMLMC7 6/21/89  
 M.C. (WB%)= 35.359  
 FUEL FEED (WET, DRY lb/hr)= 6.846 4.425  
 E.A. (%)= 80.770  
 TOTAL AIR (scfh)= 665.600  
 U.F. AIR (%)= 50.000  
 O.F. AIR (%)= 50.000

LOC in	T12 C	T11 C	O2 percent	CO2 percent	NOx ppm	CO ppm	COMB. percent		
24.000	590.300	569.270	12.600	8.222	52.000	80.667	0.000		
22.000	642.080	629.407	10.600	10.167	61.333	88.667	0.000		
20.000	661.390	661.003	11.756	9.033	60.000	72.111	0.000		
18.000	684.977	685.750	12.211	8.589	60.667	93.778	0.000		
16.000	713.753	709.083	12.311	8.522	60.111	99.111	0.000		
LOC cm	LOC in	Tavg C	Tavg F	WALL LOC in	WALL LOC cm	Twavg C	Twavg F	Taavg C	Taavg F
60.960	24.000	579.785	1075.617	0.000	0.000	211.640	412.956	31.493	88.692
55.880	22.000	635.743	1176.342	4.000	10.160	284.309	543.760		
50.800	20.000	661.197	1222.158	8.000	20.320	286.911	548.443		
45.720	18.000	685.363	1265.658	16.000	40.640	247.756	477.965		
40.640	16.000	711.418	1312.557	24.000	60.960	217.076	422.741		
Tcavg C	Tcavg F	O2avg percent	CO2avg percent	NOxavg ppm	COavg ppm	COMBavg percent	PART. g	COMB% in part.	ASH% in part.
654.701	1210.466	11.896	8.907	58.822	86.867	0.000	0.015	24.160	75.860

TEST CODE AND DATE: MMHNC8 6/21/89  
M.C. (WB%)= 35.359  
FUEL FEED (WET, DRY lb/hr)= 6.846 4.425  
E.A. (%)= 125.980  
TOTAL AIR (scfh)= 832.000  
U.F. AIR (%)= 50.000  
O.F. AIR (%)= 50.000

LOC in	T12 C	T11 C	O2 percent	CO2 percent	NOx ppm	CO ppm	COMB. percent		
24.000	584.873	561.560	15.367	5.500	36.000	119.667	0.000		
22.000	599.437	587.583	14.500	6.367	41.333	76.333	0.000		
20.000	627.847	627.077	13.822	7.033	44.000	98.333	0.000		
18.000	643.643	645.573	14.444	6.411	43.000	64.778	0.000		
16.000	663.713	662.550	14.067	6.800	46.667	76.889	0.000		
LOC cm	LOC in	Tavg C	Tavg F	WALL LOC in	WALL LOC cm	Twavg C	Twavg F	Taavg C	Taavg F
60.960	24.000	573.217	1063.794	0.000	0.000	205.644	402.163	31.118	88.016
55.880	22.000	593.510	1100.322	4.000	10.160	282.375	540.278		
50.800	20.000	627.462	1161.435	8.000	20.320	287.012	548.626		
45.720	18.000	644.608	1192.299	16.000	40.640	249.143	480.462		
40.640	16.000	663.132	1225.641	24.000	60.960	218.070	424.530		
Tcavg C	Tcavg F	O2avg percent	CO2avg percent	NOxavg ppm	COavg ppm	COMBavg percent	PART. g	COMB% in part.	ASH% in part.
620.386	1148.698	14.440	6.422	42.200	87.200	0.000	0.016	0.000	100.000

TEST CODE AND DATE: MWHMC9 6/21/89  
M.C. (WB%)= 53.920  
FUEL FEED (WET, DRY lb/hr) 9.309 4.290  
E.A. (%)= 133.130  
TOTAL AIR (scfh)= 832.000  
U.P. AIR (%)= 50.000  
O.P. AIR (%)= 50.000

LOC in	T12 C	T11 C	O2 percent	CO2 percent	NOx ppm	CO ppm	COMB. percent
24.0	599.0	576.9	13.3	7.5	47.7	83.9	0.0
22.0	612.8	604.0	13.0	7.8	51.0	81.6	0.0
20.0	618.2	618.6	14.0	6.9	47.3	90.0	0.0
18.0	616.7	619.4	14.7	6.2	48.0	143.4	0.0
16.0	645.5	646.3	13.8	7.0	52.0	201.3	0.0
14.0	677.2	672.5	13.2	7.6	67.0	108.0	0.0
12.0	671.4	662.9	15.4	5.5	50.0	140.9	0.0
10.0	699.7	687.3	14.7	6.2	43.0	192.9	0.0
9.0	693.9	683.4	15.9	5.0	36.3	176.7	0.0
8.0	741.1	727.4	13.8	7.0	48.3	96.2	0.0
7.0	737.2	720.8	15.6	5.3	37.3	91.9	0.0
6.0	807.8	795.9	15.3	5.6	40.0	85.7	0.0
5.0	848.6	851.5	13.8	7.0	50.3	82.3	0.0
4.0	848.6	851.5	12.4	8.5	55.9	70.1	0.0
3.5	903.4	827.8	11.9	8.9	61.8	68.2	0.0
3.0	905.0	849.9	11.2	9.6	66.0	65.1	0.0
2.5	817.5	824.7	13.1	7.7	56.6	66.4	0.0
2.0	797.2	898.5	12.3	8.5	56.2	345.6	0.0
1.5	847.3	899.5	8.8	11.9	20.1	3168.8	0.6
1.0	737.6	854.8	15.9	5.0	33.7	334.9	0.0

LOC cm	LOC in	Tavg C	Tavg F	WALL LOC in	WALL LOC cm	Tavg C	Tavg F	Tavg C	Tavg F
61.0	24.0	588.0	1090.3	0.0	0.0	191.6	376.9	30.8	87.4
55.9	22.0	608.4	1127.2	4.0	10.2	269.8	517.7		
50.8	20.0	618.4	1145.1	8.0	20.3	277.3	531.2		
45.7	18.0	618.0	1144.4	16.0	40.6	243.6	470.4		
40.6	16.0	645.9	1194.6	24.0	61.0	215.5	419.9		
35.6	14.0	674.8	1246.7						
30.5	12.0	667.1	1232.8						
25.4	10.0	693.5	1280.2						
22.9	9.0	688.7	1271.6						
20.3	8.0	734.2	1353.6						
17.8	7.0	729.0	1344.2						
15.2	6.0	801.8	1475.3						
12.7	5.0	850.0	1562.1						
10.2	4.0	850.0	1562.1						
8.9	3.5	865.6	1590.1						
7.6	3.0	877.4	1611.4						
6.4	2.5	821.1	1510.0						
5.1	2.0	847.9	1558.2						
3.8	1.5	873.4	1604.1						
2.5	1.0	796.2	1465.1						

PART. COMBt ASHt  
g in part.in part.  
-----  
0.022 0.000 100.000  
-----



TEST CODE AND DATE: MWLMC10 6/21/89  
 H.C. (WB%)= 53.920  
 FUEL FEED (WET, DRY lb/hr) 9.309 4.290  
 E.A. (%)= 86.500  
 TOTAL AIR (scfh)= 665.600  
 U.P. AIR (%)= 50.000  
 O.P. AIR (%)= 50.000

LOC in	T12 C	T11 C	O2 percent	CO2 percent	NOx ppm	CO ppm	COMB. percent
24.0	597.9	570.8	11.9	8.9	52.9	132.1	0.0
22.0	627.5	615.2	10.8	9.9	61.9	124.4	0.0
20.0	630.1	630.5	12.2	8.6	55.2	102.9	0.0
18.0	635.5	638.6	13.3	7.6	51.7	102.2	0.0
16.0	643.6	644.3	13.7	7.1	49.7	98.9	0.0
14.0	686.1	680.3	12.0	8.8	58.4	115.1	0.0
12.0	710.9	700.0	12.0	8.8	61.0	82.3	0.0
10.0	741.7	725.3	14.3	6.6	51.3	105.3	0.0
9.0	761.8	747.6	13.7	7.2	49.0	118.1	0.0
8.0	783.5	768.9	14.1	6.8	46.3	91.7	0.0
7.0	787.5	772.8	14.2	6.7	46.3	67.7	0.0
6.0	832.8	818.9	15.4	5.5	38.3	54.0	0.0
5.0	880.0	873.5	14.3	6.6	43.3	50.4	0.0
4.0	880.0	873.5	10.0	10.8	54.3	935.0	0.0
3.5	922.4	949.8	10.8	10.0	50.1	939.6	0.0
3.0	909.4	954.6	10.7	10.0	7.0	2833.1	0.2
2.5	893.9	957.9	11.3	9.5	6.0	3108.3	0.1
2.0	849.0	947.2	12.0	8.8	5.3	3956.0	0.3
1.5	843.8	939.0	12.1	8.7	6.0	4000.0	1.3
1.0	694.1	898.5	13.5	7.4	6.3	4000.0	0.3

LOC cm	LOC in	Tavg C	Tavg F	WALL LOC in	WALL LOC cm	Twavg C	Twavg F	Taavg C	Taavg F
61.0	24.0	584.3	1083.8	0.0	0.0	188.8	371.8	31.6	88.8
55.9	22.0	621.3	1150.4	4.0	10.2	264.0	507.2		
50.8	20.0	630.3	1166.6	8.0	20.3	271.3	520.3		
45.7	18.0	637.1	1178.7	16.0	40.6	238.4	461.1		
40.6	16.0	644.0	1191.1	24.0	61.0	211.0	411.9		
35.6	14.0	683.2	1261.7						
30.5	12.0	705.5	1301.8						
25.4	10.0	733.5	1352.4						
22.9	9.0	754.7	1390.4						
20.3	8.0	776.2	1429.2						
17.8	7.0	780.1	1436.3						
15.2	6.0	825.8	1518.5						
12.7	5.0	876.8	1610.2						
10.2	4.0	876.8	1610.2						
8.9	3.5	936.1	1717.0						
7.6	3.0	932.0	1709.6						
6.4	2.5	925.9	1698.6						
5.1	2.0	898.1	1648.6						
3.8	1.5	891.4	1636.5						
2.5	1.0	796.3	1465.3						

PART. g	COMB% in part.	ASH% in part.
0.017	0.000	100.000

TEST CODE AND DATE: MWMME11 6/21/89  
M.C. (WB%)= 53.920  
FUEL FEED (WET, DRY lb/hr) 9.309 4.290  
E.A. (%)= 109.80  
TOTAL AIR (scfh)= 748.80  
U.F. AIR (%)= 50.000 NOTE: GAS LEAK?  
O.F. AIR (%)= 50.000

LOC in	T12 C	T11 C	O2 percent	CO2 percent	NOx ppm	CO ppm	COMB. percent
24.0	575.8	551.8	18.3	2.6	20.0	382.3	0.0
22.0	606.4	593.4	16.6	4.4	28.3	161.6	0.0
20.0	636.4	636.0	16.2	4.6	29.7	134.6	0.0
18.0	666.1	671.5	15.9	5.0	31.3	104.7	0.0
16.0	669.6	670.3	16.4	4.5	33.0	61.6	0.0
14.0	687.3	682.7	16.7	4.1	32.7	50.7	0.0
12.0	714.9	704.4	16.6	4.3	32.7	59.9	0.0
10.0	714.6	704.1	16.8	4.1	31.0	47.8	0.0
9.0	731.0	718.2	17.4	3.6	26.7	36.9	0.0
8.0	763.6	749.1	16.4	4.5	30.7	28.1	0.0
7.0	783.7	768.0	16.4	4.6	31.3	26.0	0.0
6.0	835.5	822.4	17.1	3.8	27.7	22.4	0.0
5.0	862.1	866.5	17.9	3.1	27.6	47.7	0.0
4.0	862.1	866.5	18.5	2.4	22.3	32.4	0.0
3.5	930.1	858.5	17.7	3.2	24.0	25.6	0.0
3.0	903.1	897.4	17.5	3.4	24.7	29.2	0.0
2.5	914.6	942.2	17.1	3.8	27.4	30.4	0.0
2.0	974.8	967.3	16.8	4.1	27.9	44.4	0.0
1.5	955.8	945.0	13.8	7.0	42.2	66.2	0.0
1.0	963.2	930.3	14.1	6.7	43.7	211.2	0.0

LOC cm	LOC in	Tavg C	Tavg F	WALL in	LOC cm	WALL cm	LOC C	Twavg F	Taavg C	Taavg F
61.0	24.0	563.8	1046.8							
55.9	22.0	599.9	1111.8							
50.8	20.0	636.2	1177.1							
45.7	18.0	668.8	1235.8							
40.6	16.0	670.0	1237.9							
35.6	14.0	685.0	1265.0							
30.5	12.0	709.7	1309.4							
25.4	10.0	709.3	1308.8							
22.9	9.0	724.6	1336.3							
20.3	8.0	756.3	1393.4							
17.8	7.0	775.8	1428.5							
15.2	6.0	828.9	1524.1							
12.7	5.0	864.3	1587.7							
10.2	4.0	864.3	1587.7							
8.9	3.5	894.3	1641.7							
7.6	3.0	900.3	1652.5							
6.4	2.5	928.4	1703.1							
5.1	2.0	971.1	1779.9							
3.8	1.5	950.4	1742.7							
2.5	1.0	946.8	1736.2							

PART. COMB% ASH%  
g in partin part.

0.018 8.430 91.570

TEST CODE AND DATE: MMMH12 6/21/89  
 M.C. (WB)= 35.359  
 FUEL FEED (WET, DRY lb/hr) 7.097 4.588  
 E.A. (%)= 96.180  
 TOTAL AIR= 748.80 NOTE: LEAK IN GAS PROBE  
 U.F. AIR (%)= 50.000  
 O.F. AIR (%)= 50.000

LOC in	T12 C	T11 C	O2 percent	CO2 percent	NOx ppm	CO ppm	COMB. LOST
24.0	618.5	593.6	19.8	1.3	9.3	37.6	ERR
22.0	626.6	612.4	19.1	1.9	9.7	47.1	ERR
20.0	638.9	637.0	16.8	4.2	26.7	90.0	ERR
18.0	666.6	670.1	16.5	4.4	28.3	55.3	ERR
16.0	680.6	681.3	16.7	4.2	27.7	38.3	ERR
14.0	705.4	700.4	17.1	3.8	27.0	30.0	ERR
12.0	721.8	711.3	17.3	3.6	26.3	20.3	ERR
10.0	762.2	747.6	16.7	4.2	28.8	17.2	ERR
9.0	781.5	766.9	16.5	4.4	32.7	15.0	ERR
8.0	787.4	772.4	16.8	4.1	32.3	15.0	ERR
7.0	841.2	821.3	16.1	4.9	35.7	17.7	ERR
6.0	853.4	837.3	16.7	4.2	32.3	19.9	ERR
5.0	903.7	891.8	16.7	4.2	31.7	16.3	ERR
4.0	903.7	891.8	16.0	4.9	34.7	18.6	ERR
3.5	1016.3	944.8	14.0	6.9	47.0	22.0	ERR
3.0	1042.8	998.8	14.2	6.7	47.0	149.6	ERR
2.5	1096.1	1062.2	15.2	5.7	8.0	109.2	ERR
2.0	1064.6	1096.6	15.9	5.0	27.1	84.6	ERR
1.5	1077.7	1069.4	15.7	5.2	20.7	47.4	ERR
1.0	987.1	1020.4	16.1	4.8	6.0	30.7	ERR

LOC cm	LOC in	Tavg C	Tavg F	WALL in	LOC cm	WALL cm	LOC C	Twavg C	Twavg F	Taavg C	Taavg F
61.0	24.0	606.1	1123.0			0.0	0.0	215.1	419.1	207.5	405.5
55.9	22.0	619.5	1147.1			4.0		10.2	270.5		518.9
50.8	20.0	637.9	1180.3			8.0		20.3	275.4		527.8
45.7	18.0	668.4	1235.1			16.0		40.6	240.8		465.4
40.6	16.0	681.0	1257.7			24.0		61.0	215.1		419.2
35.6	14.0	702.9	1297.2								
30.5	12.0	716.5	1321.8								
25.4	10.0	754.9	1390.9								
22.9	9.0	774.2	1425.6								
20.3	8.0	779.9	1435.9								
17.8	7.0	831.3	1528.3								
15.2	6.0	845.3	1553.6								
12.7	5.0	897.7	1647.9								
10.2	4.0	897.7	1647.9								
8.9	3.5	980.6	1797.0								
7.6	3.0	1020.8	1869.5								
6.4	2.5	1079.1	1974.5								
5.1	2.0	1080.6	1977.1								
3.8	1.5	1073.6	1964.4								
2.5	1.0	1003.7	1838.7								

PART. COMB% ASH%  
 q in part in part.

0.015 0.000 100.00

TEST CODE AND DATE:					MDMMH13 6/21/89				
M.C. (WB%)=					11.200				
FUEL FEED (WET, DRY lb/hr)=					5.621		4.990		
E.A. (%)=					80.360				
TOTAL AIR (scfh)=					748.800				
U.F. AIR (%)=					50.000				
O.F. AIR (%)=					50.000				
LOC in	T12 C	T11 C	O2 percent	CO2 percent	NOx ppm	CO ppm	COMB. percent		
24.000	629.400	603.323	13.211	7.678	52.667	171.778	0.000		
22.000	666.370	652.870	13.389	7.478	52.667	132.222	0.000		
20.000	691.950	690.390	12.111	8.667	61.667	91.778	0.000		
18.000	703.590	705.140	14.322	6.544	47.667	65.111	0.000		
16.000	739.900	738.723	13.122	7.711	57.111	55.333	0.000		
LOC cm	LOC in	Tavg C	Tavg F	WALL LOC in	WALL LOC cm	Twavg C	Twavg F	Taavg C	Taavg F
60.960	24.000	616.362	1141.455	0.000	0.000	223.575	434.440	208.643	407.562
55.880	22.000	659.620	1219.320	4.000	10.160	278.335	533.008		
50.800	20.000	691.170	1276.110	8.000	20.320	282.037	539.671		
45.720	18.000	704.365	1299.861	16.000	40.640	244.639	472.355		
40.640	16.000	739.312	1362.765	24.000	60.960	217.821	424.082		
Tcavg C	Tcavg F	O2avg percent	CO2avg percent	NOxavg ppm	COavg ppm	COMBavg percent	PART. g	COMB% in part.	ASH% in part.
682.166	1259.902	13.231	7.616	54.356	103.244	0.000	0.021	0.000	100.000

TEST CODE AND DATE: LDMC4 6/21/89  
M.C. (WB%)= 11.200  
FUEL FEED (WET, DRY lb/hr)= 5.200 4.618  
E.A. (%)= 94.890  
TOTAL AIR (scfh)= 748.800  
U.F. AIR (%)= 50.000  
O.F. AIR (%)= 50.000  
AIR TEMP.= COLD

LOC in	T12 C	T11 C	O2 percent	CO2 percent	NOx ppm	CO ppm	COHB. percent
24.000	560.180	540.330	13.744	7.133	45.000	103.889	0.000
22.000	622.577	611.447	10.356	10.400	57.667	92.556	0.000
20.000	653.317	652.553	11.489	9.289	56.222	92.889	0.000
18.000	685.033	685.033	11.478	9.344	56.000	77.222	0.000
16.000	707.947	701.347	11.689	9.100	53.667	67.556	0.000
14.000	725.910	711.883	11.811	8.967	53.333	60.333	0.000
12.000	725.953	706.470	13.578	7.267	46.667	56.333	0.000
10.000	728.753	709.630	13.411	7.411	48.667	47.667	0.000
9.000	779.353	751.020	11.278	9.533	60.556	131.333	0.000
8.000	813.953	784.967	11.689	9.111	59.444	45.778	0.000
7.000	829.930	800.827	13.078	7.744	55.222	44.000	0.000
6.000	858.880	829.580	14.011	6.800	46.667	44.000	0.000
5.000	913.720	888.850	11.778	9.056	58.222	48.222	0.000
4.000	913.720	888.850	8.622	12.122	73.000	54.556	0.000
3.500	1059.730	959.530	5.700	14.922	77.889	204.333	0.000
3.000	1047.000	963.240	6.167	14.500	90.444	157.000	0.000
2.500	1053.013	977.083	8.544	12.133	68.000	113.556	0.000
2.000	1031.017	958.723	7.522	13.211	81.889	119.222	0.000
1.500	1062.413	1011.273	7.789	12.922	27.667	946.111	0.103
1.000	1015.157	983.377	15.933	4.867	28.222	188.000	0.000

LOC cm	LOC in	Tavg C	Tavg F	WALL in	LOC cm	WALL in	LOC cm	Tavg C	Tavg F	Taavg C	Taavg F
60.960	24.000	550.255	1022.463	0.000	0.000	201.639	394.955	29.515	85.130		
55.880	22.000	617.012	1142.625	4.000	10.160	273.067	523.524				
50.800	20.000	652.935	1207.287	8.000	20.320	274.535	526.166				
45.720	18.000	685.033	1265.064	16.000	40.640	234.477	454.063				
40.640	16.000	704.647	1300.368	24.000	60.960	206.947	404.509				
35.560	14.000	718.897	1326.018								
30.480	12.000	716.212	1321.185								
25.400	10.000	719.192	1326.549								
22.860	9.000	765.187	1409.340								
20.320	8.000	799.460	1471.032								
17.780	7.000	815.378	1499.685								
15.240	6.000	844.230	1551.618								
12.700	5.000	901.285	1654.317								
10.160	4.000	901.285	1654.317								
8.890	3.500	1009.630	1849.338								
7.620	3.000	1005.120	1841.220								
6.350	2.500	1015.048	1859.091								
5.080	2.000	994.870	1822.770								
3.810	1.500	1036.843	1898.322								
2.540	1.000	999.267	1830.684								

TEST CODE AND DATE: LDHMC5 6/21/89  
 M.C. (WB%)= 11.200  
 FUEL FEED (WET, DRY lb/hr)= 5.200 4.618  
 E.A. (%)= 116.540  
 TOTAL AIR (scfh)= 832.000  
 U.F. AIR (%)= 50.000  
 O.F. AIR (%)= 50.000

LOC in	T12 C	T11 C	O2 percent	CO2 percent	NOx ppm	CO ppm	COMB. percent		
24.000	609.160	589.250	14.456	6.411	34.333	97.556	0.000		
22.000	620.297	604.600	16.163	4.750	26.250	502.333	0.000		
20.000	622.633	617.267	16.522	4.389	27.889	113.333	0.000		
18.000	672.333	671.173	14.644	6.289	36.667	81.111	0.000		
16.000	706.070	700.250	14.322	6.533	39.000	64.556	0.000		
LOC cm	LOC in	Tavg C	Tavg F	WALL LOC in	WALL LOC cm	Twavg C	Twavg F	Taavg C	Taavg F
60.960	24.000	599.205	1110.573	0.000	0.000	206.143	403.061	29.530	32.004
55.880	22.000	612.448	1134.411	4.000	10.160	277.790	532.026		
50.800	20.000	619.950	1147.914	8.000	20.320	278.505	533.312		
45.720	18.000	671.753	1241.160	16.000	40.640	238.343	461.022		
40.640	16.000	703.160	1297.692	24.000	60.960	210.611	411.104		
Tcavg C	Tcavg F	O2avg percent	CO2avg percent	NOxavg ppm	COavg ppm	COMBavg percent	PART. g	COMB% in part.	ASH% in part.
641.303	1186.350	15.221	5.674	32.828	171.778	0.000	0.030	0.000	100.000

TEST CODE AND DATE:					LDLMC6 6/21/89				
M.C. (WB%)=					11.200				
FUEL FEED (WET, DRY lb/hr)=					5.200		4.618		
E.A. (%)=					73.290				
TOTAL AIR (scfh)=					665.600				
U.F. AIR (%)=					50.000				
O.F. AIR (%)=					50.000				
LOC in	T12 C	T11 C	O2 percent	CO2 percent	NOx ppm	CO ppm	COMB. percent		
24.000	640.173	614.063	11.511	9.300	54.778	70.556	0.000		
22.000	659.083	642.523	12.589	8.233	51.667	65.556	0.000		
20.000	697.763	692.730	11.956	8.856	56.333	64.222	0.000		
18.000	727.737	724.227	12.078	8.733	55.778	55.333	0.000		
16.000	762.680	752.850	11.667	9.144	54.778	50.000	0.000		
LOC cm	LOC in	Tavg C	Tavg F	WALL LOC in	WALL LOC cm	Twavg C	Twavg F	Taavg C	Taavg F
60.960	24.000	627.118	1160.817	0.000	0.000	210.122	410.224	30.880	87.588
55.880	22.000	650.803	1203.450	4.000	10.160	278.894	534.013		
50.800	20.000	695.247	1283.448	8.000	20.320	280.955	537.722		
45.720	18.000	725.982	1338.771	16.000	40.640	241.451	466.615		
40.640	16.000	757.765	1395.981	24.000	60.960	213.615	416.512		
Tcavg C	Tcavg F	O2avg percent	CO2avg percent	NOxavg ppm	COavg ppm	COMBavg percent	PART. g	COMB% in part.	ASH% in part.
691.383	1276.493	11.960	8.853	54.667	61.133	0.000	0.020	11.060	88.940

TEST CODE AND DATE: DFSW1 6/7/89  
 M.C. (WB%)= 52.660  
 FUEL FEED (WET, DRY lb/hr)= 4.780 2.514  
 E.A. (%)= 75.160  
 TOTAL AIR (scfh)= 366.400  
 U.F.AIR (%)= 35.000  
 O.F. AIR (%)= 65.000  
 AIR TEMP.= COLD

LOC	T12	T11	O2	CO2	NOX	CO	COMB.
IN	C	C	percent	percent	ppm	ppm	percent
24.000	428.553	475.323	14.467	6.389	25.000	320.889	0.000
22.000	446.617	484.903	15.244	5.611	25.778	93.556	0.000
20.000	470.363	500.567	15.078	5.800	25.667	521.222	0.000
18.000	484.157	510.133	15.533	5.356	28.333	559.778	0.000
16.000	481.890	497.173	17.033	3.878	22.667	2466.667	0.032
14.000	533.497	552.583	12.744	8.089	42.333	616.667	0.000
12.000	535.037	544.973	16.056	4.544	29.444	1935.778	0.036
10.000	557.957	568.277	14.178	4.422	38.000	333.778	0.000
9.000	557.613	566.780	15.067	3.844	28.111	2177.000	0.020
8.000	605.050	621.153	12.878	5.233	42.333	186.000	0.000
7.000	593.243	584.420	15.778	3.400	25.556	3072.111	0.044
6.000	673.313	667.027	13.644	4.733	40.000	178.667	0.000
5.000	694.920	719.793	13.944	4.578	36.778	1140.556	0.003
4.000	645.450	665.870	14.433	4.244	38.667	1156.667	0.007
3.500	576.187	590.313	14.289	4.344	33.667	1796.222	0.099
3.000	779.450	786.567	8.856	7.856	43.111	3650.333	0.201
2.500	772.830	789.803	8.811	7.878	57.556	3283.889	0.052
2.000	806.430	802.950	9.511	7.389	24.556	3951.556	0.409
1.500	752.747	729.283	14.244	4.378	37.333	1886.444	0.007
1.000	757.123	758.633	12.978	5.167	35.333	3926.556	0.186

LOC	LOC	Tavg	Tavg	WALL	LOC	WALL	LOC	Twavg	Twavg	Taavg	Taavg
CM	in	C	F	in	CM	in	CM	C	F	C	F
60.960	24.000	451.938	845.493	0.000	0.000	197.341	387.218	34.786	94.618		
55.880	22.000	465.760	870.372	4.000	10.160	262.396	504.317				
50.800	20.000	485.465	905.841	8.000	20.320	265.283	509.513				
45.720	18.000	497.145	926.865	16.000	40.640	224.789	436.624				
40.640	16.000	489.532	913.161	24.000	60.960	179.479	355.067				
35.560	14.000	543.040	1009.476								
30.480	12.000	540.005	1004.013								
25.400	10.000	563.117	1045.614								
22.860	9.000	562.197	1043.958								
20.320	8.000	613.102	1135.587								
17.780	7.000	588.832	1091.901								
15.240	6.000	670.170	1238.310								
12.700	5.000	707.357	1305.246								
10.160	4.000	655.660	1212.192								
8.890	3.500	583.250	1081.854								
7.620	3.000	783.008	1441.419								
6.350	2.500	781.317	1438.374								
5.080	2.000	804.690	1480.446								
3.810	1.500	741.015	1365.831								
2.540	1.000	757.878	1396.185								



TEST CODE AND DATE: DPSW2 6/7/89  
M.C. (WB%)= 52.660  
FUEL FEED (WET, DRY lb/hr)= 4.780 2.514  
E.A. (%)= 107.980  
TOTAL AIR (scfh)= 435.100  
U.F.AIR (%)= 35.000  
O.F. AIR (%)= 65.000  
AIR TEMP.= COLD

LOC IN	T12 C	T11 C	LONG		NOX ppm	CO ppm	COMB. percent
			O2 percent	CO2 percent			
24.000	426.733	440.183	15.467	3.567	29.667	702.889	0.000
22.000	420.607	434.060	16.522	2.911	20.889	3343.333	0.074
20.000	481.597	517.890	11.933	5.856	49.667	434.778	0.000
18.000	467.097	493.490	15.978	3.256	29.444	1017.111	0.000
16.000	482.080	500.430	14.844	3.978	28.556	2973.000	0.107
14.000	505.040	520.713	15.011	3.889	30.444	2111.222	0.051
12.000	527.627	539.853	14.844	3.967	33.333	1160.333	0.034
10.000	555.167	566.243	13.889	4.567	37.333	621.556	0.000
9.000	553.683	563.620	15.700	3.422	28.778	1587.556	0.003
8.000	572.830	580.090	15.200	3.744	33.444	579.333	0.003
7.000	546.943	548.083	17.167	2.489	23.333	1851.333	0.054
6.000	535.127	548.113	17.189	2.456	21.889	1654.111	0.030
5.000	646.970	692.573	15.700	3.456	28.444	879.222	0.000
4.000	624.843	658.263	15.378	3.656	28.333	3014.667	0.089
3.500	695.053	678.623	14.133	4.444	33.333	3341.667	0.122
3.000	697.460	691.277	12.633	5.378	45.667	3028.444	0.051
2.500	741.117	720.383	11.533	6.089	49.667	3598.111	0.111
2.000	693.727	678.583	18.244	1.811	16.667	1078.556	0.000
1.500	767.563	777.013	17.178	2.444	20.000	2090.556	0.046
1.000	745.630	784.973	17.489	2.278	18.333	1125.222	0.032

LOC cm	LOC in	Tavg C	Tavg F	WALL in	LOC cm	WALL cm	LOC C	Tavg F	Taavg C	Taavg F
60.960	24.000	433.458	812.229	0.000	0.000	174.632	346.341	32.211	89.984	
55.880	22.000	427.333	801.204	4.000	10.160	239.908	463.838			
50.800	20.000	499.743	931.542	8.000	20.320	243.529	470.357			
45.720	18.000	480.293	896.532	16.000	40.640	210.443	410.801			
40.640	16.000	491.255	916.263	24.000	60.960	170.008	338.019			
35.560	14.000	512.877	955.182							
30.480	12.000	533.740	992.736							
25.400	10.000	560.705	1041.273							
22.860	9.000	558.652	1037.577							
20.320	8.000	576.460	1069.632							
17.780	7.000	547.513	1017.528							
15.240	6.000	541.620	1006.920							
12.700	5.000	669.772	1237.593							
10.160	4.000	641.553	1186.800							
8.890	3.500	686.838	1268.313							
7.620	3.000	694.368	1281.867							
6.350	2.500	730.750	1347.354							
5.080	2.000	686.155	1267.083							
3.810	1.500	772.288	1422.123							
2.540	1.000	765.302	1409.547							

TEST CODE AND DATE: DFSD3 6/7/89  
M.C. (WB%)= 11.200  
FUEL FEED (WET, DRY lb/hr)= 2.909 2.583  
E.A. (%)= 70.460  
TOTAL AIR (scfh)= 366.400  
U.P. AIR (%)= 35.000  
O.F. AIR (%)= 65.000  
AIR TEMP.= COLD

LOC IN	T12 C	T11 C	LONG O2 percent	CO2 percent	NOX ppm	CO ppm	COMB. percent
24.000	484.257	528.957	12.800	5.311	40.333	123.111	0.000
22.000	519.047	553.023	12.778	5.333	43.000	117.222	0.000
20.000	550.727	574.783	13.083	5.100	40.667	111.667	0.000
18.000	556.823	578.210	14.511	6.322	35.000	108.778	0.000
16.000	572.507	587.033	15.022	5.878	32.333	133.000	0.000
14.000	593.527	606.547	15.600	5.322	30.778	134.333	0.000
12.000	629.940	636.850	14.244	6.644	36.667	158.333	0.000
10.000	664.577	669.207	14.078	6.811	37.444	129.444	0.000
9.000	679.277	686.657	15.556	5.311	33.000	105.444	0.000
8.000	699.817	707.220	14.089	6.733	40.889	297.000	0.000
7.000	756.883	748.223	14.000	6.822	38.333	78.333	0.000
6.000	807.953	786.040	13.156	7.644	42.444	741.222	0.009
5.000	778.890	793.130	15.756	5.178	30.444	70.778	0.000
4.000	942.557	878.013	13.733	7.111	39.000	84.333	0.000
3.500	824.007	799.500	15.500	5.356	7.667	3056.222	0.227
3.000	878.537	839.440	15.933	4.956	24.333	1465.444	0.047
2.500	923.870	877.837	16.867	4.056	22.667	1100.222	0.019
2.000	936.107	899.343	16.922	3.978	23.667	163.556	0.000
1.500	948.513	914.847	16.600	4.322	21.333	337.778	0.003
1.000	906.733	898.107	16.889	4.022	17.333	490.556	0.003

LOC cn	LOC in	Tavg C	Tavg F	WALL in	LOC cn	WALL LOC cn	Twavg C	Twavg F	Taavg C	Taavg F
60.960	24.000	506.607	943.896	0.000	0.000	193.379	380.086	33.298	91.940	
55.880	22.000	536.035	996.867	4.000	10.160	251.984	485.575			
50.800	20.000	562.755	1044.963	8.000	20.320	250.309	482.560			
45.720	18.000	567.517	1053.534	16.000	40.640	210.454	410.822			
40.640	16.000	579.770	1075.590	24.000	60.960	169.065	336.321			
35.560	14.000	600.037	1112.070							
30.480	12.000	633.395	1172.115							
25.400	10.000	666.892	1232.409							
22.860	9.000	682.967	1261.344							
20.320	8.000	703.518	1298.337							
17.780	7.000	752.553	1386.600							
15.240	6.000	796.997	1466.598							
12.700	5.000	786.010	1446.822							
10.160	4.000	910.285	1670.517							
8.890	3.500	811.753	1493.160							
7.620	3.000	858.988	1578.183							
6.350	2.500	900.853	1653.540							
5.080	2.000	917.725	1683.909							
3.810	1.500	931.680	1709.028							
2.540	1.000	902.420	1656.360							

TEST CODE AND DATE: DFSD4 6/7/89  
 M.C. (WB%)= 11.200  
 FUEL FEED (WET, DRY lb/hr)= 2.909 2.485  
 E.A. (%)= 102.000  
 TOTAL AIR (scfh)= 435.100  
 U.F. AIR (%)= 35.000  
 O.F. AIR (%)= 65.000  
 AIR TEMP.= COLD

LOC IN	T12 C	T11 C	O2 percent	CO2 percent	NOX ppm	CO ppm	COMB. percent		
24.000	489.917	510.553	18.089	2.867	17.000	74.000	0.000		
22.000	512.103	537.320	18.256	2.711	15.667	65.222	0.000		
20.000	548.797	577.820	18.389	2.589	15.667	114.889	0.000		
18.000	571.747	596.610	18.189	2.778	16.000	87.667	0.000		
16.000	614.653	633.077	18.333	2.611	18.333	75.111	0.000		
14.000	629.993	639.217	17.800	3.122	21.333	896.556	0.003		
12.000	650.807	655.053	17.578	3.356	21.000	72.444	0.000		
10.000	696.840	700.330	18.111	2.800	18.000	67.556	0.000		
9.000	722.927	729.553	17.344	3.567	22.000	60.667	0.000		
8.000	724.480	724.873	17.967	2.978	18.667	47.778	0.000		
7.000	801.700	790.177	17.300	3.522	22.000	518.444	0.007		
6.000	862.600	838.033	17.700	3.233	21.000	134.333	0.000		
5.000	880.397	882.797	17.533	3.389	21.000	52.667	0.000		
4.000	933.330	913.307	16.389	4.533	24.333	1662.333	0.076		
3.500	964.080	919.137	16.933	4.000	21.111	977.444	0.026		
3.000	906.823	875.917	17.244	3.644	23.000	1048.222	0.038		
2.500	935.877	884.793	17.378	3.522	21.889	498.667	0.011		
2.000	940.950	887.817	16.622	4.267	13.000	2180.111	0.071		
1.500	939.410	896.757	17.267	3.656	22.333	167.333	0.000		
1.000	944.303	890.697	18.078	2.867	19.000	87.778	0.000		
LOC CN	LOC in	Tavg C	Tavg F	WALL LOC in	WALL LOC CN	Tavg C	Tavg F	Taavg C	Taavg F
60.960	24.000	500.235	932.427	0.000	0.000	205.378	401.685	34.330	93.798
55.880	22.000	524.712	976.485	4.000	10.160	265.456	509.825		
50.800	20.000	563.308	1045.959	8.000	20.320	262.472	504.454		
45.720	18.000	584.178	1083.525	16.000	40.640	220.689	429.244		
40.640	16.000	623.865	1154.961	24.000	60.960	174.574	346.238		
35.560	14.000	634.605	1174.293						
30.480	12.000	652.930	1207.278						
25.400	10.000	698.585	1289.457						
22.860	9.000	726.240	1339.236						
20.320	8.000	724.677	1336.422						
17.780	7.000	795.938	1464.693						
15.240	6.000	850.317	1562.574						
12.700	5.000	881.597	1618.878						
10.160	4.000	923.318	1693.977						
8.890	3.500	941.608	1726.899						
7.620	3.000	891.370	1636.470						
6.350	2.500	910.335	1670.607						
5.080	2.000	914.383	1677.894						
3.810	1.500	918.083	1684.554						
2.540	1.000	917.500	1683.504						

TEST CODE AND DATE: DFSW5 6/7/89  
 M.C. (WB%)= 52.660  
 FUEL FEED (WET, DRY lb/hr)= 5.249 2.485  
 E.A. (%)= 110.450  
 TOTAL AIR (scfh)= 435.100  
 U.F.AIR (%)= 35.000  
 O.F. AIR (%)= 65.000  
 AIR TEMP.= MED.

LONG							
LOC IN	T12 C	T11 C	O2 percent	CO2 percent	NOX ppm	CO ppm	COMB. percent
24.000	479.690	454.413	17.011	3.900	20.333	114.778	0.000
22.000	482.790	457.897	18.644	2.333	14.667	2008.000	0.063
20.000	522.200	511.887	16.244	4.644	27.444	1177.889	0.017
18.000	527.203	519.950	17.567	3.344	20.000	1824.111	0.054
16.000	561.230	553.977	15.822	5.022	29.667	293.778	0.000
14.000	563.560	551.727	17.533	3.378	19.333	1231.889	0.004
12.000	594.573	584.263	16.289	4.611	25.667	236.889	0.000
10.000	638.670	624.843	15.589	5.267	29.000	163.444	0.000
9.000	635.663	621.070	16.989	3.911	24.667	187.444	0.000
8.000	605.430	590.883	17.711	3.200	21.333	456.111	0.000
7.000	679.810	618.533	17.000	3.900	21.444	2941.889	0.084
6.000	779.417	697.200	15.956	4.944	28.444	640.333	0.000
5.000	701.633	691.057	16.300	4.589	27.444	122.667	0.000
4.000	780.697	735.083	14.044	6.800	34.444	3133.778	0.102
3.500	844.317	778.067	14.200	6.644	35.667	1718.556	0.030
3.000	844.620	781.593	13.778	7.044	32.556	1473.556	0.029
2.500	844.930	803.790	15.278	5.622	31.667	275.778	0.007
2.000	830.160	773.737	14.822	6.056	36.000	698.667	0.013
1.500	767.887	787.323	15.167	5.711	33.333	2037.556	0.020
1.000	793.657	746.663	14.589	6.311	9.333	4000.000	0.833

LOC cm	LOC in	Tavg C	Tavg F	WALL in	LOC cm	Twavg C	Twavg F	Taavg C	Taavg F
60.960	24.000	467.052	872.697	0.000	0.000	198.158	388.689	96.546	205.787
55.880	22.000	470.343	878.622	4.000	10.160	268.209	514.780		
50.800	20.000	517.043	962.682	8.000	20.320	265.947	510.709		
45.720	18.000	523.577	974.442	16.000	40.640	226.607	439.897		
40.640	16.000	557.603	1035.690	24.000	60.960	176.467	349.644		
35.560	14.000	557.643	1035.762						
30.480	12.000	589.418	1092.957						
25.400	10.000	631.757	1169.166						
22.860	9.000	628.367	1163.064						
20.320	8.000	598.157	1108.686						
17.780	7.000	649.172	1200.513						
15.240	6.000	738.308	1360.959						
12.700	5.000	696.345	1285.425						
10.160	4.000	757.890	1396.206						
8.890	3.500	811.192	1492.149						
7.620	3.000	813.107	1495.596						
6.350	2.500	824.360	1515.852						
5.080	2.000	801.948	1475.511						
3.810	1.500	777.605	1431.693						
2.540	1.000	770.160	1418.292						

TEST CODE AND DATE: DFSW6 6/7/89  
M.C. (WB%)= 52.660  
FUEL FEED (WET, DRY lb/hr)= 5.249 2.485  
E.A. (%)= 110.450  
TOTAL AIR (scfh)= 435.100  
U.F.AIR (%)= 35.000  
O.F. AIR (%)= 65.000  
AIR TEMP.= HOT

LONG							
LOC IN	T12 C	T11 C	O2 percent	CO2 percent	NOX ppm	CO ppm	COMB. percent
24.000	466.187	448.560	13.733	7.122	30.000	191.444	0.000
22.000	464.663	454.327	15.378	5.467	25.556	190.444	0.000
20.000	479.647	478.110	14.767	6.100	32.333	1123.222	0.007
18.000	535.433	540.393	12.078	8.744	42.222	703.889	0.000
16.000	518.643	512.913	16.500	4.378	31.444	499.556	0.000
14.000	460.577	443.697	19.333	1.611	12.667	2869.556	0.036
12.000	513.737	499.973	14.900	5.989	31.111	2422.556	0.046
10.000	595.137	582.527	12.622	8.200	47.889	366.556	0.000
9.000	570.340	558.507	15.833	5.033	32.333	602.444	0.003
8.000	602.120	572.650	14.144	6.733	33.667	2597.111	0.110
7.000	696.107	647.797	11.944	8.844	51.000	274.444	0.000
6.000	762.280	683.337	13.589	7.244	40.333	410.333	0.000
5.000	757.483	737.427	12.211	8.633	47.333	228.778	0.000
4.000	825.780	762.547	8.911	11.844	61.556	1918.000	0.106
3.500	644.020	628.977	15.422	5.444	35.667	1809.889	0.033
3.000	773.563	730.067	11.922	8.878	50.000	587.222	0.003
2.500	842.827	811.297	10.433	10.344	51.222	3289.889	0.278
2.000	834.803	799.723	13.222	7.622	46.000	581.778	0.009
1.500	835.173	790.933	14.100	6.767	37.667	1398.000	0.070
1.000	814.373	786.190	14.444	6.400	31.667	2350.889	0.269

LOC cn	LOC in	Tavg C	Tavg F	WALL LOC in	WALL LOC cn	Twavg C	Twavg F	Taavg C	Taavg F
60.960	24.000	457.373	855.276	0.000	0.000	180.055	356.103	207.494	405.494
55.880	22.000	459.495	859.095	4.000	10.160	248.999	480.203		
50.800	20.000	478.878	893.985	8.000	20.320	249.041	480.278		
45.720	18.000	537.913	1000.248	16.000	40.640	215.926	420.671		
40.640	16.000	515.778	960.405	24.000	60.960	170.270	338.490		
35.560	14.000	452.137	845.850						
30.480	12.000	506.855	944.343						
25.400	10.000	588.832	1091.901						
22.860	9.000	564.423	1047.966						
20.320	8.000	587.385	1089.297						
17.780	7.000	671.952	1241.517						
15.240	6.000	722.808	1333.059						
12.700	5.000	747.455	1377.423						
10.160	4.000	794.163	1461.498						
8.890	3.500	636.498	1177.701						
7.620	3.000	751.815	1385.271						
6.350	2.500	827.062	1520.715						
5.080	2.000	817.263	1503.078						
3.810	1.500	813.053	1495.500						
2.540	1.000	800.282	1472.511						

TEST CODE AND DATE: PHC3 6/1/89  
 FUEL M.C. (PERCENT W.B.): 8.400  
 FUEL FEED RATE: 4.669 4.277  
 TOTAL AIR (SCFH)= 593.950  
 EXCESS AIR PERCENT= 68.350  
 PERCENT U.F. AIR= 35.000  
 PERCENT O.F. AIR= 65.000

LOC IN	T12 C	T11 C	O2 percent	CO2 percent	NOx ppm	CO ppm	COMB. percent
24.000	630.746	678.840	8.080	12.647	101.000	0.000	0.000
22.000	713.322	763.596	4.767	15.873	149.800	0.000	0.000
20.000	767.590	810.854	4.747	15.880	145.133	8.533	0.041
18.000	761.708	787.264	8.513	12.220	103.267	0.000	0.000
16.000	756.990	775.886	10.167	10.607	94.000	0.000	0.000
14.000	779.956	799.208	9.560	11.187	104.400	0.000	0.000
12.000	817.862	839.468	7.847	12.873	121.667	0.000	0.000
10.000	914.830	930.092	3.673	16.927	168.200	0.000	0.000
9.000	857.600	859.538	10.527	10.253	89.267	0.000	0.000
8.000	914.692	892.160	7.360	13.353	128.200	0.000	0.000
7.000	982.518	935.312	6.760	13.933	130.133	0.000	0.000
6.000	1097.668	1043.668	1.027	19.493	127.533	1250.867	0.043
5.000	1156.644	1095.414	0.287	20.220	113.667	603.200	0.028
4.000	1162.084	1122.564	0.000	20.533	23.933	4000.000	6.347
3.500	1100.338	1094.138	0.000	20.587	19.600	4000.000	7.290
3.000	1070.810	1076.440	0.000	20.573	14.200	4000.000	7.290
2.500	1059.838	1060.614	0.000	20.533	10.000	4000.000	5.857
2.000	1036.996	1048.432	0.000	20.507	9.000	4000.000	5.317
1.500	1024.146	1029.704	0.000	20.513	8.800	4000.000	2.803
1.000	984.046	959.396	0.673	19.867	41.133	4000.000	2.853
0.500	993.028	1016.938	6.120	14.500	11.800	4000.000	0.913

LOC IN	LOC CM	Tavg C	Tavg F	WALL LOC IN	WALL LOC CM	Twavg C	Twavg F	Taavg F/C
24.000	60.960	654.793	1210.631	0.000	0.000	208.250	406.854	C
22.000	55.880	738.459	1361.230	4.000	10.160	297.847	568.129	32.983
20.000	50.800	789.222	1452.604	8.000	20.320	303.270	577.889	F
18.000	45.720	774.486	1426.079	16.000	40.640	262.851	505.135	91.373
16.000	40.640	766.438	1411.592	24.000	60.960	225.712	438.285	
14.000	35.560	789.582	1453.252					
12.000	30.480	828.665	1523.601					
10.000	25.400	922.461	1692.434					
9.000	22.860	858.569	1577.428					
8.000	20.320	903.426	1658.171					
7.000	17.780	958.915	1758.051					
6.000	15.240	1070.668	1959.206					
5.000	12.700	1126.029	2058.856					
4.000	10.160	1142.324	2088.187					
3.500	8.890	1097.238	2007.032					
3.000	7.620	1073.625	1964.529					
2.500	6.350	1060.226	1940.411					
2.000	5.080	1042.714	1908.889					
1.500	3.810	1026.925	1880.469					
1.000	2.540	971.721	1781.102					
0.500	1.270	1004.983	1840.973					

TEST CODE AND DATE: KMP2 6/1/89  
 FUEL M.C. (PERCENT W.B.): 6.600  
 FUEL FEED RATE: 4.442 4.149  
 TOTAL AIR (SCFH)= 576.480  
 EXCESS AIR PERCENT= 73.500  
 PERCENT U.F. AIR= 35.000  
 PERCENT O.F. AIR= 65.000

LOC IN	T12 C	T11 C	O2 percent	CO2 percent	NOx ppm	CO ppm	COMB. percent
24.000	625.306	685.212	9.060	11.680	202.600	0.000	0.000
22.000	657.410	715.750	8.787	11.933	203.933	0.000	0.000
20.000	675.248	726.746	9.740	11.007	187.333	0.000	0.000
18.000	692.930	737.338	10.340	10.387	184.533	0.000	0.000
16.000	721.880	758.540	9.733	11.027	192.267	0.000	0.000
14.000	763.298	801.250	8.607	12.113	210.667	0.000	0.000
12.000	762.374	796.022	10.213	10.560	192.067	0.000	0.000
10.000	804.908	839.414	8.693	12.067	215.267	0.000	0.000
9.000	856.002	879.284	7.993	12.733	213.000	0.000	0.000
8.000	930.244	931.466	5.640	15.033	269.733	0.000	0.000
7.000	1003.146	977.108	5.100	15.560	287.200	0.000	0.000
6.000	1021.094	1003.962	8.433	12.340	208.600	0.000	0.000
5.000	996.486	1036.040	5.967	14.700	235.867	0.000	0.000
4.000	1002.258	1054.080	0.000	20.487	154.267	3915.667	0.357
3.500	1047.444	1073.224	0.000	20.507	16.400	4000.000	5.737
3.000	1040.382	1064.304	0.000	20.507	19.000	4000.000	5.276
2.500	1024.436	1051.080	0.000	20.507	12.200	4000.000	3.371
2.000	1009.826	1062.778	0.000	20.500	11.000	4000.000	5.124
1.500	999.858	1049.826	0.000	20.500	10.200	4000.000	5.163
1.000	989.178	1077.160	0.000	20.513	14.200	4000.000	4.735
0.500	996.100	1032.420	15.740	5.133	12.400	4000.000	0.023

LOC IN	LOC CM	Tavg C	Tavg F	WALL LOC IN	WALL LOC CM	Twavg C	Twavg F	Taavg F/C
24.000	60.960	655.259	1211.470	0.000	0.000	216.188	421.142	C
22.000	55.880	686.580	1267.848	4.000	10.160	294.872	562.774	32.404
20.000	50.800	700.997	1293.799	8.000	20.320	295.860	564.552	F
18.000	45.720	715.134	1319.245	16.000	40.640	254.421	489.962	90.332
16.000	40.640	740.210	1364.382	24.000	60.960	218.101	424.587	
14.000	35.560	782.274	1440.097					
12.000	30.480	779.198	1434.560					
10.000	25.400	822.161	1511.894					
9.000	22.860	867.643	1593.761					
8.000	20.320	930.855	1707.543					
7.000	17.780	990.127	1814.233					
6.000	15.240	1012.528	1854.554					
5.000	12.700	1016.263	1861.277					
4.000	10.160	1028.169	1882.708					
3.500	8.890	1060.334	1940.605					
3.000	7.620	1052.343	1926.221					
2.500	6.350	1037.758	1899.968					
2.000	5.080	1036.302	1897.348					
1.500	3.810	1024.842	1876.720					
1.000	2.540	1033.169	1891.708					
0.500	1.270	1014.260	1857.672					

TEST CODE AND DATE: BCCP161 6/1/89  
 M.C. (WB%)= 8.300  
 FUEL FEED (WET, DRY lb/hr) 4.570 4.190  
 E.A. (%)= 71.400  
 TOTAL AIR (scfh)= 601.400  
 U.F.AIR (%)= 35.000  
 O.F. AIR (%)= 65.000

LOC IN	T12 C	T11 C	O2 percent	CO2 percent	NOx ppm	CO ppm	COMB. percent	PART. g
24.0	702.2	810.0	3.6	17.0	104.1	477.3	0.0	0.040
22.0	725.2	825.8	5.3	15.4	93.8	318.1	0.0	-----
20.0	712.1	791.0	9.1	11.6	70.3	192.6	0.0	COMB%
18.0	741.7	826.4	7.2	13.5	82.9	172.2	0.0	in part.
16.0	737.9	806.3	9.8	11.0	70.4	108.2	0.0	-----
14.0	756.3	831.3	8.8	11.9	72.9	77.0	0.0	14.540
12.0	820.9	903.5	5.9	14.7	87.4	67.5	0.0	-----
10.0	817.8	874.3	9.2	11.5	70.7	49.1	0.0	ASH%
9.0	778.7	814.2	12.1	8.7	59.1	40.1	0.0	in part
8.0	848.7	880.9	8.2	12.5	77.0	34.6	0.0	-----
7.0	865.8	879.4	10.2	10.6	69.2	35.5	0.0	85.460
6.0	898.9	924.1	12.2	8.6	55.5	27.3	0.0	-----
5.0	937.5	1024.4	8.3	12.4	77.8	35.5	0.0	
4.0	1043.1	1088.9	0.0	20.5	14.3	3962.7	3.6	
3.5	1037.5	1079.4	0.0	20.5	7.8	4000.0	3.2	
3.0	1021.3	1075.5	0.0	20.5	7.4	4000.0	2.3	
2.5	1014.8	1054.1	0.0	20.5	9.4	4000.0	3.0	
2.0	1040.9	1090.5	0.0	20.6	10.0	4000.0	4.9	
1.5	1023.4	1082.2	0.9	19.6	44.5	4000.0	0.2	
1.0	941.2	1016.0	11.1	9.6	37.3	0.0	0.4	
0.5	924.3	984.1	19.7	1.3	14.0	0.0	0.0	

LOC IN	LOC CM	Tavg C	Tavg F	WALL IN	LOC CM	Twavg C	Twavg F	Taavg F/C
24.000	61.0	756.1	1393.0	0.0	0.0	225.8	438.4	C
22.000	55.9	775.5	1427.9	4.0	10.2	292.2	557.9	30.9
20.000	50.8	751.5	1384.8	8.0	20.3	290.5	554.8	F
18.000	45.7	784.0	1443.2	16.0	40.6	241.6	466.9	87.7
16.000	40.6	772.1	1421.8	24.0	61.0	199.9	391.8	
14.000	35.6	793.8	1460.9					
12.000	30.5	862.2	1584.0					
10.000	25.4	846.0	1554.9					
9.000	22.9	796.5	1465.7					
8.000	20.3	864.8	1588.6					
7.000	17.8	872.6	1602.6					
6.000	15.2	911.5	1672.7					
5.000	12.7	980.9	1797.6					
4.000	10.2	1066.0	1950.8					
3.500	8.9	1058.5	1937.2					
3.000	7.6	1048.4	1919.2					
2.500	6.4	1034.4	1894.0					
2.000	5.1	1065.7	1950.2					
1.500	3.8	1052.8	1927.1					
1.000	2.5	978.6	1793.5					
0.500	1.3	954.2	1749.5					